Small Molecule Transcriptional Activation Domains

by

Sara J. Buhrlage

A dissertation submitted in partial fulfillment
of the requirements for the degree of
Doctor of Philosophy
(Chemistry)
in The University of Michigan
2008

Doctoral Committee:

Associate Professor Anna K. Mapp, Chair
Professor Richard R. Neubig
Associate Professor Hashim Al-Hashimi
Associate Professor Melanie S. Sanford

© Sara J. Buhrlage

All rights reserved
2008

To Dad

Acknowledgements

I owe more gratitude than I can express in two short pages to the many people who have provided me encouragement, support, mentorship, and understanding before, during, and I'm sure what will be after, completion of this degree. When I didn't know what I wanted to do as an undergraduate at Miami University Dr. Ben Gung suggested I work in his lab for a summer and that opportunity is what made me realize how much I enjoy science. After college I took an industry job and undoubtedly the confidence in my abilities as a scientist my boss Dr. Jack Amburgey gave me with, along with his encouragement, is what led me to graduate school and the last five years at the University of Michigan.

From probably day one of my rotation in the Mapp lab I knew I had landed in the right place. The enthusiasm the lab has for its research projects is contagious and the supporting and fun environment was invaluable to me. I particularly want to thank Amelia Fuller and Aaron Minter, I am very fortunate to have had the opportunity to work with such talented scientists and what became great friends during my first years of graduate school. Additionally, throughout my time at Michigan I have been fortunate to work closely with Caleb Bates, Brian Brennan, Matt Leathern, and Steve Rowe. I have been very lucky to be able to come to work every day and be surrounding by great scientists and friends, and occasionally punching bags (sorry Caleb!). Anna, I am very grateful that I had to opportunity to spend five years in your lab, I don't know if I would have accomplished this feat anywhere else. It goes without saying that your research vision is incredible and I have thoroughly enjoyed the work I have done over the last five years. Beyond science, I have grown from observing your professionalism, the high standard you hold yourself to, the way you treat everyone with respect, and your patience; this truly motivates me to expect the same of myself.

My thesis committee members have all provided me with valuable, yet different, support during my time here. My opportunity to work with Professor Melanie Sanford

during what was both of our first summers here provided me excellent training as I was learning lab techniques directly from her. Professor Hashim al-Hashimi has been an invaluable collaborator on a number of project during almost my entire time here. Last, but not least, Professor Richard Neubig, taught me the valuable lesson in my candidacy exam that you need to think critically about every aspect of your project in order for it to succeed, even if aspects of the project are carried out by a colleague. Outside of Michigan, I was afforded the unique opportunity to work in the lab of Professor David Wemmer at the University of California, Berkeley. I sincerely thank him for that opportunity, it not only enriched my thesis project but it was just really enjoyable spending three months on the west coast.

I would like to thank the people I have spent time with outside of lab for keeping me from going crazy at times. From vacationing with Therese Nash, Eileen Merkle, Chris Liu, Brian Brennan, Sarah Kissell, and my family to playing soccer once a week with a great group of girls to catching lunch and Grey's Anatomy with Tasha Francis, it has been nice to have these opportunities to get relax.

Most importantly, I would like to thank my family for unwavering support, encouragement, confidence in me, care packages, and love. I would not have gotten here, gotten through the hard times or finished this without you. My entire family knows how valuable they are to my life, but I would like to highlight two people. I owe nearly all, if not all of my success, to my father. His guidance, support, encouragement, confidence, and emphasis on education have made the person I am today and I will always be grateful to have had him in my life. I only wish it could have been for even longer. Secondly, I am fortunate to have met Chris Liu during graduate school. His support in- and outside of lab have been invaluable and I am very grateful o have him in my life.

Table of Contents

List of Figures

Chapter I

Chatper II

Chatper III

Chapter IV

Chapter V

Appendix

List of Schemes

Chapter II

Chapter IV

Appendix

List of Tables

Chapter III

Appendix

List of Abbreviations

A	alanine
AEEA	8-amino-3,6,-dioxaoctanoic acid
ATF-14	artificial transcription factor-14
$BF_3 \bullet OEt_2$	boron trifluoride diethyl etherate
BnBr	benzylbromide
BnMgCl	benzylmagnesium chloride
Bpa	bnezophenone alanine
*t*BuOCl	*tert*-butyl hypochlorite
*t*BuOH	*tert*-butanol
CBP	CREB binding protein
CH_2Cl_2	dicholoromethane
CH_3CN	acetonitrile
ChIP	chromatin immunoprecipitation
CREB	cAMP response element-binding protein
DBD	DNA binding domain
DHFR	dihyrofolate reductase
DIBAL	diisobutylaluminum hydride
DMF	N, N-dimethylformamide
DMSO	dimethylsulfoxide
DNA	deoxyribonucleic acid
EC_{50}	concentration at half-maximal stimulation
EtMgBr	ethyl magnesiumbromide
Et_3N	triethyl amine
Et_2O	diethyl ether
F	phenylalanine
Fmoc	9-fluorenylmethoxycarbonyl
FP	fluorescence polarization
g	gram
HeLa	Henrietta Lacks cervical cancer cells
HBTU	2-(1H-benzotrizol-1-yl)-1,1,3,3-tetramethyluronium hexafluorophosphate
hMDM2	human double-minute 2
HOBT	N-hydrozybenzotrizole
HPLC	high pressure liquid chromatography
IPTG	isopropyl β-D-1-thiogalactopyranoside
K_d	dissociation constant at equilibrium
HSQC	heteronuclear single quantum coherence
Kid	kinase inducible domain
L	leucine
LB	Luria-Bertani media

Med	Mediator protein 150 kD
MeOH	methanol
MLL	mixed lineage lekemia
mRNA	messenger ribonucleic acid
MsCl	methane sulfonylchloride
NaH	sodium hydride
$NaBH_4$	sodium borohydride
$NaIO_4$	sodium periodate
NaN_3	sodium azide
NMO	N-methylmorpholine-N-oxide
NMR	nuclear magnetic resonance
NSRF	neuron-restrictive silencer factor
OsO_4	osmium tetroxide
OxDex	oxidized dexamethasone
pKid	phosphorylated kinase inducible domain
p53	protein 53 kiltodaltons
PBS	phosphate buffered saline
PEG	polyethylene glycol
PNA	peptide nucleic acid
PPh_3	triphenylphosphine
$i Pr_2NEt$	diisopropyl ethyl amine
REST	response element-1 silencing transcription factor
RNA	ribonucleic acid
Srebp	steroid response element binding protein
TA	transcriptional activator
TAD	transcriptional activation domain
TAF	TBP-associated factor
TBAF	tetrabutylammonium fluoride
TBP	TATA binding protein
TBS	*tert*-butyl dimethylsilane
TFO	triplex forming oligonucleotide
THF	tetrahydrofuran
VP16	viral protein 16
ZF	zinc finger

Abstract

Small Molecule Transcriptional Activation Domains

By

Sara J. Buhrlage

Chair: Anna K. Mapp

Transcriptional activators are essential for high fidelity transcription, responsible for seeking out particular genes and up-regulating them to precise levels in a signal responsive fashion. Indeed the altered transcription patterns observed in disease states can often be attributed to malfunctioning and/or misregulated transcriptional activators. Thus, molecules that can reconstitute the function of transcriptional activators, artificial transcription activators, are highly desirable commodities as mechanistic tools and transcription-targeted therapeutics. Transcriptional activators control the specificity and extent of gene upregulation through two domains: the DNA binding domain (DBD) is responsible for the former and the transcriptional activation domain (TAD) dictates the level of gene expression. It has proven quite challenging to identify TAD replacements with functional properties comparable to the natural system despite their likely advantages in terms of stability, delivery, and and/or immunogenic properties. This is

likely due to the many open questions surrounding how natural transcriptional activation domains function.

To address the need for the development and characterization of small molecule TADs we have employed a combination of organic chemistry, NMR spectroscopy, and biological evaluations to a class of isoxazolidines that functionally mimic natural TADs. We prepared five stereochemically pure isoxazolidine isomers, each of which contained identical functional groups (benzyl, isobutyl and hydroxyl) arranged in different positions around the isoxazolidine ring. All of these amphipathic isoxazolidines functioned as TADs in a cell-free assay, revealing that analogous to endogenous TADs, a particular positioning of functional groups is not required for transcription function. Similar functional trends were observed in a cellular assay. We further demonstrated that the small molecule TADs interact with at least a subset of the same coactivator proteins as do natural TADs. In particular, interaction with the KIX domain of Creb Binding Protein is correlated with transcription function, although binding interactions with Tra1, Med15 and Med23 are also observed. These molecules are thus anticipated to be an excellent starting point for the design of more potent small molecule regulators of transcription.

Chapter I

Introduction to Small Molecule Control of Transcription Initiation

A. Project Focus

Transcriptional activators are essential for high fidelity transcription, responsible for seeking out particular genes and up-regulating them to precise levels in a signal responsive fashion.[1] Indeed, malfunctioning transcriptional activators are correlated with altered transcription patterns in disease states.[1-3] There is thus tremendous interest in the development of artificial transcriptional activators as potential transcription-targeted therapeutics and mechanistic probes of disease. Transcriptional activators carry out their gene targeting and up-regulating functions through two different domains: the DNA binding domain (DBD) performs the former and the transcriptional activation domain (TAD) controls the extent of gene expression.[1-3] Of these two domains it has proven significantly more challenging to identify TAD replacements with functional properties comparable to the natural system despite their likely advantages in terms of stability, delivery, and and/or immunogenic properties. In fact, at the outset of my thesis work there was only a single example of a small molecule TAD.[4] Thus the focus of my thesis project was to design, synthesize and evaluate novel analogs of that molecule to probe its mode of action and yield future generations of small molecule TADs.

B. Introduction to Transcription

Transcription, the process by which DNA is transcribed to mRNA, is the first step in the ultimate production of protein product from the information encoded in DNA. RNA polymerase II is the key enzyme in transcribing mRNA from DNA but this enzyme requires a large number of accessory proteins to function.[1-3] A general schematic of the process of transcription is shown in Figure I-1a. Transcriptional activator proteins, in response to intra- or extra-cellular signals, seek out a specific sequence of DNA within

the nucleus of a cell and recruit chromatin remodeling enzymes to alter the chromatin structure. The same transcriptional activator proteins then recruit RNA polymerase II (RNA Pol II) to the gene of interest through direct binding interaction with proteins termed coactivators that serve as a bridge between the transcriptional activators and RNA Pol II. The complex of RNA Pol II, associated factors and enzymes, and coactivators are collectively referred to as the transcriptional machinery. The availability of transcriptional activators to regulate transcription is controlled in part by masking proteins (Figure I-1b) that prevent proteolysis and aggregation of activators until signals are received indicating appropriate timing for gene upregulation.[1, 3, 5]

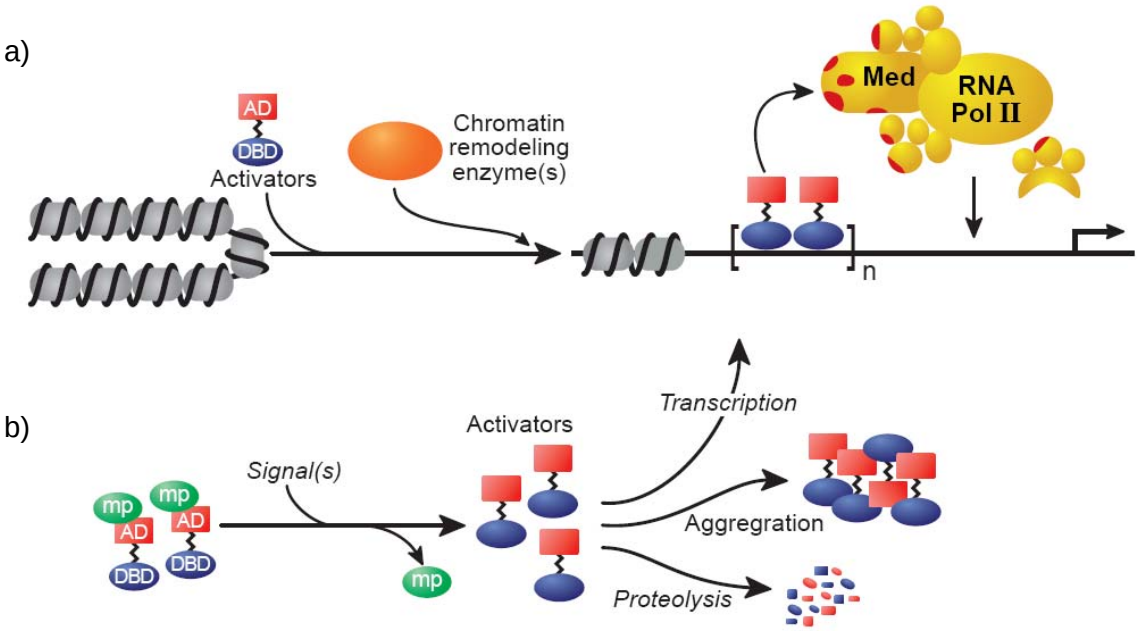

Figure I-1. General schematic of transcription initiation. a) In the nucleus activators localize to a specific sequence of genomic DNA and recruit chromatin remodeling enzymes, coactivators such as Mediator, Med, and RNA polymerase II, RNA Pol II. b) Masking proteins control, in part, the concentration of activators available in the nucleus.[1-3]

C. Transcriptional Activators

The interactions that transcriptional activators participate in with DNA and with enzyme and coactivator proteins in the transcriptional machinery result in the activators having a significant role in controlling both the specificity and extent of gene

upregulation. The proteins can minimally accomplish this using two domains, the DNA binding domain and transcriptional activation domain.[1] The DNA binding domain (DBD), as the name insinuates, confers gene-targeting specificity to the activator by localizing to a specific sequence of genomic DNA. The transcriptional activation domain, or TAD, recruits the transcriptional machinery through direct binding interactions with coactivator proteins. Transcriptional activators often have additional protein interaction and signaling domains, but they are not required for function.[1] The two essential modules, the DBD and TAD, can be linked either covalently or noncovalently and typically function independently.[1] For example, chimeric molecules composed of a DBD from one transcriptional activator protein and a TAD from another can be fused together and function to activate transcription (Figure I-2b).[1, 6, 7] Importantly, this enables the study of each module individually.

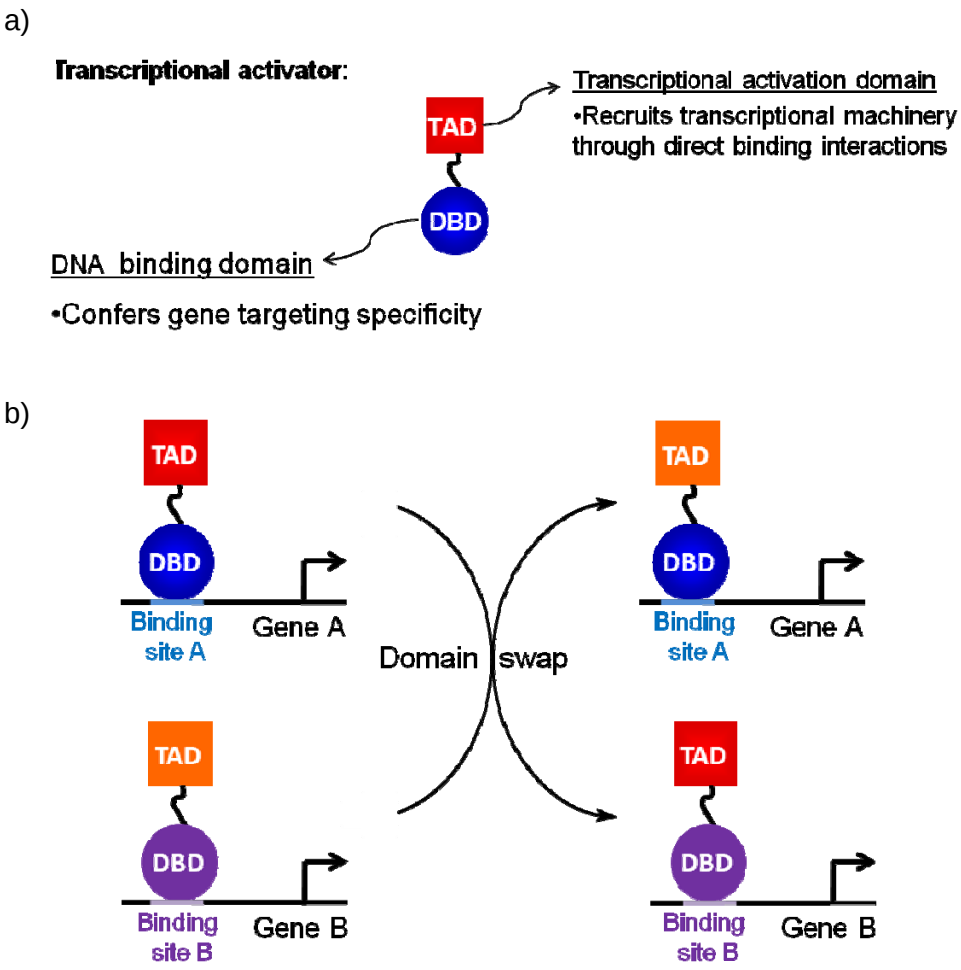

Figure I-2. Transcriptional activators contain two critical modules for function. a) Architecture of a transcriptional activator. b) Domain swapping experiments demonstrated the DBD and TAD modules function independently.[1, 6, 7]

D. Misregulated Transcription, Disease, and Protein-Based Therapeutics

Due to the important role that transcriptional activators play in controlling gene expression it is not surprising that malfunctioning or miscued transcriptional activators are correlated with a wide range of consequences including several leukemias, diabetes, and medulloblastoma.[8-10] Artificial transcriptional activators, nonnatural replacements of these powerful proteins, are thus highly sought after commodities as potential transcription-targeted therapeutics.[1] An ideal artificial transcriptional activator would reconstitute all aspects of natural transcriptional activator function: signal responsive up-regulation of selected genes to predetermined levels in a tissue-specific and time-sensitive manner.[1] This of course requires an artificial activator be effectively delivered

to a specific tissue, localize to the nucleus, and upregulate transcription of a specific gene to the appropriate level in response to a natural signal. Achieving this is quite challenging due to the complex network of events involved in upregulating a single gene. The current state of the art in artificial transcriptional activator based therapeutics is protein-based artificial transcriptional activators containing the minimal DBD and TAD modules. Examples of the successful utilization of protein-based artificial transcriptional activators are presented below.

In the case of medulloblastoma, the most malignant pediatric brain tumor, the disease is caused by the overexpression of the transcriptional repressor REST/NSRF.[8] This repressor causes suppression of genes critical for proper differentiation of neuronal cells that when down-regulated result in tumor formation. The therapeutic potential of artificial transcriptional activators has been demonstrated for this disease. An artificial transcriptional activator that swapped the repression domain of REST for the activation domain of VP16 competed for DNA binding with the REST/NSRF repressor and restored expression at the neuronal promoters ultimately leading to apoptosis of the cancer cells.[11, 12]

In a second example, a zinc finger artificial transcriptional activator that up-regulates the VEGF-A gene is in Phase II clinical trials as a treatment for diabetic peripheral sensory motor neuropathy.[13] Diabetic neuropathy is one of the most common complications of diabetes and has symptoms ranging from numbness and tingling in mild cases to loss of feeling and motor function as nerve damage progresses. This loss of sensation often leads to untreated injuries and infections resulting in the high number of leg amputations obtained among the diabetic population.[14] VEGF-A possesses potent neurotrophic and neuroprotective properties and upregulation of expression of this protein by the artificial activator has been effective in protecting motor and sensory nerve function in a diabetic rat model.[13] The same company, Sangamo BioSciences, Inc., also has ongoing Phase I clinical trials for another zinc finger artificial transcriptional activator as a therapeutic for peripheral artery disease.

E. Small Molecule Artificial Transcriptional Activators

The above examples highlight the power of artificial transcriptional activators, but there are significant challenges facing protein variants, including delivery, cellular stability and immunogenicity concerns. Small molecule artificial transcriptional activators are thus an attractive alternative as they are likely to address many of these issues. Ideally, a small molecule transcriptional activator would consist of a low molecular weight small molecule that sequence specifically binds DNA and a second low molecular weight small molecule that functions as a TAD, recruiting the transcriptional machinery through direct binding interactions. Towards this, significant progress has been achieved in the development of synthetic DNA binding domains that can be used in cell-free, cellular, and, in some cases, in vivo settings.[15, 16] However, the development of small molecule transcriptional activation domains that can reconstitute the function of their endogenous counterparts has proven to be quite challenging, likely due to the lack of detailed information regarding the mechanism by which natural TADs function.

As alluded to above, transcriptional activation domains have multiple binding partners in the transcriptional machinery.[1, 17] Thus the challenge is to identify a single small molecule that can interact with multiple proteins in the transcriptional machinery while maintaining specificity for coactivator proteins over nonproductive interactions with other cellular proteins. Further complicating this task is the fact that the identities of all coactivator proteins have not been elucidated, making binding-based screens for small molecule TADs difficult to implement. There is also little structural data for either TADs alone or TADs in complex with coactivators, and there is not enough data for true structure-based design of small molecule TADs.[1] The following section focuses on what is known about transcriptional activation domains, coactivators, how the two protein classes interact, and concludes with how this information influenced the design of the first small molecule transcriptional activation domain.

F. TADs and Their Protein Binding Partners

1) Transcriptional Activation Domains

The most well studied class of transcriptional activation domains, amphipathic TADs, contain interspersed hydrophobic and polar residues, but there is little sequence homology within the class.[1, 18, 19] Mutagenesis experiments have revealed that the hydrophobic groups are particularly important for binding with loss of interaction of a hydrophobic residue with a coactivator binding site abrogating binding and function more significantly than mutagenesis of a polar group.[20, 21] Examples of TADs that bind coactivator proteins are shown in Figure I-3a.[22-25] These particular examples also highlight the observation that relatively short peptide sequences are capable of activating transcription. In fact, several groups have utilized peptide sequences of only 8 amino acids to construct TADs.[1, 18, 19, 26] The amphipathic sequences of transcriptional activation domains have been shown to be unstructured in solution but to adopt a defined conformation, most commonly an amphipathic helix, upon binding coactivator targets (Figure I-3b)[27, 28], although there is some evidence for alternate secondary structure.[29, 30] In an early example Verdine and coworkers utilized NMR spectroscopy to show that in the case of the C-terminal VP16 TAD 12 of the TAD residues (472-483) undergo a transition from random coil to helix upon binding the coactivator protein $TAF_{II}31$.[28] The mode by which folding is coupled to binding for these intrinsically disordered proteins has gained significant interest and recently the mechanism of folding for the pKID peptide of the activator Creb to the KIX domain of the coactivator protein CBP was described.[31] pKID forms an ensemble of transient encounter complexes upon binding KIX and evolves by way of an intermediate to the fully bound α-helical state without dissociation from KIX. Interestingly, the encounter complexes are also formed with a second binding site contained in the KIX domain but do not evolve to the fully bound state.

a)

MLL	2847	DIMDFVLKNT
Myb	295	IKELELLL
SREBP1a	26	LTDIEDML
KBP 2.20	47	SWAVYELLFGS

b)

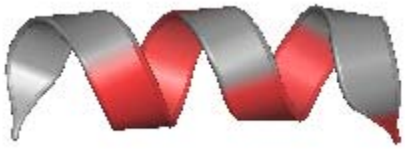

MLL

Figure I-3. Natural TADs. a) Sequences are comprised of interspersed hydrophobic and polar residues. b) Amphipathic helix is the most common secondary structure of amphipathic TADs. MLL is shown here and hydrophobic residues are colored red.[32] Figure adapted from 2agh.

2) Transcriptional Activation Domain Binding Partners

Two key classes of proteins that TADs interact with are masking proteins and transcriptional coactivator proteins. The structure and function of co-complexes of TADs and masking proteins are well-characterized compared to the complexes formed between TADs and transcriptional machinery proteins.

a) Masking Proteins

The role of masking proteins is to regulate the function, aggregation, and proteolysis of TADs until signals are received indicating appropriate timing for upregulation of a particular gene.[1] The interactions between TADs and masking proteins occur with high affinity and specificity compared to interactions with coactivators. It has thus been relatively straightforward to utilize screens, for example, to discover small molecules that bind masking proteins. For example, the complex formation of Gal4 with its masking protein Gal80 occurs with a K_D of 2 nM,[33] whereas Gal4 binds several coactivator proteins in the low micromolar range.[17, 34, 35] In a second example, p53 binds its masking protein MDM2 (Figure I-4a) with a K_D of 420 nM and the coactivator protein CBP with a K_D of 40 μM.[36, 37] A subset of the small molecules that bind MDM2 are

shown in Figure I-4b.[38] Interestingly, evidence suggests masking proteins and coactivators may sample TAD sequences differently. For example, certain point mutations in the Gal4 TAD negatively impacted the ability of the TAD to bind its masking protein Gal80 but did not affect the ability of the TAD to activate target genes in vivo.[39] Thus, inhibitors such as **I-1**-**I-3** which are more straightforward to discover than small molecules that bind coactivator proteins may serve as excellent starting points for the generation of small molecule TADs.

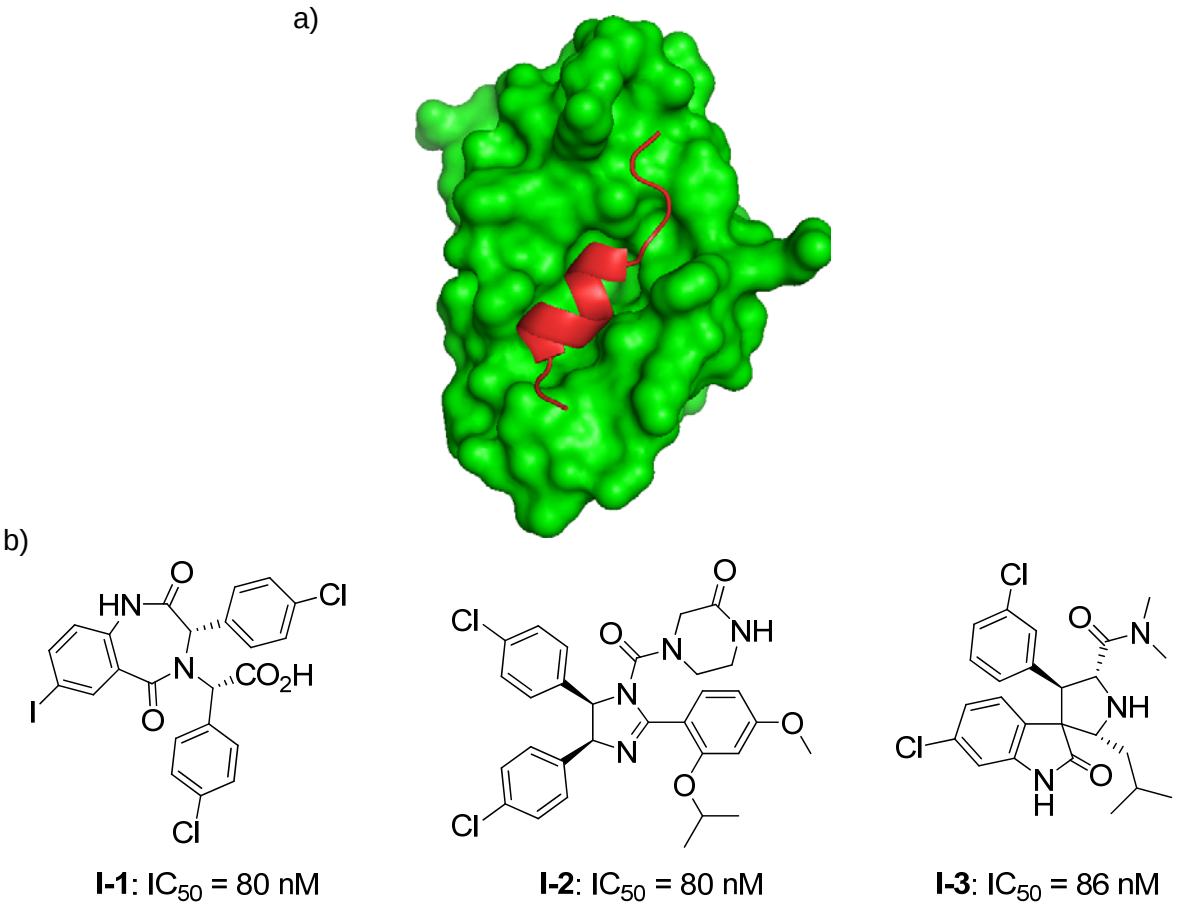

Figure I-4. p53•MDM2 complex and inhibitors. a) Cocrystal structure of p53•MDM2.[36] b) Inhibitors of the p53•MDM2 interaction.[38] Figure adapted from 1ycr.

b) Coactivators

To initiate transcription, the TAD must facilitate assembly of the transcriptional machinery through direct binding interactions with one or more coactivators. The

identity, however, of the binding partners remains a source of debate, and additional binding partners are still being elucidated. Further, particular coactivators at a given promoter vary based on factors such as tissue-type and the timing of the transcription cycle. This needs references

Transcriptional machinery proteins and protein complexes that have been identified as targets of transcriptional activators include CBP, Mediator, SAGA, NuA4, Swi/Snf and TBP-associated factors (TAFs).[40-46] Individual coactivator proteins can reside in multiple complexes and a single complex may fulfill multiple roles. For example, the SAGA complex functions both in chromatin remodeling and as a coactivator and contains overlapping protein components with Mediator. The protein complexes within the transcriptional machinery range from large, approximately 25 proteins comprise Mediator, to small and easier to study.[47] CBP, for example is currently believed to function independently or in complex with 1-2 other coactivator proteins.[42, 48]

The prevailing evidence suggests that transcriptional activators interact with several coactivators, between 3 and 10, in order to recruit the transcriptional machinery to DNA.[1] Particularly compelling evidence arises from in vitro crosslinking experiments conducted by Hahn and co-workers with DNA-bound transcriptional activators. Two well-characterized amphipathic activators, Gal4 and GCN4, were exposed to nuclear extracts, and under these conditions both activators were found to directly interact with three coactivators proteins, Tra1, Med15, and Taf12.[40, 41] Tra1 and Taf12 are components of the SAGA chromatin remodeling complex and Med15 is a component of the Mediator complex.[45, 49] In another recent example of the necessity of recruitment of multiple coactivators, activator by-pass experiments found that minimally two complexes, SAGA and Mediator, must be recruited to DNA for gene expression to occur.[50] In activator by-pass experiments, the coactivator is directly attached to a DBD and the ability of the chimeric protein to function as a transcriptional activator is evaluated. Significant in vitro binding data has also been collected as evidence for a multipartner binding profile. For example more than five binding partners have been identified each for activators p53 and VP16 using a variety of techniques.[51]

Along similar lines, a single transcriptional machinery protein often interacts with multiple TADs. For example, the four transcriptional activation domains shown in Figure I-4 are all binding partners of CBP and all interact with the same motif within CBP, the KIX domain.[24, 52, 53] Similarly, natural TADs GCN4, Gal4 and VP16 as well as the non-natural TAD XL_Y are believed to all function, in part, through interaction with the Mediator protein Med15.[19, 54-58] This implies that individual binding sites are permissive and recognize a variety of presentations of amphipathic functionality. At least in the case of the KIX domain of CBP, sufficient structural data has been collected to show that in fact a single binding site recognizes multiple activators.[32, 52, 53, 59-62]

3) Structural Details of TAD•Coactivator Interactions

The number of structural studies of TAD•coactivator co-complexes is small. Nonetheless, the available studies have been valuable in providing insight in to design criteria for nonnatural transcriptional activation domains. Perhaps the most well-characterized TAD•coactivator complexes are between the KIX domain of CBP and activators Creb, Myb, and MLL and the Tfb1 domain of TFIIH in complex with activators VP16 and p53.[27, 32, 51, 52, 58, 60, 63] The CBP KIX domain is comprised of five helices and interacts with greater than 10 transcriptional activations; the solution structures have been solved for three of these in complex with the KIX domain.[27] The solution structures of the Tfb1 domain of TFIIH in complex with two different activators p53 and VP16 have also been solved.[51, 63] The Tfb1 protein is comprised of one α-helix and 7 β-sheets. In all cases the TADs were bound as amphipathic helices with the hydrophobic face contacting the coactivator binding site; the length of the helices ranged from 9-15 amino acids. The solution structures suggest that a precise arrangement of functional groups is not necessary for binding. For example, the hydrophobic faces of p53 and VP16 that bind the same site on the Tfb1 domain consist of different residues. In the case of p53 the three residues are Ile, Phe, and Trp,[63] whereas for VP16 it is a Met and two Phe.[51] Although the hydrophobic face of the helix inserts into the binding surface in all cases at least one polar residue, either a serine or threonine, makes an important hydrogen bonding or ionic interaction with the protein. The solution structure

of VP16•Tfb1 is shown in Figure I-5a and the MLL•KIX•Myb ternary complex is shown in Figure I-5b.[32, 51]

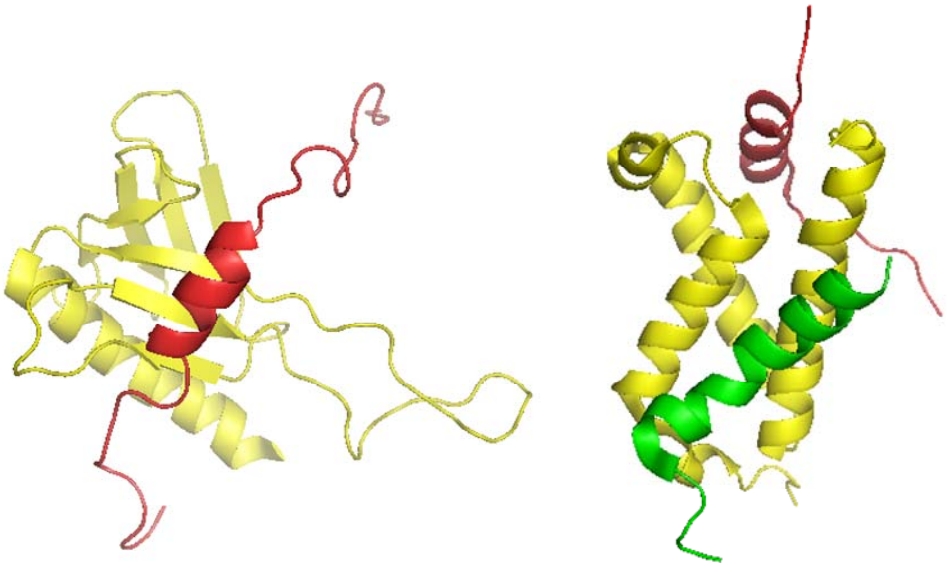

Figure I-5. TAD•coactivator complexes. a) VP16•Tfb1, Tfb1 is in yellow and VP16 is shown in red.[51] Figure adapted from 2k2u. b) Myb•KIX•MLL, KIX is shown in yellow, Myb is in green and MLL is in red.[32] Figure adapted from 2agh.

G. Design of the First Small Molecule TAD

The multi-partner, moderate affinity binding profile of TADs with coactivator proteins suggested that screening methods would be unsuccessful in identifying small molecule TADs. Indeed, screens against a single transcriptional machinery protein have typically yielded TADs that do not function as well as natural TADs.[29, 57] However, the permissiveness of coactivator binding sites, which recognize multiple presentations of amphipathic functionality, led to the idea that perhaps designing a small molecule TAD could be straightforward. The hypothesis was that a small molecule that mimics the general characteristics of endgenous TADs would be able to interact with at least a subset of the permissive binding sites for TADs within the transcriptional machinery and by doing so activate transcription. Thus, relatively simple criteria based on what is known about endogenous TADs were outlined as design guidelines for a small molecule TAD. The design criteria included that the small molecule contain a rigid core to adequately

project functionality into the binding site similarly to a helix. Secondly, the rigid core would need to be appended with both hydrophobic and polar sidechains that mimic the functionality commonly contained in endogenous TADs.

Former coworkers identified isoxazolidine **I-4** as a small molecule that fit the above criteria (Figure I-6). The five-membered heterocycle imparts the desired rigidity, and further, the synthetic methods to access this scaffold allow for dense functionalization of the core with a variety of sidechains. Amphipathic isoxazolidine **I-4** was thus prepared and covalently linked to a DNA binding functionality for evaluation as were analogs that were either significantly more hydrophobic (**I-5**) or more polar (**I-6**).[4] This 'top-down' approach proved successful, with **I-4** being the first reported small molecule transcriptional activation domain. This molecule activated transcription 5-7 fold in a cell-free transcription assay. Analogous to the endogenous system isoxazolidines **I-5** and **I-6** that do not maintain an appropriate balance of amphipathic character did not activate transcription.

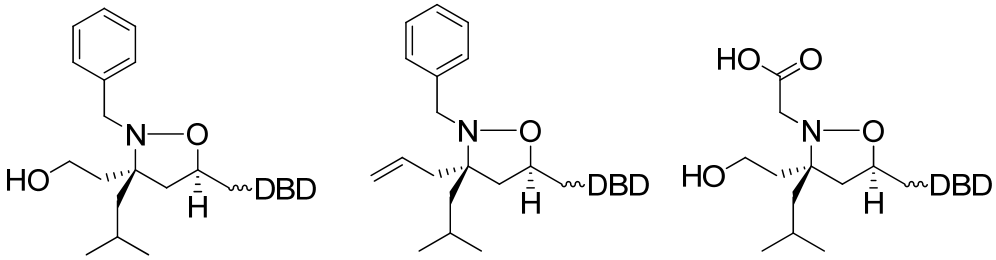

I-4 **I-5** **I-6**

Figure I-6. Isoxazolidines evaluated as TADs. Amphipathic isoxazolidine **I-4** activated transcription, whereas **I-5** and **I-6** do not.[4]

This first example of a small molecule TAD, referred to as iTAD for isoxazolidine transcriptional activation domain, had been a long sought after milestone in the artificial control of gene expression and thus there was tremendous interest in elucidating the mode of action of iTAD **I-5** as well as investigating the ability of the molecule to function in cells; answering these questions was the focus of my thesis work.

H. Thesis Outline

To expand our understanding of small molecule TADs the key questions my research efforts sought to answer were do iTADs function by a similar mode of action as endogenous TADs and will the molecules function in cells. Towards the former the particular comparisons I investigated were whether iTADs target the same coactivator binding sites as endogenous amphipathic TADs and do they mimic the functional profile in that a precise presentation of functionality is not a critical determinant of function.

In Chapter II the ability of amphipathic isoxazolidines differing in placement of amphipathic side chains were evaluated for ability to upregulate transcription. A facile synthetic approach for the generation of chiral isoxazolidines was established and utilized for the rapid generation of target molecules. Analogous behavior to natural amphipathic TADs, in which there is not a strict requirement for functional group placement, was observed for iTADs suggesting that the small molecule TADs function by a similar mechanism. Consistent with this, the small molecules were evaluated in cells and potently activated transcription.

In Chapter III the coactivator binding partners of iTADs were investigated and four binding partners of iTAD **I-4** were identified supporting that iTADs exhibit a multipartner, low K_D binding profile analogous to their endogenous counterparts. Of particular note, iTAD **I-4** binds CBP, a ubiquitously expressed histone acetyltransferase and coactivator that is an important node in many signaling networks, interacting in fact with greater than 300 TADs. Thus **I-5** should be a valuable commodity for elucidating the functional role of particular CBP molecular recognition events. The ability of additional isoxazolidines to interact with the same motif within CBP was evaluated using NMR spectroscopy and it was observed that small structural changes alter the binding profile of the small molecules suggesting that some degree of specificity for a given activator or activator class may indeed be achievable within this framework.

Surreptitious repeats are often encountered in TADs and the repeated sequences have been shown to synergistically activate transcription compared to the minimal domain. Thus an iterative synthetic approach to bis-isoxazolidines was designed and implemented in an effort to produce small molecules with enhanced potency compared to

monomeric iTADs. In Chapter IV the synthesis of a variety of bis-isoxazolidines is presented; the molecules bind the CBP KIX domain with enhanced affinity but this did not translate to synergistic levels of function, likely attributable to attenuated cellular permeability.

Together, the investigation of the monomeric and dimer isoxazolidines for ability to bind coactivator proteins yielded evidence that the ability of iTADs to stimulate transcription is linked to a binding interaction with CBP. Characterization of the iTAD binding site within CBP via NMR spectroscopy revealed a remarkable similarity to endogenous activators such as MLL that utilize this site.

In sum, the preponderance of evidence suggests that iTADs are similar to endogenous counterparts in terms of function and shared binding sites within the transcriptional machinery. Consistent with this iTADs function in cells and when attached to a variety of DBDs suggesting the molecules should be able to activate endogenous genes. Further these molecules should serve as an excellent starting point for the generation of small molecule inhibitors of transcription, long a challenging endeavor.

I. References

1. Mapp, A. K.; Ansari, A. Z., *ACS Chem Biol* **2007,** *2* (1), 62-75.
2. Majmudar, C. Y.; Mapp, A. K., *Curr Opin Chem Biol* **2005,** *9* (5), 467-74.
3. Lum, J. K.; Mapp, A. K., *Chembiochem* **2005,** *6* (8), 1311-5.
4. Minter, A. R.; Brennan, B. B.; Mapp, A. K., *J Am Chem Soc* **2004,** *126* (34), 10504-5.
5. Majmudar, C. Y.; Lum, J. K.; Prasov, L.; Mapp, A. K., *Chem Biol* **2005,** *12* (3), 313-21.
6. Keegan, L.; Gill, G.; Ptashne, M., *Science* **1986,** *231* (4739), 699-704.
7. Ma, J.; Ptashne, M., *Cell* **1987,** *51* (1), 113-9.
8. Schoenherr, C. J.; Anderson, D. J., *Science* **1995,** *267* (5202), 1360-3.
9. Perou, C. M.; Sorlie, T.; Eisen, M. B.; van de Rijn, M.; Jeffrey, S. S.; Rees, C. A.; Pollack, J. R.; Ross, D. T.; Johnsen, H.; Akslen, L. A.; Fluge, O.; Pergamenschikov,

A.; Williams, C.; Zhu, S. X.; Lonning, P. E.; Borresen-Dale, A. L.; Brown, P. O.; Botstein, D., *Nature* **2000,** *406* (6797), 747-52.

10. Slack, J. L.; Gallagher, R. E., *Cancer Treat Res* **1999,** *99*, 75-124.

11. Fuller, G. N.; Su, X.; Price, R. E.; Cohen, Z. R.; Lang, F. F.; Sawaya, R.; Majumder, S., *Mol Cancer Ther* **2005,** *4* (3), 343-9.

12. Lawinger, P.; Venugopal, R.; Guo, Z. S.; Immaneni, A.; Sengupta, D.; Lu, W.; Rastelli, L.; Marin Dias Carneiro, A.; Levin, V.; Fuller, G. N.; Echelard, Y.; Majumder, S., *Nat Med* **2000,** *6* (7), 826-31.

13. Urnov, F. D.; Miller, J. C.; Lee, Y. L.; Beausejour, C. M.; Rock, J. M.; Augustus, S.; Jamieson, A. C.; Porteus, M. H.; Gregory, P. D.; Holmes, M. C., *Nature* **2005,** *435* (7042), 646-51.

14. Andersen, C. A.; Roukis, T. S., *Surg Clin North Am* **2007,** *87* (5), 1149-77, x.

15. Weatherman, R. V., *Org Biomol Chem* **2003,** *1* (19), 3257-60.

16. Nielsen, P. E., *Methods Enzymol* **2001,** *340*, 329-40.

17. Melcher, K., *J Mol Biol* **2000,** *301* (5), 1097-112.

18. Mapp, A. K.; Ansari, A. Z.; Ptashne, M.; Dervan, P. B., *Proc Natl Acad Sci U S A* **2000,** *97* (8), 3930-5.

19. Lu, X.; Ansari, A. Z.; Ptashne, M., *Proc Natl Acad Sci U S A* **2000,** *97* (5), 1988-92.

20. Drysdale, C. M.; Duenas, E.; Jackson, B. M.; Reusser, U.; Braus, G. H.; Hinnebusch, A. G., *Mol Cell Biol* **1995,** *15* (3), 1220-33.

21. Cress, W. D.; Triezenberg, S. J., *Science* **1991,** *251* (4989), 87-90.

22. Ernst, P.; Wang, J.; Huang, M.; Goodman, R. H.; Korsmeyer, S. J., *Molecular and Cellular Biology* **2001,** *21* (7), 2249-2258.

23. Liu, Y. P.; Chang, C. W.; Chang, K. Y., *FEBS Lett* **2003,** *554* (3), 403-9.

24. Frangioni, J. V.; LaRiccia, L. M.; Cantley, L. C.; Montminy, M. R., *Nat Biotechnol* **2000,** *18* (10), 1080-5.

25. Zor, T.; Mayr, B. M.; Dyson, H. J.; Montminy, M. R.; Wright, P. E., *J Biol Chem* **2002,** *277* (44), 42241-8.

26. Lum, J. K.; Majmudar, C. Y.; Ansari, A. Z.; Mapp, A. K., *ACS Chem Biol* **2006,** *1* (10), 639-43.

27. Radhakrishnan, I.; Perez-Alvarado, G. C.; Parker, D.; Dyson, H. J.; Montminy, M. R.; Wright, P. E., *Cell* **1997,** *91* (6), 741-52.

28. Uesugi, M.; Nyanguile, O.; Lu, H.; Levine, A. J.; Verdine, G. L., *Science* **1997,** *277* (5330), 1310-3.

29. Liu, B.; Alluri, P. G.; Yu, P.; Kodadek, T., *J Am Chem Soc* **2005,** *127* (23), 8254-5.

30. Buskirk, A. R.; Landrigan, A.; Liu, D. R., *Chem Biol* **2004,** *11* (8), 1157-63.

31. Sugase, K.; Dyson, H. J.; Wright, P. E., *Nature* **2007,** *447* (7147), 1021-5.

32. De Guzman, R. N.; Goto, N. K.; Dyson, H. J.; Wright, P. E., *Journal of Molecular Biology* **2006,** *355* (5), 1005-1013.

33. Parthun, M. R.; Jaehning, J. A., *J Biol Chem* **1990,** *265* (1), 209-13.

34. Wu, Y.; Reece, R. J.; Ptashne, M., *EMBO J* **1996,** *15* (15), 3951-63.

35. Koh, S. S.; Ansari, A. Z.; Ptashne, M.; Young, R. A., *Mol Cell* **1998,** *1* (6), 895-904.

36. Kussie, P. H.; Gorina, S.; Marechal, V.; Elenbaas, B.; Moreau, J.; Levine, A. J.; Pavletich, N. P., *Science* **1996,** *274* (5289), 948-53.

37. Teufel, D. P.; Freund, S. M.; Bycroft, M.; Fersht, A. R., *Proc Natl Acad Sci U S A* **2007,** *104* (17), 7009-14.

38. Murray, J. K.; Gellman, S. H., *Biopolymers* **2007,** *88* (5), 657-86.

39. Ansari, A. Z.; Reece, R. J.; Ptashne, M., *Proc Natl Acad Sci U S A* **1998,** *95* (23), 13543-8.

40. Fishburn, J.; Mohibullah, N.; Hahn, S., *Mol Cell* **2005,** *18* (3), 369-78.

41. Reeves, W. M.; Hahn, S., *Mol Cell Biol* **2005,** *25* (20), 9092-102.

42. Chan, H. M.; La Thangue, N. B., *J Cell Sci* **2001,** *114* (Pt 13), 2363-73.

43. Malik, S.; Roeder, R. G., *Trends Biochem Sci* **2000,** *25* (6), 277-83.

44. Malik, S.; Baek, H. J.; Wu, W.; Roeder, R. G., *Mol Cell Biol* **2005,** *25* (6), 2117-29.

45. Bhaumik, S. R.; Raha, T.; Aiello, D. P.; Green, M. R., *Genes Dev* **2004,** *18* (3), 333-43.

46. Alley, S. C.; Trakselis, M. A.; Mayer, M. U.; Ishmael, F. T.; Jones, A. D.; Benkovic, S. J., *J Biol Chem* **2001,** *276* (42), 39340-9.

47. Kornberg, R. D., *Proc Natl Acad Sci U S A* **2007,** *104* (32), 12955-61.

48. Goodman, R. H.; Smolik, S., *Genes Dev* **2000,** *14* (13), 1553-77.

49. Brown, C. E.; Howe, L.; Sousa, K.; Alley, S. C.; Carrozza, M. J.; Tan, S.; Workman, J. L., *Science* **2001,** *292* (5525), 2333-7.

50. Cheng, J. X.; Gandolfi, M.; Ptashne, M., *Curr Biol* **2004,** *14* (18), 1675-9.

51. Langlois, C.; Mas, C.; Di Lello, P.; Jenkins, L. M.; Legault, P.; Omichinski, J. G., *J Am Chem Soc* **2008,** *130* (32), 10596-604.

52. Goto, N. K.; Zor, T.; Martinez-Yamout, M.; Dyson, H. J.; Wright, P. E., *Journal of Biological Chemistry* **2002,** *277* (45), 43168-43174.

53. Zor, T.; De Guzman, R. N.; Dyson, H. J.; Wright, P. E., *J Mol Biol* **2004,** *337* (3), 521-34.

54. Jeong, C. J.; Yang, S. H.; Xie, Y.; Zhang, L.; Johnston, S. A.; Kodadek, T., *Biochemistry* **2001,** *40* (31), 9421-7.

55. Lee, Y. C.; Park, J. M.; Min, S.; Han, S. J.; Kim, Y. J., *Mol Cell Biol* **1999,** *19* (4), 2967-76.

56. Park, J. M.; Kim, H. S.; Han, S. J.; Hwang, M. S.; Lee, Y. C.; Kim, Y. J., *Mol Cell Biol* **2000,** *20* (23), 8709-19.

57. Wu, Z.; Belanger, G.; Brennan, B. B.; Lum, J. K.; Minter, A. R.; Rowe, S. P.; Plachetka, A.; Majmudar, C. Y.; Mapp, A. K., *J Am Chem Soc* **2003,** *125* (41), 12390-1.

58. Zhang, F.; Sumibcay, L.; Hinnebusch, A. G.; Swanson, M. J., *Mol Cell Biol* **2004,** *24* (15), 6871-86.

59. Campbell, K. M.; Lumb, K. J., *Biochemistry* **2002,** *41* (47), 13956-64.

60. Radhakrishnan, I.; Perez-Alvarado, G. C.; Parker, D.; Dyson, H. J.; Montminy, M. R.; Wright, P. E., *J Mol Biol* **1999,** *287* (5), 859-65.

61. Vendel, A. C.; Lumb, K. J., *Biochemistry* **2004,** *43* (4), 904-8.

62. Vendel, A. C.; McBryant, S. J.; Lumb, K. J., *Biochemistry* **2003,** *42* (43), 12481-7.

63. Di Lello, P.; Jenkins, L. M. M.; Jones, T. N.; Nguyen, B. D.; Hara, T.; Yamaguchi, H.; Dikeakos, J. D.; Appella, E.; Legault, P.; Omichinski, J. G., *Molecular Cell* **2006,** *22* (6), 731-740.

Chapter II

Stereochemical Promiscuity of iTADs[a]

A. Abstract

Small molecule replacements of transcriptional activation domains are highly desirable targets due to their utility as mechanistic tools and their long-term therapeutic potential for a variety of human diseases. Here we examine the ability of amphipathic isoxazolidines differing only in the placement of constituent side chains to function as transcriptional activation domains in a cell-free system. The results reveal that precise positioning of functional groups within a conformationally constrained small molecule scaffold is not required for transcription function; rather, the balance of polarity and hydrophobicity within the scaffold is the more important determinant of transcription function. This is analogous to the natural amphipathic TADs the small molecules were designed to mimic, suggesting that the small molecule TADs function via a similar mechanism. Consistent with this model, the small molecules also function as transcriptional activation domains in cell culture.

B. Introduction

According to the prevailing model, transcriptional activators initiate transcription by assembling the large, multicomponent transcriptional machinery complex through the interaction of their transcriptional activation domains (TADs) and several distinct binding partners.[1] In vitro crosslinking studies with a labeled version of the yeast activator Gal4, for example, showed that its TAD contacts at least three coactivator proteins during transcription initiation: Med15(Gal11), a component of the Mediator complex, and two proteins in the SAGA chromatin remodeling complex, Tra1 and Taf12.[2] It is a single

[a] Portions of this Chapter are reported in: Buhrlage, S. J.; Brennan, B. B.; Minter, A. R. Mapp, A. K. *J. Am. Chem. Soc*. **2005**, *127*, 12456-12457; Rowe, S. P.; Casey, R. J.; Brennan, B. B.; Buhrlage, S. J.; *J. Am. Chem. Soc.* **2007**, *129*, 10654-10655.

peptide sequence that mediates these different binding interactions, suggesting that there are somewhat conserved TAD binding motifs present in different transcriptional machinery proteins. Remarkably, an amphipathic TAD with no sequence homology to Gal4, GCN4, interacts with the same set of coactivators as the Gal4 TAD, suggesting that the TAD binding sites within coactivators are also somewhat permissive, not requiring a single placement of particular side chains.[3] In another example of this phenomenon, the KIX domain of the coactivator CBP (Creb binding protein) interacts with at least 10 amphipathic TADs with little sequence homology.[4]

The first small molecule TAD, isoxazolidine TAD (iTAD) **II-1**,[5] was designed as a generic mimic of natural amphipathic TADs, with the hypothesis being that a conformationally constrained amphipathic small molecule should be able to interact with at least a subset of the permissive binding sites for TADs within the transcriptional machinery and by doing so activate transcription. Consistent with this hypothesis, the amphipathic isoxazolidines functioned as TADs in a standard cell-free transcription assay whereas more hydrophobic or more polar isoxazolidines did not.[5] Here we describe positional 'mutagenesis' experiments in which we evaluated analogs of **II-1** bearing identical side chains in various locations within the isoxazolidine scaffold.[6] The results reveal that the iTADs mimic the functional profile of natural TADs in that precise positioning of the amphipathic side chains is not a critical determinant for function. Further, we demonstrate that the function in a cell-free environment can be translated to cellular activity, yielding the first small molecule TADs with function in living cells.[7]

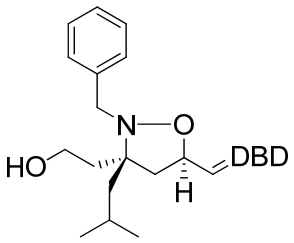

(±)-**II-1**

Figure II-1. Isoxazolidine TAD (iTAD) **II-1**.[5]

C. Design and Synthesis of Isomeric Isoxazolidines

To assess whether isoxazolidine TADs mimic the functional profile of natural TADs in that precise positioning of the amphipathic side chains is not a critical determinant for function,[1] we performed stereochemical and positional "mutagenesis" experiments in which stereochemical isomers of **II-1** and analogs bearing identical sidechains in various locations within the isoxazolidine scaffold were evaluated. In the original experiments, all isoxazolidines were prepared as racemates and were tested as stereoisomeric mixtures.[5] We thus targeted each enantiomer of the original isoxazolidine (**II-2** and **II-3**) as well as a diastereomer (**II-4**) and three positional isomers (**II-5**, **II-6**, and **II-7**) for this study (**Figure II-2**). The compounds contain the same functional groups found in the original active compound but in varying three-dimensional orientations.

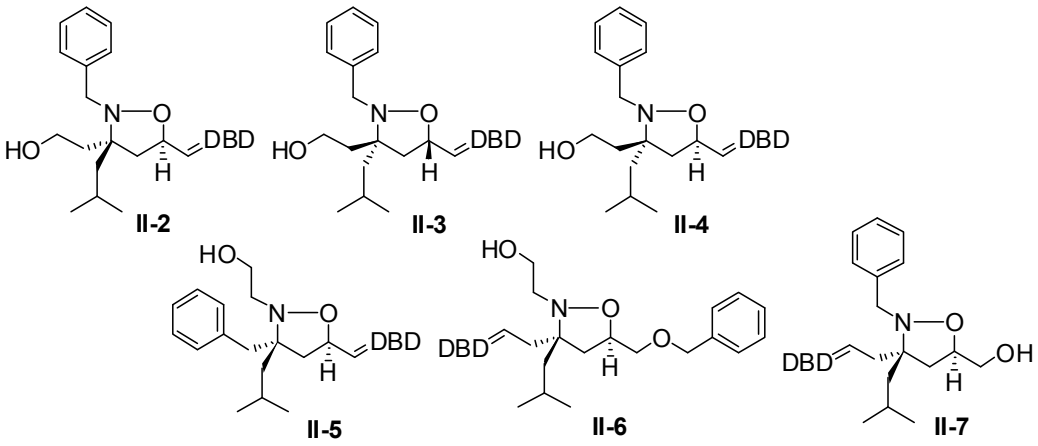

Figure II-2. Isomeric iTAD mimics. DBD = DNA Binding Domain.

The first step towards the target molecules was a 1,3-dipolar cycloaddition between a nitrile oxide generated from an oxime and an allylic alcohol to produce an isoxazoline.[8-10] The starting oxime **II-8** was generated in a single step from 3-methylbutyraldehyde[11, 12] and the starting allylic alcohol was generated as a single enantiomer in two steps from (*R*)-glycidol using established protocols.[13, 14] Towards isoxazoline **II-10**, oxime **II-8** was treated with *t*BuOCl to afford generation of the hydroximinoyl chloride. The hydroximinoyl chloride was then combined with the allylic

alcohol and the components underwent a 1,3-dipolar cycloaddition to give isoxazoline **II-10** in 88% yield as a single regioisomer and diastereomer, as determined by analysis of the crude material by ^{1}H NMR spectroscopy. Isoxazoline **II-10** is a common intermediate towards four of the target molecules, **II-2**, **II-4**, **II-5** and **II-6**. Towards three of these, nucleophilic addition to the C=N bond of isoxazoline **II-10** was afforded by treatment of **II-10** with the Grignard reagent allylmagnesium chloride in the presence of the strong Lewis acid, BF_3•OEt_2. This reaction yielded a 5:1 mixture of diastereomeric products **II-11** and **II-12** in a combined 71% yield. Analogous to previously reported isoxazolidines the major diastereomer obtained resulted from approach of the nucleophile to the face opposite the bulky C5 sidechain as confirmed by NOE analysis.[10] Isoxazolidine **II-11** is an intermediate towards **II-2** and **II-6** and the details of the synthesis of these two compounds is shown in Scheme II-2.

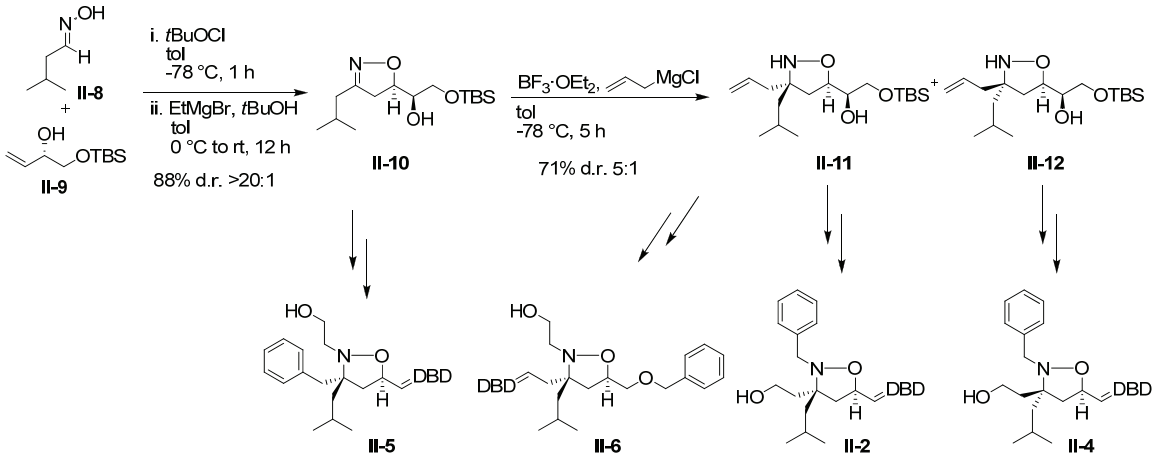

Scheme II-1. Synthetic strategy for the generation of isomeric iTAD mimics.

The first step in the functionalization of **II-11** towards **II-2** was alkylation of the isoxazolidine ring nitrogen with benzyl bromide. This reaction proceeded in 89% yield using microwave-accelerated conditions.[5] The conditions were utilized as the alkylation of the isoxazolidine ring nitrogen does not proceed or proceeds in only low yields under standard conditions. One concern was competitive alkylation of the secondary alcohol under these conditions, but it was not detected, although small quantities of material were obtained in which the silyl group had transferred to the secondary alcohol (≥5%). Following alkylation, the double bond moiety on C3 of isoxazolidine **II-13** was

oxidatively cleaved to yield the desired alcohol at that position. This functional group conversion was afforded by an initial dihydroxylation of the olefin by treatment with a catalytic amount of OsO_4 and a stoichiometric amount of the oxidant NMO. The crude diol was subsequently cleaved to the aldehyde by treatment with $NaIO_4$ and in the final step of the oxidative cleavage, the crude aldehyde was reduced to the desired primary alcohol by treatment with $NaBH_4$. The oxidative cleavage sequence proceeded in 81% yield to give isoxazolidine **II-14** that contains the three desired sidechains, benzyl, isobutyl, and hydroxyl. The functionality on C5 of **II-14** served as the point of attachment of the densely functionalized isoxazolidine to methotrexate, necessary as part of the DNA binding strategy.[15] Treatment of **II-14** with TBAF afforded deprotection of the C5 silyl ether to reveal a diol. Treatment of the diol with $NaIO_4$ yielded an aldehyde that was combined with methotrexate hydrazide to produce isoxazolidine conjugate **II-2** in which the isoxazolidine is tethered to methotrexate through a hydrazone linkage.

Also shown in Scheme II-2 is the generation of positional isomer **II-6** from isoxazolidine **II-11**. In that direction the C5 sidechain was manipulated first. The silyl ether protecting group was removed from **II-11** by treatment with TBAF. The resultant diol was cleaved to the aldehyde by treatment with $NaIO_4$ and the crude aldehyde was reduced to the primary alcohol by treatment with $NaBH_4$. The primary alcohol was then selectively alkylated with benzyl bromide over the secondary amine using non-microwave conditions. The reaction sequence from **II-11** to **II-15** proceeded in 55% yield. The ring nitrogen was then alkylated with methyl bromoacetate using microwave accelerated conditions and subsequently, the methyl ester was reduced to the primary alcohol by treatment with DIBAL to produce **II-16** in 72% yield. Isoxazolidine **II-16** was then tethered to methotrexate at the C3 olefin moiety. For this, the olefin was dihydroxylated and the resultant diol was cleaved to the aldehyde using the same reaction conditions described above. The aldehyde was then combined with methotrexate functionalized with a hydrazide to yield target **II-6**.

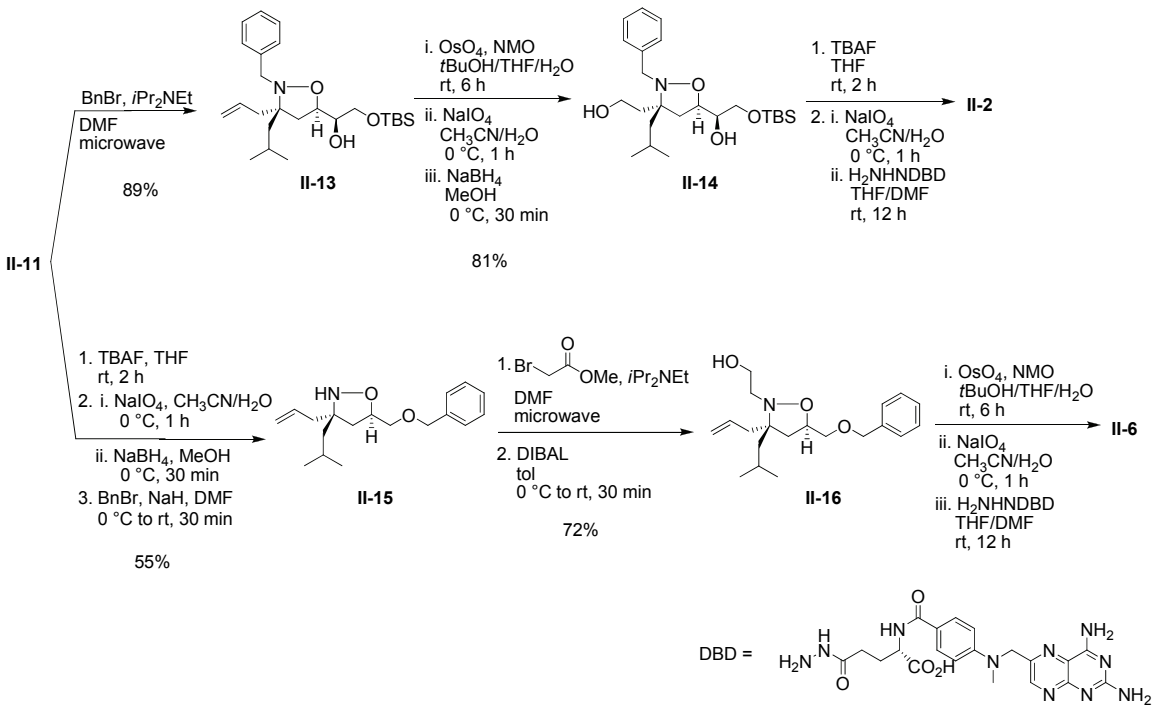

Scheme II-2. Synthesis of isoxazolidine targets **II-2** and **II-6**.

The preparation of isoxazolidine-DBD conjugate **II-5** from isoxazoline **II-10** is depicted in Scheme **II-3**. In that direction the secondary alcohol of isoxazoline **II-10** was protected as the silyl ether in 85% yield. Subsequently nucleophilic addition to the C=N bond was afforded by treatment with benzylmagnesium chloride in the presence of a strong Lewis acid to produce **II-18** in 80% yield as a single stereoisomer. Alkylation of the ring nitrogen with allylbromide using microwave accelerated conditions yielded **II-19** and the newly introduced double bond was oxidatively cleaved by dihydroxylation, cleavage to the aldehyde, and finally reduction to the primary alcohol. The silyl ethers were unmasked, the resultant diol was cleaved to the aldehyde and the aldehyde was condensed with methotrexate hydrazide to produce the final target **II-5**. Isoxazolidine-DBD conjugate **II-4** was prepared analogously to **II-2** from **II-12** and **II-3** was prepared analogously to **II-2** using the chiral allylic alcohol derived from (*S*)-glycidol in the cycloaddition. Each isoxazolidine-methotrexate conjugate was purified to homogeneity by reverse-phase HPLC prior to functional evaluation.

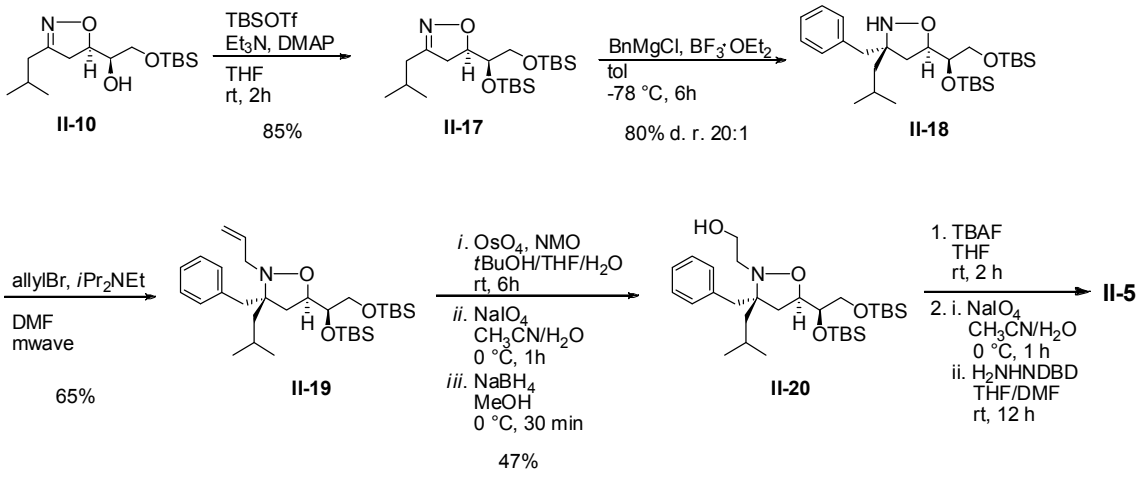

Scheme II-3. Synthesis of **II-5**.

D. In Vitro Assessment of iTAD Activity

My colleague Dr. Brian Brennan evaluated the function of isoxazolidines **II-2-II-7** in a standard two-hybrid in vitro transcription assay (**Figure II-3**). In this assay the fusion protein LexA-DHFR served as the DNA binding domain, localizing isoxazolidines to the promoter via the specific and high affinity interaction of methotrexate with DHFR.[15] The construct placed a reporter gene under control of two LexA binding sites 75 bp upstream of the start site. The assay employed HeLa nuclear extracts and methotrexate was utilized as the negative control with the natural activation domain ATF14 as the positive control.

Figure II-3. Two hybrid in-vitro transcription assay.

Figure II-4 shows the activation observed for each compound reported as percent activation relative to the positive control ATF14; for reference, the maximal activation in this assay corresponds to 5-7-fold above DNA binding domain alone.[6, 16] The first set of compounds that were evaluated for ability to activate transcription were **II-2** and **II-3**, each isoxazolidine enantiomer. The activity of the two compounds was indistinguishable

from that of iTAD **II-1** containing both enantiomers of the isoxazolidine ring. This parallels the functional behavior of the *d*- and *l*-peptide versions of ATF29.[17] Isoxazolidines **II-4**-**II-7** more significantly differ in the presentation of the amphipathic functional groups due to stereochemical or positional changes within the ring. Nonetheless, all functioned well as iTADs. Isoxazolidine **II-5** for example, swaps the positioning of the alcohol and benzyl moieties compared to the initial compound **II-1** and again the activity of the two molecules is indistinguishable. The isoxazolidine portion of **II-4** is a diastereomer of the original compound; similar activity was observed for the two compounds further supporting that the permissiveness of binding sites within the transcriptional machinery towards endogenous activators extends to iTADs. Isoxazolidine conjugates **II-6** and **II-7** differ from the others in that the isoxazolidine is attached to the DNA binding moiety at the C3 rather than C5 position. An approximate 40% attenuation in activity was observed for one of these compounds, **II-7**, while **II-6** exhibited activation levels essentially the same as the others tested. A significant difference between **II-7** and the other compounds tested is reduced projection of the benzyl moiety away from the DBD; if the benzyl functionality of iTADs makes particularly important binding interactions with at least of subset of iTAD co-activator targets the reduced availability of the benzyl group would impact function. This would be consistent with mutagenesis studies of natural activators that show the disruption of an interaction between a hydrophobic sidechain of a TAD and co-activator usually more significantly impacts activation levels compared to elimination of an interaction with a polar sidechain.[18]

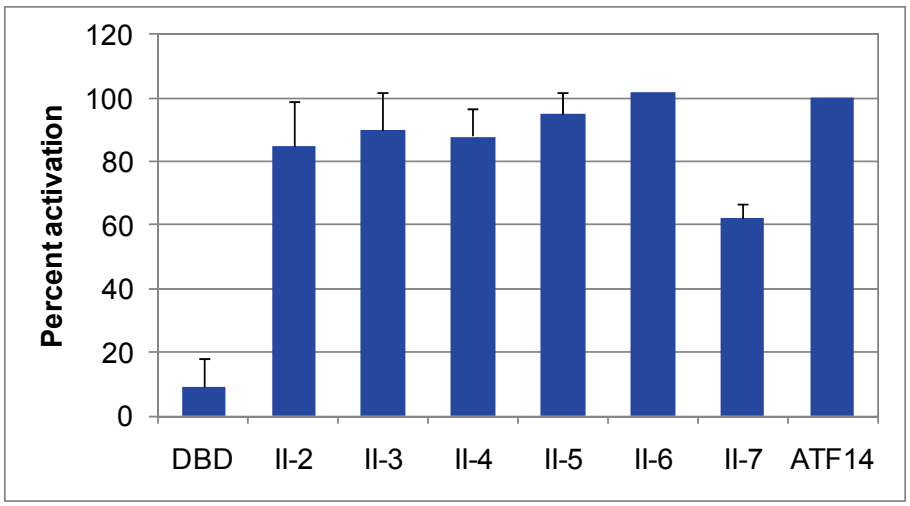

ATF14 = CGSDALDDFDLDML

Figure II-4. Results from in vitro transcription assays. The DBD is the fusion protein LexA-DHFR; the high affinity interaction between DHFR and methotrexate localizes the Mtx-tagged small molecules (50 nM) to DNA.[11] Each activity is the average of at least 3 independent experiments with the indicated error (SDOM). The maximal activation is 7-fold relative to background.

The conserved activity across amphipathic, isomeric isoxazolidines, including both enantiomers, parallels the functional behavior of endogenous amphipathic TADs that this molecular class was originally designed to mimic. These data support the original hypothesis that drove the design of the first iTAD (**II-1**): that precise positioning of functional groups is not necessary for function, but rather general mimics of endogenous TADs should be able to reconstitute their function. Thus, other conformationally constrained small molecule scaffolds containing an amphipathic mix of sidechains should also function as TADs.

E. Ability of iTADs to Function in Cells

We have shown that isoxazolidines reconstitute the function of endogenous TADs in cell-free systems. In the cell-free assay, however, cellular permeability, nuclear localization, and cellular stability are not assessed. In addition, there is a much more limited range of potential protein binding partners relative to the cellular environment. This latter issue is particularly important since natural and nonnatural TADs have been shown to exhibit promiscuous binding profiles, interacting with many different

hydrophobic surfaces.[1] A small molecule that can activate transcription in cells would be a significant step forward in the development of transcription-targeted therapeutics and thus we evaluated iTAD **II-21** as well as isoxazolidine **II-22** (Figure II-5), a molecule that does not activate transcription in the cell free system, to activate transcription in HeLa cells.[5] Isoxazolidines **II-21** and **II-22** differ only in the DBD portion compared to the molecules discussed above. The DBD localizing moiety is oxidized dexamethosone, OxDex, a steroid utilized to localize the molecules to DNA in a 2-hybrid system.

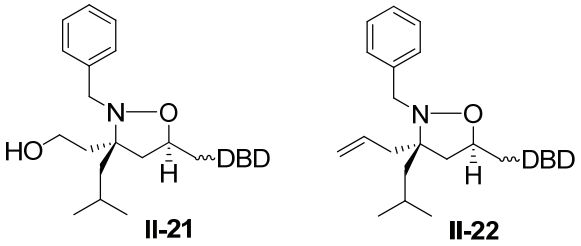

Figure II-5. Isoxazolidine targets for evaluating iTAD activity in cells.

1) Synthesis of Isoxazolidine-DBD Targets

The synthesis of **II-21** is shown in Scheme II-4. Isoxazolidine intermediate **II-23** was generated from **II-13** by a silyl deprotection, cleavage of the resultant diol to an aldehyde and reduction of the crude aldehyde to the primary alcohol.[5] Treatment of compound **II-23** with methane sulfonylchloride transformed the primary alcohol into the mesylate which was subsequently displaced by sodium azide. The two steps proceeded in high yield (89%). The C3 olefin moiety was then oxidatively cleaved to the primary alcohol using the reaction sequence described previously with product obtained in 76% yield. The appropriately functionalized isoxazolidine was then tethered to OxDex using the C5 functionality. The azide was reduced to an amine by treatment with PPh_3 and the crude amine was coupled to a short PEG linker using standard peptide coupling conditions. The other terminus of the linker contained an Fmoc protected amine that was unmasked by treatment with 20% piperidine in DMF. The OxDex moiety was then coupled to the linker through an amide bond linkage, again using standard amide bond formation conditions. The hydrophobic isoxazolidine-OxDex conjugate **II-22** was

synthesized by my colleague Ryan Casey and both molecules were purified by reverse phase HPLC prior to evaluation in cells.

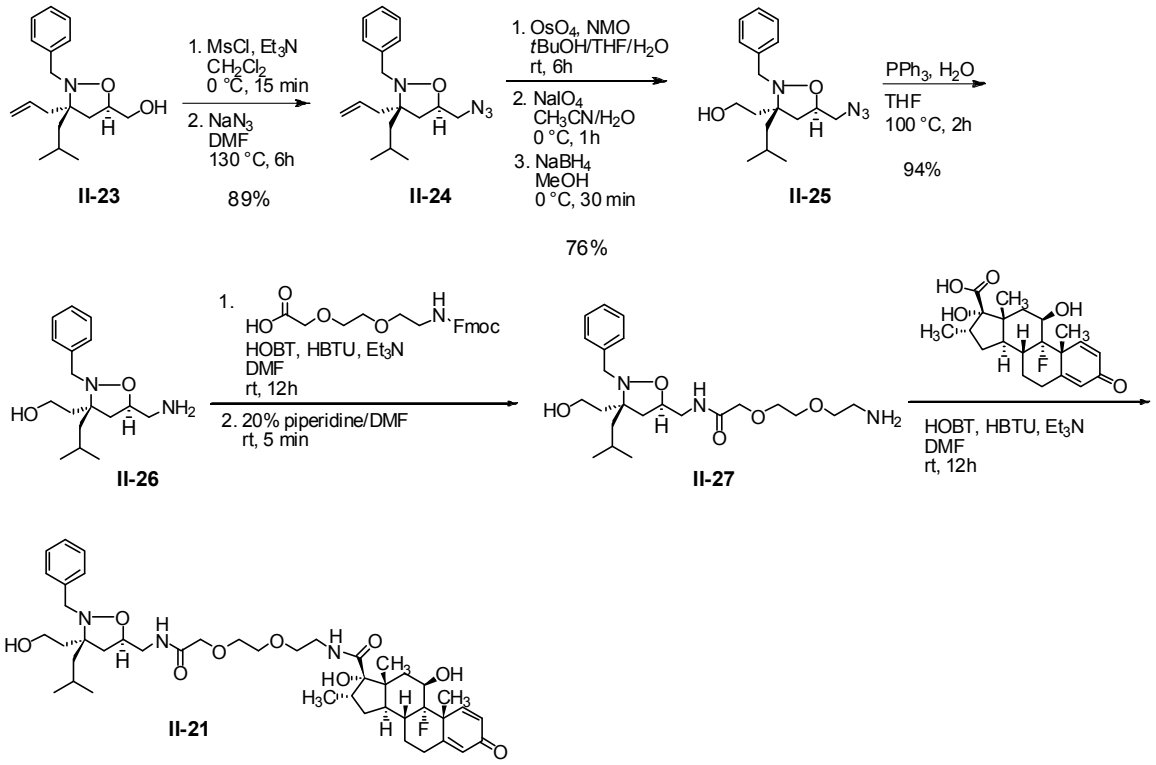

Scheme II-4. Synthesis of **II-21**.

2) Function of iTADs: Ability to Upregulate Transcription in a Cellular System

To test the small molecules in cells we used a system developed in the Kodadek lab in which a fusion protein consisting of a Gal4 DBD and the minimal ligand binding domain of the glucocorticoid receptor is constitutively expressed (**Figure II-6**).[19] The HeLa cells were transiently transfected with a plasmid containing five Gal4 binding sites located upstream of a firefly luciferase reporter gene. The isoxazolidines were attached to oxidized dexamethasone (OxDex), which binds the glucocorticoid ligand binding domain localizing the transcriptional activator to DNA. The assays evaluating the small molecules were carried out by Dr. Steve Rowe and Dr. Brian Brennan.

Figure II-6. 2-hybrid cell based transcription assay.

As illustrated in **Figure II-7**, amphipathic isoxazolidine **II-21** exhibited a remarkable 80-fold level of activation at 1 μM and was active even at low nanomolar concentrations (5 fold at 5 nM).[7] The EC_{50} of isoxazolidine **II-21** is 33 ± 6 nM. Analogous to the cell free results, hydrophobic isoxazolidine **II-22** did not activate over the concentration range investigated.

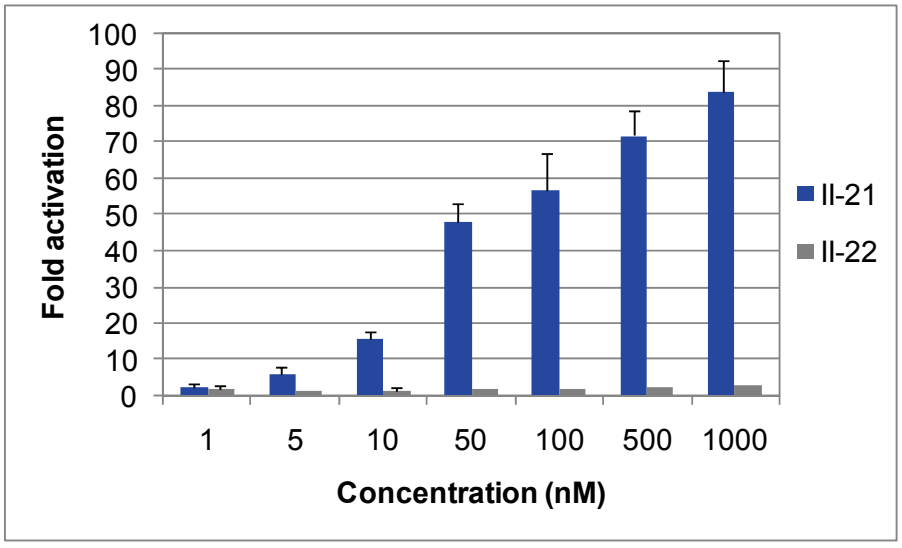

Figure II-7. iTAD function in cell culture.

This first reported small molecule TAD to function in cells was an important demonstration towards the long-term goal of developing transcription-targeted therapeutics. Prior to this example only one nonnatural TAD, peptoid **II-28** (Figure II-8), had been reported to activate transcription in cells and this molecule does not fit a drug-like profile.[19] It has a molecular weight of >1000 g/mol and a high EC_{50} value (10 μM). In contrast, iTAD **II-21** is low molecular weight (<300 g/mol) and is potent at low concentrations (EC_{50} = 33 nM).

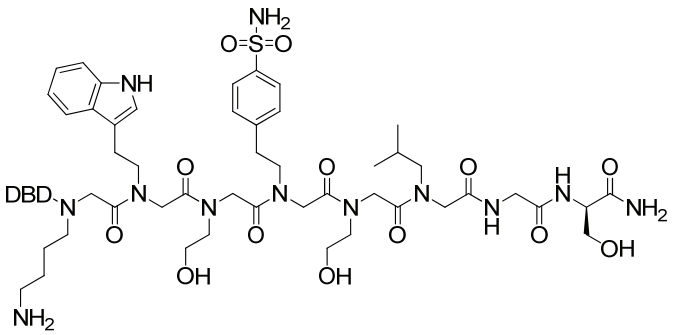

II-28

Figure II-8. Peptoid TAD.

3) Portability of iTADs

One characteristic of natural transcriptional activators is that the DBD and TAD function independently.[1] To evaluate if that holds true in the iTAD system, two key experiments were conducted. First, a competitive inhibition or 'squelching' experiment of the TAD was carried out. Increasing concentrations of isoxazolidine **II-25** (free TAD) was added to a constant concentration of isoxazolidine activator **II-21**. Depicted in Figure II-9 is that **II-21** showed a dose dependent decrease in activation with approximately 70% inhibition upon addition of 100 μM **II-25**.[7] This is consistent with the DBD being a functionality inert DNA localizing scaffold. In a second experiment, 'squelching' of DNA localization was performed (data not shown).[7] Increasing concentrations of an inactive transcriptional activator, **II-22**, were added to a constant concentration of isoxazolidine activator **II-21**. The inactive conjugate **II-22** occupied a portion of the OxDex binding sites resulting in a dose dependent reduction in transcription. It is important to note that the isoxazolidine portion alone of **II-22** does not squelch transcription by **II-21**. Together, these experiments suggested that the TAD is portable and should function when attached to alternative DNA localizing moieties. Thus we evaluated iTADs attached to a synthetic DBD resulting in the generation of the first entirely small molecule based transcriptional activator.

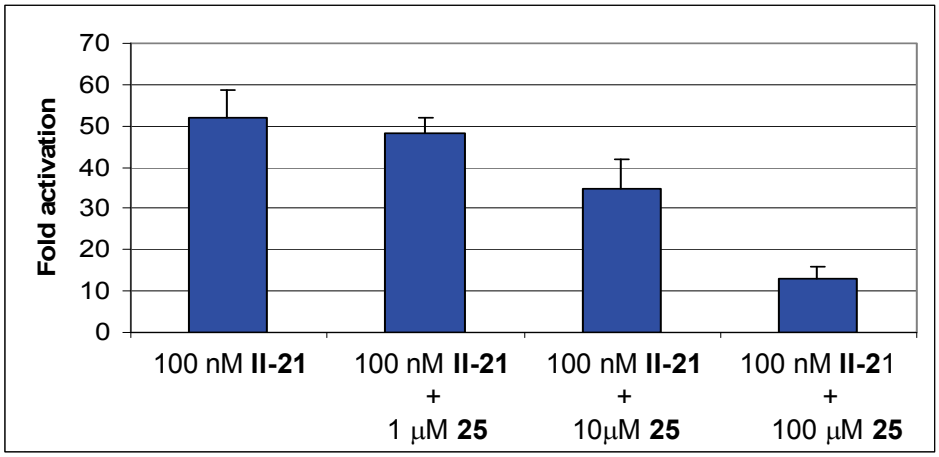

Figure II-9. 'Squelching' of **II-21**. The transcriptional function of **II-21** is inhibited by increasing concentrations of **II-25**. Experiment conducted by former colleague Dr. Brian Brennan.

F. An Entirely Synthetic Transcriptional Activator

The isoxazolidine-polyamide conjugate **II-29** shown in Figure II-10 was synthesized. This molecule consists of an amphipathic isoxazolidine with activation function in human HeLa cells and a polyamide that binds the sequence WGWWWW, where W = A or T. Dr. Brian Brennan constructed a reporter plasmid with the firefly luciferase gene under control of six sites containing the appropriate binding sequence. Compound **II-29** showed approximately 4 -old activation at a concentration of 3 μM. This was a very exciting initial result as it represents the first entirely non-biopolymer based transcriptional activator to upregulate gene expression in cells. The Dervan group had previously reported a small molecule-polyamide conjugate that activated in cell-free assays, but the molecule was not cell permeable.[20] In another related example the Kodadek lab prepared a peptoid-polyamide conjugate that activated 5 fold at 3 μM in cells.[21, 22] Similar to iTADs, this was a significant attenuation in activity compared to evaluations in a 2-hybrid assay. We are hopeful, however, that modifications to our construction of **II-29** that improve cellular uptake and reduce binding of cognate DNA sequences can result in a boost in activity. There have been reports in the literature since our evaluation of **II-29** that suggest modes for accomplishing this. Recently, Dervan and co-workers reported that introduction of an amino group to the diamino-butyric acid linking the two polyamide strands can increase affinity of the polyamide construct for

DNA 15 fold.[23] In another study, the group showed that modification of the linker region between the polyamide and TAD led to improved cellular uptake and nuclear localization of polyamides.[24] Currently, another graduate student, Ryan Casey is collaborating with Professor Peter Dervan's lab to obtain a polyamide-isoxazolidine conjugate with high specificity for endogenous binding sites.

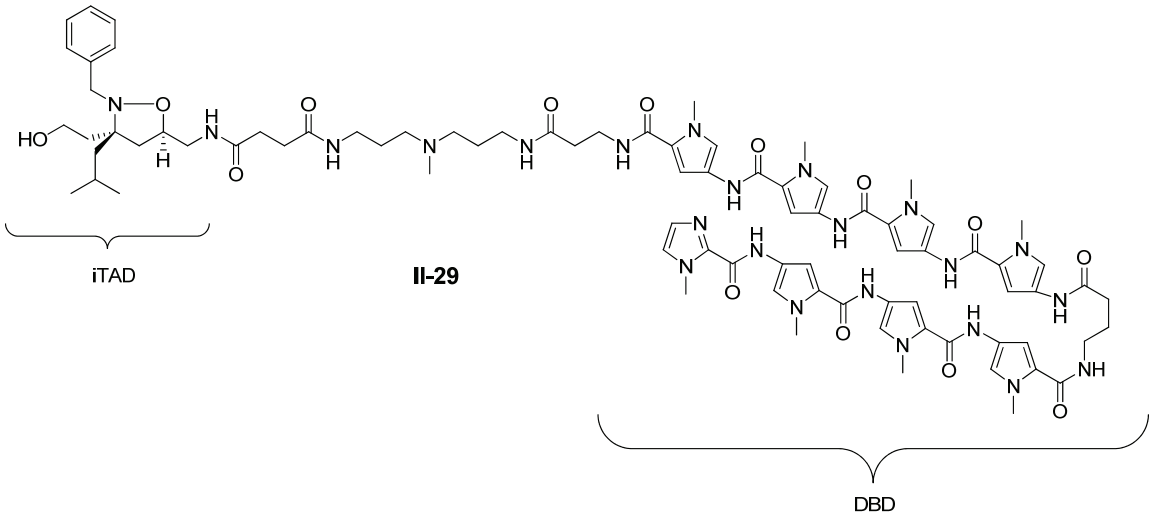

Figure II-10. An entirely small molecule based transcriptional activator.

G. Conclusions

A facile synthetic approach for generation of chiral isoxazolidines was utilized to enable the rapid generation of isomeric isoxazolidines for evaluation as TADs.[6] All stereochemical and positional isomers of the original iTAD, **II-1**, functioned well as TADs supporting that the molecule recognition profile of iTADs and the natural counterparts they were designed to mimic are similar. For both class of TADs precise positioning of the amphipathic sidechains is not a critical determinant of function. An implication of this data is that isoxazolidines are unlikely to be the only suitable scaffold for the construction of small molecule transcriptional activation domains. Rather, a variety of appropriately functionalized conformationally constrained small molecules should also function well, a prediction for which preliminary results obtained in lab suggest to be true. This strategy obviates the need to identify high affinity ligands for single protein targets and takes advantage of the remarkable functional flexibility of the endogenous transcriptional regulatory system.

iTAD **II-21** was the first small molecule to function as a TAD in cell culture. This molecule elicits a maximal activation of 80-fold and exhibits measurable activity even at low nanomolar concentrations in human HeLa cells.[7] Upon conjugation of the iTAD to a DNA binding hairpin polyamide cellular activation was retained, although attenuated, suggesting that entirely small molecule based transcriptional activators can be utilized to upregulate endogenous genes. In support of this a peptoid-polyamide conjugate activated the expression of 45 genes upon addition to HeLa cells.[21]

In sum, these experiments demonstrate that artificial transcriptional activators can be generated, using relatively simple criteria, that mimic the function and mode of action of endogenous transcriptional activators. Such molecules are important both as transcription-targeted therapeutics and as probes for deciphering mechanistic details of disease as altered transcription patterns are associated with nearly every disease state as either a cause or an effect.[1]

H. Experimental

General.

Unless otherwise noted, starting materials were obtained from commercial suppliers and used without further purification. CH_2Cl_2, THF, CH_3CN and toluene were dried by passage through activated alumina columns and degassed by stirring under a dry N_2 atmosphere.[25] BF_3•OEt_2 and Et_3N were distilled from CaH_2, MeOH was distilled from sodium metal, and *t*-BuOH was distilled from $MgSO_4$. All reactions involving air- or moisture-sensitive reagents were performed under a dry N_2 atmosphere. Purification by column chromatography was carried out with E. Merck Silica Gel 60 (230-400 mesh) according to the procedure of Still, Kahn, and Mitra.[26] ^1H and ^{13}C NMR spectra were recorded in $CDCl_3$ at 500 MHz and 125 MHz, respectively, unless otherwise specified. IR spectra were measured as thin films on NaCl plates. Reverse-phase HPLC purification was performed on a Varian ProStar 210 equipped with Rainin Dynamax UV-D II detector using a C18 (8 x 100 mm) Radial-PakTM cartridge using a gradient mixture of 20 mM NH_4OAc (pH = 6.9) and MeOH (λ = 254 nm) unless otherwise specified.[27] UV-vis spectra were measured in MeOH. In order to determine the concentration of all methotrexate conjugates (**II-2**-**II-7**), the characteristic UV-vis absorptions of

methotrexate at λ_{max} = 257, 302, and 370 nm with extinction coefficients of 23,000, 22,000, and 7,100 $M^{-1}cm^{-1}$, respectively, was used. Once the concentration was determined, the sample was aliquoted, lyophilized, and stored at –78 °C. The in vitro transcription assays were carried out as previously described. The buffer used for transcription assays contains 5 mM $MgCl_2$, 400 mM of each NTP, 10 μg of salmon sperm carrier DNA, 10 mM HEPES (pH 7.9), 50 mM KCl, 0.1 mM EDTA, 0.25 mM DTT, and 10% glycerol. Full fluorescence spectra were run on all methotrexate conjugates to insure no spectral overlap with the molecular beacon fluorophores. Compounds that do not appear in the text are numbered **S1**-**S9.**

3-Methylbutyraldehyde oxime (**II-8**) was prepared in accordance with standard protocols from 3-methyl-butyraldehyde.[11] Allylic alcohols **II-9** and *ent*-**II-9** were prepared in two steps from (*R*)-glycidol or (*S*)-glycidol, respectively.[13, 14] Methotrexate hydrazide was prepared according to literature procedures. Compound **II-7** was prepared as previously described.[4] Spectroscopic data on the purified products was consistent with reported values for those compounds.

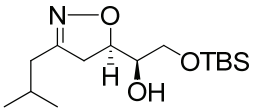

II-10

2-(*tert*-Butyl-dimethyl-silanyloxy)-(1*R*)-1-[(5*R*)-3-isobutyl-4,5-dihydro-isoxazol-5-yl]-ethanol (II-10): To a solution of oxime **II-8** (780 mg, 7.6 mmol, 1.0 eq) in toluene (38 mL), cooled in a dry ice-acetone bath was added *t*-BuOCl (0.90 mL, 7.6 mmol, 1.0 eq) over 20 min. The resulting mixture was stirred 2 h with continued cooling at which time TLC analysis indicated complete conversion to the hydroximinoyl chloride. In a separate flask, chiral allylic alcohol **II-9** (2.0 g, 9.9 mmol, 1.3 eq) was dissolved in toluene (99 mL) and cooled in an ice-H_2O bath. To this solution was added *t*-BuOH (25 mmol, 3.3 eq) followed by dropwise addition of EtMgBr (7.6 mL of a 2.0 M solution in Et_2O, 23 mmol, 3.0 eq) and the solution stirred 1 h with continued cooling. The solution of hydroximinoyl chloride was then transferred via canula to the allylic alcohol solution and the mixture allowed to slowly warm to ambient temperature and stirred for 15 h. Sat. aq. NH_4Cl (10 mL) was added to the reaction mixture followed by further dilution with H_2O. The organic and aqueous layers were separated and the aqueous extracted with CH_2Cl_2 (3

x 20 mL). The combined organic extracts were washed with brine (1 x 20 mL), dried over $MgSO_4$, filtered, and concentrated. Purification by flash chromatrography (1:1 hexanes/EtOAc) yielded 2.0 g of isoxazoline **II-10** as a clear solid in 88% yield as a single stereoisomer. IR: 3400, 2955, 2858, 1463, 1255 cm^{-1}; ^1H NMR: δ -5.26, (s, 6H), 0.90 (s, 9H), 0.96 (d, 3H, J = 6.6), 0.97 (d, 3H, J = 6.8), 1.90-1.93 (m, 1H), 2.23 (d, 2H, J = 7.3), 2.97 (d, 2H, J = 8.8), 3.58-3.62 (m, 1H), 3.65-3.73 (m, 2H), 4.62-4.67 (m, 1H); ^{13}C NMR (100 MHz): δ -5.26, 18.44, 22.54, 22.74, 26.04, 26.43, 36.66, 39.56, 64.19, 73.26, 79.22, 159.14; HRMS (ESI) calcd for $[C_{15}H_{31}NO_3Si + Na]^+$: 324.1971, found: 324.1985; $[\alpha]_D^{25}$ = -56.17 (*c* 0.84, $CHCl_3$).

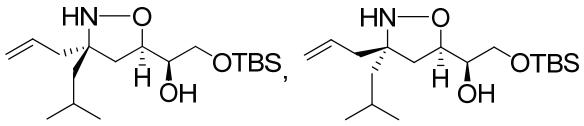

II-11 **II-12**

II-11 and **II-12**: To a solution of isoxazoline **II-10** (1.5 g, 5.0 mmol, 1.0 eq) in 50 mL toluene cooled in a dry ice-acetone bath was added distilled $BF_3 \bullet OEt_2$ (1.9 mL, 15 mmol, 3.0 eq) and the resultant mixture was stirred with continued cooling for 30 min. Allylmagnesium chloride (15 mL of a 2.0 M solution in THF, 30 mmol, 6.0 eq) was added dropwise over 10 min. The reaction mixture was allowed to stir with continued cooling until the reaction was complete by TLC analysis (6 h). H_2O (5 mL) was added and the mixture stirred for 20 min. H_2O (20 mL) was added and the aqueous and organic layers were separated. The aqueous layer was extracted with EtOAc (3 x 20 mL) and the combined organic extracts were washed with H_2O (1 x 20 mL) and brine (1 x 20 mL), dried over $MgSO_4$, filtered and concentrated *in vacuo*. A diastereomeric ratio of 5:1 was determined by crude ^1H NMR. The major diastereomer (**II-11**) (1.0 g) and the minor diastereomer (**II-12**) (200 mg) were each isolated (both as colorless oils) following purification by flash chromatography (1:4 hexanes/EtOAc). The combined yield of diastereomers was 71%.

(1*R*)-1-[(3*S*, 5*R*)-3-Allyl-3-isobutyl-isoxazolidin-5-yl]-2-(*tert*-butyl-dimethyl-silanyloxy)-ethanol (II-11): IR: 3362, 2917, 2849, 1812, 1700, 1076 cm^{-1}; ^1H NMR: δ 0.050 (s, 3H), 0.054 (s, 3H) 0.88 (s, 9H), 0.92 (d, 3H, J = 2.9), 0.93 (d, 3H, J = 2.9), 1.40 (dd, 1H, J = 6.8, 14.2), 1.46 (dd, 1H, J = 6.3, 14.2), 1.77-1.86 (m, 1H), 1.93 (dd, 1H, J = 6.8, 12.2), 2.19 (dd, 2H, J = 7.8, 14.2), 2.33 (dd, 1H, J = 6.8, 14.2), 2.51 (bs, 1H), 3.57-

3.63 (m, 2H), 3.66-3.72 (m, 1H), 4.02 (bs, 1H), 5.06-5.12 (m, 2H), 5.34 (bs, 1H), 5.80-5.88 (m, 1H); ^{13}C NMR (100 MHz): δ -5.52, -5.51, 18.12, 23.91, 24.18, 25.76, 39.98, 40.24, 42.63, 64.25, 64.66, 67.06, 74.13, 117.4, 134.5; HRMS (ESI) calcd for $[C_{18}H_{37}NO_3Si + Na]^+$: 366.2440, found: 366.2435; $[\alpha]_D^{24}$ = -22.03 (*c* 0.81, $CHCl_3$).

(1*R*)-1-[(3*S*, 5*R*)-3-Allyl-3-isobutyl-isoxazolidin-5-yl]-2-(*tert*-butyl-dimethyl-silanyloxy)-ethanol (II-12): IR: 3400, 2929, 147, 1253, 1113, 836 cm^{-1}; ^{1}H NMR (400 MHz): δ 0.05 (s, 6H), 0.88 (s, 9H), 0.93 (d, 3H, J = 6.8), 0.96 (d, 3H, J = 6.4), 1.39 (dd, 1H, J = 5.9, 14.2), 1.47 (dd, 1H, J = 6.1, 14.4), 1.76-1.84 (m, 1H), 1.99-2.07 (m, 2H), 2.24 (dd, 1H, J = 7.8, 14.2), 2.44 (dd, 1H, J = 6.8, 14.2), 2.49 (bs, 1H), 3.60-3.69 (m, 3H), 4.02-4.06 (m, 1H), 5.10-5.13 (m, 2H), 5.78-5.87 (m, 1H); ^{13}C NMR (100 MHz): δ -5.43, 18.24, 24.33, 24.40, 25.85, 39.20, 40.22, 41.89, 44.49, 63.94, 64.61, 73.40, 118.8, 133.6; HRMS (ESI) calcd for $[C_{18}H_{37}NO_3Si + Na]^+$: 366.2440, found: 366.2446.

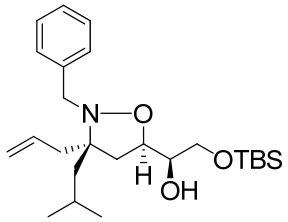

II-13

(1*R*)-[(3*S*, 5*R*)-3-Allyl-2-benzyl-3-isobutyl-isoxazolidin-5-yl]-2-(*tert*-butyl-dimethyl-silanyloxy)-ethanol (II-13): To a solution of isoxazolidine **II-11** (210 mg, 0.61 mmol, 1.0 eq) in DMF (3.0 mL) was added *i*Pr$_2$NEt (0.31 mL, 1.8 mmol, 3.0 eq) and BnBr (0.48 mL, 3.7 mmol, 6.0 eq). The reaction mixture was irradiated in a 1000 W microwave (6 x 20 s) @ 20% power with mixing between each interval. Upon cooling to ambient temperature the solution was diluted with H_2O (3 mL) and extracted with Et_2O (3 x 5 mL). The combined organic extracts were washed with H_2O (1 x 5 mL) and brine (1 x 5 mL), dried over Na_2SO_4, filtered, and concentrated *in vacuo*. Purification of the crude mixture by flash chromatography (95:5 hexanes/EtOAc) yielded 200 mg of **II-13** in 77% yield as a clear oil. IR: 3326, 2917, 1803, 1720, 1457, 1081 cm^{-1}; ^{1}H NMR: δ -0.01 (s, 3H), -0.02 (s, 3H), 0.85 (s, 9H), 0.96 (d, 3H, J = 2.9), 0.98 (d, 3H, J = 2.9), 1.39 (dd, 1H, J = 7.3, 14.6), 1.63 (dd, 1H, J = 4.6, 14.4), 1.87-1.95 (m, 1H), 2.26 (m, 2H), 2.32 (dd, 1H, 8.8, 12.2), 2.44 (dd, 1H, J = 7.1, 13.9), 3.13 (bs, 1H), 3.41 (dd, 1H, J = 6.3, 8.8), 3.46-3.53 (m, 2H), 3.80 (d, 1H, J = 14.2), 3.85 (d, 1H, J = 14.2), 4.03-4.06 (m, 1H), 5.09-5.12

(m, 2H), 5.91-5.99 (m, 1H), 7.21-7.24 (m, 1H), 7.28-7.34 (m, 4H); ^{13}C NMR (100 MHz): δ -5.42, 18.31, 24.10, 24.33, 25.33, 25.91, 38.53, 39.56, 44.08, 53.67, 64.34, 68.62, 74.92, 117.62, 126.93, 128.27, 128.28, 135.19, 138.61; HRMS (ESI) calcd for $[C_{25}H_{43}NO_3Si]^+$: 434.3090, found: 434.3089; $[\alpha]_D^{24}$ = -15.61 (*c* 1.95, $CHCl_3$).

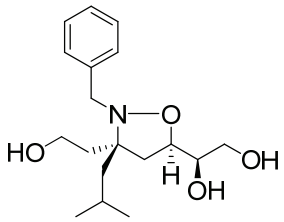

II-S1

(1*R*)-1-[(3*S*, 5*R*)-2-Benzyl-3-(2-hydroxy-ethyl)-3-isobutyl-isoxazolidin-5-yl]-ethane-1,2-diol (II-S1): To a solution of isoxazolidine **II-13** (0.15 g, 0.34 mmol, 1.0 eq) in *t*-BuOH (2.5 mL), THF (0.67 mL), and H_2O (0.17 mL) was added NMO (47 mg, 0.40 mmol, 1.2 eq) followed by OsO_4 (0.34 ml of a 2.5 wt% solution in *t*-BuOH, 0.03 mmol, 0.10 eq). The reaction mixture was stirred at ambient temperature until complete by TLC analysis (5 h). The mixture was cooled in an ice-H_2O bath, Na_2SO_3 (20 mg) was added, and the mixture stirred 1 h. The mixture was diluted with H_2O (10 mL) and extracted with EtOAc (3 x 10 mL). The combined organic extracts were dried over Na_2SO_4, filtered and concentrated *in vacuo*. The crude diol was taken up in 1.9 mL CH_3CN and 1.9 mL H_2O and cooled in an ice-H_2O bath. Sodium periodate (0.10 g, .45 mmol, 1.2 eq) was added and the reaction mixture stirred at ambient temperature until complete by TLC analysis (2 h). The reaction mixture was diluted with H_2O (10 mL) and extracted with Et_2O (3 x 10 mL). The combined organic extracts were washed with H_2O (1 x 10 mL) and brine (1 x 10 mL), dried over Na_2SO_4, filtered and concentrated *in vacuo*. The crude aldehyde thus obtained was dissolved in 3.7 mL MeOH and cooled in an ice-H_2O bath prior to addition of $NaBH_4$ (21 mg, 0.56 mmol, 1.5 eq). Upon completion as noted by TLC analysis (1h), H_2O (5 mL) was added and the reaction extracted with EtOAc (3 x 10 mL). The combined organic extracts were dried over Na_2SO_4, filtered and concentrated *in vacuo*. The crude material was passed through a plug of SiO_2 to remove baseline impurities (7:3 hexanes/EtOAc). To a portion of the product (0.20 mmol, 1.0 eq) in THF (1.0 mL) cooled in an ice-H_2O bath was added TBAF (0.41 mL of a 1 M solution in THF, 0.41 mmol, 2.0 eq). The reaction mixture was allowed to stir at ambient temperature

until complete by TLC analysis (2 h). The mixture was then diluted with H_2O (10 mL) and extracted with EtOAc (5 x 15 mL). The combined organic extracts were dried over Na_2SO_4, filtered, and concentrated *in vacuo*. Purification by flash chromatography (93:7 CH_2Cl_2: MeOH) provided 83 mg of **II-S1** in 59% yield from compound **II-13** as a colorless oil. IR: 3349, 2952, 1453, 1063 cm^{-1}; ^1H NMR (400 MHz): δ 0.99 (d, 3H, J = 6.6), 1.01 (d, 3H, J = 6.6), 1.44 (dd, 1H, J = 8.1, 13.9), 1.71-1.82 (m, 2H), 1.83-2.00 (m, 2H), 2.22-2.34 (m, 2H), 3.50-3.61 (m, 3H), 3.77-3.85 (m, 3H), 4.01 (d, 1H, J – 13.6), 4.10-4.19 (m, 1H), 7.11-7.38 (m, 5H); ^{13}C NMR (100 MHz): δ 23.55, 24.77, 25.16, 35.30, 39.93, 42.82, 54.79, 59.61, 63.98, 64.94, 70.45, 73.53, 127.31, 128.44, 128.56, 137.63; HRMS (ESI) calcd for $[C_{18}H_{29}NO_4 + Na]^+$: 346.1994, found: 346.1993; $[\alpha]_D^{27}$ = + 0.09 (*c* 0.29, $CHCl_3$).

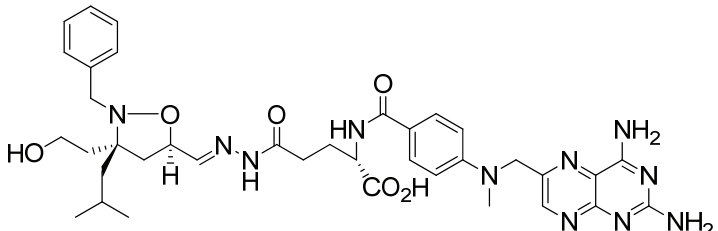

II-2

4-[(3*S*, 5*R*)-2-Benxyl-3-(2-hydroxy-ethyl)-3-isobutyl-isoxazolidin-5-ylmethylene-hydrazinocarbonyl]-2-{4-[(2,4-diamino-pteridin-6-ylmethyl)-methyl-amino]-benzoylamino}-(*S*)-butyric acid (II-2): To a solution of diol **II-S1** (9.7 mg, 0.03 mmol, 1.0 eq) in CH_3CN (0.15 mL) and H_2O (0.15 mL) cooled in an ice-H_2O bath was added $NaIO_4$ (5.3 mg, 0.02, 0.80 eq). The solution was slowly warmed to ambient temperature and the formation of aldehyde was monitored by TLC analysis. After 2 h the mixture was diluted with H_2O (2 mL), extracted with Et_2O (3 x 3 mL), and the combined organic extracts washed with brine (2 x 2 mL), dried over Na_2SO_4, filtered, and concentrated *in vacuo*. The crude aldehyde (0.003 mmol, 1.0 eq) in THF (0.16 mL) was added to methotrexate hydrazide (0.003 mmol, 1.0 eq) in DMF (0.16 mL). The reaction was stirred at ambient temperature, shielded from light for 24 h. The mixture was then concentrated to half-volume under high pressure (0.05 mm Hg) and purified by reverse-phase HPLC. Following purification by reverse-phase HPLC, the compound was stored at –78 °C, shielded from light. The purity of **II-2** was confirmed by analytical reverse-phase HPLC immediately after isolation and again prior to use in any *in vitro*

transcription assays. The identity was verified by mass spectral and UV analysis of the isolated conjugate. UV (λ_{max} nm): 257, 297, 373; HRMS (ESI) calcd for $[C_{37}H_{47}N_{11}O_6 + Na]^+$: 764.3608, found: 764.3605.

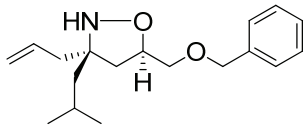

II-15

(3*S*,5*R*)-3-allyl-5-(benzyloxymethyl)-3-isobutylisoxazolidine (II-15): The silyl ether deprotection, cleavage of the diol to the aldehyde and reduction to the primary alcohol was carried out analogously to the C5 diol of **II-11**. To a stirring solution of that intermediate (200 mg, 1.0 mmol, 1.0 eq) in THF (10 mL) cooled in an ice-H_2O bath was added NaH (80 mg of a 60% dispersion in mineral oil, 2.0 mmol, 2.0 eq). The resulting mixture was stirred for 20 minutes at which point BnBr (130 µl, 1.0 mmol, 1.0 eq) was added dropwise and the solution was allowed to slowly warm to rt. TLC analysis indicated completion of the reaction after 12 hours and the mixture was cooled in an ice-H_2O bath and excess reagent was quenched with NH_4Cl (5 mL). Upon warming to rt, the solution was further diluted with H_2O (10 mL) and extracted with EtOAc (3 x 10 mL). The combined organic extracts were washed with brine (1 x 10 mL), dried over Na_2SO_4, filtered, and concentrated in vacuo. Purification by flash chromatography (90:10 hexanes/EtOAc) yielded 180 mg of product as a colorless oil in 64% yield. ^{1}H NMR: δ 0.88 (d, 3H, J = 6.3), 0.90 (d, 3H, J = 6.8), 1.38 (dd, 1H, J = 6.3, 14.2), 1.43 (dd, 1H, J = 6.3, 14.2), 1.73-1.83 (m, 2H), 2.18-2.25 (m, 2H), 2.35 (dd, 1H, J = 6.8, 14.2), 3.49 (dd, 1H, J = 4.4, 10.2), 3.62, (dd, 1H, J = 3.4, 10.2), 4.27 (bs, 1H), 4.51-4.58 (m, 2H), 5.07-5.13 (m, 2H), 5.80-5.88 (m, 1H), 7.25-7.36 (m, 5H).

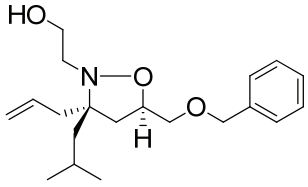

II-16

2-((3*S*,5*R*)-3-allyl-5-(benzyloxymethyl)-3-isobutylisoxazolidin-2-yl)ethanol (II-16): To a solution of **II-15** (180 mg, 0.62 mmol, 1.0 eq) in DMF (3.1 mL) was added methyl bromoacetate (470 µl, 5.0 mmol, 8.0 eq) and *i*Pr_2NEt (330 µl, 1.9 mmol, 3.0 eq). The

mixture was irradiated in a 1000W microwave for 20 sec at 10% power, cooled to rt, and the irradiation repeated. After 10 rounds TLC analysis indicated completion of the reaction. Following cooling to rt the mixture was diluted with H_2O (5 mL) and extracted with Et_2O (3 x 5 mL). The combined organic extracts were washed with H_2O (2 x 5 mL) and brine (1 x 5 mL), dried over Na_2SO_4, filtered, and concentrated in vacuo. The product was passed through a short plug of silica gel (80:20 hexanes/EtOAc) and utilized in the subsequent reduction of the methyl ester to the primary alcohol. To a solution of DIBAL (340 µl of a 1.5 M solution in tol, 0.51 mmol, 2.1 eq) in tol (170 µl) cooled in an ice-H_2O bath was added the methyl ester (90 mg, 0.25 mmol, 1.0 eq) and the solution was stirred for 30 min at which point TLC analysis indicated complete consumption of starting material. MeOH (350 µl) followed by 750 µl 1N HCl was added to the reaction mixture and the precipitate was immediately filtered away. The filtrate was diluted with H2O (5 mL) and extracted with EtOAc (3 x 5 mL). The combined organic extracts were washed with brine (1 x 10 mL), dried over Na_2SO_4, filtered, and concentrated in vacuo. Purification by flash chromatography (80:20 hexanes/EtOAc) yielded 67 mg of a colorless oil in 80% yield. ^{1}H NMR: δ 0.92 ("apparent triplet," 6H, J = 6.6), 1.31 (dd, 1H, J = 6.6, 13.6), 1.54 (dd, 1H, J = 5.5, 14.5), 1.75-1.81 (m, 1H), 1.88 (bs, 1H), 2.24-2.37 (m, 2H), 2.87 (bs, 1H), 3.47-3.50 (m, 2H), 3.55 (d, 1H, J = 6.6), 3.58 (d, 1H, J = 6.6), 3.67-3.74 (m, 2H), 4.23 (bs, 1H), 4.56 (s, 2H), 5.07-5.12 (m, 2H), 5.84-5.95 (m, 1H), 7.27-7.35 (m, 5H).

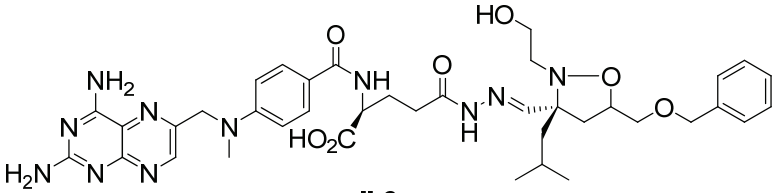

II-6

(2*S*)-5-((*E*)-2-(((3*R*)-5-(benzyloxymethyl)-2-(2-hydroxyethyl)-3-isobutylisoxazolidin-3-yl)methylene)hydrazinyl)-2-(4-(((2,4-diaminopteridin-6-yl)methyl)(methyl)amino)benzamido)-5-oxopentanoic acid (II-6): Following dihydroxylation of the C3 olefin of III-X, the preparation, purification, storage, and purity occurred analogously to **3**. The identity was verified by mass spectral and UV analysis of the isolated conjugate. UV (λ_{max} nm): 258, 291, 370.

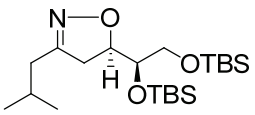

II-17

2-(*tert*-Butyl-dimethyl-silanyloxy)-(1*R*)-1-[(5*R*)-(3-isobutyl-4,5-dihydro-isoxazol-5-yl)-ethanol] (II-17): To a solution of isoxazoline **II-10** (360 mg, 1.3 mmol, 1.0 eq) in THF (6.5 mL) cooled in an ice-H_2O bath was added DMAP (16 mg, 0.13 mmol, 0.l0 eq) and Et_3N (0.35 mL, 2.9 mmol, 2.2 eq). TBSOTf (0.67 mL, 2.9 mmol, 2.2 eq) was then added dropwise and the solution slowly warmed to ambient temperature. The reaction was complete in 2 h as indicated by TLC analysis. The mixture was again cooled in an ice-H_2O bath, diluted with sat. NH_4Cl (3 mL), and extracted with Et_2O (3 x 5 mL). The combined organic extracts were washed with brine (1 x 10 mL), dried over Na_2SO_4, filtered, and concentrated *in vacuo*. Purification of the crude product by flash chromatography (95:5 hexanes/EtOAc) yielded 460 mg of isoxazoline **II-17** in 85% yield as a clear oil. IR: 3400, 2955, 2858, 1594, 1463, 1255, 1124 cm^{-1}; ^1H NMR: δ 0.01 (s, 3H), 0.02 (s, 3H), 0.04 (s, 3H), 0.05 (s, 3H), 0.83 (s, 9H), 0.84 (s, 9H), 0.90 (d, 3H, J = 6.6), 0.91 (d, 3H, J = 6.6), 1.84-1.87 (m, 1H), 2.13-2.16 (m, 2H), 2.81-2.84 (m, 2H), 3.53-3.56 (m, 1H), 3.61-3.66 (m, 2H), 4.52-4.58 (m, 1H); ^{13}C (100 MHz): δ -5.27, -4.54, -4.20, 18.31, 18.50, 22.64, 22.80, 25.99, 26.11, 26.26, 36.90, 38.78, 64.61, 74.30, 80.52, 158.12; HRMS (ESI) calcd for $[C_{21}H_{45}NO_3Si_2 + Na]^+$: 438.2836, found: 438.2839; $[\alpha]_D^{25}$ = -62.28 (*c* 0.50, $CHCl_3$).

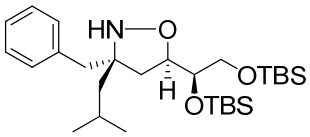

II-18

(3*S*, 5*R*)-3-Benzyl-5-[(1*R*)-1,2-bis-(tert-butyl-dimethyl-silanyloxy)-ethyl]-3-isobutyl-isoxazolidine (II-18): Benzylmagnesium chloride (4.5 mL of a 2.0 M solution in THF, 9.0 mmol, 10 eq) was added to 370 mg of isoxazoline **II-17** (9.0 mmol, 1.0 eq) in 8.9 ml THF in the presence of $BF_3 \bullet OEt_2$ (0.34 mL, 2.7 mmol, 3.0 eq) by using a procedure analogous to that used for the preparation of **II-11**. A diastereomeric ratio of 10:1 was determined by crude ^1H NMR. Purification by flash chromatography (9:1 hexanes/EtOAc) yielded 320 mg of the major diastereomer in 80% yield as a colorless

oil. IR: 2954, 2929, 2858, 1472, 1255 cm^{-1}; ^1H NMR: δ 0.03 (s, 3H), 0.03 (s, 3H), 0.05 (s, 3H), 0.06 (s, 3H), 0.85 (s, 9H), 0.87 (s, 9H), 0.91 (d, 3H, J = 6.6), 0.96 (d, 3H, J = 6.6), 1.26 (m, 2H), 1.79-1.84 (m, 1H), 2.02 (m, 1H), 2.18-2.23 (m, 1H), 2.66 (d, 1H, J = 13.9), 2.92 (d, 1H, J = 13.5), 3.53-3.59 (m, 2H), 3.72 (bs, 1H), 4.30 (bs, 1H), 5.20 (bs, 1H), 7.14-7.19 (m, 1H), 7.22-7.24 (m, 4H); ^{13}C NMR: δ -5.17, -4.29, -4.12, 18.18, 18.57, 24.18, 24.62, 24.85, 25.18, 26.13, 40.69, 42.27, 42.98, 64.61, 68.79, 72.31, 78.96, 126.300, 128.04, 130.91, 138.69; HRMS (ESI) calcd for $[C_{28}H_{53}NO_3Si_2 + Na]^+$: 530.3462, found: 530.3464; $[\alpha]_D^{25}$ = -64.98 (*c* 0.26, MeOH).

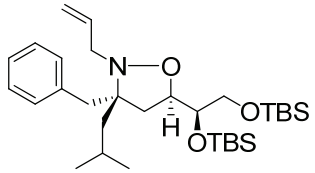

II-19

(5*R*, 3*S*)-2-Allyl-3-benzyl-5-[(1*R*)-1,2-bis-(*tert*-butyl-dimethyl-silanyloxy)-ethyl]-3-isobutyl-isoxazolidine (II-19): To a solution of 150 mg of isoxazolidine **II-18** (0.29 mmol, 1.0 eq) in DMF (1.4 mL) was added *i*Pr_2NEt (110 mg, 0.86 mmol, 3.0 eq) and allylBr (0.20 mL, 2.3 mmol, 8.0 eq). The reaction mixture was irradiated in a 1000 W microwave (6 x 20 s) @ 20 % power with mixing between each interval. A second portion of allylBr was added (.20 mL, 2.3 mmol, 8.0 eq) and the mixture was irradiated in a 1000 W microwave (6 x 20 s) @ 20 % power with mixing between each interval. The solution was diluted with H_2O (3 mL) and extracted with Et_2O (3 x 5 mL). The combined organic extracts were washed with H_2O (1 x 5 mL) and brine (1 x 5 mL), dried over Na_2SO_4, filtered, and concentrated *in vacuo*. Product was isolated as a colorless oil in 65% yield (100 mg) following purification by flash chromatography (97:3 hexanes/EtOAc). IR: 3349, 2929, 1761, 1456, 1255, 1081 cm^{-1}; ^1H NMR (400 MHz): δ 0.01 (s, 3H), 0.02 (s, 3H), 0.07 (s, 6H), 0.84 (d, 3H, J = 7.3), 0.86 (s, 9H), 0.87 (s, 9H), 0.94 (d, 3H, J = 6.6), 1.21-1.26 (m, 2H), 1.47-1.52 (m, 1H), 1.77-1.86 (m, 1H), 1.90-2.02 (m, 2H), 2.66 (d, 1H, J = 12.5), 2.86 (d, 1H, J = 13.2), 3.27 (dd, 1H, J = 6.6, 13.9), 3.37 (dd, 1H, J = 5.9, 13.9), 3.54 (dd, 1H, J = 6.6, 11.7), 3.66-3.70 (m, 2H), 4.09 (dt, 1H, J = 5.1, 8.1), 5.06 (dd, 1H, J = 1.5, 10.3), 5.19 (dd, 1H, J = 1.5, 16.8), 5.89-5.99 (m, 1H), 7.17-7.26 (m, 5H); ^{13}C (100 MHz): δ -5.40, -4.58, -4.48, 18.25, 18.36, 23.79, 24.52, 25.27, 25.97, 36.87, 39.57, 42.11, 52.90, 65.39, 69.24, 75.26, 116.03, 125.99, 127.89,

130.76, 136.22, 138.81; HRMS (ESI) calcd for $[C_{31}H_{57}NO_3Si]^+$: 548.3955, found: 548.3953; $[\alpha]_D^{25}$ = -33.17 (*c* 1.19, MeOH).

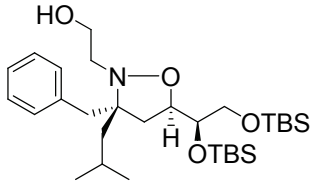

II-20

2-{(3*S*, 5*R*)-3-Benzyl-5-[(1*R*)-1,2-bis-(*tert*-butyl-dimethyl-silanyloxy)-ethyl]-3-isobuty-isoxazolidin-2-yl}-ethanol (II-20): Oxidative cleavage of the allyl group on **II-19** to form isoxazolidine **II-20** was carried out using a procedure analogous to that used for the preparation of **II-14** starting with 95 mg of **II-19** (0.17 mmol) except that the product was purified and isolated prior to silyl deprotection. Purification by flash chromatography yielded 45 mg of **II-20** in 47% yield as a colorless oil. IR: 3369, 2849, 1772, 1472, 1258, 1078 cm^{-1}; ^1H NMR (400 MHz): δ 0.02 (s, 3H), 0.04 (s, 3H), 0.07 (s, 6H), 0.86-0.88 (m, 21H), 0.93 (d, 3H, J = 6.6), 1.21 (dd, 1H, J = 5.9, 13.9), 1.48 (dd, 1H, J = 3.7, 13.9), 1.80-1.89 (m, 1H), 1.97 (dd, 1H, J = 8.8, 12.5), 2.05 (dd, 1H, J = 7.7, 12.1), 2.68 (d, 1H, J = 13.2), 2.74 (t, 1H, J = 5.86), 2.78-2.92 (m, 2H), 3.55 (dd, 1H, J = 7.3, 11.7), 3.62 (dd, 2H, J = 5.1, 11.7), 3.74 (m, 2H), 4.12-4.19 (m, 1H), 7.16-7.27 (m, 5H); ^{13}C NMR: δ -5.46, -5.43, -4.65, -4.48, 18.15, 18.34, 24.52, 25.26, 25.87, 25.93, 37.46, 39.67, 42.13, 51.09, 60.87, 65.224, 69.28, 44.63, 126.18, 127.96, 130.69, 138.37; HRMS (ESI) calcd for $[C_{30}H_{57}NO_4Si_2]^+$: 552.3904, found: 552.3912; $[\alpha]_D^{25}$ = -13.51 (*c* 0.70, MeOH).

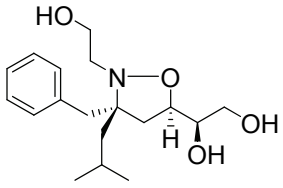

II-S2

(1*R*)-1-[(3*S*, 5*R*)-3-Benzyl-2-(2-hydroxy-ethyl)-3-isobutyl-isoxazolidin-5-yl]-ethane-1,2-diol (II-S2): Treatment of 44 mg of isoxazolidine **II-20** (0.08 mmol, 1.0 eq) in THF (0.80 mL) cooled in an ice-H_2O bath with TBAF (0.32 mL of a 1 M solution in THF, 0.32 mmol, 4.0 eq) afforded removal of both silyl protecting groups in 2 h by TLC analysis. The solution was diluted with H_2O (5 mL), extracted with EtOAc (3 x 5 mL),

dried over Na_2SO_4, filtered, and concentrated *in vacuo*. Purification by flash chromatography (92:8 CH_2Cl_2:MeOH) yielded 25 mg of product in 98% yield as an oil. IR: 3369, 2954, 1456, 1056 cm^{-1}; ^1H NMR: δ 0.87 (d, 3H, J = 6.8), 0.95 (d, 3H, J = 6.3), 1.30 (dd, 1H, J = 6.3, 14.6), 1.58 (dd, 1H, J = 4.4, 14.6), 1.83-1.91 (m, 1H), 2.02-2.07 (m, 1H), 2.17-2.26 (m, 2H), 2.63 (d, 1H, J = 12.7), 2.87 (d, 1H, J = 13.2), 2.93 (m, 2H), 3.59-3.63 (m, 2H), 3.67-3.69 (m, 1H), 3.78-3.86 (m, 2H), 4.09 (td, 1H, J = 3.7, 7.6), 7.15-7.17 (m, 2H), 7.20-7.23 (m, 1H), 7.26-7.29 (m, 2H); ^{13}C NMR (100 MHz): δ 23.55, 24.57, 25.38, 37.42, 39.38, 42.27, 51.09, 61.37, 64.38, 69.77, 74.10, 126.36, 128.14, 130.77, 138.02; HRMS (ESI) calcd for $[C_{18}H_{29}NO_4 + Na]^+$: 346.1994, found: 346.1991; $[\alpha]_D^{25}$ = -19.47 (*c* 0.19, MeOH).

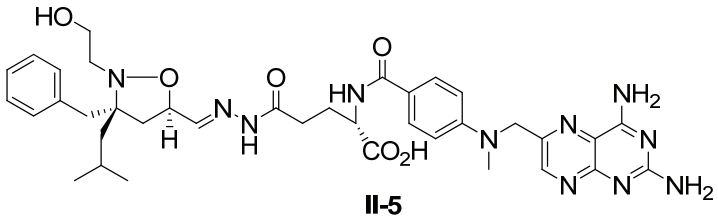

II-5

4-[(3*S*, 5*R*)-3-Benxyl-2-(2-hydroxy-ethyl)-3-isobutyl-isoxazolidin-5-ylmethylene-hydrazinocarbonyl]-2-{4-[(2,4-diamino-pteridin-6-ylmethyl)-methyl-amino]-benzoylamino}-(*S*)-butyric acid (II-5): Purification, storage, and purity confirmation was carried out analogously to **II-2**. The identity was verified by mass spectral and UV analysis of the isolated conjugate. UV (λ_{max} nm): 258, 295, 373; LRMS (ESI) calcd for $[C_{37}H_{47}N_{11}O_6 + H]^+$: 742.8, found: 742.6.

Characterization of II-4 and appropriate intermediates from II-12.

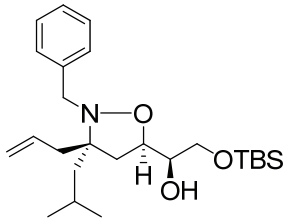

II-S3

(1*R*)-[(3*R*, 5*R*)-3-Allyl-2-benzyl-3-isobutyl-isoxazolidin-5-yl]-2-(*tert*-butyl-dimethyl-silanyloxy)-ethanol (II-S3): Isoxazolidine **II-S3** was prepared using the procedure for the preparation of **II-14** from 200 mg (0.58 mmol) of **II-12**. Purification by flash

chromatography (95:5 hexanes/EtOAc) gave **II-S3** in 81% yield (200 mg) as an oil. IR: 3430, 2928, 1463, 1253, 1115, 837 cm^{-1}; ^1H NMR: δ -0.02 (s, 6H), 0.84 (s, 9H), 0.98 (d, 3H, J = 8.3), 1.00 (d, 3H, J = 8.3), 1.46 (dd, 1H, J = 4.4, 13.2), 1.78-1.86 (m, 1H), 2.21-2.36 (m, 3H), 2.47 (dd, 1H, J = 6.8, 13.7), 3.42 (dd, 1H, J = 8.3, 11.7), 3.49-3.53 (m, 2H), 3.72 (d, 1H, J = 13.2), 3.84 (d, 1H, J = 13.2), 4.08 (bs, 1H), 5.10-5.13 (m, 2H), 5.89-5.98 (m, 1H), 7.20-7.23 (m, 1H), 7.27-7.33 (m, 4H); ^{13}C NMR: δ -5.46, 18.28, 24.61, 24.94, 25.03, 25.90, 39.20, 40.17, 40.25, 41.54, 53.60, 64.34, 74.34, 117.87, 117.92, 126.92, 128.24, 128.48, 134.35; HRMS (ESI) calcd for $[C_{25}H_{43}NO_3Si]^+$: 434.3090, found: 434.3086; $[\alpha]_D^{25}$ = -1.50 (*c* 0.20, MeOH).

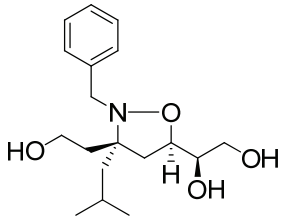

II-S4

(1*R*)-1-[(3*R*, 5*R*)-2-Benzyl-3-(2-hydroxy-ethyl)-3-isobutyl-isoxazolidin-5-yl]-ethane-1,2-diol (II-S4): Oxidative cleavage of the allyl functionality on isoxazolidine **II-S4** was carried out on 200 mg (0.48 mmol) of **II-S3** using a procedure analogous to the one used for the oxidative cleavage of **II-13**. The final TBS deprotection was carried out on 100 mg (0.23 mmol) of the intermediate alcohol following passage of the crude product through a plug of silica (7:3 hexanes/EtOAc). Purification of the crude oil by flash chromatography (92:8 CH_2Cl_2: MeOH) gave 47 mg of **II-S4** in 64% yield as a clear oil. IR: 3334, 2954, 1456, 1067 cm^{-1}; ^1H NMR: δ 0.99 (d, 3H, J = 6.3), 1.01 (d, 3H, J = 6.3), 1.57 (dd, 2H, J = 6.8, 13.7), 1.66-1.79 (m, 2H), 2.10 (m, 1H), 2.28 (dd, 1H, J = 5.9, 12.7), 2.38 (dd, 1H, J = 8.8, 12.7), 3.52 (dd, 1H, J = 5.1, 11.5), 3.61 (dd, 1H, J = 3.9, 11.7), 3.67 (m, 1H), 3.75 (d, 1H, J = 13.7), 3.82-3.91 (m, 2H), 4.01 (d, 1H, J = 13.2), 4.27-4.31 (m, 1H), 7.25-7.35 (m, 5H); ^{13}C NMR (100 MHz): 24.23, 25.06, 25.00, 35.74, 38.76, 41.40, 53.30, 59.32, 63.90, 72.97, 127.74, 128.62, 128.82, 137.21; HRMS (ESI) calcd for $[C_{18}H_{29}NO_4 + Na]^+$: 346.1994, found: 346.1999; $[\alpha]_D^{25}$ = +3.21 (*c* 0.20, MeOH).

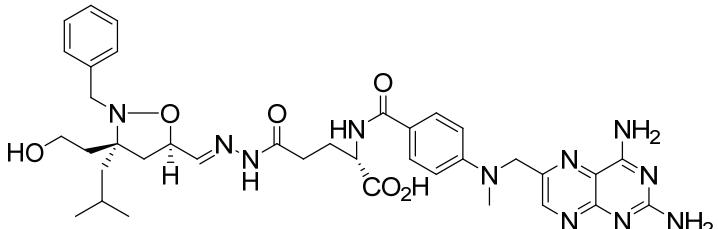

II-4

4-[(3*R*, 5*R*)-2-Benxyl-3-(2-hydroxy-ethyl)-3-isobutyl-isoxazolidin-5-ylmethylene-hydrazinocarbonyl]-2-{4-[(2,4-diamino-pteridin-6-ylmethyl)-methyl-amino]-benzoylamino}-(*S*)-butyric acid (II-4): II-4 was prepared, purified, and stored by the same methods as **II-2**. The identity was verified by mass spectral and UV analysis of the isolated conjugate. UV (λ_{max} nm): 258, 298, 378; HRMS (ESI) calcd for $[C_{37}H_{47}N_{11}O_6 + Na]^+$: 764.3608, found: 764.3599.

Characterization of II-3 and appropriate intermediates from II-S5.

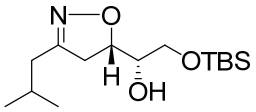

II-S5

2-(*tert*-Butyl-dimethyl-silanyloxy)-(1*S*)-1-[(5*S*)-3-isobutyl-4,5-dihydro-isoxazol-5-yl]-ethanol (II-S5): Isoxazoline **II-S5** was prepared using a procedure analogous to that used for the preparation of **II-10** except 190 mg (1.9 mmol) of **II-8** and 500 mg (2.5 mmol) of *ent*-**II-9** were used. Purification by flash chromatography (2:3 hexanes/EtOAc) yielded 410 mg of isoxazoline **II-S5** as a colorless oil in 79% yield. Spectral data was identical to that of **10**. $[\alpha]_D^{25} = +59.50$ (*c* 0.87, $CHCl_3$).

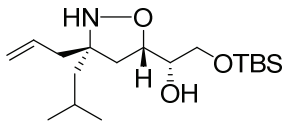

II-S6

(1*S*)-1-[(3*R*, 5*S*)-3-Allyl-3-isobutyl-isoxazolidin-5-yl]-2-(*tert*-butyl-dimethyl-silanyloxy)-ethanol (II-S6): Isoxazolidine **II-S6** was prepared by the same procedure used for the preparation of **II-11** except 390 mg (1.4 mmol) of isoxazoline **II-S5** was used as the starting material. Purification of the crude oil by flash chromatography (1:4 hexanes/EtOAc) yielded 300 mg of **II-S6** as a colorless oil. Spectroscopic data was identical to that obtained for **11**; $[\alpha]_D^{24} = +25.70$ (*c* 1.42, $CHCl_3$).

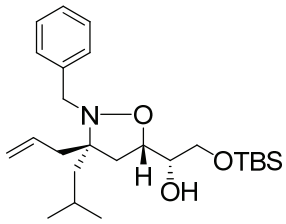

II-S7

(1*S*)-[(3*R*, 5*S*)-3-Allyl-2-benzyl-3-isobutyl-isoxazolidin-5-yl]-2-(*tert*-butyl-dimethyl-silanyloxy)-ethanol (II-S7): Isoxazolidine **II-S7** was prepared by the procedure used for the preparation of **II-13** except 460 mg (1.3 mmol) of isoxazolidine **II-S6** was used as the starting material. Purification by flash chromatography (95:5 hexanes/EtOAc) gave 470 mg (80% yield) of product isolated as a clear oil. Spectroscopic data was identical to the enantiomer **II-13**. $[\alpha]_D^{24}$ = +11.32 (*c* 1.12, $CHCl_3$).

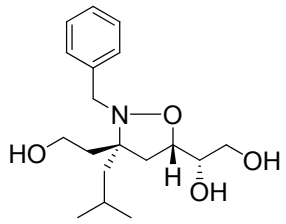

II-S8

(1*S*)-1-[(3*R*, 5*S*)-2-Benzyl-3-(2-hydroxy-ethyl)-3-isobutyl-isoxazoldin-5-yl]-ethane-1,2-diol (II-S8): Experimental conditions for the conversion of **II-S7** (150 mg, 0.34 mmol) to **II-S8** followed the procedure used for the conversion of **II-13** to **II-S1**. Purification by flash chromatography (93:7 CH_2Cl_2:MeOH) provided 81 mg of **II-S8** in 75% yield as a colorless oil. Spectroscopic data was identical to that obtained for **II-S1**. $[\alpha]_D^{27}$ = -0.08 (*c* 0.29, $CHCl_3$).

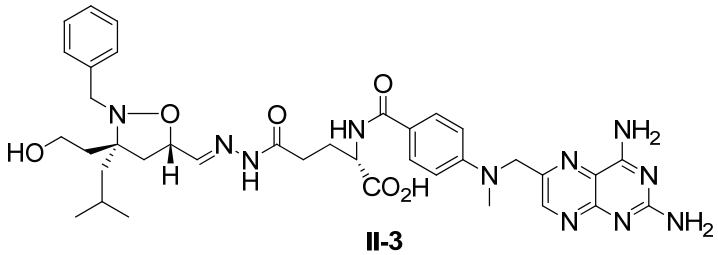

II-3

4-[(3*R*, 5*S*)-2-Benxyl-3-(2-hydroxy-ethyl)-3-isobutyl-isoxazolidin-5-ylmethylene-hydrazinocarbonyl]-2-{4-[(2,4-diamino-pteridin-6-ylmethyl)-methyl-amino]-benzoylamino}-(*S*)-butyric acid (II-3): II-3 was prepared, purified, and stored by the same methods as **II-2**. The identity was verified by mass spectral and UV analysis of the

isolated conjugate. UV (λ_{max} nm): 259, 299, 375; HRMS (ESI) calcd for [$C_{37}H_{47}N_{11}O_6$ + Na]$^+$: 764.3608, found: 764.3608.

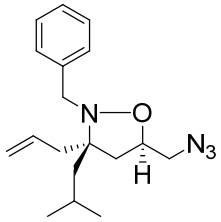

II-24

(3*S*,5*R*)-3-allyl-5-(azidomethyl)-2-benzyl-3-isobutylisoxazolidine (II-24): To a solution of isoxazolidine **II-23** (35 mg, 0.12 mmol, 1.0 eq) in CH_2Cl_2 (1.2 mL) cooled in an ice-H_2O bath was added Et_3N (18 µl, 0.13 mmol, 1.1 eq) and methane sulfonylchloride (10 µl, 0.13 mmol, 1.1 eq). The mixture was stirred for 20 min at which point TLC analysis indicated completion of the reaction. The mixture was diluted with H_2O (5 mL) and Et_2O (5 mL) and the layers separated. The aqueous was extracted with Et_2O (3 x 5 mL) and the combined organic extracts were washed with brine (5 mL), dried over Na_2SO_4, filtered, and concentrated in vacuo. The crude product was dissolved in DMSO (1.2 mL) and NaN_3 (78 mg, 1.2 mmol, 10 eq) was added. The flask was fitted with a reflux condenser and heated at 100 °C for 12 h at which point mass spectral analysis indicated completion of the reaction. The reaction mixture was diluted with H_2O (5 mL) and Et_2O (5 mL) and the organic and aqueous separated. The aqueous was extracted with Et_2O (3 x 5 mL) and the combined organic extracts were washed with H_2O (2 x 5 mL) and brine (5 mL), dried over Na_2SO_4, filtered, and concentrated in vacuo. Purification by flash chromatography (95:5 hexanes/EtOAc) yielded 34 mg of product as a colorless oil in 89 % yield. IR: 2955, 2869, 2099, 1454, 1278, 916, 732 cm^{-1}; ^{1}H NMR: δ 0.96 (d, 3H, J = 6.6), 0.98 (d, 3H, J = 6.6), 1.37 (dd, 1H, J = 6.6, 14.7), 1.59 (dd, 1H, J = 5.5, 14.5), 1.80-1.91 (m, 2H), 2.26 (dd, 1H, J = 7.4, 13.9), 2.31 (dd, 1H, J = 8.6, 12.7), 2.44 (dd, 1H, J = 7.0, 13.7), 3.06 (dd, 1H, J = 3.3, 12.3), 3.44 (dd, 1H, J = 7.3, 12.7), 3.87 (m, 1H), 3.89 (m, 1H), 4.10-4.15 (m, 1H), 5.06-5.15 (m, 2H), 5.85-5.98 (m, 1H), 7.19-7.41 (m, 5H); ^{13}C NMR: δ 24.09, 24.60, 25.21, 38.65, 40.19, 43.54, 53.26, 54.37, 68.28, 74.47, 117.8, 126.7, 128.0, 128.1, 134.9, 138.6; HRMS (ESI) calcd for [$C_{18}H_{26}N_4O$ + H]$^+$: 315.2185, found 315.2171.

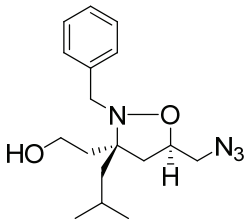

II-25

2-((3*S*,5*R*)-5-(azidomethyl)-2-benzyl-3-isobutylisoxazolidin-3-yl)ethanol (II-25): Oxidative cleavage of the allyl group on **II-24** to form isoxazolidine **II-25** was carried out using a procedure analogous to that used for the preparation of **II-14** starting with 34 mg of **13** (0.11 mmol). Purification by flash chromatography yielded 25 mg of **II-25** in 76% yield as a colorless oil. IR: 3358, 2955, 2870, 2100, 1455, 1280, 1045, 733, 697 cm^{-1}: ^{1}H NMR: δ 0.99 (s, 3H), 1.00 (s, 3H), 1.50-1.60 (m, 1H), 1.65-1.95 (m, 5H), 2.07 (dd, 1H, J = 8.1, 12.7), 2.36 (dd, 1H, J = 8.0, 12.7), 3.41 (d, 2H, J = 4.7), 3.78-3.92 (m, 3H), 3.99 (d, 1H, J = 13.9), 4.19-4.27 (m, 1H), 7.22-7.37 (m, 5H); ^{13}C NMR: δ24.31, 24.89, 25.24, 35.61, 40.82, 43.00, 53.69, 54.49, 59.67, 70.43, 127.2, 128.4, 128.6, 137.6; HRMS (ESI) calcd for $[C_{17}H_{26}N_4O_2 + H]+$: 319.2134, found: 319.2122.

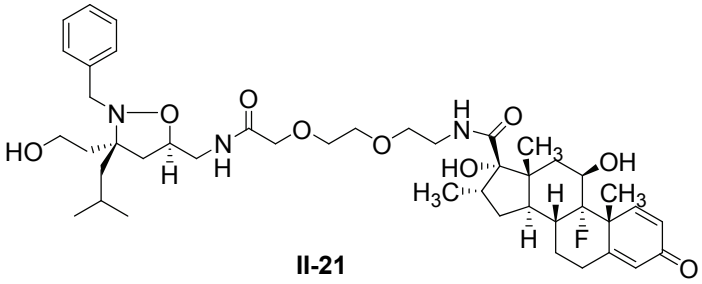

II-21

(8*R*,9*S*,10*R*,11*R*,13*R*,14*R*,16*S*,17*S*)-N-(2-(2-(2-(((3S,5R)-2-benzyl-3-(2-hydroxyethyl)-3-isobutylisoxazolidin-5-yl)methylamino)-2-oxoethoxy)ethoxy)ethyl)-9-fluoro-11,17-dihydroxy-10,13,16-trimethyl-3-oxo-6,7,8,9,10,11,12,13,14,15,16,17-dodecahydro-3H-cyclopenta[a]phenanthrene-17-carboxamide (II-21): To a solution of **II-25** (25 mg, 0.07 mmol, 1.0 eq) in THF (700 µl) was added PPh_3 (37 mg, 0.14 mmol, 2.0 eq) and H_2O (13 µl, 0.7 mmol, 10 eq) and the flask was fitted with a reflux condenser and the mixture heated at 100 °C for 2 h at which point TLC analysis indicated completion of the reaction. An acid, base work-up yielded the crude amine which was immediately coupled to a short PEG linker, 8-amino-3,6,-dioxaoctanoic acid (AEEA). Towards this AEEA (32 mg, 0.08 mmol, 1.2 eq) in DMF (4.6 mL) was stirred with HOBT (11 mg.

0.08 mmol, 1.2 eq) and HBTU (34 mg, 0.08 mmol, 1.2 eq) for 1 h at which point a solution of the crude amine and Et_3N (10 μl, 0.07 mmol, 1.0 eq) in DMF (2.4 mL) was added dropwise and the solution stirred for 12 h. At this point mass spectral analysis indicated production and 1.8 mL of piperidine was added to generate an overall 20% piperidine in DMF solution to afford deprotection of the Fmoc. After 5 min mass spectral analysis indicated product formation and the mixture was thus concentrated in vacuo. The crude product was purified by reverse-phase HPLC using a 0.1% TFA in H_2O/CH_3CN gradient. The product was subsequently coupled to OxDex. Towards this OxDex (8 mg, 0.02 mmol, 1.2 eq) in DMF (1.0 mL) was stirred with HOBT (3 mg. 0.02 mmol, 1.2 eq) and HBTU (8 mg, 0.02 mmol, 1.2 eq) for 1 h at which point a solution of the amine (5 mg, 0.017 mmol, 1.0 eq) and Et_3N (2 μl, 0.017 mmol, 1.0 eq) in DMF (0.54 mL) was added dropwise and the solution stirred for 12 h. At this point mass spectral analysis indicated product formation and the mixture was concentrated in vacuo and purified using reverse-phase HPLC (0.1% TFA in H_2O/CH_3CN gradient). The identity was confirmed by mass spectral analysis UV analysis and the purity was assessed by analytical HPLC. HRMS (ESI) calcd for $[C_{44}H_{64}FN_3O_9 + H]^+$: 798.4705, found: 798: 4692.

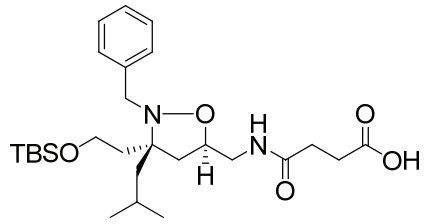

II-S9

4-(((3*S*,5*R*)-2-benzyl-3-(2-(tert-butyldimethylsilyloxy)ethyl)-3-isobutylisoxazolidin-5-yl)methylamino)-4-oxobutanoic acid (II-S9): To a solution of **II-25** (55 mg, 0.17 mmol, 1.0 eq) in THF (1.7 mL) cooled in an ice-H_2O bath was added DMAP (2 mg, 0.02 mmol, 0.1 eq), Et_3N (26 μl, 0.19 mmol, 1.1 eq) and TBSOTf (44 μl, 0.19 mmol, 1.1 eq) and the mixture stirred 1 h with continued cooling at which TLC analysis indicated complete consumption of starting material. The mixture was diluted with sat. NH_4Cl (5 mL) and extracted with Et_2O (3 x 5 mL). The combined organic extracts were washed with brine (5 mL), dried over Na_2SO_4, filtered, and concentrated in vacuo. Purification by flash chromtogarphy (elution in 80:20 hexanes/EtOAc) yielded 60 mg of product as

colorless oil in 82% yield. A portion of the product (39 mg, 0.09 mmol) was reduced to the amine using identical conditions utilized for the reduction of **II-25** to yield 34 mg of product in 92% yield. To the amine in 800 μl DMF was added DMAP (1 mg, 0.01 mmol, 0.1 eq) and Et_3N (11 μl, 0.08 mmol, 1.0 eq) and succinic anhydride (8 mg, 0.08 mmol, 1.0 eq) and the resulting solution was stirred for 12 hours at which point TLC analysis indicated complete consumption of starting material. The mixture was diluted with H_2O (5 mL) and extracted with EtOAc (3 x 5 mL) and the combined organic extracts were washed with brine (5 mL), dried over Na_2SO_4, filtered, and concentrated in vacuo. Purification (elution in 90:10 benzene/MeOH) produced 30 mg of product in 75% yield. ^{1}H NMR: δ 0.08 (s, 6H), 0.91 (s, 9H), 0.97 (d, 3H, J = 6.8), 1.0 (d, 3H, J = 6.8), 1.39 (dd, 1H, J = 6.1, 14.4), 1.62 (dd, 1H, J = 5.4, 14.2), 1.80-1.90 (m, 2H), 1.95 (dd, 1H, J = 6.3, 12.6), 2.38-2.41 (m, 1H), 2.44 (dd, 1H, J = 8.8, 12.7), 2.51-2.57 (m, 2H), 2.85 (singlet, 2H), 2.98 (singlet, 2H), 3.28 (dd, 1H, J = 6.3, 13.7), 3.33 (dd, 1H, J = 4.9, 13.7), 3.80-3.90 (m, 3H)< 4.09-4.15 (m, 1H), 7.18-7.21 (m, 1H), 7.26-7.29 (m, 2H), 7.35 -7.36 (m, 2H); LRMS calcd for $[C_{27}H_{46}N_2O_5Si + H]^+$: 507.3, found 507.3.

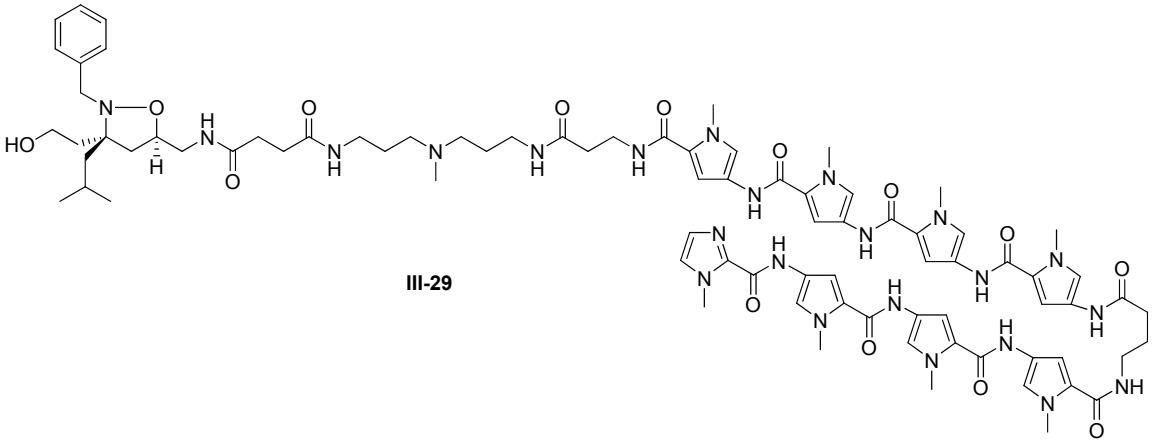

III-29

N1-(((3*S*,5*R*)-2-benzyl-3-(2-hydroxyethyl)-3-isobutylisoxazolidin-5-yl)methyl)-N4-(3-(methyl(3-(3-(1-methyl-4-(1-methyl-4-(1-methyl-4-(1-methyl-4-(4-(1-methyl-4-(1-methyl-4-(1-methyl-1H-imidazole-2-carboxamido)-1H-pyrrole-2-carboxamido)-1H-pyrrole-2-carboxamido)-1H-pyrrole-2-carboxamido)butanamido)-1H-pyrrole-2-carboxamido)-1H-pyrrole-2-carboxamido)-1H-pyrrole-2-carboxamido)-1H-pyrrole-2-carboxamido)propanamido)propyl)amino)propyl)succinamide (II-29): To a solution of **II-S9** (5 mg, 0.01 mmol, 1.0 eq) in DMF (250 μl) was added HOBT (1.5 mg, 0.01

mmol, 1.0 eq) and HBTU (4 mg, 0.01 mmol, 1.0 eq) and the solution was stirred 1 h. At this point a solution of polyamide containing a free amine (4 mg, 0.12 mmol, 1.2 eq) and Et3N (2 μl, 0.012 mmol, 1.2 eq) in DMF (250 μl) was added to the **II-S9** solution dropwise and the resultant solution stirred for 12 h at which point mass spectral analysis indicated product formation. The solution was diluted with 1N HCl (500 μl) and stirred 30 min to afford removal of the silyl ether protecting group. The crude product was concentrated in vacuo and purified by reverse phase HPLC (0.1% TFA in H_2O/CH_3CN gradient). LRMS (ESI) calcd for $[C_{82}H_{107}N_{23}O_{14} + H]^+$: 1638.9, found 1639.3.

I. Appendix of Selected ^{1}H NMR Spectra and HPLC traces

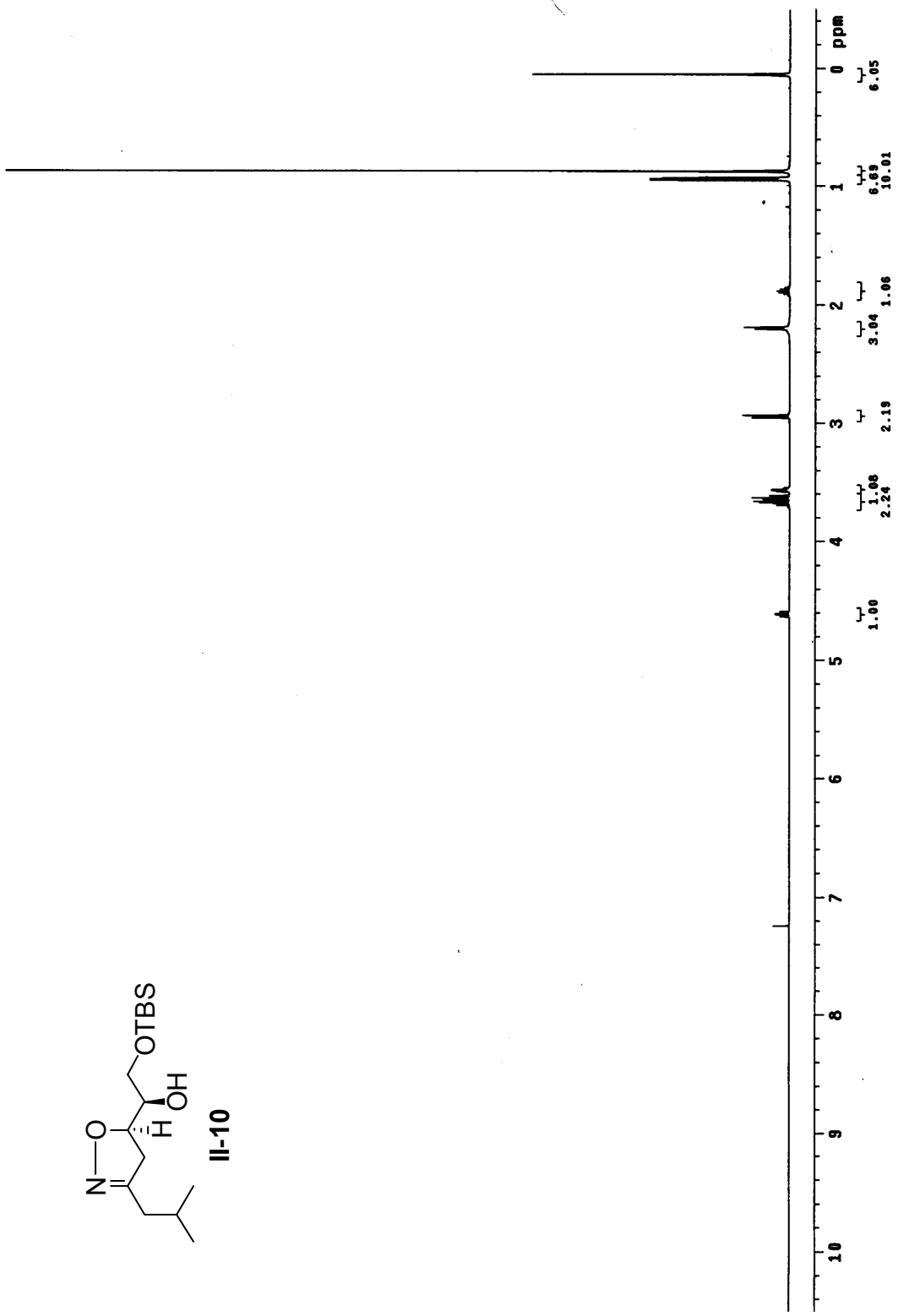

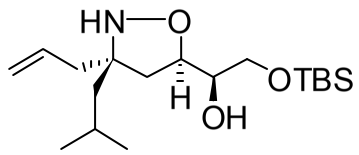
HN
O
OTBS
H
OH

II-11

10
9
8
7
6
5
4
3
2
1
0
ppm
1.00
2.07
1.01
1.03
1.33
1.68
0.95
2.09
1.06
1.15
0.93
2.17
0.42
1.49
6.47
5.72

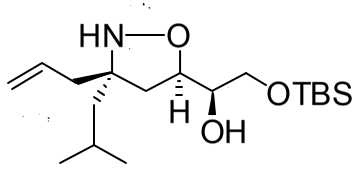

II-12

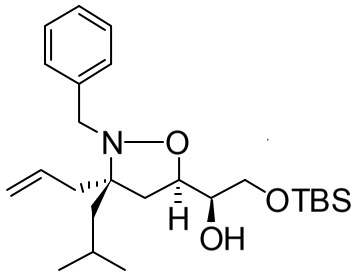
N
O
H
OH
OTBS

II-13

10
9
8
7
6
5
4
3
2
1
0
ppm
3.85
0.86
1.00
2.02
0.95
2.05
2.02
1.00
0.78
3.09
1.01
1.02
1.02
0.99
6.14
9.12
5.50

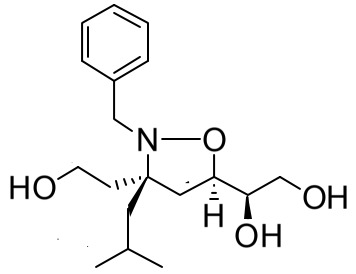

II-S1

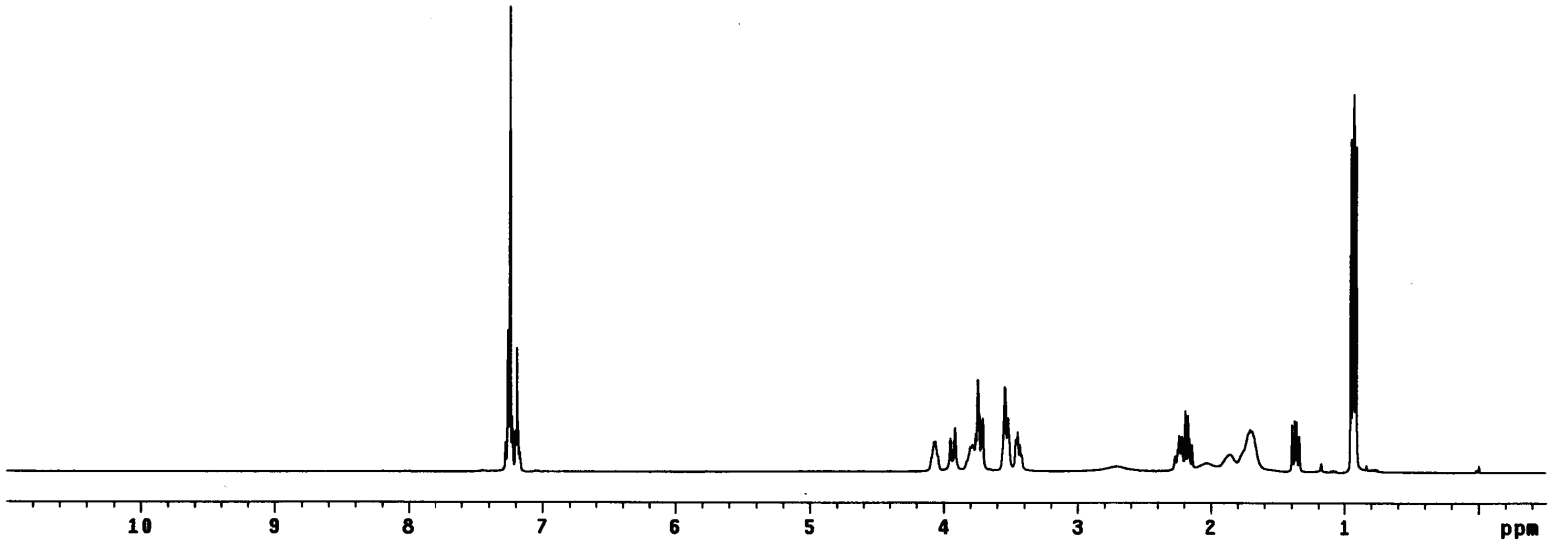

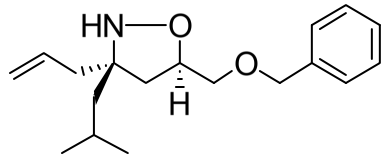

II-15

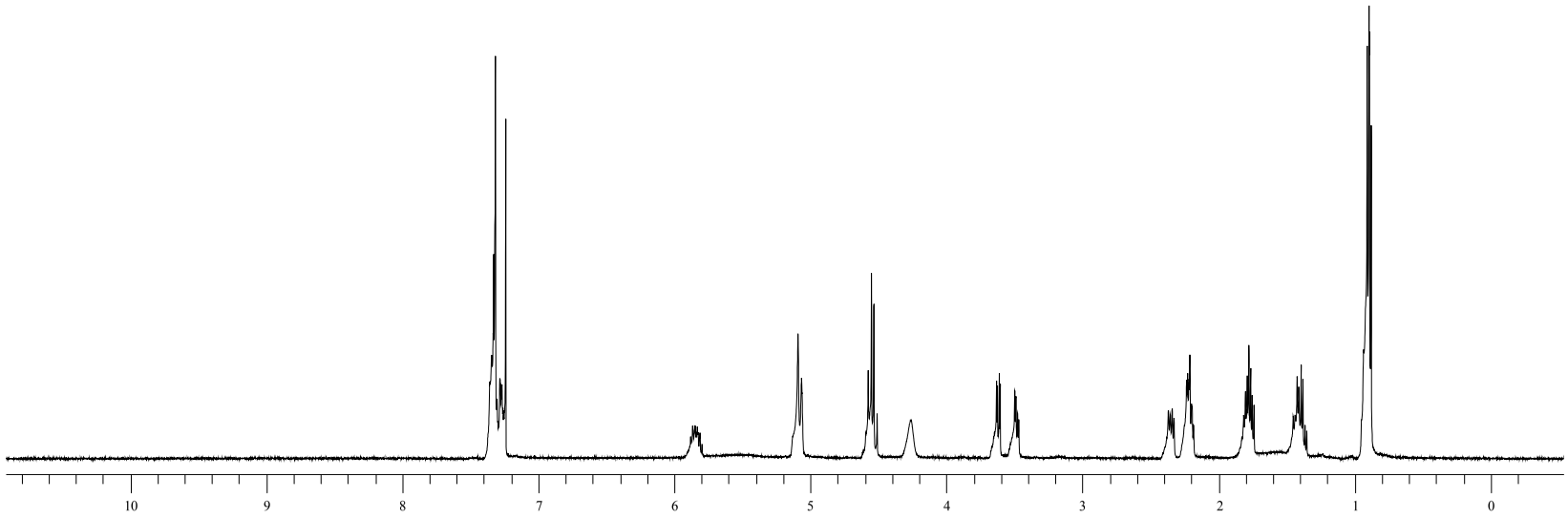

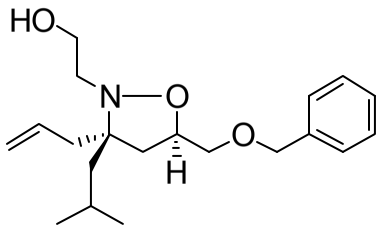

II-16

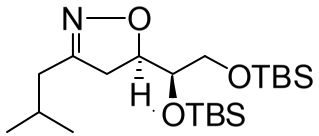
N
O
H
OTBS
OTBS

II-17

10
9
8
7
6
5
4
3
2
1
0
ppm
1.00
1.03
2.07
1.93
2.00
0.96
6.25
18.83
10.98

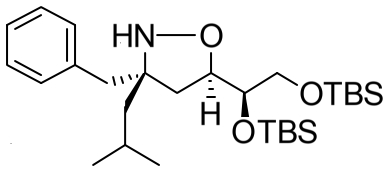
HN
O
OTBS
H
OTBS

II-18

10
9
8
7
6
5
4
3
2
1
0 ppm
4.16
1.06
1.00
0.07
0.81
0.92
2.10
0.95
0.95
0.86
0.90
0.91
1.69
2.68
11.11

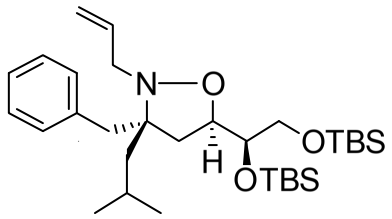

II-19

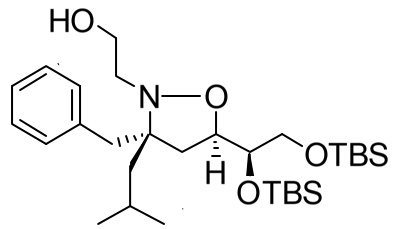
HO
N
O
H
OTBS
OTBS

II-20

10
9
8
7
6
5
4
3
2
1
0
ppm
13.13
1.00
2.05
1.93
0.95
3.10
1.12
1.21
0.95
1.04
1.96
1.59
3.28
21.03
10.80

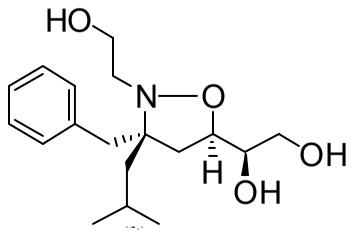

II-S2

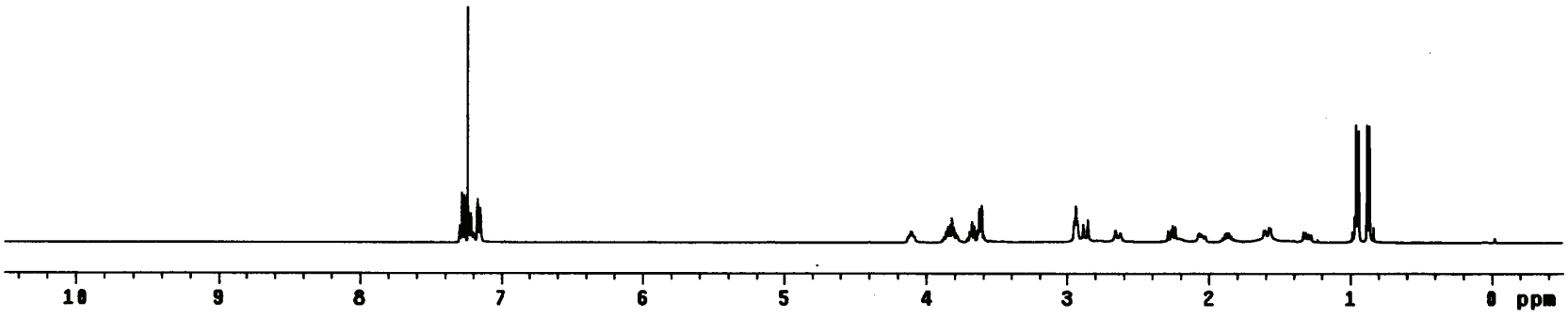

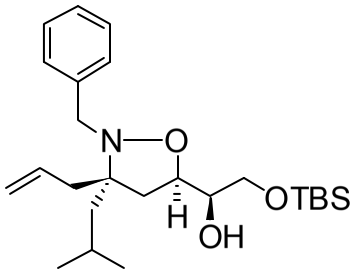
N
O
H
OH
OTBS

II-S3

10
9
8
7
6
5
4
3
2
1
0 ppm
3.86
1.05
1.00
2.02
0.99
1.08
1.14
1.99
1.12
0.82
1.06
3.23
1.20
2.35
1.21
6.62
9.68
5.52

OH
OH
H
O
N
HO

II-S4

10
9
8
7
6
5
4
3
2
1
0 ppm
5.16
1.00
1.14
2.18
1.071.29
1.18
3.90
3.71
6.35

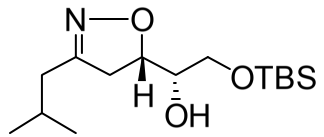
N
O
OTBS
H
OH

II-S5

10
9
8
7
6
5
4
3
2
1
0 ppm
1.00
1.06
2.13
2.13
0.96
2.09
1.02
9.56
6.46
5.86

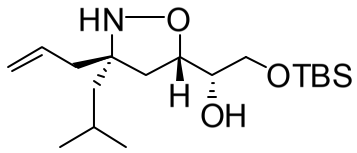
HN
O
H
OH
OTBS

II-S6

10
9
8
7
6
5
4
3
2
1
0
ppm
1.00
0.86
2.05
0.98
1.04
2.11
0.85
0.99
1.98
0.99
1.03
2.03
6.04
9.76
5.85

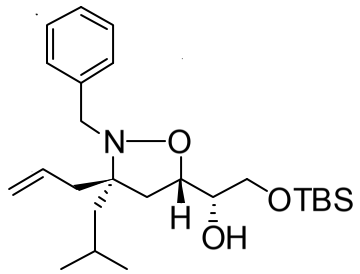

II-S7

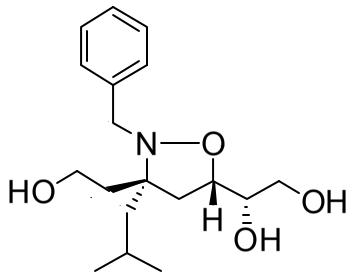

II-S8

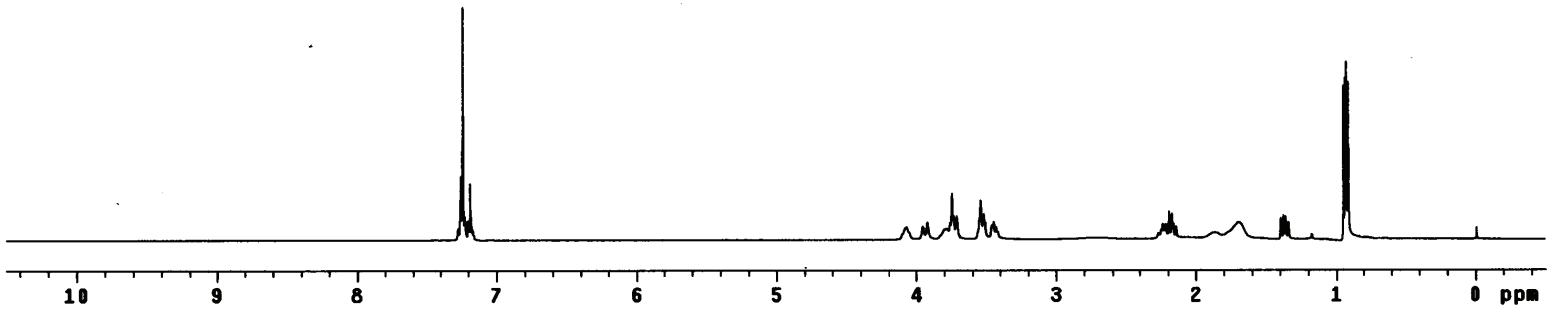

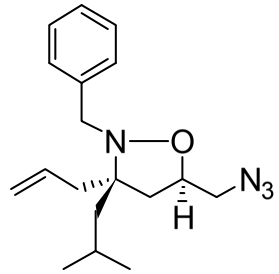

II-24

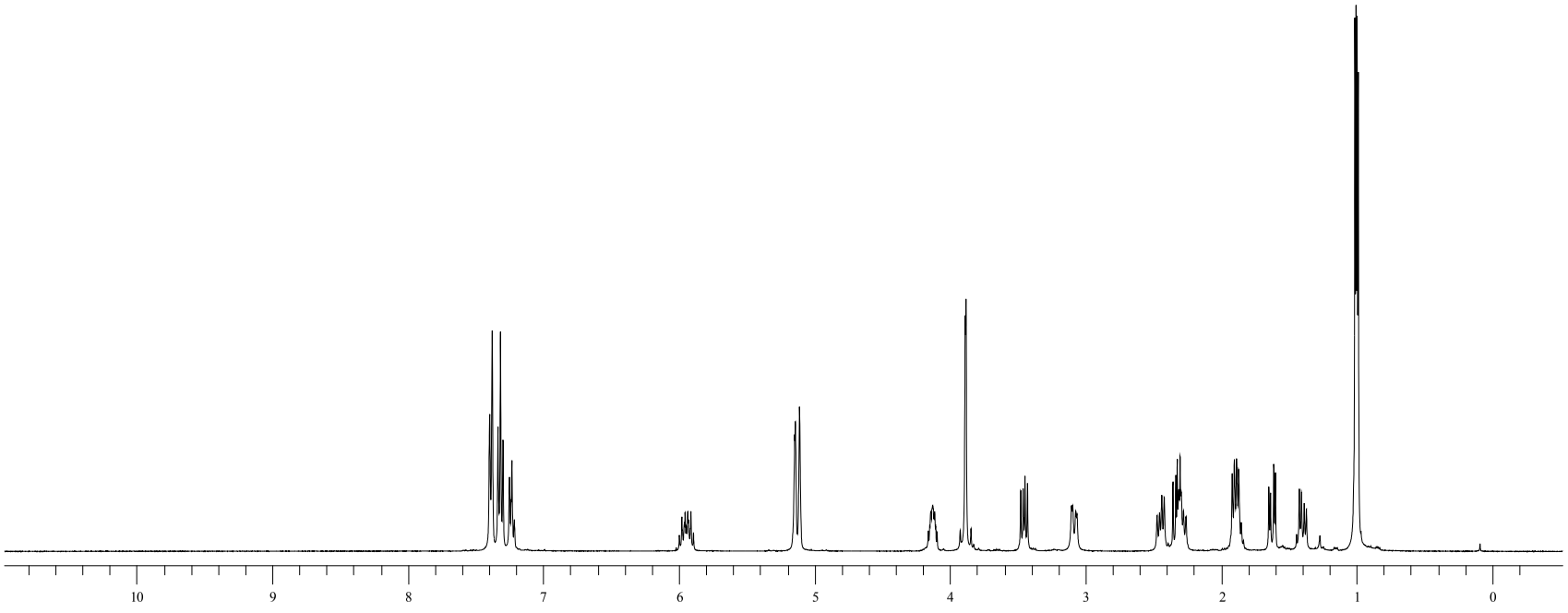

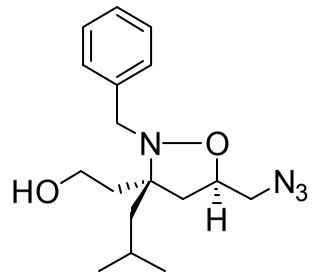

II-25

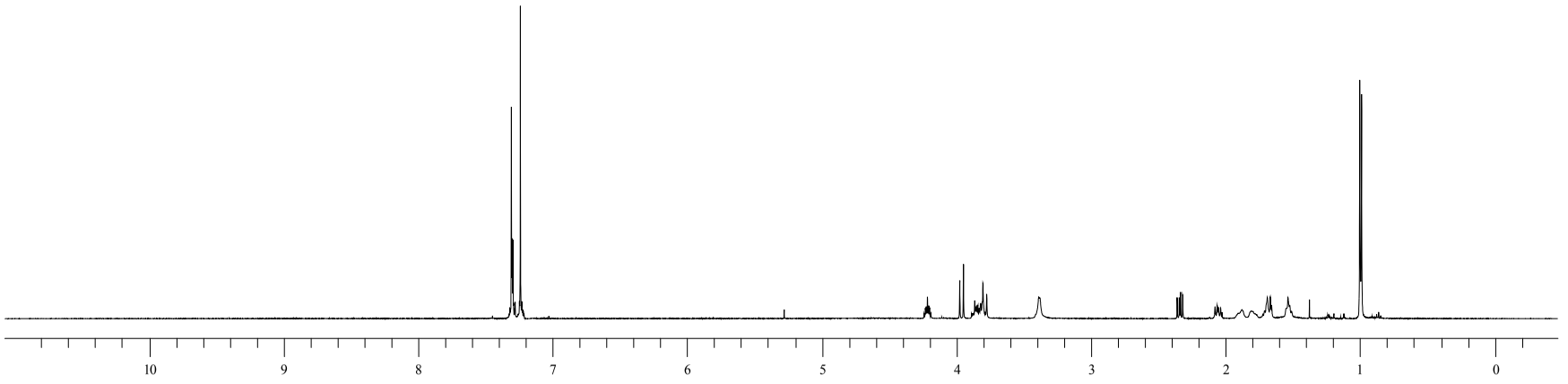

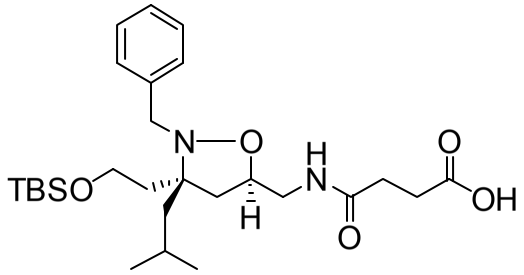

II-S9

HPLC traces of compounds **II-3-II-5**. Compounds **II-4** and **II-5** are present as a mixture of E/Z isomers as confirmed by ^{1}H NMR. **II-25** is a mixture of diastereomers as confirmed by ^{1}H NMR.

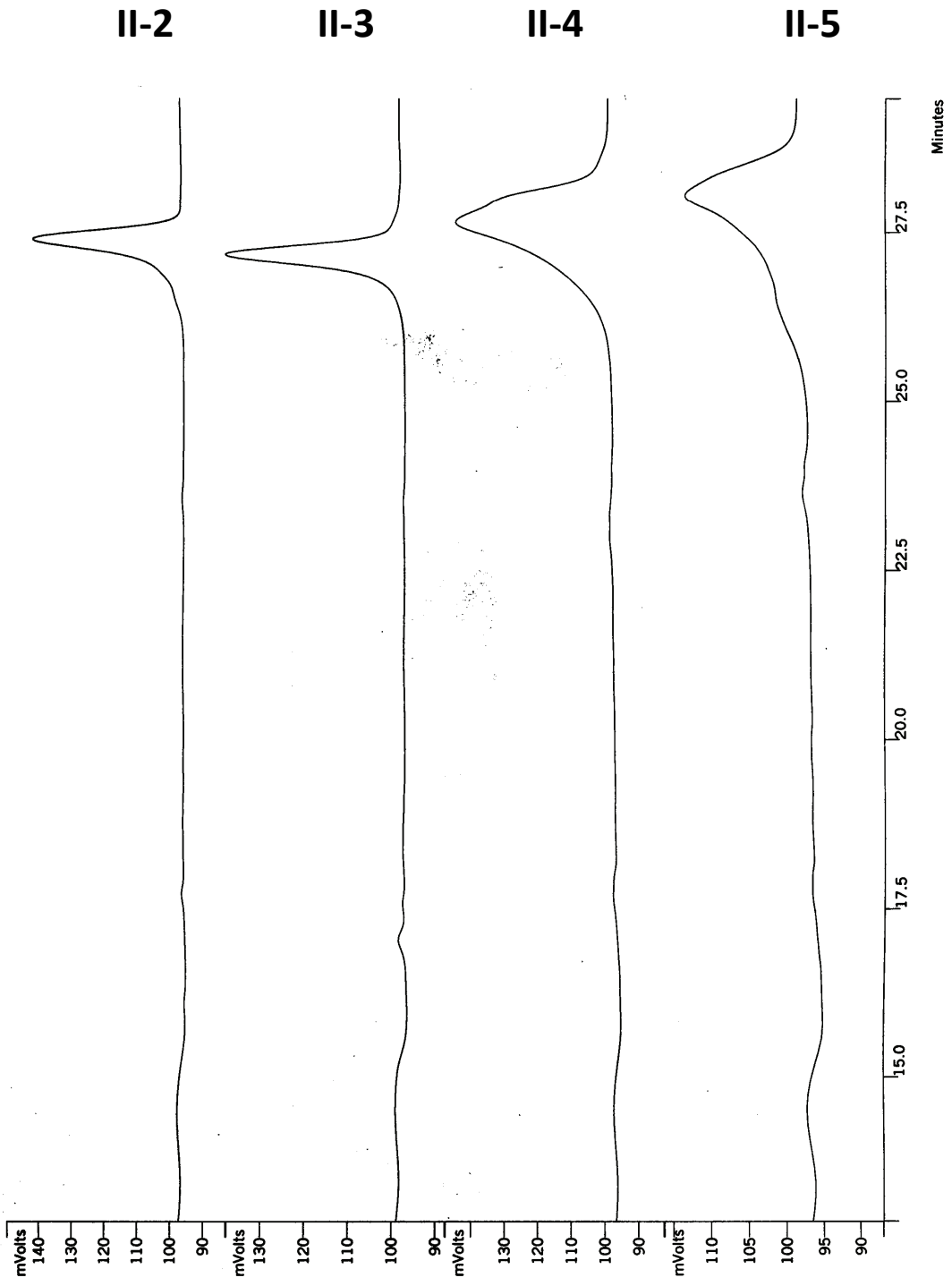

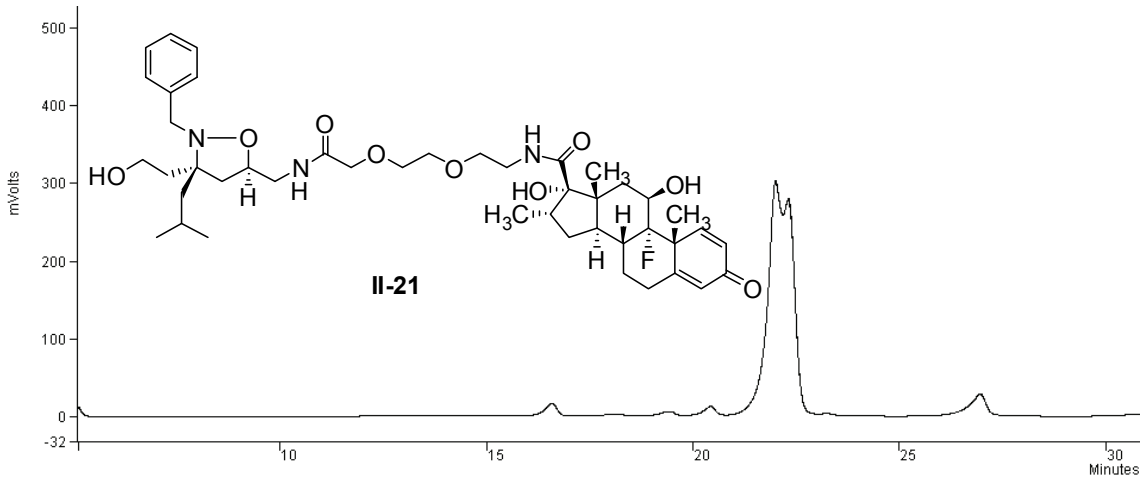

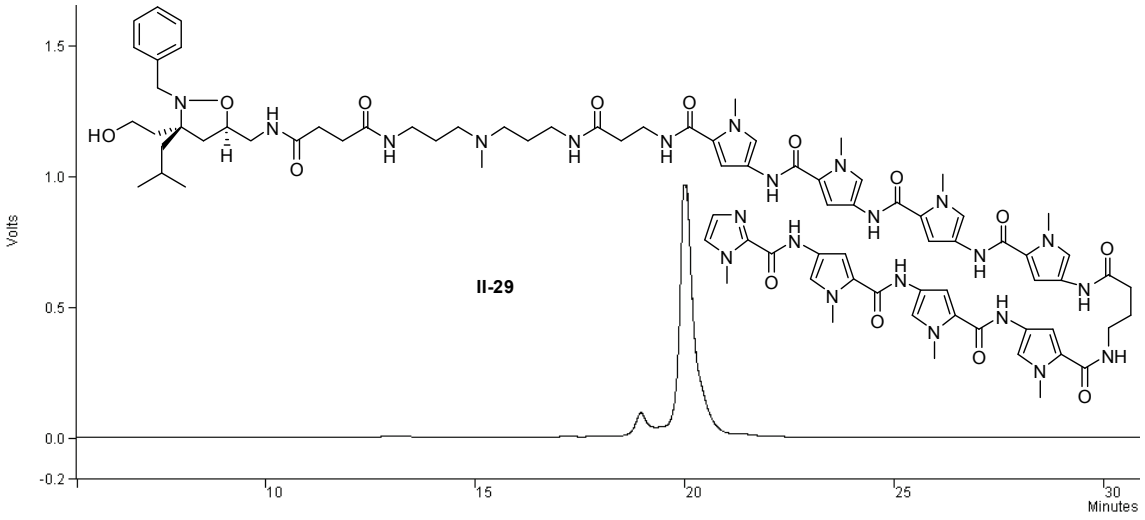

J. References

1. Mapp, A. K.; Ansari, A. Z., *ACS Chem Biol* **2007,** *2* (1), 62-75.

2. Reeves, W. M.; Hahn, S., *Mol Cell Biol* **2005,** *25* (20), 9092-102.

3. Fishburn, J.; Mohibullah, N.; Hahn, S., *Mol Cell* **2005,** *18* (3), 369-78.

4. Schanda, P.; Brutscher, B.; Konrat, R.; Tollinger, M., *J Mol Biol* **2008,** *380* (4), 726-41.

5. Minter, A. R.; Brennan, B. B.; Mapp, A. K., *J Am Chem Soc* **2004,** *126* (34), 10504-5.

6. Buhrlage, S. J.; Brennan, B. B.; Minter, A. R.; Mapp, A. K., *J Am Chem Soc* **2005,** *127* (36), 12456-7.

7. Rowe, S. P.; Casey, R. J.; Brennan, B. B.; Buhrlage, S. J.; Mapp, A. K., *Journal of the American Chemical Society* **2007,** *129* (35), 10654-+.

8. Kanemasa, S. N., M; Kamimura, A.; Hori, K. J., *J. Am. Chem. Soc.* **1994,** *116*, 2324-2439.

9. Bode, J. W.; Fraefel, N.; Muri, D.; Carreira, E. M., *Angew Chem Int Ed Engl* **2001,** *40* (11), 2082-2085.

10. Minter, A. R.; Fuller, A. A.; Mapp, A. K., *J Am Chem Soc* **2003,** *125* (23), 6846-7.

11. Karabatsos, G. J. T., R. A., *Tetrahedron* **1968,** *24*, 3347-3360.

12. Kurbanov, S. S., A.; Sen, N., *Org. Prep. Proced. Int.* **1999,** *31*, 681-688.

13. Wang, J. C. J., G. J., *J. Org. Chem.* **1999,** *64*, 8090-8097.

14. Davoille, R. J. R., D. T.; Christie, S. D. R., *Tet. Lett.* **2000,** *41*, 1255-1259.

15. Baker, K.; Bleczinski, C.; Lin, H.; Salazar-Jimenez, G.; Sengupta, D.; Krane, S.; Cornish, V. W., *Proc Natl Acad Sci U S A* **2002,** *99* (26), 16537-42.

16. Stanojevic, D.; Young, R. A., *Biochemistry* **2002,** *41* (23), 7209-16.

17. Nyanguile, O.; Uesugi, M.; Austin, D. J.; Verdine, G. L., *Proc Natl Acad Sci U S A* **1997,** *94* (25), 13402-6.

18. Drysdale, C. M.; Duenas, E.; Jackson, B. M.; Reusser, U.; Braus, G. H.; Hinnebusch, A. G., *Mol Cell Biol* **1995,** *15* (3), 1220-33.

19. Liu, B.; Alluri, P. G.; Yu, P.; Kodadek, T., *J Am Chem Soc* **2005,** *127* (23), 8254-5.

20. Kwon, Y.; Arndt, H. D.; Mao, Q.; Choi, Y.; Kawazoe, Y.; Dervan, P. B.; Uesugi, M., *J Am Chem Soc* **2004,** *126* (49), 15940-1.

21. Xiao, X.; Yu, P.; Lim, H. S.; Sikder, D.; Kodadek, T., *Angew Chem Int Ed Engl* **2007,** *46* (16), 2865-8.

22. Xiao, X.; Yu, P.; Lim, H. S.; Sikder, D.; Kodadek, T., *J Comb Chem* **2007,** *9* (4), 592-600.

23. Dose, C.; Farkas, M. E.; Chenoweth, D. M.; Dervan, P. B., *J Am Chem Soc* **2008,** *130* (21), 6859-66.

24. Nickols, N. G.; Jacobs, C. S.; Farkas, M. E.; Dervan, P. B., *Nucleic Acids Res* **2007,** *35* (2), 363-70.

25. Pangborn, A. B.; Giardello, M. A.; Grubbs, R. H.; Rosen, R. K.; Timmers, F. J., *Organometallics* **1996,** *15* (5), 1518-1520.

26. Still, W. C. K., M.; Mitra, A., *J. Org. Chem.* **1978,** *43*, 2923.

27. Seeger, D. R. C., D. B.; Smith, J. M.; Huitquist, M. E. , *J. Am. Chem. Soc.* **1949,** *71*, 1753.

Chapter III

Binding Partners of iTADs

A. Abstract

Prevailing evidence suggests that transcriptional activators interact with several coactivators in the transcriptional machinery to initiate transcription. This presents a challenging molecular recognition profile to mimic with a small molecule with only a single class of molecules, iTADs, having been reported to reconstitute this function in cells. Here we show that iTADs interact with several coactivator targets of endogenous activators. Of particular note, the small molecules are the first reported to bind the KIX domain within CBP at a site that is utilized by endogenous transcriptional activators. Further there is evidence for a link between the ability of iTADs to bind CBP and activate transcription. Thus these compounds should be valuable tools for elucidating the functional role of particular CBP molecular recognition events.

B. Introduction

We recently reported the first example of a small molecule transcriptional activation domain (TAD), **III-1** (Figure III-1a).[1] When localized to a promoter the isoxazolidine TAD (iTAD) **III-1** activated transcription both in cell-free assays and in cells (Chapter 2), with up to 80-fold upregulation observed.[1, 2] This molecule and related iTADs were designed to mimic the composition and structural commonalities among endogenous TADs (Figure III-1b) with hydrophobic and polar functional groups displayed on a conformationally constrained scaffold similar to a helix.[3-5] In the previous chapter several key aspects of the function of iTADs were shown to be analogous to their endogenous counterparts. It was shown, for example, that analogous to endogenous TADs, iTADs with multiple presentations of amphipathic functionality activate

transcription and that iTADs function when attached to different DBDs.[4] Here we show additional key characteristics are conserved, that iTADs interact with overlapping transcriptional machinery binding sites utilized by endogenous TADs and, further, that iTADs have multiple coactivator binding partners. Using NMR spectroscopy and fluorescence polarization experiments binding partners of iTADs were identified and include CBP, Tra1, Med15, and Med23, all of which are also binding partners of endogenous amphipathic TADs. Similar evaluations of additional isoxazolidines, both active (**III-2**) and inactive (**III-3** and **III-4**), yielded evidence that the ability of iTADs to stimulate transcription is linked to a binding interaction with the coactivator and histone acetyltransferase CBP (Creb Binding Protein). Characterization of the iTAD binding site within CBP via NMR spectroscopy revealed a remarkable similarity to endogenous transcriptional activators such as the mixed lineage leukemia (MLL) factor that utilize the same site.[6] CBP is a node in many cellular signaling networks and iTADs should thus be valuable tools for elucidating the functional role of particular CBP molecular recognition events.[7, 8]

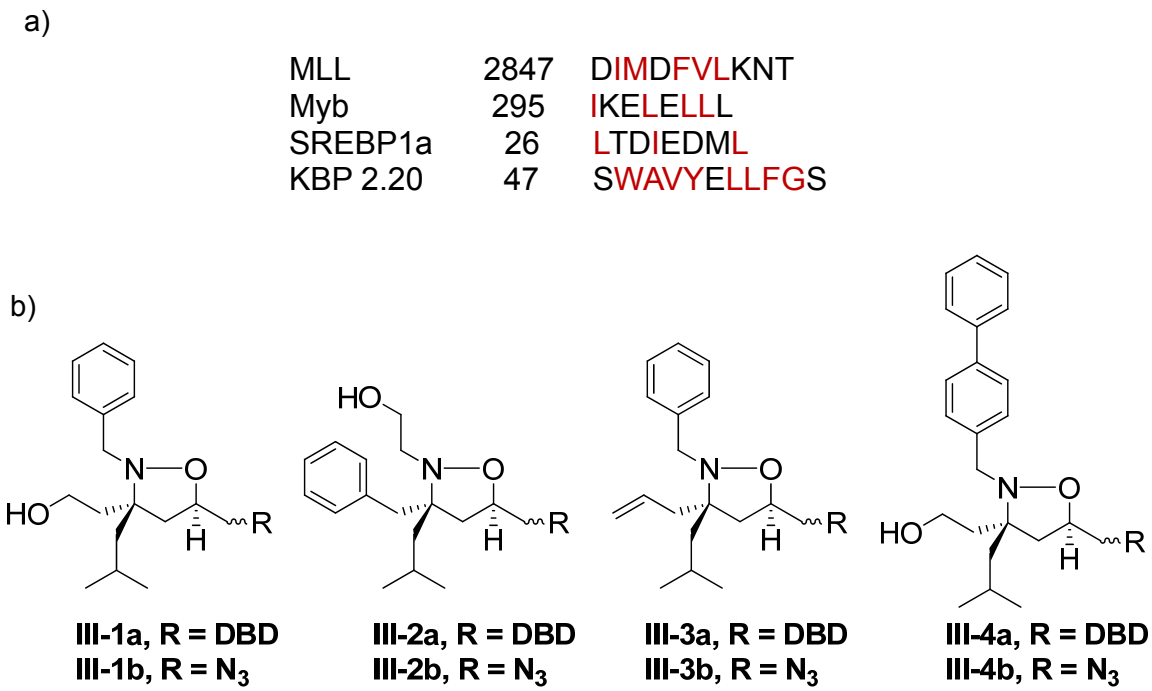

Figure III-1. TADs are composed of interspersed hydrophobic and polar residues. a) Amphipathic isoxazolidines **III-1** and **III-2** functions as TADs, whereas hydrophobic analogs **III-2** and **III-3** do not.[1, 4] DBD = DNA binding domain. b) Natural TAD sequences.

1) Identification of Binding Partners of iTADs

To identify potential coactivator targets of iTAD **III-1** crosslinking and competitive inhibition experiments were conducted by colleagues in the Mapp lab. The crosslinking experiments were conducted by Caleb Bates. A variant of iTAD **III-1** (**III-1-Bpa-biotin**) was prepared that contains a photoactivatable crosslinking group, benzophenone alanine (Bpa), at the C5 position as well as a biotin tag. Upon irradiation with 365 nm light, the benzophenone moiety is converted to a diradical species that undergoes C-H insertion with nearby amino acid residues.[9] Isoxazolidine **III-1-Bpa-biotin** was combined with HeLa nuclear extracts and following irradiation, the mixture was purified on avidin beads. Western blot analysis of the resulting mixture revealed that one interaction partner of isoxazolidine TADs is CBP (Figure **III-2**). The six other bands revealed upon probing with strepavidin are still under investigation.

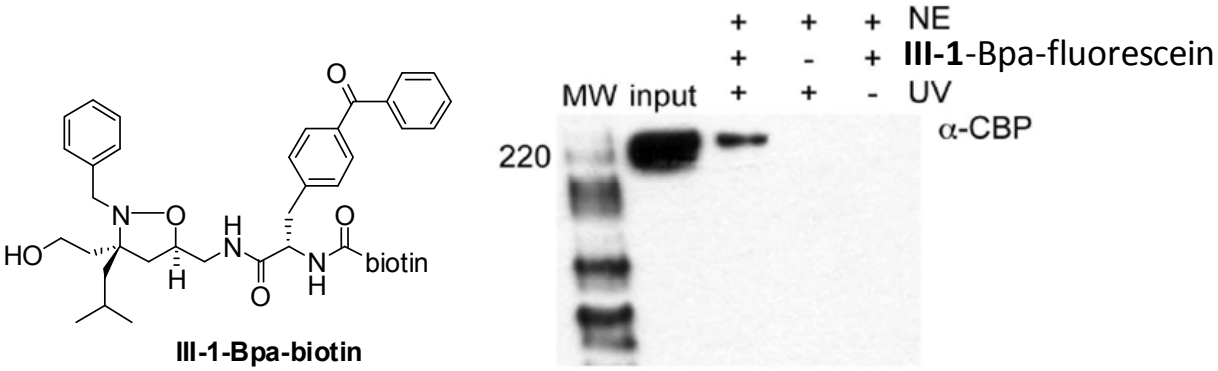

Figure III-2. Crosslinking identified CBP as a binding partner of iTADs. Isoxazolidine **III-1-Bpa-biotin** crosslinks to CBP upon incubation with nuclear extracts (NE) and irradiation with UV light.

The competitive inhibition or 'squelching' experiments were conducted by former coworkers, Dr. Brian Brennan and Dr. Steve Rowe. Well-characterized transcriptional activation domains were expressed as Gal4 DBD fusion proteins in HeLa cells and the ability of iTAD **III-1b** to inhibit gene upregulation by the activators was assessed over a concentration range of 0-100 μM. Of particular note, **III-1b** produced dose-dependent inhibition of two different activators (**Figure III-3**), a VP16-derived TAD and KBP 2.20, both of which are thought to function at least in part through interaction with CBP.[10, 11]

VP-16 derived transcriptional activation domains have been used extensively in mechanistic studies of transcription and as a component of activator ATFs. KBP 2.20 was originally identified in a 'bottom-up' experiment as a ligand for the KIX domain of CBP.[11] Taken together, these results suggested that CBP and, more specifically the KIX domain of CBP as at least one cellular interaction partner of **III-1**.

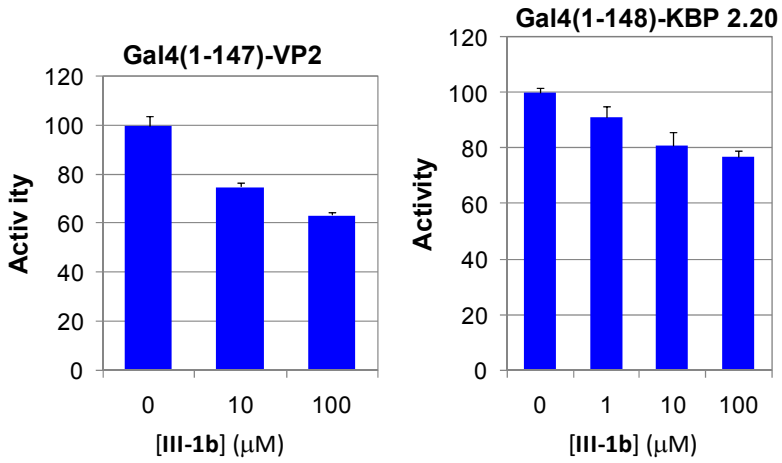

Figure III-3. **III-1b** inhibits activation by TADs VP2 and KBP 2.20.

2) Focus on the CBP KIX Domain

Of the two CBP-targeting transcriptional activators that iTAD **III-1b** inhibits the function of, the interaction domain of one of these, KBP 2.20, is the KIX domain;[11] this suggested the KIX domain is the motif iTAD **III-1** interacts with as well. The KIX domain was originally identified in CBP and has since been found in several eukaryotic coactivators in mammals, plants, and fungi,[12-15] and it is hypothesized to be a conserved TAD binding motif. In support of this, the KIX domain of the mammalian coactivator protein Arc105 and the CBP KIX domain both interact with Srebp-1a, a transcriptional activator responsible for controlling cholesterol and lipid homeostasis.[14, 16]

The KIX domain of CBP is an 87 amino acid module comprised of three α-helices and two 3_{10} helices, the solution structure for which was solved by Professor Peter Wright's research group in 1997.[17] The KIX domain interacts with greater than 15 transcriptional activators through two distinct hydrophobic binding sites.[6, 13, 18, 19] A

larger, more shallow binding site, shown bound by Myb on the left in Figure III-4a is formed at the interface of α1 (L599, H602, L603, K606, L607, and A610) and α3 (Y650, L653, A654, I657, Y658, Q661, and K662).[17, 20] A smaller but deeper binding site on the opposite and top face of the protein is formed by the sidechains of the C-terminus of α1 (I611), L_{12} (F612), the N-terminal half of α2 (R624, L628, and Y631) and the C-terminus of α3 (L664) and is shown bound by MLL in the diagram on the right in Figure III-4a.[6, 21] Examples of other transcriptional activation domains that bind each site are listed and their sequences are shown in Figure III-4b. The factors that lead to a TAD utilizing one site over another have not been elucidated. Thus, in addition to confirming that iTAD **III-1** interacts with the KIX domain, there was an additional query of binding site specificity.

a)

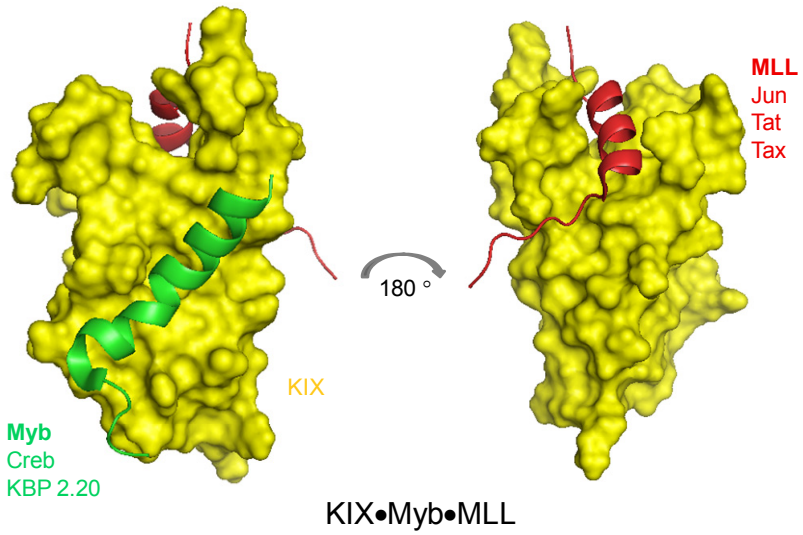

b)

Larger binding site:

Myb 291 KEKRIKELELLLMSTENELKGQQAL 315
Creb 119 TDSQKRREILSRRPSYRKILNDLSSDAPG 147

Smaller binding site:

MLL 2840 DCGNILPSDIMDFVLKNTP 2858
cJun 47 GSLKPHLRAKNSDLLTSPDVGLLKLASPELERLIIQSS NGHIT 89
Tat 1 MEPVDPRLEPWKHPGSQPKTACTN 24
Tax 59 IDGRVIGSALQFLIPRLPSFPTQRTSKTLKVLTPPIT 95

Figure III-4. CBP KIX domain and its TAD binding partners. a) The CBP KIX domain contains two binding sites. Each interacts with multiple TADs.[6] Figure adapted from 2agh. b) TADs that interact with the same binding site within the KIX domain have little sequence homology.

C. iTAD III-1 Interaction With the CBP KIX Domain

1) Initial Assessment

To assess whether **III-1** interacts with the KIX domain, one-dimensional ^{13}C, ^{1}H-HSQC experiments were carried out with a variant of **III-1** (**III-5**), in which a ^{13}C label was installed at the benzylic position, in the absence and presence of a hexahistidine-tagged murine KIX domain [CBP(586-672)] with a polar linker (His_6KIX), Figure III-5a. The ^{13}C labeled small molecule was synthesized with minor modification to the route utilized to access **II-25** (page 30). The spectrum of the small molecule in the absence of protein contained two resonances, one for each benzylic proton. In the presence of protein, with the small molecule in excess, a second set of peaks appeared corresponding to the small molecule in the bound form. The dual set of peaks is consistent with a slow exchange process. To assess the affinity of the co-complex of iTAD **III-1**•KIX a fluorescence polarization experiment was conducted by my colleague Dr. Steve Rowe with **III-1-fluorescein** and His_6KIX and yielded a K_D of 38 μM ± 4 μM (Figure III-5b). This is consistent with dissociation constants for endogenous KIX ligands (K_Ds ranging from 300 nM to 40 μM).[17, 19-22] From this point, NMR spectroscopy was used to identify the binding site(s) and further characterize the interaction.

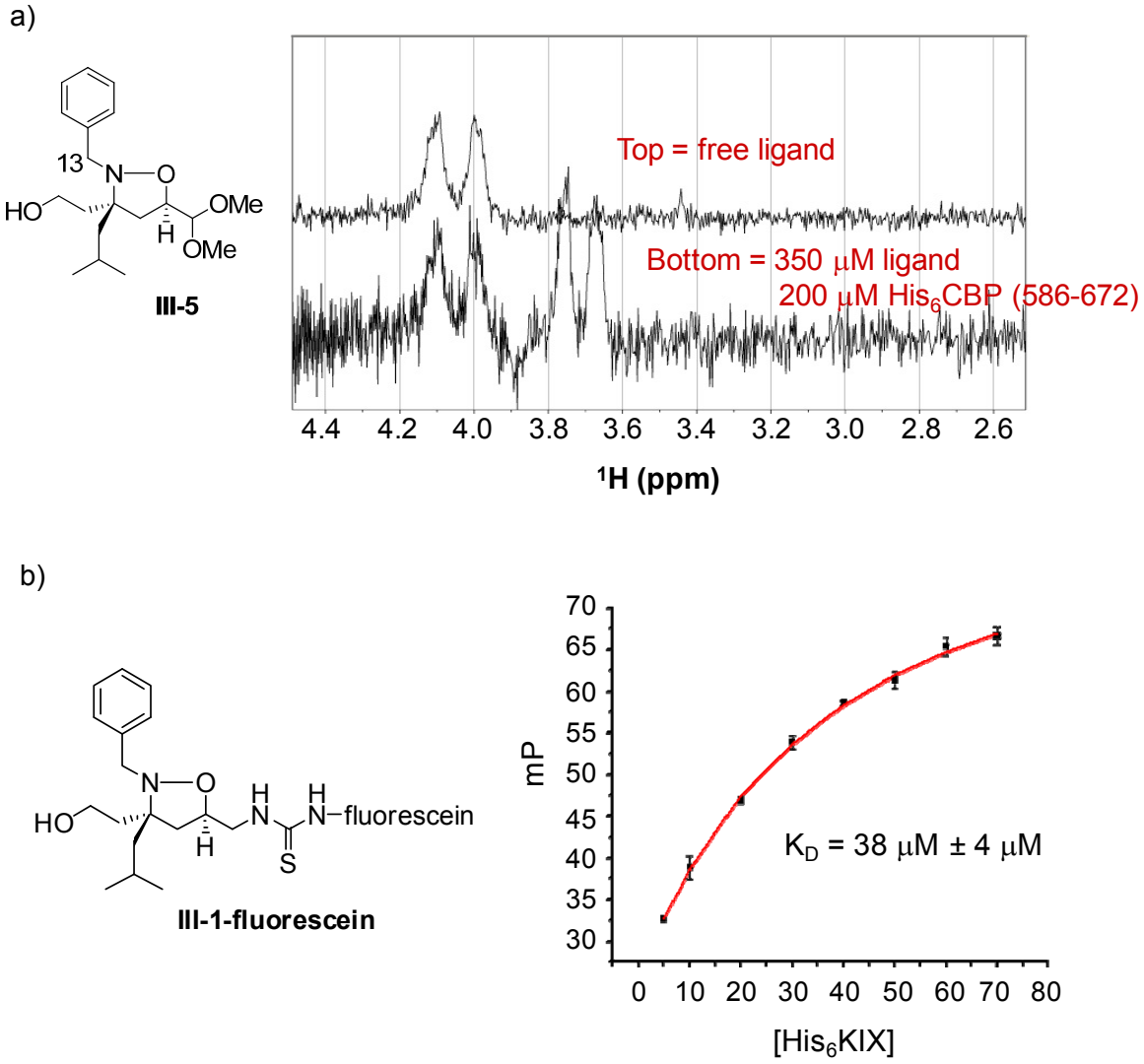

Figure III-5. iTAD **III-1** binds the CBP KIX domain. a) 1D ^{13}C, ^{1}H-HSQC of **III-5** in the absence and presence of His_6KIX. b) The interaction occurs with a K_D of 38 μM ± 4 μM.

2) Binding Site Identification

To identify the binding site(s) of iTAD **III-1**, His_6KIX uniformly labeled with ^{15}N was overexpressed and purified and a ^{15}N, ^{1}H-HSQC spectrum of the protein in the absence and presence of **III-1b** was recorded. NMR samples consisted of 400 μM ^{15}N-His_6KIX in 90% H_2O/10% D_2O 10 mM phosphate buffer with 150 mM NaCl and 1% (vol/vol) CD_3OD at pH 7.2 and varying concentration of ligand as indicated. Spectra were recorded at 27 °C. The spectrum of this fragment of CBP without a tag has been fully assigned by the research group of Professor Peter Wright and facilitated assignment

of this His-tagged variant.[17] Approximately 90% of the 87 KIX residues assignments could be transferred to the spectrum of our protein; not all residues could be assigned at this pH due to chemical shift degeneracy and line broadening effects. The full spectrum with resonances labeled is shown in Figure III-6. Resonances not visible at the contour level shown, but visible at higher contours are shown in purple. Resonances originating from a polar linker between the histidine-tag and KIX protein are indicated by red boxes and stars.

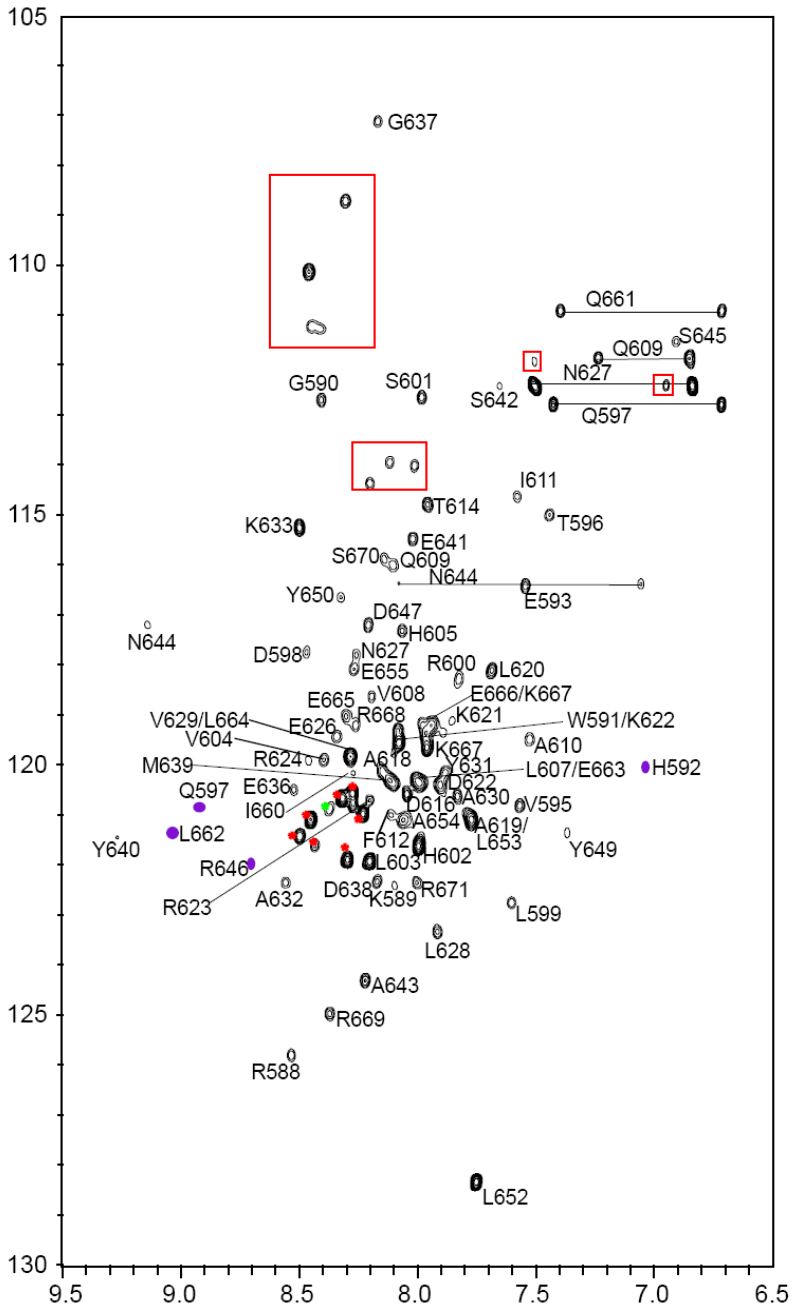

Figure III-6. 2D ^{15}N, ^{1}H-HSQC of ^{15}N-His$_6$KIX. Resonances from amino acids that comprise a linker between the histidine-tag and protein are indicated by red boxes and stars. Purple resonances are not observed at the countour level shown here, but are visible at higher contours.

A titration experiment was conducted in which increasing concentrations of **III-1b** were added to ^{15}N-His$_6$KIX; this induced progressive changes in the ^{1}H and ^{15}N chemical shifts, indicating that complex formation is occurring in the fast exchange regime. Similar evaluations for three endogenous TADs that bind the KIX domain have been conducted by the Wright and Lumb research groups. These show that two, Jun and Tax,[19, 22] also interact with the KIX domain on the fast exchange timescale and one, MLL,[6] binds in the slow exchange regime as indicated by concomitant disappearance and reappearance of peaks. Thus, by this evaluation iTAD **III-1** exhibits similar kinetic behavior as at least a subset of the endogenous activators that function through binding interactions with CBP. Interestingly, the small molecule exhibits slow exchange and the protein exhibits fast exchange. While not commonly reported, this is possible and in fact has been observed for the CREB transcriptional activation domain (Kid) in complex with KIX.[17, 23]

A region of the spectrum of His$_6$KIX upon addition of saturating quantities of **III-1b** is shown in red overlayed on the spectrum of the free protein in black in Figure III-7a and residues that shifted are labeled. To facilitate binding site identification by chemical shift perturbation mapping, the chemical shifts were quantitated, $\delta\Delta = [(\delta\Delta_{HN})^2 + 0.1(\delta\Delta_N)^2]^{1/2}$, and plotted against residue number (Figure III-7b). Chemical shift perturbation mapping has proven to be a reliable method for binding site identification with the KIX domain.[19, 22, 24] The average chemical shift was 0.016 ppm and the largest shift was 0.066 ppm for R623. The black line in Figure III-7b indicates the average shift. The magnitude of the shifts observed upon binding iTAD **III-1** is comparable to endogenous ligands; for example the average chemical shift observed for KIX residues upon binding Tax or Jun is 0.02 ppm with the largest shift for those ligands just over 0.1 ppm.[19, 25] In the case of **III-1**, the plot of chemical shifts revealed that the shifts are not uniform across the sequence, but clustered, indicative of specific binding. Residues that experienced chemical shifts greater than two standard deviations above the average are V608, A618, L620, K621, and R623. Residues that experienced shifts one standard deviation above the average are I611, T614, R624, and E665. The shifts map onto the C-terminus of α1, L_{12}, G2, and the N-terminus of α2, corresponding to the MLL/Tax/Jun/Tat binding site.[19, 21, 24, 25] As a visualization of the shared binding site, the

residues that experience the largest chemical shift perturbation upon binding iTAD **III-1**, MLL, and Jun are highlighted in red in the space filling diagrams of the KIX domain in Figure III-7c.[19, 21]

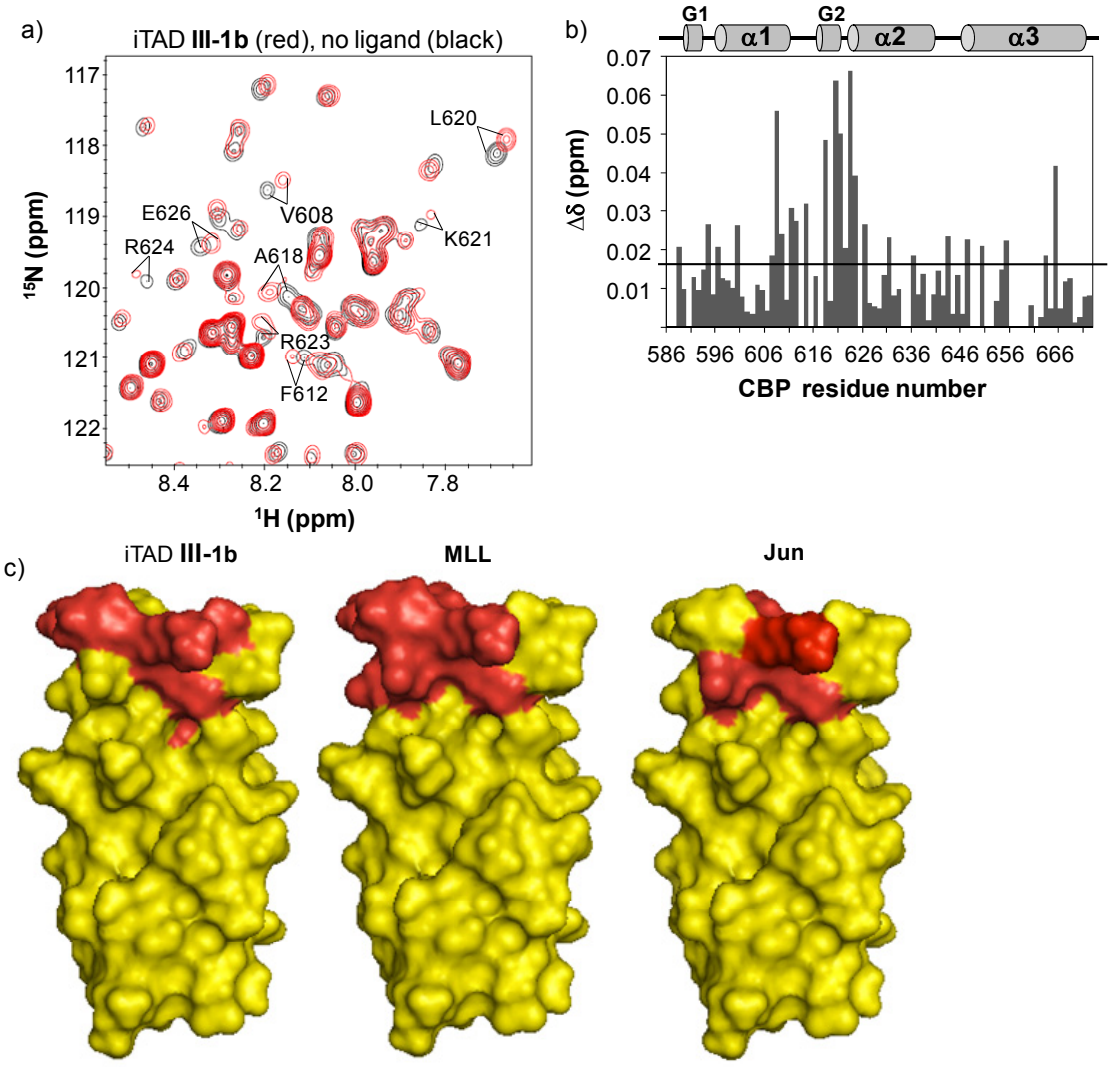

Figure III-7. iTAD **III-1** binds the MLL/Jun/Tat/Tax site. a) ^{15}N, ^{1}H-HSQC spectrum of ^{15}N-His$_6$KIX in the presence of five-fold excess iTAD **III-1b** (red) is overlayed on the spectrum on the free ^{15}N-His$_6$KIX (black). b) Chemical shift perturbation map of KIX upon binding **III-1**. c) **III-1**, MLL, and Jun share a binding site. The residues in red in the space filling diagrams experience that largest chemical shift upon binding the respective ligand. Figures were adapted from 1kdx.

These experiments demonstrated that, in fact, iTADs function as intended by binding at least a subset of the same coactivator binding sites as their endogenous

counterparts. Further, similarities between iTAD **III-1** and endogenous TADs extend to both thermodynamic and kinetic parameters. Importantly, this is also the first example of a small molecule to selectively bind one of the KIX domain binding sites utilized by endogenous TADs and thus **III-1** should be a valuable tool for elucidating the functional role of particular CBP molecular recognition events. CBP is a large 250 kD protein that is an important node in many signaling networks and suggested to be present in limiting quantities in cells.[7, 8, 26, 27] Deletion of CBP is embryonic lethal and loss of a single CBP allele leads to severe development defects.[28-30] Additionally, CBP is involved in mediating the function of several viral transcriptional activators including those associated with HIV and the adult T-cell leukemia virus as well transcriptional activators involved in angiogenesis, lipid homeostasis and myeloid leukemias.[31-35] Reflective of the importance of CBP in mediating transcription, CBP interacts with >300 transcriptional activators through 5 protein binding motifs.[36]

D. Additional iTADs Interact with CBP

As outlined above, the KIX domain of CBP interacts with ≥15 amphipathic TADs despite differences in sequence and significant changes in the identity and spacing of the hydrophobic side chains do not preclude binding to this domain. Thus it might be predicted that iTADs with different side chains and/or side chain arrangement would maintain KIX binding ability. To test this, we examined the interaction of three additional isoxazolidines with CBP (Figure III-8). Isoxazolidine **III-2** has the same functional groups as **III-1** but in a different orientation. Hydrophobic isoxazolidine **III-3** maintains the two key hydrophobic functional groups present in **III-1** (benzyl, isobutyl) but lacks the C3 hydroxyl moiety. In the case of **III-4**, the C3 substituents are identical to **III-1** but the N2 substituent is now a larger, biphenyl sidechain.

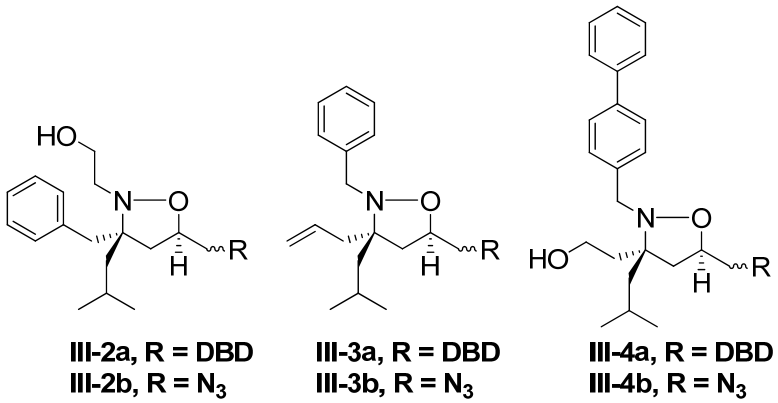

Figure III-8. Additional isoxazolidines evaluated for KIX binding.

To assess binding of iTAD **III-2** to the CBP KIX domain a ^{15}N, ^{1}H-HSQC of ^{15}N-His$_6$KIX was collected in the presence of ligand and compared to the spectrum of the free protein. Figure III-9 shows the spectrum of ^{15}N-His$_6$KIX bound by **III-2** (cyan) overlayed on the protein bound by **III-1** (red) and free protein (black). The residues that shift upon addition of **III-2** to ^{15}N-His$_6$KIX are nearly identical to those observed for **III-1** as was the direction and magnitude of the shifts. A subset of these residues is labeled in Figure III-9a.

Subsequently the two isoxazolidines (**III-3** and **III-4**) with increased hydrophobic surface area for binding protein surfaces, surface area that would presumably enhance the interaction with coactivator binding surfaces, were evaluated analogously for binding the CBP KIX domain. This revealed there is not an interaction between the KIX domain and either **III-3** or **III-4**. The spectra of the CBP KIX domain in the presence of **III-3** (green) and **III-4** (purple) are overlayed on the spectrum of free protein (black) in Figure III-9b. A portion of the residues that experienced chemical shift perturbation upon binding **III-1** are labeled. These results are unlikely due to compromised solubility or aggregation. The ^{1}H NMR spectrum of **III-3b** alone in NMR buffer showed a sharp, well-defined spectrum (Figure III-9c) analogous to that obtained in organic solvents. However upon combination with ^{15}N-His$_6$KIX, **III-2b** did not bind either of the protein's binding sites. The resonances of R600 and F612 are the only two that experienced a significant chemical shift perturbation in the presence of **III-3** and **III-4** perhaps attributable to hydrophobic or ∏-stacking interactions with the small molecules.

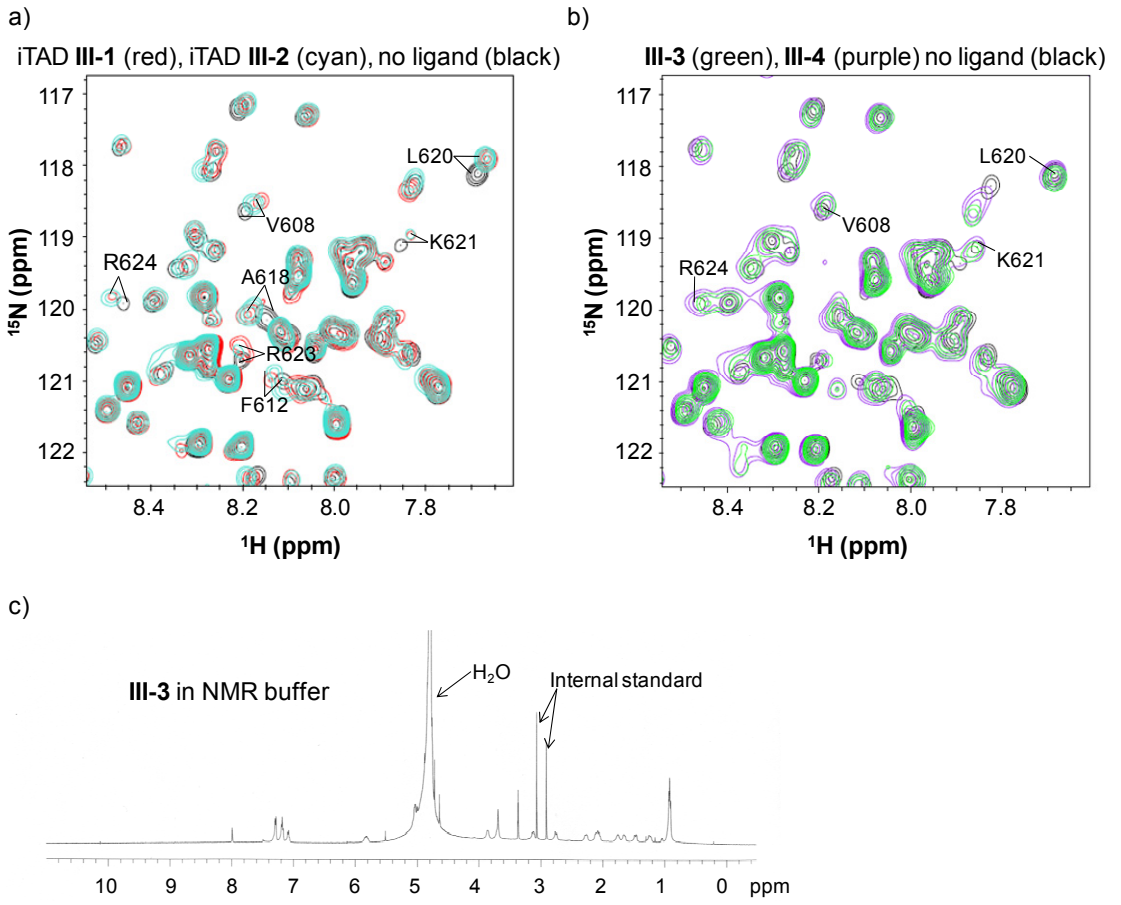

Figure III-9. Evaluation of KIX binding of **III-2**, **III-3** and **III-4**. a) Overlay of the ^{15}N, ^{1}H-HSQC of ^{15}N-His$_6$KIX in the presence of **III-2b** (cyan), **III-1b** (red) and no ligand (black). b) Overlay of the ^{15}N, ^{1}H-HSQC of ^{15}N-His$_6$KIX in the presence of **III-3b** (green), **III-4b** (purple) and no ligand (black). c) ^{1}H spectrum of **III-3** in NMR buffer.

This result suggests that although coactivator binding sites are large hydrophobic grooves the presence and positioning of polar functionality is important in the molecular recognition of at least a subset of binding sites.[17, 37] One possible hypothesis is that while polar groups of TADs typically make minimal contributions in terms of binding affinity the interactions of these sidechains may be important in controlling specificity. As a probe of this and the ability of iTADs to bind multiple coactivator proteins the ability of **III-1, III-3** and **III-4** to interact with other coactivators was evaluated.

E. Interaction of Isoxazolidines III-1, III-3 and III-4 with Other Coactivators

Mediator proteins Med15 and Med23, and Tra1, a component of the SAGA and NuA4 complexes, all common targets of endogenous TADs, were evaluated as binding partners of **III-1, III-3,** and **III-4** using binding assays (Table III-1). The fluorescein-tagged variant, **III-1-fluorescein**, of iTAD **III-1** described above (Figure III-5) interacted with all three coactivators: Tra1 with a K_D = 9 μM (Chinmay Majmudar), Med15 with a low μM K_D (Steve Winter) and Med23 with a K_D = 6 μM (JP Desaulnier).

A fluroescein-tagged variant of **III-3** was also prepared for assessment of binding Tra1, Med15 and Med23 using fluorescence polarization experiments. The single experiment conducted thus far determined that **III-3** binds Med23 with a K_D = 500 nM. Dr. J. P. Desauliner showed that **III-4** binds Sur2 and Med23, both in the low μM range.

Overall, these experiments yielded two important results. First, analogous to endogenous TADs, iTAD **III-1** exhibits a low K_D, multipartner binding profile with transcriptional machinery proteins. Second, these experiments unexpectedly revealed that one distinguishing feature of iTADs is the ability to interact with the CBP KIX domain. During the course of this work, the solution structure of the KIX domain in complex with MLL was published and based upon comparison to that structure a binding model for **III-1** is put forth.[6] Further examination of the KIX•MLL structure provides a rational for the inability of **III-3** and **III-4** to interact with the KIX domain.

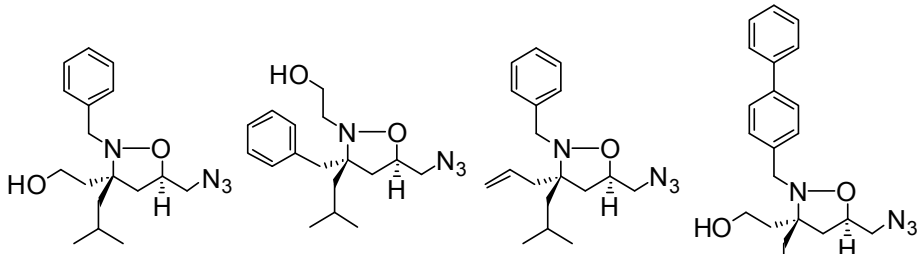

	III-1	III-2	III-3	III-4
Functions as an iTAD	+	+	−	−
CBP	+	+	−	−
Sur2	+		+	+
Tra1	+			
Med15	+			+

Table III-1. Summary of identified isoxazolidine coactivator binding partners.

F. iTAD III-1•KIX Binding Model

Of the many endogenous TADs that bind the same site on the CBP KIX domain as iTAD **III-1**, only in the case of MLL has a structure of a TAD in complex with the KIX domain been solved, enabling a more detailed comparison with the small molecules. Of the human MLL fragment 2842-2869 that was utilized by the Wright group to solve the solution structure only 2847-2857 (Figure III-10a) adopt an amphipathic helical structure upon binding the protein; for clarity only these residues are utilized in the picture of MLL•KIX in Figure III-10b.[6] Of these residues, the side chains of five, one polar (T2857) and four hydrophobic (I2849, F2852, V2853, and L2854), make extensive contacts with the KIX binding groove contributing to a K_D of 3 μM.[21] In the view of the KIX domain shown bound by MLL in Figure III-10b, looking down the top of the protein, three of the five critical residues for binding can be seen, a phenylalanine, leucine, and threonine. Remarkably, the side chains of these residues are nearly identical to the three functional groups of iTAD **III-1**, one polar (C3 hydroxyl) and two

hydrophobic (N2 benzyl and C3 isobutyl), for interacting with the KIX domain; the substituent at C5 (the point of attachment for DNA binding functionality in the context of activation) does not contribute significantly to binding as an analog of **III-1** containing the larger and more polar dimethoxyacetal substituent at the C5 position exhibits nearly identical binding behavior. Further, the relative spacing of the three substituents is also comparable suggesting a binding orientation in which each of the iTAD substituents projects into the same subsite as the analogous MLL sidechain. While the iTAD core is smaller than the helix of MLL, the binding site on the KIX domain that recognizes these ligands has been shown to undergo significant structural rearrangement upon binding MLL and this flexible nature may enable the binding site to adapt to recognize the smaller ligand.[6, 18] Consistent with this hypothesis several residues in or near the binding pocket are line broadened in our experiments (for example, V608, K621, R624, and K621) suggesting flexibility of that region.

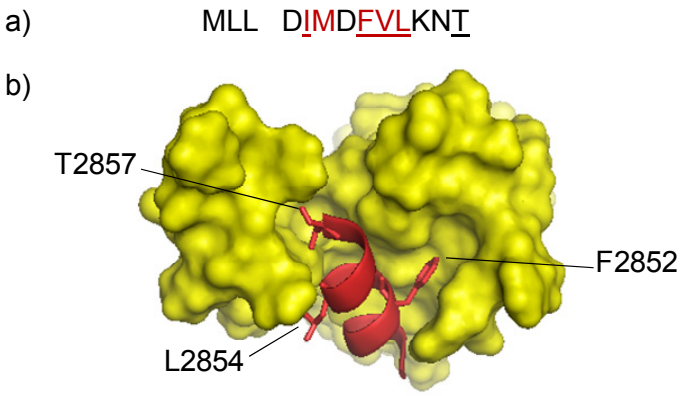

Figure III-10. MLL•KIX solution structure. a) I2849, F2852, V2853, L2854, and T2857 of MLL make extensive hydrophobic contacts with the KIX domain upon binding. Only the MLL residues shown form an amphipathic helice upon binding. b) The position of MLL residues F2852, L2854, and T2857 can be seen viewing the protein from the top.[6] Figure adapted from 2agh.

The recognition of **III-2**, a positional isomer of **III-1**, by the KIX domain supports that as it does to bind endogenous TADs, the binding site can tailor itself to recognize iTADs with different functional group orientation. The observation that **III-3**, which lacks the C3 hydroxyl but otherwise mimics **III-1**, does not bind the KIX domain

is consistent with a polar group mimicking the binding interaction of the threonine side chain and both hydrophobic groups being required for interaction. In the case of **III-4**, which contains the larger biphenyl moiety, an examination of the TADs that interact with this KIX site revealed that only a single large hydrophobic amino acid (W at residue 11 of Tat) that would be similar in size to the biphenyl moiety.[19, 21, 24, 25] Further, a F2852Y mutation within the MLL TAD abrogates binding to KIX and concomitantly reduces MLL-mediated transcription by 60%.[38] Thus, at least in the case of this TAD-binding site, large hydrophobic groups do not appear to be well-tolerated.

G. Conclusions

The NMR and fluorescence polarization experiments evaluating complex formation between iTAD **III-1** and coactivators demonstrate that analogous to its endogenous counterpart iTAD **III-1** interacts with multiple transcriptional machinery proteins, including CBP, Med15, Med23, and Tra1. Of these, the interaction with CBP was investigated in detail resulting in the discovery of the first small molecule to target a site on the CBP KIX domain utilized by endogenous TADs. Further, isoxazolidine **III-1** forms a complex with this binding partner with similar thermodynamic parameters as endogenous TADs that use the same site. In fact, iTAD **III-1** shows remarkable similarity to the endogenous transcriptional activators such as MLL in terms of functional group content and structure.

The activity of the isoxazolidines evaluated parallels their ability to bind the CBP KIX domain suggesting that CBP binding is an essential component of iTAD function. An initial assessment of this suggests that screening for molecules that bind either of the binding sites on the KIX domain should produce small molecules that function as TADs. This strategy has been pursued and proven unsuccessful, however. The Montminy lab conducted an NMR screen of 762 small molecules for binding to the KIX domain and only two hits were obtained and neither molecule bound a KIX site utilized by endogenous activators.[39] Consistent with this small structural changes within the isoxazolidine scaffold significantly altered the binding profile with the KIX domain. This ultimately suggests that some degree of specificity for a given coactivator or coactivator class may indeed be achievable within this framework.

H. Experimental

General.

Unless otherwise noted, starting materials were obtained from commercial suppliers and used without further purification. CH_2Cl_2, THF, CH_3CN and toluene were dried by passage through activated alumina columns and degassed by stirring under a dry N_2 atmosphere. BF_3•OEt_2 and Et_3N were distilled from CaH_2. All reactions involving air- or moisture-sensitive reagents were performed under a dry N_2 atmosphere.[40] Purification by column chromatography was carried out with E. Merck Silica Gel 60 (230-400 mesh) according to the procedure of Still, Kahn, and Mitra.[41] ^1H and ^{13}C NMR spectra were recorded in $CDCl_3$ at 500 MHz and 125 MHz, respectively, unless otherwise specified. IR spectra were measured as thin films on NaCl plates. The synthesis of **III-1b** and, **III-3b** were reported in Chapter II. **III-4** was prepared by JP Desaulnier. **III-2** is reported here, compounds that do not appear in the text are numbered **S1-S3.**

Hexa-histidine tagged CBP (586-672) with polar linker, His_6KIX, sequence.

Lower case corresponds to the linker, upper case corresponds to KIX residues 586-672:

mrgshhhhhhgmasmtggqqmgrdlyddddkdpssrsGVRKGWHEHVTQDLRSHLVHKLVQAI
FPTPDPA ALKDRRMENLVAYAKKVEGDMYESANSRDEYYHLLAEKIYKI QKEL
EEKRRSRL

^{15}N-His_6KIX overexpression and purification.

The His_6KIX plasmid, prepared by Dr. Steve Rowe as reported in his PhD thesis, was transformed into freshly grown Rosetta pLysS cells. The transformed cells were grown on an LB agar plate supplemented with 0.1 mg/mL ampicillin and 0.034 mg/mL chloramphenicol. The cells were grown for approximately 18 hours at 37 °C. Single colonies were selected from the plate and used to inoculate 50-mL cultures of LB supplemented with 0.1 mg/mL ampicillin and 0.034 mg/mL chloramphenicol. The cultures were grown for 12 h at 37 °C with shaking at 250 rpm. 25 mL of the starter culture were then used to inoculate 1 L M9 minimal media (recipe below) supplemented with 0.1 mg/mL ampicillin. The 1 L cultures were grown until the OD_{600} reached 0.4, typically 12 hours. The temperature on the incubator was lowered to 25 °C and

expression of the protein was induced with 0.5 mM IPTG for 12 hours. The cells were then centrifuged for 20 min at 6,000 rpm and the pellets were stored at -80 °C overnight.

For protein isolation the cells were resuspended in 25 mL lysis buffer (100 mM PBS, pH 7.2) per 2L culture volume and lysed using a sonic dismembrator (120 s total with 30 s on, 30 s off intervals). The cells were kept on ice throughout the sonication. The crude lysis solution was centrifuged at 9500 rpm for 30 min at 4 °C. The resultant supernatant was batch bound to 1 mL (per L culture volume) of Ni-NTA beads (Qiagen) for 1 h at 4 °C. The solution was centrifuged at 2500 rpm for 2 min at 4 °C and the supernatant discarded. The resin was washed six times with 2 mL aliquots of wash buffer (100 mM PBS, 30 mM imidazole, pH 7.2) and the protein was then eluted from the beads with 3-5 mL elutions with elution buffer (100 mM PBS, 300 mM imidazole, pH 7.2). The first elution occurred for 1 h and the subsequent two for 30 min each. The combined eluted fractions were lyophilized to a powder. The powder, including imidazole and phosphate salts, was resuspended in 50/50 CH_3CN/H_2O and centrifuged at 2500 rpm for 30 sec to pellet the insoluble fraction. The supernatant was loaded onto PD-10 desalting columns (GE Healthcare) and eluted with 50/50 CH_3CN/H_2O. The solution was lyophilized to a powder and immediately utilized in NMR experiments.

^{15}N-His$_6$KIX NMR experiments.

The uniformly ^{15}N-labelled His$_6$KIX protein was prepared as a 300-400 μM solution in 90% H_2O/10% D_2O 10 mM phosphate buffer with 150 mM NaCl and 1% v/v CD_3OD at pH 7.2. Protein concentration was determined by Bradford assay. Samples containing small molecule ligands were prepared by adding 0.25-5.0 equivalents of the small molecule as a solution in CD_3OD to achieve a final CD_3OD concentration of 1%. ^{15}N, ^{1}H-heteronuclear single quantum coherence experiments were recorded at 27 °C on an Avance Bruker 600 MHz NMR spectrometer equipped with a triple-resonance 5 mm cryogenic probe. Typical experiments consisted of 256 complex increments defined by 40 or 56 transients and 1024 complex points. Data was processed using NMRPIPE and analyzed using Sparky.

Small molecule synthesis and characterization.

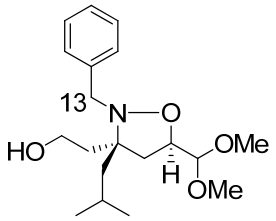

III-5

2-((3S,5R)-2-^{13}C-benzyl-5-(dimethoxymethyl)-3-isobutylisoxazolidin-3-yl)ethanol (III-5): Isoxazolidine **III-5** was prepared analogously to the previously reported unlabelled version;[1] all spectroscopy data was identical and incorporation of the ^{13}C-label was confirmed by mass spectrometry. HRMS calcd for $[C_{20}H_{31}NO_4 + Na]^+$: 361.2184, found 361.2180.

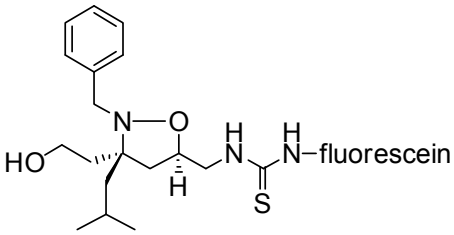

III-1-fluorescein

2-((3*S*,5*R*)-5-(azidomethyl)-2-benzyl-3-isobutylisoxazolidin-3-yl)ethanol 5-(3-(((3*S*,5*R*)-2-benzyl-3-(2-hydroxyethyl)-3-isobutylisoxazolidin-5-yl)methyl)thioureido)-2-(6-hydroxy-3-oxo-3H-xanthen-9-yl)benzoate (III-1-fluorescein): To a solution of **II-26** (5 mg, 0.02 mmol, 1.0 eq) in 200 μl DMF was added Et_3N (2.8 μl, 0.02 mmol, 1.0 eq) and FITC (7.8 mg, 0.02 mmol, 1.0 eq). The mixture was shielded from light and stirred at rt for 12 h at which point product formation was observed by ESI-MS. The solution was diluted with 1.8 mL of a 50/50 CH_3CN/0.1% TFA in H_2O mixture and purified by reverse phase HPLC using a 0.1% TFA in H_2O/CH_3CN gradient. The purity of compound SI was confirmed by analytical reverse-phase HPLC and product identify confirmed by mass spectral analysis. LRMS calcd for $[C_{38}H_{39}N_3O_7S + H]^+$: 682.9, found 682.3.

Characterization of III-2b and appropriate intermediates from III-S1.

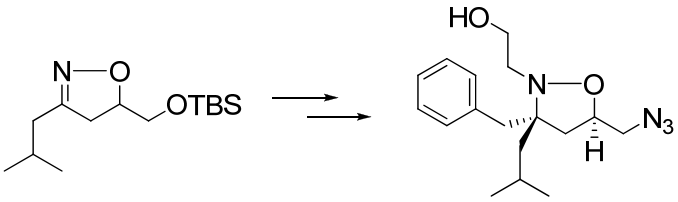

III-S1 **III-2b**

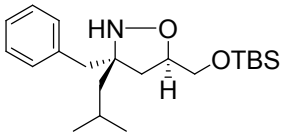

III-S2

(3*S*,5*R*)-3-benzyl-5-((tert-butyldimethylsilyloxy)methyl)-3-isobutylisoxazolidine (III-S2): To a solution of **III-S1** (500 mg, 1.8 mmol, 1.0 eq) in tol (12 mL) cooled in a dry ice-acetone bath was added $BF_3 \bullet OEt_2$ (670 µl, 5.4 mmol, 3.0 eq) over 15 min then the mixture was stirred an additional 30 min with continued cooling. Benzylmagnesium chloride (5.5 mL of a 2.0 M solution in THF, 11 mmol, 6.0 eq) was then added dropwise over 30 min. The reaction mixture stirred with continued cooling for 6h at which point TLC analysis indicated consumption of starting material. The mixture was diluted with saturated NH_4Cl (10 mL) and transferred to an ice-H_2O bath. After slowly warming to rt the mixture was diluted with H_2O (10 mL) and Et_2O (20 mL) and the aqueous and organic layers were separated. The aqueous was extracted with Et_2O (3 x 15 mL), and the combined organic extracts were washed with H_2O (15 mL) and brine (15 mL), dried over Na_2SO_4, filtered, and concentrated in vacuo. Purification by flash chromatography (elution in 95:5 hexanes/EtOAc) yielded 570 mg of a single diastereomer of product as a colorless oil in 87% yield. IR: 2927, 2858, 1603, 1494, 1452, 1254, 1118, 833 cm^{-1}; ^1H NMR: δ 0.04 (s, 3H), 0.05 (s, 3H), 0.88 (s, 9H), 0.96 (s, 3H), 0.97 (s, 3H), 1.29-1.40 (m, 2H), 1.87 (dd, 1H, J = 12.2, 6.4), 1.97-2.04 (m, 1H), 2.20 (dd, 1H, J = 12.0, 8.6), 2.69 (d, 1H, J = 13.2), 2.92 (d, 1H, J = 13.7), 3.56 (dd, 1H, J = 10.7, 2.4), 3.82 (bs, 1H), 4.18 (bs, 1H), 5.32 (bs, 1H), 7.18-7.28 (m, 5H); ^{13}C NMR: δ -5.54, -5.50, 18.20, 24.10, 24.36, 24.46, 25.85, 41.05, 41.22, 42.93, 65.83, 68.58, 80.03, 126.1, 127.8, 130.6, 138.3; HRMS (ESI) calcd for $[C_{21}H_{37}NO_2Si + H]^+$: 364.2672, found: 364.2666.

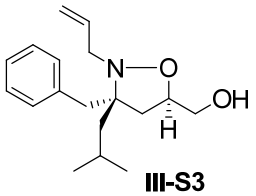

III-S3

((3*S*,5*R*)-2-allyl-3-benzyl-3-isobutylisoxazolidin-5-yl)methanol (III-S3): To a solution of **III-S2** (320 mg, 0.88 mmol, 1.0 eq) in 4.4 mL DMF was added allylbromide (460 µl, 5.3 mmol, 6.0 eq) and *i*Pr_2NEt (450 µl, 2.6 mmol, 3.0 eq). The mixture was irradiated in a 1000W microwave for 15 seconds at 20% power. The solution was cooled and irradiated 8 additional times, each time for 15 seconds at 20% power, with cooling between each interval. Upon completion of the reaction, as indicated my TLC analysis, the mixture was diluted with H_2O and Et_2O, the layers separated, and the aqueous layer extracted with Et_2O (3 x 10 mL). The combined organic extracts were washed with H_2O (2 x 10 mL) and brine (1 x 10 mL), dried over Na_2SO_4, filtered, and concentrated in vacuo. The crude product was dissolved in 4.4 mL THF and cooled in an ice-H_2O bath. TBAF (2.6 mL of a 1M solution in THF, 2.6 mmol, 3.0 eq) was added and the mixture was allowed to slowly warm to rt. The reaction was stirred 3h, at which point TLC analysis indicated complete consumption of the starting material. The reaction mixture was diluted with H_2O and Et_2O and the layers separated. The aqueous layer was extracted with Et_2O (3 x 10 mL) and the combined organic extracts were washed with brine (1 x 10 mL), dried over Na_2SO_4, filtered, and concentrated in vacuo. The crude product was purified by flash chromatography (elution in 80:20 hexanes/EtOAc) to yield 170 mg of **III-S3** as a colorless oil in 68% yield. IR: 3428, 2954, 1645, 1453, 1031, 702 cm^{-1}; ^{1}H NMR: δ 0.86 (d, 3H, J = 6.35), 0.94 (d, 3H, J = 6.8), 1.30 (dd, 1H, J = 6.8, 14.7), 1.59 (dd, 1H, J = 3.9, 14.7), 1.82-1.89 (m, 1H), 1.89 (dd, 1H, J = 6.8, 12.7), 2.18 (dd, 1H, J = 8.3, 12.7), 2.40 (bs, 1H), 2.61 (d, 1H, J = 13.2), 2.91 (d, 1H, J = 13.2), 3.37 (m, 2H), 3.55 (m, 1H), 3.69 (ddd, 1H, J = 3.2, 5.4, 11.5), 4.10-4.14 (m, 1H), 5.14 (dd, 1H, J = 1.5, 10.3), 5.25 (dd, 1H, J = 1.5, 17.1), 5.93-6.01 (m, 1H), 7.16-7.17 (m, 2H), 7.19-7.22 (m, 1H), 7.26-7.29 (m, 2H); ^{13}C NMR: δ 24.52, 25.33, 36.57, 39.21, 42.40, 52.18, 53.36, 65.54, 69.28, 75.55, 116.3, 126.1, 128.0, 130.7, 135.4, 138.4; HRMS (ESI) for $[C_{18}H_{27}NO_2 + Na]^+$: 312.1939; found: 312.1946.

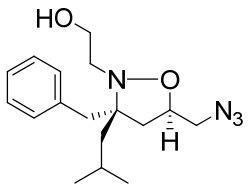

III-2b

2-((3*S*,5*R*)-5-(azidomethyl)-3-benzyl-3-isobutylisoxazolidin-2-yl)ethanol (III-2b): To a solution of **III-S3** (150 mg, 0.52 mmol, 1.0 eq) in CH_2Cl_2 (5.2 mL) cooled in an ice-H_2O bath was added Et_3N (80 µl, 0.57 mmol, 1.1 eq) followed methanesulfonyl chloride (44 µl, 0.57 mmol, 1.1 eq). TLC analysis indicated complete conversion to the mesylate after 30 min and the reaction mixture was diluted with 5 mL H_2O. The organic and aqueous layers were separated and the aqueous was extracted with CH_2Cl_2 (3 x 5 mL). The combined organic extracts were washed with brine (1 x 10 mL), dried over Na_2SO_4, filtered, and concentrated in vacuo. The crude mixture was dissolved in DMF (5.2 mL) and NaN_3 (340 mg, 5.2 mmol, 10 eq) was added to the solution. The flask was fitted with a reflux condenser and heated for 12 h at reflux at which point TLC analysis indicated complete consumption of starting material. The mixture was diluted with H_2O (10 mL) and extracted with Et_2O (3 x 10 mL). The combined organic extracts were washed with H_2O (2 x 10 mL) and brine (10 mL), dried over Na_2SO_4, filtered, and concentrated in vacuo. The crude product was passed through a plug of silica gel to remove polar impurities and utilized in subsequent oxidative cleavage of the olefin. To a solution of the product (120 mg, 0.38 mmol, 1.0 eq) in *t*BuOH (2.85 mL), THF (760 µl) and H_2O (190 µl) was added NMO (54 mg, 0.46 mmol, 1.2 eq) followed by OsO_4 (410 µl of a 2.5 wt% solution in *t*BuOH, 0.04 mmol, 0.1 eq). The reaction mixture was stirred for 6h at which time TLC indicated completion of the reaction. Na_2SO_3 (100 mg) was added to quench excess reagents and the mixture was stirred for 1h. The mixture was then diluted with EtOAc (5 mL) and H_2O (5 mL) and the layers separated. The aqueous layer was extracted with EtOAc (3 x 5 mL). The combined organic extracts were washed with brine (1 x 10 mL), dried over Na_2SO_4, filtered, and concentrated in vacuo. The crude diol product was dissolved in CH_3CN (1.9 mL) and H_2O (1.9 mL) and $NaIO_4$ (98 mg, 0.46 mmol, 1.2 eq) was added. TLC analysis indicated complete consumption of the starting material after stirring at rt for 1h. The reaction mixture was diluted with H_2O (5 mL) and Et_2O (5 mL) and the aqueous and organic layers separated. The aqueous layer was

extracted with Et_2O (3 x 5 mL) and the combined organic extracts were washed with H_2O (10 mL) and brine (10 mL), dried over Na_2SO_4, filtered, and concentrated in vacuo. To the crude mixture dissolved in MeOH (3.8 mL) cooled in an ice-H_2O bath was added $NaBH_4$ (41 mg, 1.1 mmol, 3.0 eq) and the reaction was stirred for 30 min at which time TLC analysis indicated complete consumption of the starting material. The reaction mixture was diluted with H_2O (5 mL) to quench excess reagent and allowed to slowly warm to rt. Et_2O (10 mL) was added to the mixture and the organic and aqueous layers separated. The aqueous layer was extracted with Et_2O (3 x 10 mL) and the combined organic extracts were washed with brine (15 mL), dried over Na_2SO_4, filtered, and concentrated in vacuo. The crude product was purified by flash chromatography (elution in 30:70 hexanes/EtOAc) to yield 130 mg of product in 78% yield as a colorless oil. IR: 3440, 2954, 2098, 1453, 1278, 1057 cm^{-1}; ^1H NMR: δ 0.89 (d, 3H, J = 6.8), 0.97 (d, 3H, J = 6.8), 0.97 (d, 3H, J = 6.8), 1.33 (dd, 1H, J = 5.9, 14.7), 1.56 (dd, 1H, J = 4.9, 14.7), 1.77-1.84 (m, 2H), 2.20 (dd, 1H, J = 8.3, 12.7), 2.49 (t, 1H, J = 5.9), 2.61 (d, 1H, J = 13.2), 2.87 (d, 1H, J = 13.2), 2.92 (m, 2H), 3.21 (dd, 1H, J = 3.7, 12.9), 3.34 (dd, 1H, J = 6.8, 12.7), 3.75-3.85 (m, 2H), 4.16-4.21 (m, 1H), 7.14-7.15 (m, 2H), 7.20-7.23 (m, 1H), 7.26-7.29 (m, 2H); ^{13}C NMR: δ 24.72, 25.36, 38.05, 39.38, 42.17, 51.09, 54.45, 60.98, 69.34, 74.97, 126.4, 128.2, 130.8, 138.0; HRMS (ESI) calcd for $[C_{17}H_{26}N_4O_2 + Na]^+$: 341.1953; found: 341.1958.

I. Appendix of Select ^{1}H NMR spectra and HPLC traces.

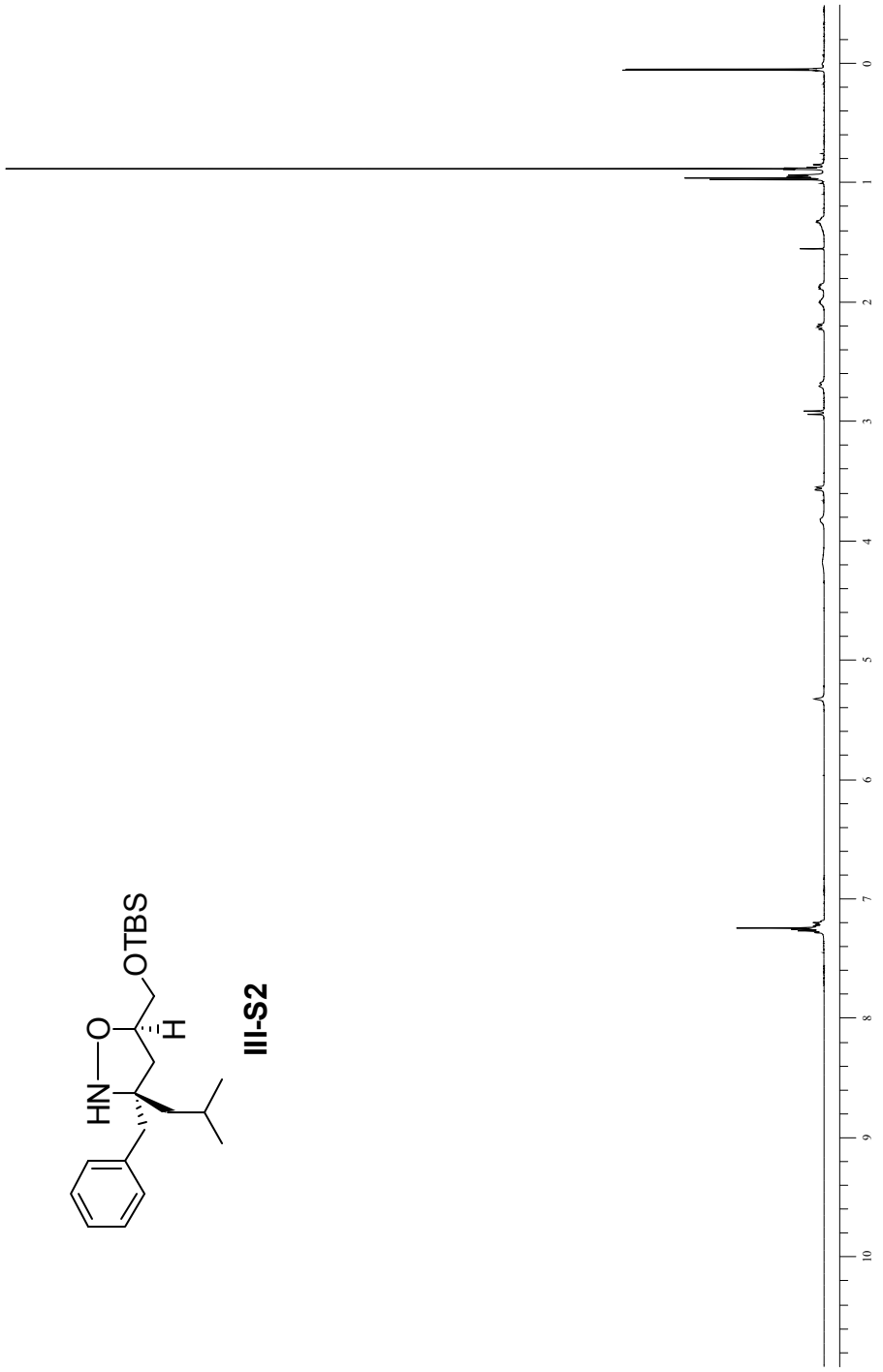

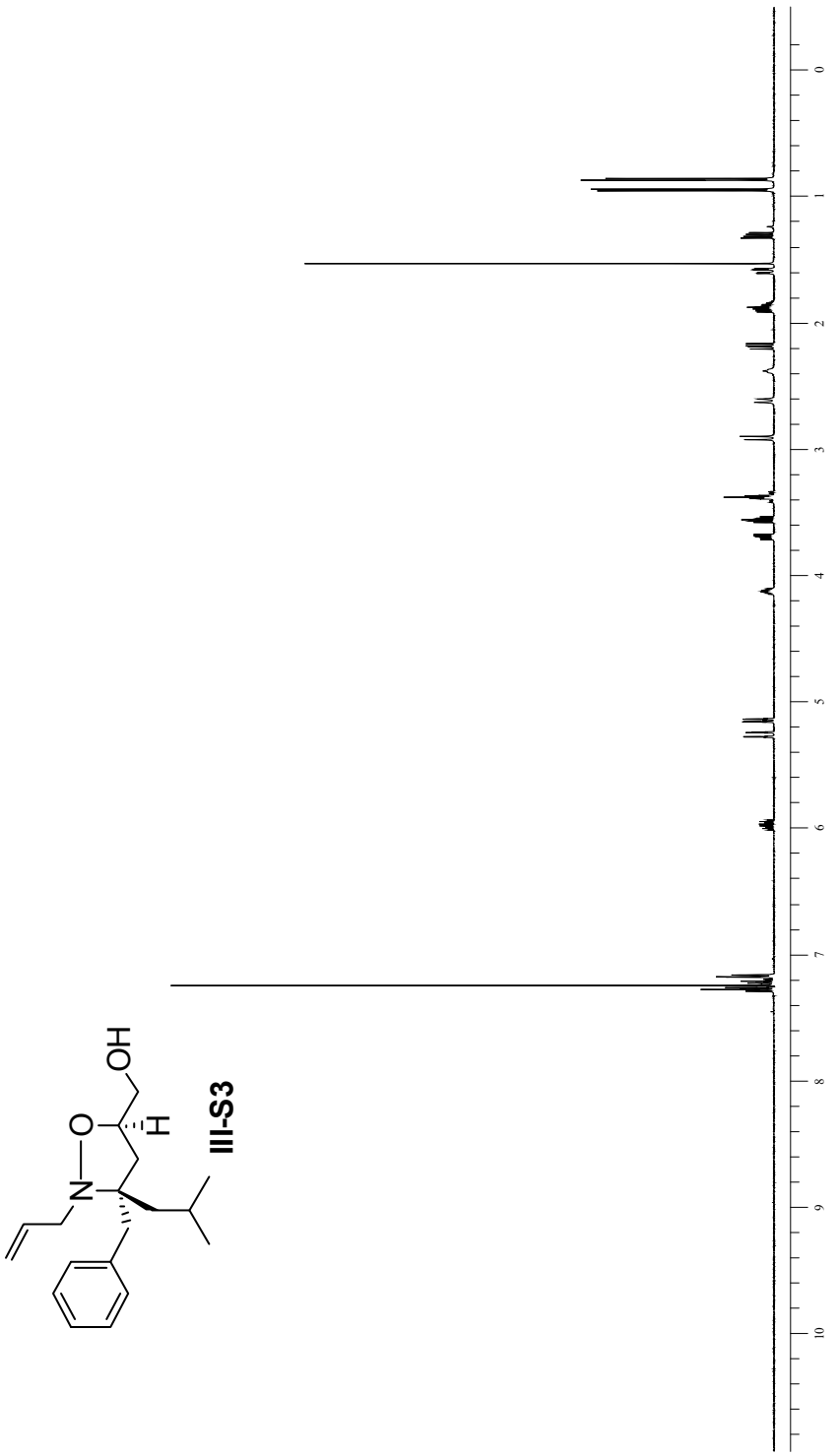
OH
H
O
N
III-S3

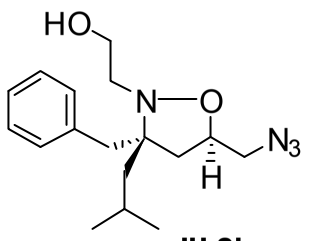

III-2b

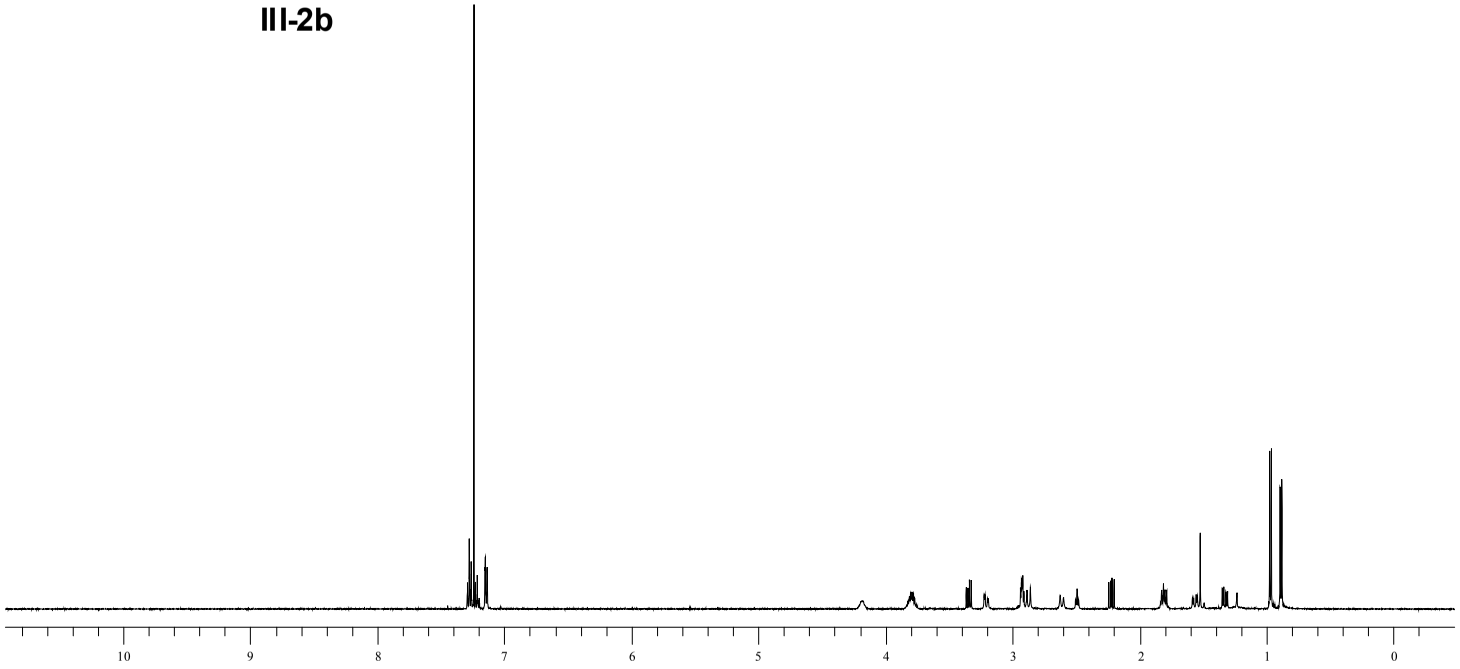

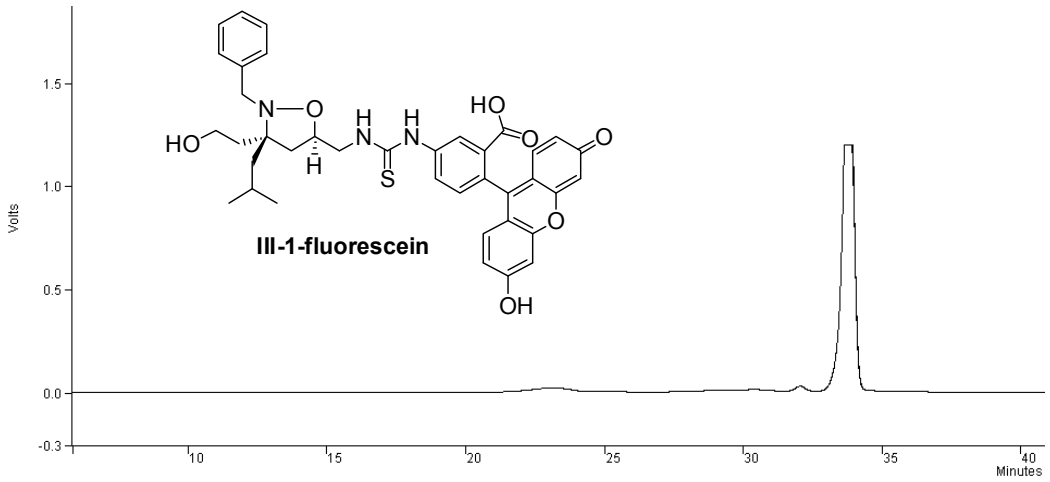

J. References

1. Minter, A. R.; Brennan, B. B.; Mapp, A. K., *J Am Chem Soc* **2004,** *126* (34), 10504-5.

2. Rowe, S. P.; Casey, R. J.; Brennan, B. B.; Buhrlage, S. J.; Mapp, A. K., *Journal of the American Chemical Society* **2007,** *129* (35), 10654-+.

3. Mapp, A. K.; Ansari, A. Z.; Ptashne, M.; Dervan, P. B., *Proc Natl Acad Sci U S A* **2000,** *97* (8), 3930-5.

4. Buhrlage, S. J.; Brennan, B. B.; Minter, A. R.; Mapp, A. K., *J Am Chem Soc* **2005,** *127* (36), 12456-7.

5. Casey, R. J.; Desaulniers, J. P.; Hojfeldt, J. W.; Mapp, A. K., *Bioorg Med Chem* **2008**.

6. De Guzman, R. N.; Goto, N. K.; Dyson, H. J.; Wright, P. E., *Journal of Molecular Biology* **2006,** *355* (5), 1005-1013.

7. Goodman, R. H.; Smolik, S., *Genes Dev* **2000,** *14* (13), 1553-77.

8. Chan, H. M.; La Thangue, N. B., *J Cell Sci* **2001,** *114* (Pt 13), 2363-73.

9. Dorman, G.; Prestwich, G. D., *Biochemistry* **1994,** *33* (19), 5661-73.

10. Herrera, F. J.; Triezenberg, S. J., *J Virol* **2004,** *78* (18), 9689-96.

11. Frangioni, J. V.; LaRiccia, L. M.; Cantley, L. C.; Montminy, M. R., *Nat Biotechnol* **2000,** *18* (10), 1080-5.

12. Parker, D.; Ferreri, K.; Nakajima, T.; LaMorte, V. J.; Evans, R.; Koerber, S. C.; Hoeger, C.; Montminy, M. R., *Mol Cell Biol* **1996,** *16* (2), 694-703.

13. Radhakrishnan, I.; Perez-Alvarado, G. C.; Parker, D.; Dyson, H. J.; Montminy, M. R.; Wright, P. E., *Cell* **1997,** *91* (6), 741-52.

14. Yang, F.; Vought, B. W.; Satterlee, J. S.; Walker, A. K.; Jim Sun, Z. Y.; Watts, J. L.; DeBeaumont, R.; Saito, R. M.; Hyberts, S. G.; Yang, S.; Macol, C.; Iyer, L.; Tjian, R.; van den Heuvel, S.; Hart, A. C.; Wagner, G.; Naar, A. M., *Nature* **2006,** *442* (7103), 700-4.

15. Thakur, J. K.; Arthanari, H.; Yang, F.; Pan, S. J.; Fan, X.; Breger, J.; Frueh, D. P.; Gulshan, K.; Li, D. K.; Mylonakis, E.; Struhl, K.; Moye-Rowley, W. S.; Cormack, B. P.; Wagner, G.; Naar, A. M., *Nature* **2008,** *452* (7187), 604-9.

16. Naar, A. M.; Beaurang, P. A.; Robinson, K. M.; Oliner, J. D.; Avizonis, D.; Scheek, S.; Zwicker, J.; Kadonaga, J. T.; Tjian, R., *Genes Dev* **1998,** *12* (19), 3020-31.

17. Radhakrishnan, I.; Perez-Alvarado, G. C.; Parker, D.; Dyson, H. J.; Montminy, M. R.; Wright, P. E., *J Mol Biol* **1999,** *287* (5), 859-65.

18. Schanda, P.; Brutscher, B.; Konrat, R.; Tollinger, M., *J Mol Biol* **2008,** *380* (4), 726-41.

19. Campbell, K. M.; Lumb, K. J., *Biochemistry* **2002,** *41* (47), 13956-64.

20. Zor, T.; De Guzman, R. N.; Dyson, H. J.; Wright, P. E., *J Mol Biol* **2004,** *337* (3), 521-34.

21. Goto, N. K.; Zor, T.; Martinez-Yamout, M.; Dyson, H. J.; Wright, P. E., *Journal of Biological Chemistry* **2002,** *277* (45), 43168-43174.

22. Vendel, A. C.; Lumb, K. J., *Biochemistry* **2003,** *42* (4), 910-6.

23. Sugase, K.; Dyson, H. J.; Wright, P. E., *Nature* **2007,** *447* (7147), 1021-5.

24. Vendel, A. C.; Lumb, K. J., *Biochemistry* **2004,** *43* (4), 904-8.

25. Vendel, A. C.; McBryant, S. J.; Lumb, K. J., *Biochemistry* **2003,** *42* (43), 12481-7.

26. Kamei, Y.; Xu, L.; Heinzel, T.; Torchia, J.; Kurokawa, R.; Gloss, B.; Lin, S. C.; Heyman, R. A.; Rose, D. W.; Glass, C. K.; Rosenfeld, M. G., *Cell* **1996,** *85* (3), 403-14.

27. Horvai, A. E.; Xu, L.; Korzus, E.; Brard, G.; Kalafus, D.; Mullen, T. M.; Rose, D. W.; Rosenfeld, M. G.; Glass, C. K., *Proc Natl Acad Sci U S A* **1997,** *94* (4), 1074-9.

28. Petrij, F.; Giles, R. H.; Dauwerse, H. G.; Saris, J. J.; Hennekam, R. C.; Masuno, M.; Tommerup, N.; van Ommen, G. J.; Goodman, R. H.; Peters, D. J.; et al., *Nature* **1995,** *376* (6538), 348-51.

29. Tanaka, Y.; Naruse, I.; Maekawa, T.; Masuya, H.; Shiroishi, T.; Ishii, S., *Proc Natl Acad Sci U S A* **1997,** *94* (19), 10215-20.

30. Tanaka, Y.; Naruse, I.; Hongo, T.; Xu, M.; Nakahata, T.; Maekawa, T.; Ishii, S., *Mech Dev* **2000,** *95* (1-2), 133-45.

31. Marzio, G.; Tyagi, M.; Gutierrez, M. I.; Giacca, M., *Proc Natl Acad Sci U S A* **1998,** *95* (23), 13519-24.

32. Jeang, K. T., *Cytokine Growth Factor Rev* **2001,** *12* (2-3), 207-17.

33. Kallio, P. J.; Okamoto, K.; O'Brien, S.; Carrero, P.; Makino, Y.; Tanaka, H.; Poellinger, L., *EMBO J* **1998,** *17* (22), 6573-86.

34. Arany, Z.; Huang, L. E.; Eckner, R.; Bhattacharya, S.; Jiang, C.; Goldberg, M. A.; Bunn, H. F.; Livingston, D. M., *Proc Natl Acad Sci U S A* **1996,** *93* (23), 12969-73.

35. Oliner, J. D.; Andresen, J. M.; Hansen, S. K.; Zhou, S.; Tjian, R., *Genes Dev* **1996,** *10* (22), 2903-11.

36. Kasper, L. H.; Fukuyama, T.; Biesen, M. A.; Boussouar, F.; Tong, C.; de Pauw, A.; Murray, P. J.; van Deursen, J. M.; Brindle, P. K., *Mol Cell Biol* **2006,** *26* (3), 789-809.

37. Langlois, C.; Mas, C.; Di Lello, P.; Jenkins, L. M.; Legault, P.; Omichinski, J. G., *J Am Chem Soc* **2008,** *130* (32), 10596-604.

38. Ernst, P.; Wang, J.; Huang, M.; Goodman, R. H.; Korsmeyer, S. J., *Molecular and Cellular Biology* **2001,** *21* (7), 2249-2258.

39. Best, J. L.; Amezcua, C. A.; Mayr, B.; Flechner, L.; Murawsky, C. M.; Emerson, B.; Zor, T.; Gardner, K. H.; Montminy, M., *Proc Natl Acad Sci U S A* **2004,** *101* (51), 17622-7.

40. Pangborn, A. B.; Giardello, M. A.; Grubbs, R. H.; Rosen, R. K.; Timmers, F. J., *Organometallics* **1996,** *15* (5), 1518-1520.

41. Still, W. C. K., M.; Mitra, A., *J. Org. Chem.* **1978,** *43*, 2923.

Chapter IV

Synthesis, Coactivator Binding and Activator Function of Bis-isoxazolidines

A. Abstract

Monomeric isoxazolidines are the first reported class of small molecule transcriptional activation domains, molecules capable of initiating gene upregulation when localized to a promoter. Many characteristics of the molecules parallel their endogenous counterparts, such as permissive binding and a low micromolar multipartner binding profile with the same coactivator targets of endogenous TADS. An additional characteristic of endogenous transcriptional activation domains is that the function of short peptidic TADs is enhanced upon multimerization and thus we hypothesized that multimers of isoxazolidines would show enhanced activity relative to their monomeric counterparts. Here we show the design and synthesis of short isoxazolidine oligomers. Initial evaluations indicate that the molecules have enhanced binding to coactivators but this did not translate to enhanced potency as a TAD.

B. Introduction

In 2004 the first small molecule to function as a transcriptional activation domain was reported, isoxazolidine **IV-1**.[1] Since that initial report significant evidence has been collected to support that iTADs possess similar features and mode of action as their endogenous counterparts. Both require amphipathic character and a rigid conformation, but neither have a strict requirement for specific placement of functionality on the helices of endogenous TADs or the isoxazolidine ring of iTADs.[2-4] For example, Figure IV-1 shows the helical region of four TADs and all contain different arrangements of interspersed hydrophobic and polar functionality.[4, 5] Similarly, several amphipathic isoxazolidines including both enantiomers as well as positional isomers (such as **IV-2**) of

the original racemic iTAD **IV-1** all activate to similar levels.[2] It also has been shown endogenous TADs and iTADs containing different orientations of amphipathic functionality have multiple protein binding partners in the transcriptional machinery and at least a subset of the protein targets are overlapped for the two classes.[4] For example, the four TADs shown in Figure IV-1a all bind the same motif, the KIX domain,[6-9] within the coactivator protein Creb Binding Protein (CBP), as do iTADs **IV-1** and **IV-2**.

a)

MLL	2847	DIMDFVLKNT
Myb	295	IKELELLL
SREBP1a	26	LTDIEDML
KBP 2.20	47	SWAVYELLFGS

b)

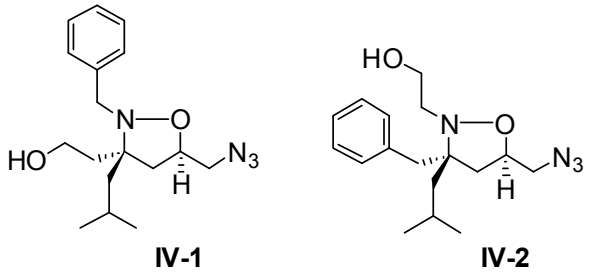

IV-1 **IV-2**

Figure IV-1. Endogenous TADs and iTADs do not require a specific arrangement of functionality. a) The TADs of MLL, Myb, SREBP1a and KBP 2.20 contain amphipathic character, but no sequence homology and all interact with the CBP KIX domain. b) Isoxazolidines **IV-1** and **IV-2** both activate transcription and bind the CBP KIX domain.

The similarities between iTADs and their endogenous counterparts suggested to us that small molecules with more significant modifications including changes not only in position of functionality but also functional group content likely will be tolerated by coactivator proteins and function as iTADs. In particular a modification predicted to be advantageous in term of activation is increased hydrophobic surface area. The typical binding sites on coactivator proteins are shallow, hydrophobic and quite large. For example, binding of the coactivator CBP through its KIX domain by the transcriptional activator c-Myb buries 1480 Å^2 of predominantly hydrophobic surface area.[10] Thus is it somewhat surprising that the only example of a small molecule TAD to function in cells has a molecular weight of <300 g/mol. In fact, the only other nonnatural molecule that functions as an TAD in cells is a 800 g/mol peptoid (Figure II-8, page 31).[11] It was thus

hypothesized that organic molecules larger than the minimal isoxazolidine domain will perform the same function, perhaps even more potently. The first approach the lab utilized towards this goal was to increase the hydrophobic surface area of the monomeric compounds by appending larger hydrophobic functional groups to the ring.[12] This strategy unfortunately was unsuccessful as all analogs evaluated showed attenuated activity and hence we adopted a new framework, short isoxazolidine oligomers (such as **IV-3**-**IV-5**). More specific evidence for the isoxazolidine oligomer approach comes from a study published by Tanaka showing that a dimer of the TAD of VP2 activates approximately three times more potently than the parent compound.[13] Further, surreptitious repeats of 6-14 amino acids are often contained in natural TADs.[3, 14, 15]

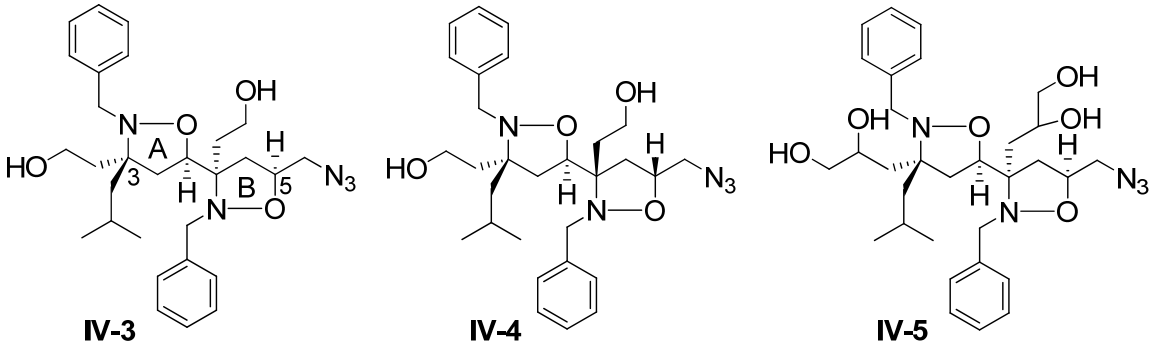

Figure IV-2. Bis-isoxazolidine targets.

1) Diastereomeric Targets

Diastereomeric bis-isoxazolidines such as **IV-3** and **IV-4** were both chosen as targets as these bis-isoxazolidines are predicted to populate a preferred conformation dictated by stereochemistry along the backbone. This hypothesis is based on analogy to bis-pyrollinones (**IV-6**, Figure IV-3) investigated by Hirschmann, Smith, and coworkers.[16-18] They have shown that both in the solid state and in solution dimeric pyrrolinones populate a preferred conformation with a dihedral angle of 168-177° due to restricted rotation around the C-C ring connecting bond. The preferred conformation does not vary with substitution along the backbone, suggesting that stereochemistry is the primary dictator of conformation. Bis-isoxazolidines such as **IV-3**-**IV-5** link the monomer units together in a fashion similar to **IV-6** and the substitution pattern is also similar suggesting the molecules will also adopt a defined conformation dictated by

stereochemistry. Coordinate driving (MMFF94) molecular modeling experiments supported that bis-isoxazolidines have a high barrier to rotation around the C-C ring connecting bond and this was experimentally confirmed by variable temperature NMR experiments.[19]

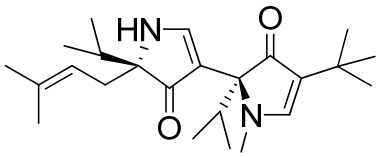

IV-6

Figure IV-3. Dimeric pyrollinones populate defined conformations.[16-18]

2) Targets with Different Polarity

Bis-isoxazolidine targets **IV-3** and **IV-5** contain the same hydrophobic face by having identical substitution of hydrophobic groups and stereochemical relationships along the backbone, but **IV-5** is overall more polar due to the presence of diol moieties rather than mono-alcohols at C3 of each ring. Both **IV-3** and **IV-5** were chosen as targets as limited solubility of the more hydrophobic **IV-3** is a concern, however the drawback to **IV-5** is that stereochemical complexity is introduced at both diols.

3) Bis-isoxazolidines and the iTAD•KIX Binding Model

While investigation of the larger bis-isoxazolidine ligands as iTADs can be argued as rational based simply on the surface area of coactivator binding sties, more specific support was provided by considering the binding model for monomeric iTADs with the KIX domain. In Chapter III it was shown using NMR spectroscopy that iTADs **IV-1** and **IV-2** bind the CBP KIX domain and a binding model for **IV-1** was proposed based on comparison to the solution structure of MLL in complex with the KIX domain.[20] Briefly, five MLL resides, one polar and four hydrophobic, make extensive contacts with the KIX domain and the three sidechains of **IV-1**, benzyl, isobutyl, and hydroxyl are predicted to project into the same subsites as three of these, F2852, L2854, and T2857, respectively (Figure IV-4). Indicative of the reduced surface area for binding the K_D for **IV-1** is 38 μM compared to 3 μM for MLL.[21] A fourth of the five residues, I2849 is located one helical turn from F2852 and thus if ring A of a bis-isoxazolidine

binds in the same orientation as **IV-1**, one of the sidechains on ring B should be poised to project into the subsite targeted by I2849 (Figure IV-4). Based on this model bis-isoxazolidines will have a total of four groups interacting with the KIX domain, likely leading to a higher affinity complex.

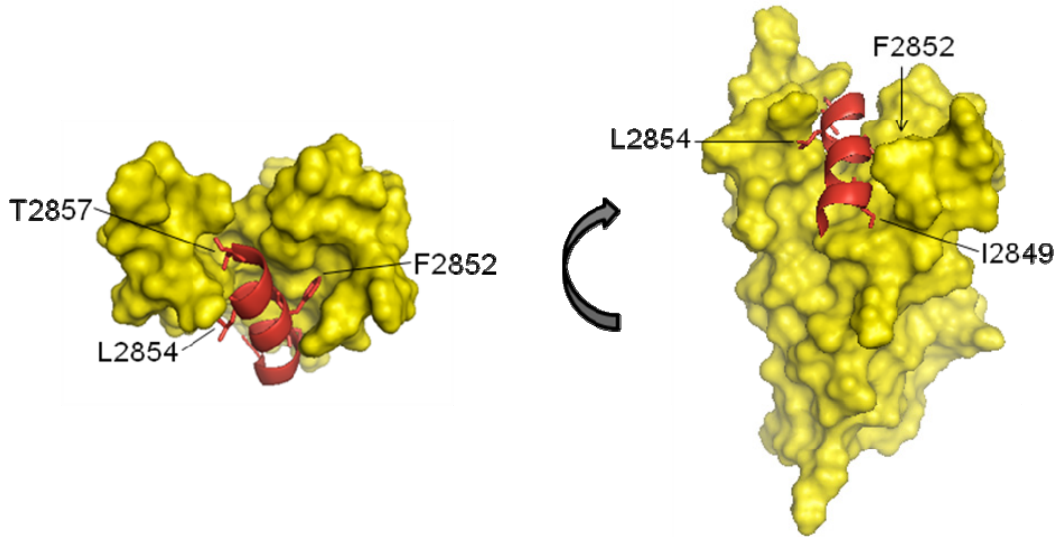

Figure IV-4. Solution structure of MLL•KIX.[20, 21] Figure adapted from 2agh.

4) Synthetic Strategy to Bis-isoxazolidines

The synthetic strategy envisioned to access bis-isoxazolidines targets is an iterative approach in which successive 1,3-dipolar cycloaddition reactions are employed to install the two rings (Figure IV-5). The first cycloaddition yields an isoxazoline that can be functionalized using reactions discussed in Chapter II to yield a densely functionalized mono-isoxazolidine.[2, 22] The C5 masked diol can then be manipulated to yield an oxime at that position which is utilized in the second cycloaddition to yield an isoxazoline that can be functionalized repeating the same reactions, with the same or varied nucleophiles and alkylating agents, used to functionalize the first isoxazoline ring.

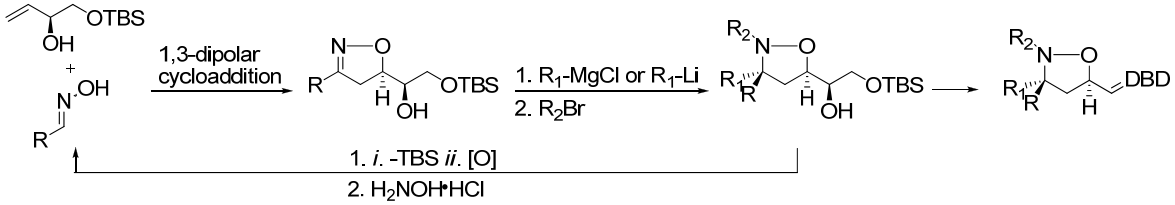

Figure IV-5. Synthetic strategy towards bis-isoxazolidines.

5) Strategy for Studying Bis-isoxazolidines

Several variables, including stereochemistry and overall polarity, are anticipated to significantly impact the function of bis-isoxazolidines. In this chapter the synthesis of molecules to probe these variables, several series of diastereomers of bis-isoxazolidines with varied polarity are presented. The major diastereomer has been utilized in initial binding and functional evaluations and the results and implications of these experiments are presented

C. Synthesis of Bis-isoxazolidine Diastereomers

The goal was to develop a synthetic route to bis-isoxazolidines that enables access to all possible diastereomeric combinations of ring B. Based on the synthetic strategy discussed above, the first step towards dimeric isoxazolidines from previously reported mono-isoxazolidines was installation of an oxime moiety at the C5 position. Formation of the oxime was afforded from **IV-7** in 87% yield by a Parikh-Doering oxidation of the alcohol to an aldehyde followed by condensation of the aldehyde with hydroxylamine hydrochloride (Scheme IV-1). With the oxime in hand, the feasibility and selectivity of the second cycloaddition and nucleophile addition to the newly formed ring was evaluated.

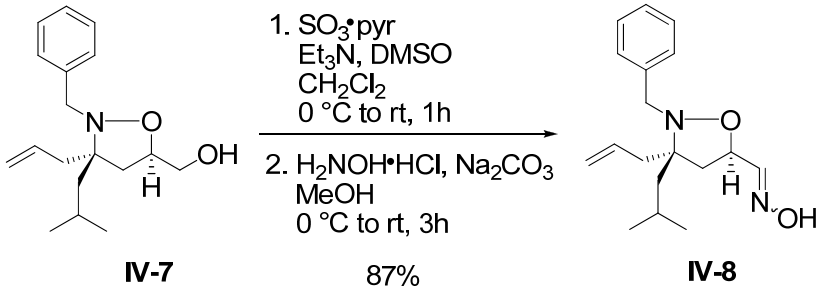

IV-7 87% **IV-8**

Scheme IV-1. Synthesis of oxime **IV-8**.

Towards the synthesis of multiple diastereomers of the final amphipathic targets we wanted to access both diastereomers of the isoxazoline ring following the second cycloaddition and initially considered two synthetic approaches to do so. The first option shown in Scheme IV-2a was to utilize the same selective cycloaddition conditions utilized for generation of the first ring and to conduct two separate reactions, each with one enantiomer of the allylic alcohol.[23, 24] The second option we considered depicted in Scheme IV-2b was to utilize non-selective reaction conditions to obtain a mixture of diastereomers that could subsequently be separated. Each set of reaction conditions produced three products: the desired product, a byproduct resulting from dimerization of the nitrile oxide generated in situ, and a byproduct resulting from intermolecular cycloaddition between the nitrile oxide and the C3 olefin moiety. Using the selective reaction conditions, in which magnesium coordination with the nitrile oxide and allylic alcohol controls the selectivity, the desired product was obtained in only trace quantities whereas the undesired byproducts were the major products. In contrast, using the non-selective cycloaddition conditions the desired product was obtained in 63% yield with isolation of each byproduct in less than 10% yield. Consistent with these results, Kanemasa and coworkers have previously observed in a similar system that dimerization of the nitrile oxide was favored over cycloaddition with less reaction allylic alcohols and hydrophobic oximes.[23] The desired product **IV-11** from the non-selective conditions was obtained as a 1:1 mixture of diastereomers, that were readily separated by preparative scale HPLC.

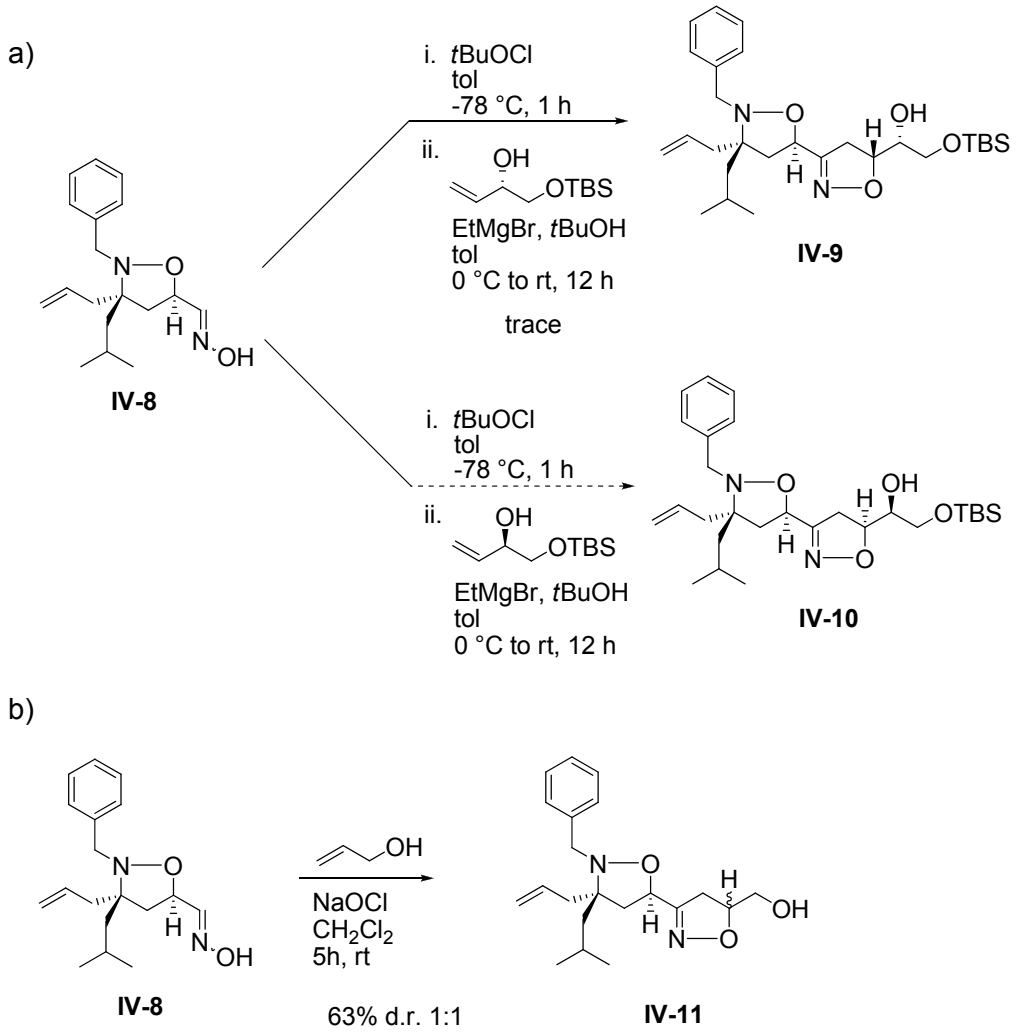

Scheme IV-2. Isoxazoline ring B formation.

The feasibility and selectivity of nucleophile addition to the C=N bond of the two diastereomeric products, **IV-12** and **IV-13** (Scheme IV-3) from the non-selective cycloaddition reaction were evaluated next. Each diastereomer was treated with the Grignard reagents allylmagnesium chloride and benzylmagnesium chloride in the presence of the strong Lewis acid, $BF_3 \bullet OEt_2$ (Scheme IV-3). Grignard addition to compound **IV-12** proceeded with high selectivity to give **IV-14** as the major product in high yield. In contrast, nucleophilic addition to ring B of compound **IV-13** proceeded in excellent yield to produce both possible diastereomers **IV-16** and **IV-17**. All diastereomers were individually isolated upon preparative scale HPLC and the four

diastereomers resulting from addition of allylmagnesium chloride to diastereomers **IV-12** and **IV-13** were peracetylated and stereochemistry was assigned using 1D NOE and 2D NOESY (Figure IV-6). Stereochemical assignments by through space interactions are appropriate for these compounds because the molecules populate a defined conformation in solution at room temperature as confirmed by molecular modeling and variable temperature NMR experiments.[19]

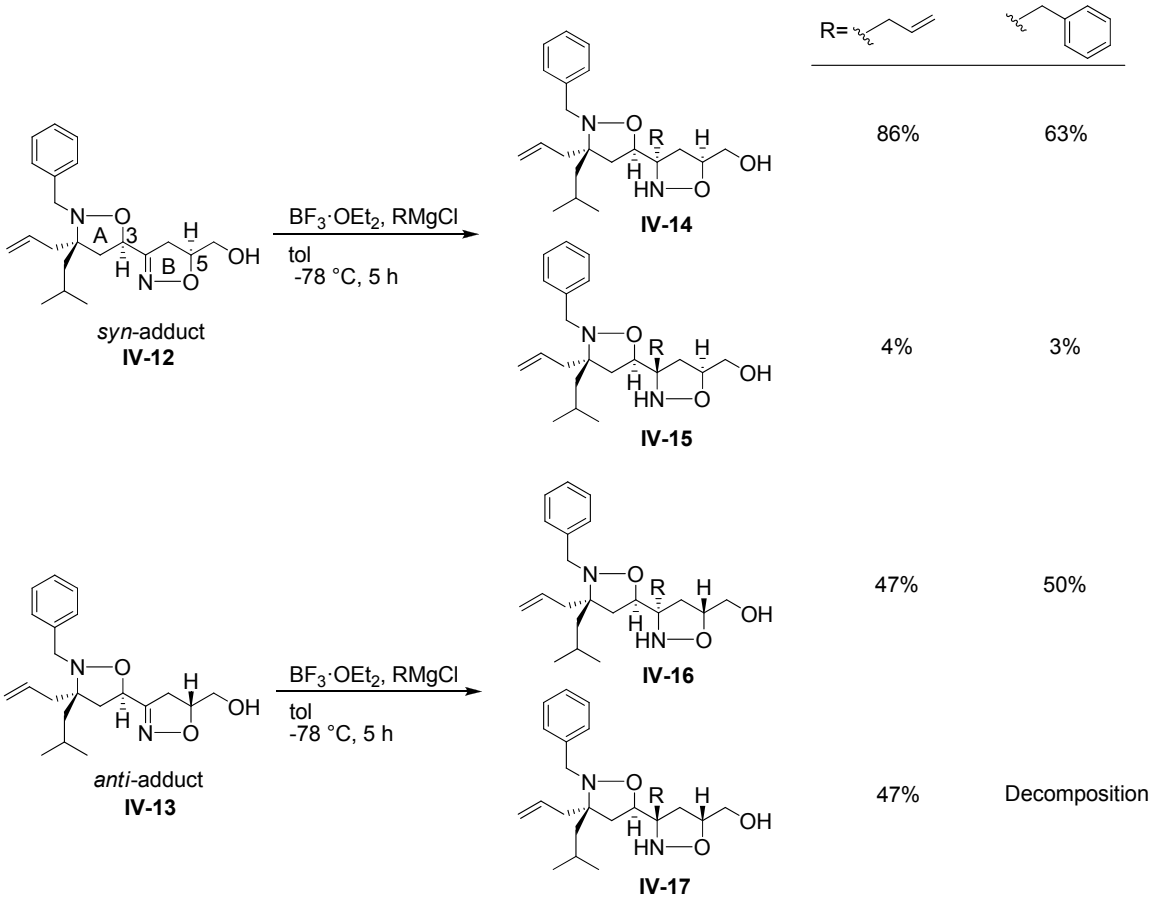

Scheme IV-3. Grignard addition to ring B of bis-isoxazolidines.

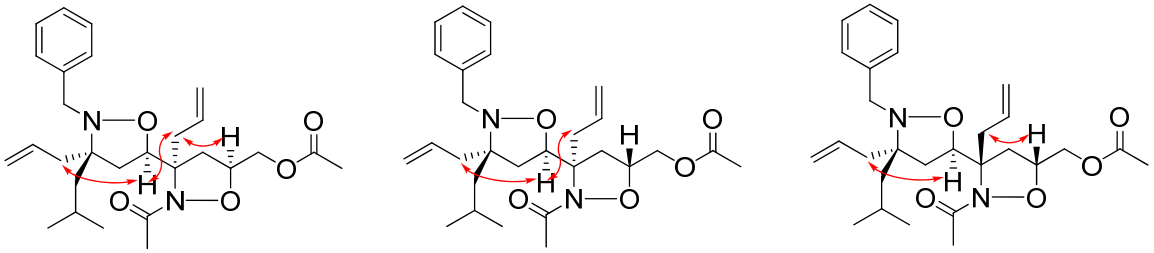

IV-18 IV-19 IV-20

Figure IV-6. Key through space interactions that facilitated bis-isoxazolidine stereochemical assignments.

Bis-isoxazolidine **IV-21** was utilized to investigate the remaining steps to the fully functionalized targets **IV-3** and **IV-5** (Scheme IV-4). Installation of the benzyl moiety on N2 of ring B of **IV-21** required first protection of the primary alcohol and this was masked as the *tert*-butyldimethy silyl ether. Alkylation of the secondary nitrogen was then accomplished using microwave-accelerated conditions and the crude product was immediately treated with TBAF to afford deprotection of the primary alcohol. The overall yield for this sequence was 77%. Subsequently the alcohol moiety was treated with methanesulfonlyl chloride and the resultant mesylate was displaced with sodium azide to yield **IV-23**. The azide served as an amine handle for tethering the bis-isoxazolidines to a DBD.

The remaining functional group transformation to **IV-5** was dihydroxylation of the two double bonds and subsequent conversion of the two diols into primary alcohols to yield **IV-3**. The typical conditions employed for this transformation on the corresponding mono-isoxazolidine structures described in Chapter II are dihydroxylation, cleavage to the aldehyde, and reduction to the alcohol. The dihydroxylation proceeded as expected in 93% yield to yield **IV-5**. However, with the bis-isoxazolidine substrate, only one of the diols (presumably, the one on ring A) could be cleaved to the aldehyde. A variety of reagents, including $NaIO_4$, $Pb(OAc)_4$ and MnO_2, and reaction conditions, including microwave irradiation with $NaIO_4$, were evaluated, but all proved unsuccessful in cleavage of both diols. This is presumably due to steric hindrance of the substituent at C3 of ring B. Generation of bis-isoxazolidine **IV-3** from **IV-23** by ozonoylsis of the two double bonds resulted in decomposition, and hydroboration was also unsuccessful. Thus,

as outlined below, an alternative strategy was explored. The other two synthetically accessible diastereomers of **IV-5** were prepared analogously to **IV-5**.

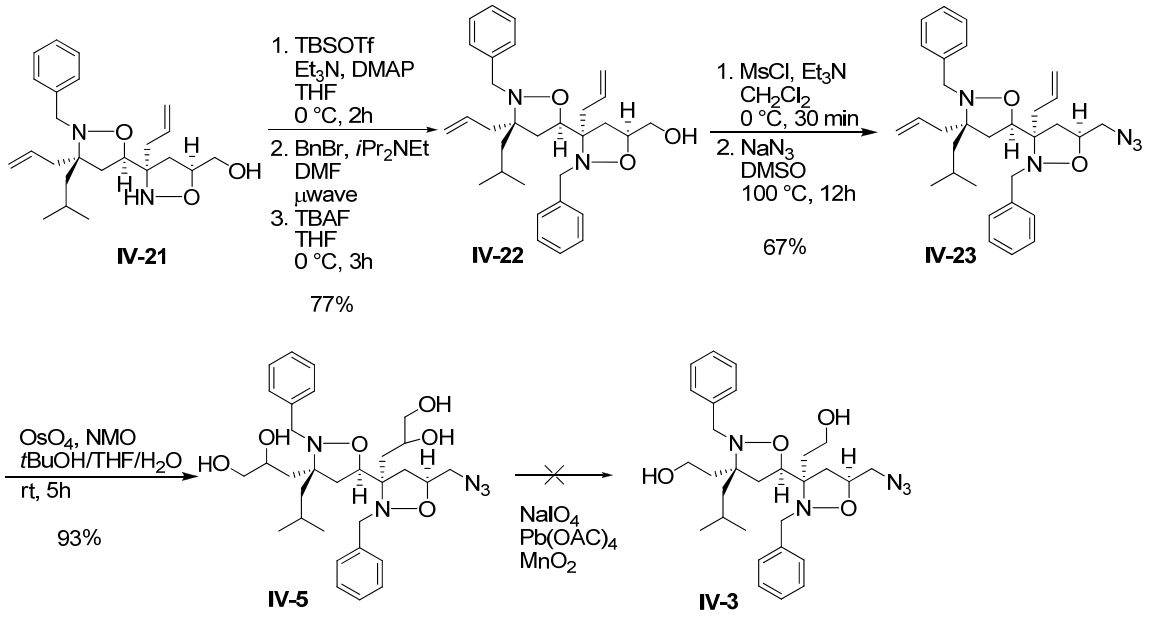

Scheme IV-4. Synthesis of bis-isoxazolidine **IV-5**.

Access to **IV-3** was afforded by adopting fa modified synthetic route. For this oxime **IV-24**, Scheme IV-5, that replaced the C3 olefin moiety with a protected alcohol sidechain was prepared and utilized in the cycloaddition reaction. The cycloaddition between the nitrile oxide of **IV-24** generated in situ and allyl alcohol proceeded in 75% to give a 1.5:1 mixture of diastereomeric products at C5 of ring B. The formation of by-products resulting from dimerization of the nitrile oxides or intermolecular cycloaddition between two isoxazolidines was suppressed, presumably due to the increased polarity of the oxime.[23] The mixture of diastereomers was treated with TBSOTf to afford protection of the primary alcohols at which stage the two diastereomers could be separated by column chromatography. The two diastereomeric products **IV-25** and **IV-26** were treated individually with allylmagnesium chloride in the presence of the Lewis acid $BF_3 \bullet OEt_2$. Similar selectivities were observed as had been obtained for the substrate containing a C3 double bond moiety on ring A. Compound **IV-27** was isolated as a single diastereomer from **IV-25** in good yield. Nucleophilic addition to the cycloaddition product with the two C5 protons on opposite faces of the molecule (**IV-26**) again proceeded non-

selectively. In this example the ratio of diastereomers was 2:1 as compared to 1:1 with substrate **IV-13**. The three diastereomers were carried on the fully functionalized bis-isoxazolidines. Scheme IV-5 shows the synthetic details for the major diastereomer. The same reaction sequences as employed for the preparation of **IV-5** were utilized; with this substrate, however, the ring B C3 double bond was successfully cleaved to the aldehyde with $NaIO_4$ and $NaBH_4$ reduction afforded the primary alcohol (**IV-32**). In the final step the MOM ether protecting group was removed by treatment with 50% HCl/*i*PrOH to yield **IV-3**.

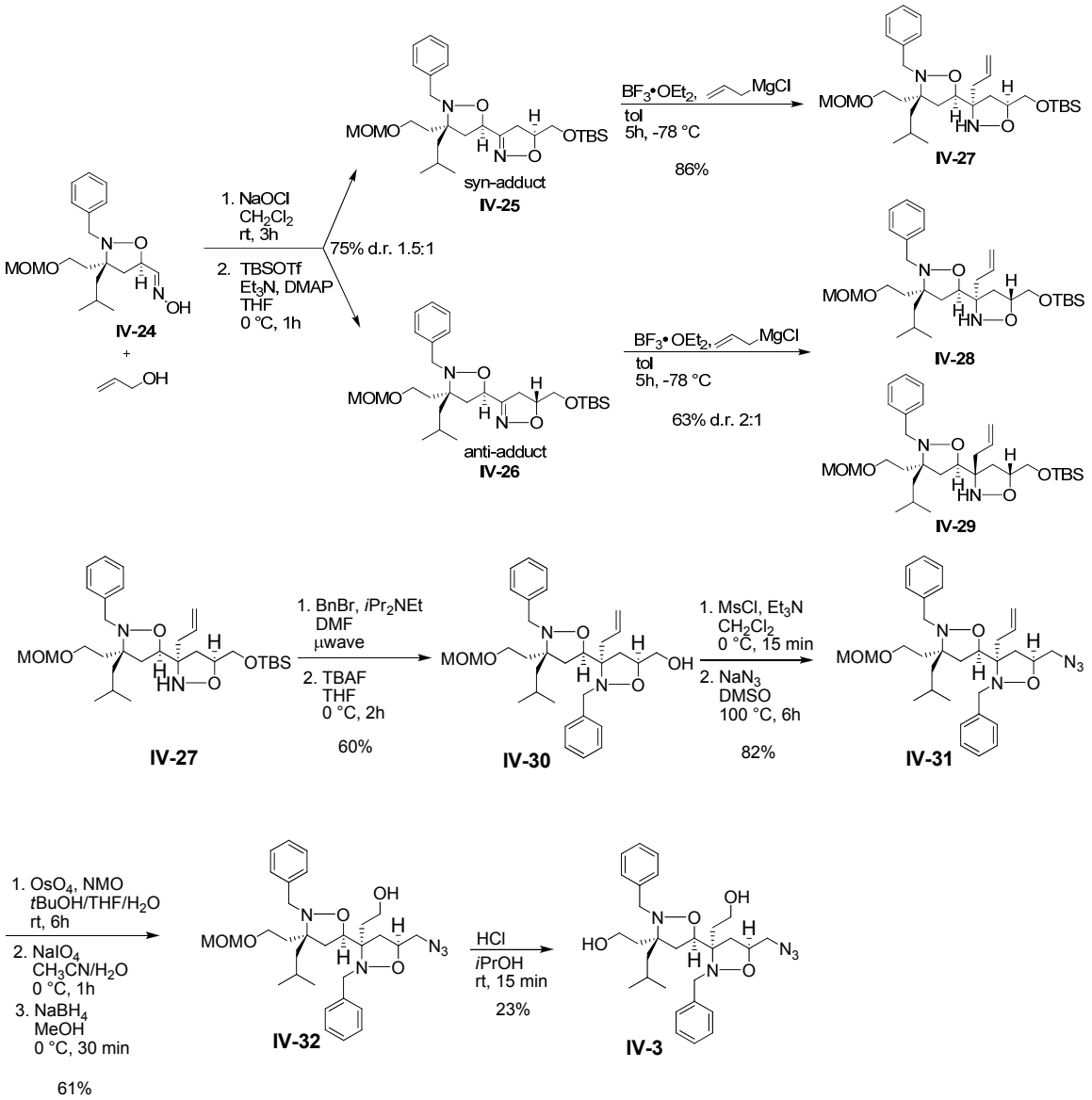

Scheme IV-5. Synthesis of bis-isoxazolidine **IV-3**.

With the synthetic methods established for access to three of the four possible diastereomeric combinations of ring B, the major diastereomer of each was evaluated for ability to upregulate transcription and to bind the CBP KIX domain. For the former, **IV-3** and **IV-5** were tethered to a DNA localizing moiety (OxDex), at the C5 position of the second ring (ring B). The synthetic details for the transformation of **IV-3** are shown in Scheme IV-6. The azide was reduced to an amine by treatment with PPh_3 and the crude amine was coupled to a short PEG linker-OxDex conjugate using standard peptide coupling conditions. **IV-5-DBD** was prepared using a slightly modified route in which the azide of **IV-5** was reduced to an amine, coupled to the PEG linker that contained a protected amine functionality which upon unmasking was coupled to OxDex. Final products were purified by reverse phase HPLC prior to evaluation in cells.

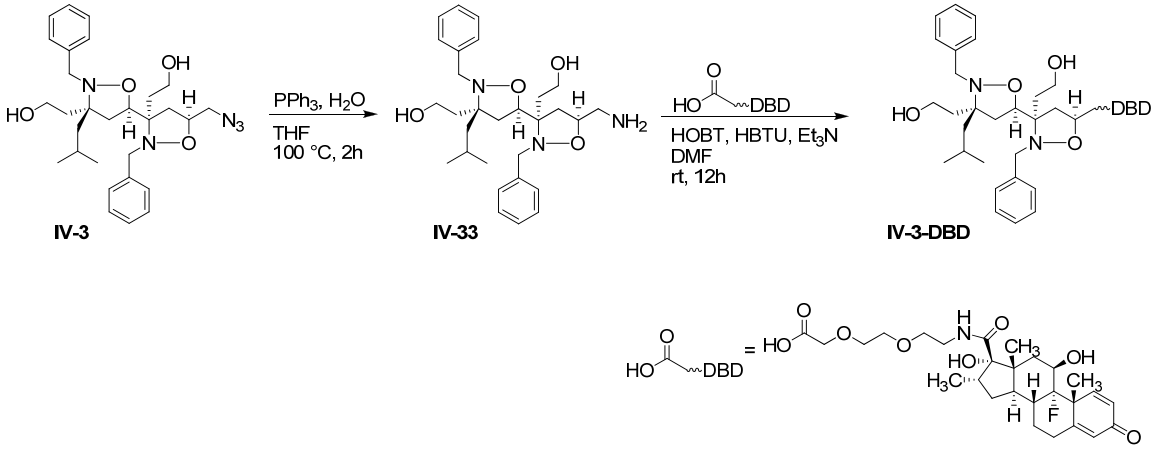

Scheme IV-6. Synthesis of bis-isoxazolidine **IV-3-DBD**.

D. Assessment of Bis-isoxazolidines IV-3 and IV-5

Analogous to monomeric isoxazolidines discussed in Chapters II and III, bis-isoxazolidines **IV-3** and **IV-5** were evaluated for ability to upregulate transcription in a 2-hybrid transcription assay in HeLa cells and for ability to bind the CBP KIX domain using NMR spectroscopy.

1) Ability to Upregulate Transcription in a Cellular System

The same system was utilized to evaluate bis-isoxazolidines as was used to evaluate monomeric iTAD **IV-1** in cells, as described previously.[11] Briefly, HeLa cells were transfected with a plasmid expressing a Gal4-GR LBD fusion protein, a second

plasmid bearing five Gal4-binding sites upstream of a firefly luciferase reporter gene, and a transfection control. OxDex binds the GR LBD localizing the isoxazolidine to DNA. The activation assays were carried out by colleagues Jonas Hojfeldt and Dr. Steve Rowe.

Bis-isoxazolidine **IV-3**, the more hydrophobic of the two molecules, did not activate transcription over the concentration range evaluated (10 nM to 10 μM). However, bis-isoxazolidine **IV-5**, a more polar variant of **IV-3** with an analogous hydrophobic face was a potent TAD with a maximal 50-fold activation observed at 1 μM (Figure IV-7). This was an initial encouraging result as it demonstrated bis-isoxazolidines are cell permeable and do interact with transcriptional machinery proteins. While the activity of **IV-5** is not enhanced but comparable to the most potent monomeric iTADs the bis-isoxazolidine scaffold offers many possibilities for optimization toward potent activators or perhaps inhibitors of transcription. The other synthetically accessible diastereomers may present functionality to coactivator subsites in a more optimal arrangement. Further, changes in functional group position or composition (for ring B) can be evaluated. Thus, this will be an active area of investigation in the future.

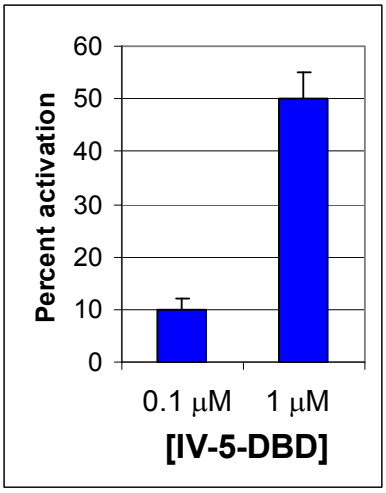

Figure IV-7. Transcription upregulation by **IV-5-DBD**.

2) Binding the CBP KIX Domain

The second evaluation of **IV-3** and **IV-5** to interact with coactivator proteins was a direct evaluation of binding the CBP KIX domain using NMR spectroscopy. The ability of each molecule to bind the KIX domain was assessed using two-dimensional ^{15}N, ^{1}H-HSQCs in which spectrum of the protein was collected in the absence and

presence of ligand. NMR samples consisted of 400 μM ^{15}N-His$_6$KIX in 90% H_2O/10% D_2O 10 mM phosphate buffer with 150 mM NaCl and 1% (vol/vol) CD_3OD at pH 7.2 and varying concentration of ligand as indicated. Experiments were conducted at 27 °C.

In the case of bis-isoxazolidine **IV-3** an accurate evaluation of binding was hindered by limited solubility of the molecule in aqueous buffer. A ^{15}N, ^{1}H-HSQC spectrum was recorded (purple) in the presence of low concentrations of bis-isoxaozlidine **IV-3** and is shown overlayed on a spectrum of free protein (black) in Figure IV-8. No resonances exhibited a significant chemical shift perturbation. There were several amide resonances however that exhibited small chemical shift perturbations (A618, L620, and R624) that are consistent with a ligand binding the same site as monomeric iTADs, MLL, Jun, and others. In contrast, several amide resonances that shift upon binding of ligands to this site, such as V608, E626, and E665, did not detectably shift.

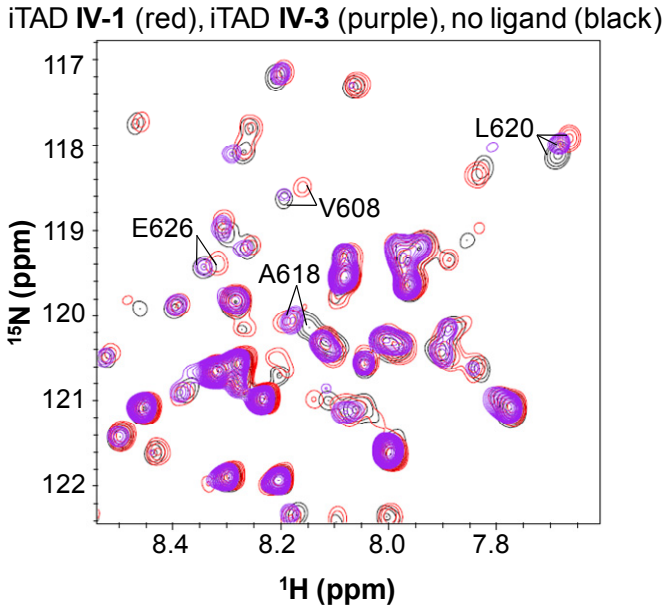

Figure IV-8. Two-dimensional ^{15}N, ^{1}H-HSQC of ^{15}N-His$_6$KIX in the absence (black) and presence (red) of **IV-3**. KIX bound by iTAD **IV-1** is in red.

Two-dimensional ^{15}N, ^{1}H-HSQC spectrum of His$_6$KIX recorded in the absence and presence of bis-isoxazolidine **IV-5** showed that there is an interaction between the protein and small molecule as indicated by chemical shift perturbation of a portion of amide residues upon addition of **IV-5**. Figure IV-9a shows the spectrum of **IV-5** (blue)

overlayed on the spectrum of unbound protein (black); for comparison the spectrum of iTAD **1V-1** (red) is also overlayed. Evaluation of the three spectra revealed that nearly all the residues that shift upon binding iTAD **IV-1** also shift upon binding iTAD **IV-5**, with the shifts being of larger magnitude for iTAD **IV-5**. Reflective of the larger surface area of **IV-5** compared to **IV-1** additional shifts are also observed upon binding the larger ligand. The chemical shifts observed for the KIX domain upon binding by **IV-5** were quantitated, $\Delta\delta=[\Delta\delta(^{1}H)^{2} + 0.1\Delta\delta(^{15}N)^{2}]^{1/2}$, and plotted against residue number (Figure IV-9b). The average chemical shift was 0.04 ppm and the largest shift is 0.25 ppm for L620. The black line on the chemical shift perturbation map indicates the average shift. The average chemical shift upon binding this site by endogenous ligands range from 0.02 ppm to 0.20 ppm with the largest shifts ranging from slightly larger than 0.1 ppm to 2.0 ppm; bis-isoxazolidines exhibit behavior in the same range suggesting similar kinetic behavior. Figure IV-9c highlights (in red) the KIX residues that experience significant chemical shift perturbation upon binding iTAD **IV-5** and MLL. These pictures demonstrate that that bis-isoxazolidine **IV-5** does bind the same site on KIX as iTAD **IV-1** and MLL.[20, 21]

In addition to the residues that shift upon addition of iTAD **IV-1** shifts obtained with small molecule **IV-5** also extend along α2 and additional shifts are observed in the C-terminus of α3, analogous to MLL. Interestingly, the additional shifts along α2 (Figure IV-10b) are located in the same region that the side chain of MLL residue I2849 contacts. The proposed binding model of bis-isoxazolidines discussed in the Introduction suggested that functionality on ring B would be poised to project into the same KIX subsite as I2849. This is consistent with the experimental evidence, although further experiments will be needed to confirm a mode of binding. Malathy Krisnamurthy is currently attempted to obtain a crystal structure of the protein in complex with iTADs such as **IV-1** and **IV-5**.

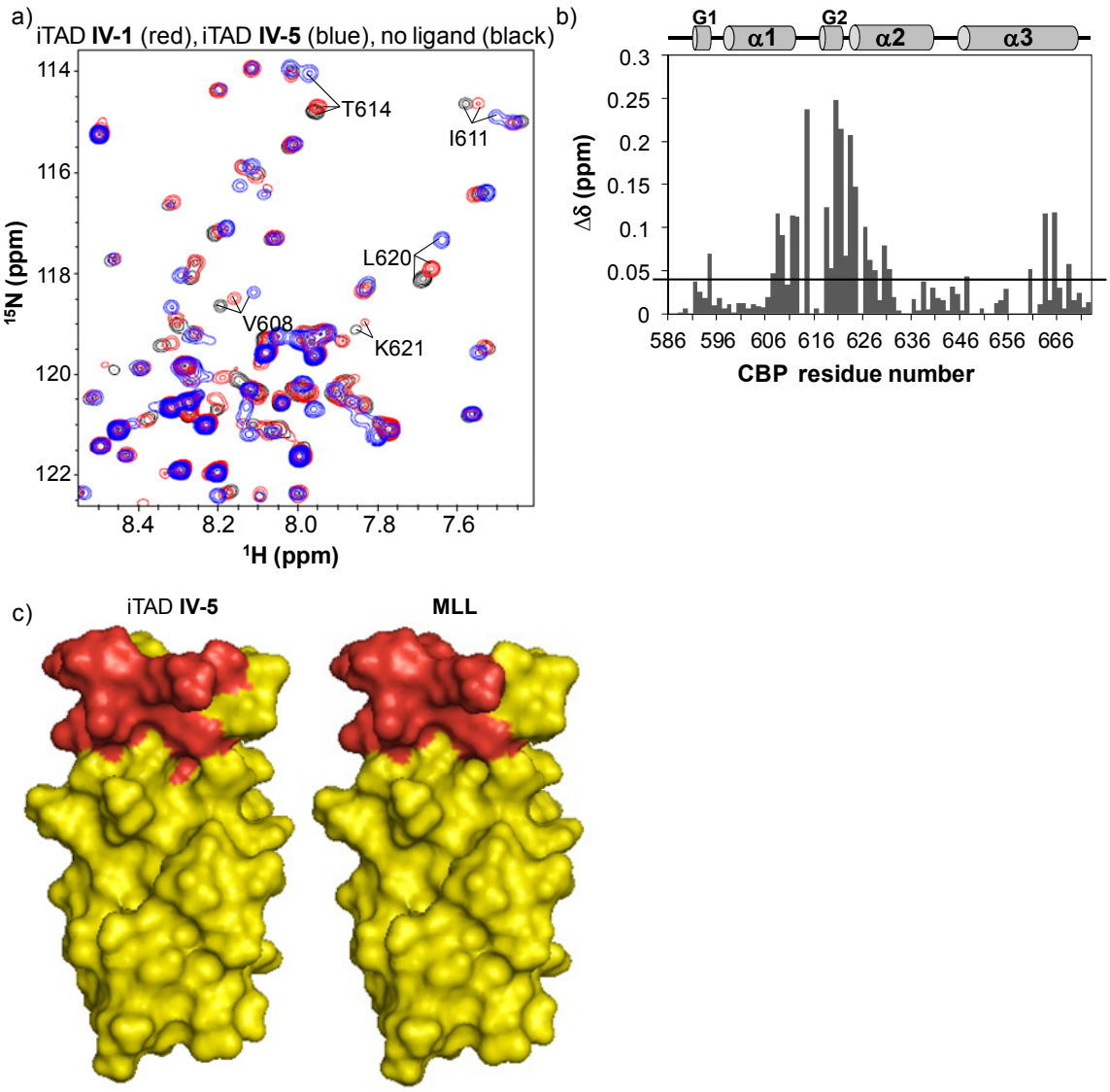

Figure IV-9. iTAD **IV-5** binds the CBP KIX domain. a) Overlay of the ^{15}N,^{1}H-HSQC of ^{15}N-His$_6$KIX bound by iTAD **IV-5** (blue) and **IV-1** (red) on unbound protein (black). b) Chemical shift perturbation map of ^{15}N-His$_6$KIX upon binding iTAD **IV-5**. c) Space filling diagrams of the KIX domain have the residues that experience the largest chemical shift perturbation upon binding iTAD **IV-5** and MLL colored in red. Figures adapted from 1kdx.

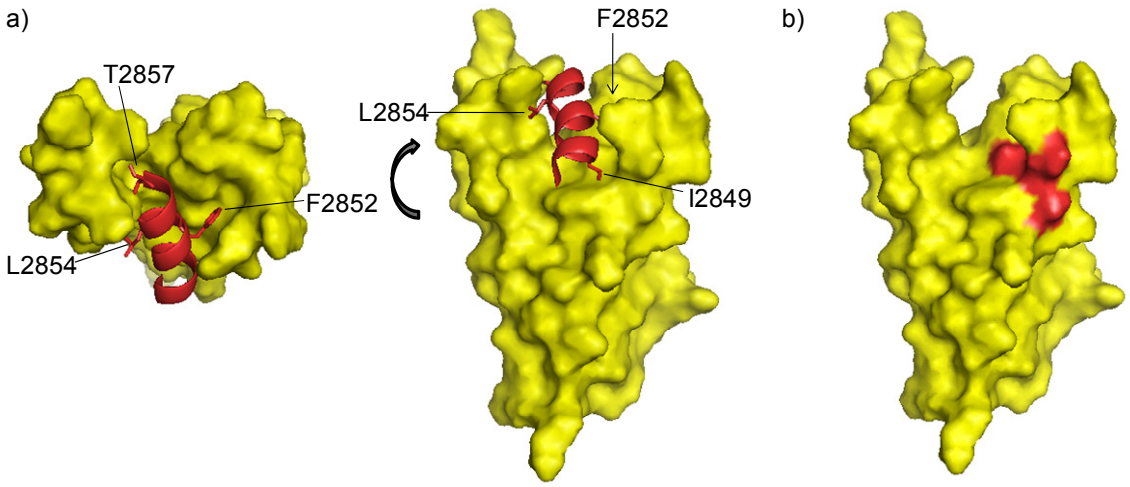

Figure IV-10. Comparison of bis-isoxazolidines to MLL•KIX. a) MLL•KIX solution structure. b) Residues that shift upon binding dimeric iTAD **IV-5**, but not monomeric iTAD **IV-1**, are highlighted in red. Figures are adapted from 2agh.

E. Conclusions

The synthetic methods to access multiple diastereomers of densely functionalized bis-isoxazolidines were established and utilized to prepare molecules for evaluation as small molecule regulators of transcription. It was determined that the more polar and stereochemically complex analog **IV-5**, compared to **IV-3**, possessed the preferable features for functioning as a TAD. The evaluation of **IV-5** in complex with the KIX domain via NMR suggested that, in fact, bis-isoxazolidine **IV-5** does project functionality such that four sidechains interact with the CBP KIX domain compared to three for iTAD **IV-1**. The ability of bis-isoxazolidines to interact with a large surface area within the KIX domain binding site suggests these molecules should be excellent starting points for the design of inhibitors of TADs that target this same site.

F. Experimental

General.

Unless otherwise noted, starting materials were obtained from commercial suppliers and used without further purification. CH_2Cl_2, THF, CH_3CN and toluene were dried by passage through activated alumina columns and degassed by stirring under a dry N_2 atmosphere.[25] BF_3•OEt_2 and Et_3N were distilled from CaH_2, MeOH was distilled

from sodium metal, and *t*-BuOH was distilled from $MgSO_4$. All reactions involving air- or moisture-sensitive reagents were performed under a dry N_2 atmosphere. Purification by column chromatography was carried out with E. Merck Silica Gel 60 (230-400 mesh) according to the procedure of Still, Kahn, and Mitra.[26] ^1H and ^{13}C NMR spectra were recorded in $CDCl_3$ at 500 MHz and 125 MHz, respectively, unless otherwise specified. IR spectra were measured as thin films on NaCl plates. Compounds that do not appear in the text are numbered **S1-S3.** The synthesis of **III-1b** and, **III-3b**, small molecules utilized in NMR experiments in this chapter, were reported in Chapter II. **III-4** was prepared by JP Desaulnier.

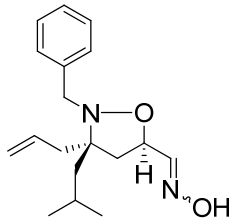

IV-8

(5*R*)-3-allyl-2-benzyl-3-isobutylisoxazolidine-5-carbaldehyde oxime (IV-8): $NaIO_4$ (1.1 g, 5.3 mmol, 1.2 eq) was added to a stirring solution of **IV-7** (1.4 g, 4.4 mmol, 1.0 eq) in 22 ml CH_3CN and 22 ml H_2O cooled in an ice-H_2O bath. Complete consumption of the starting material was afforded after stirring 1h with continued cooling, as indicated by TLC analysis. The mixture is diluted with H_2O (10 ml) and extracted with Et_2O (3 x 15 ml). The combined organic extracts were washed with H_2O (1 x 15 ml) and brine (1 x 15 ml), dried over Na_2SO_4, filtered, and concentrated *in vacuo*. The crude aldehyde was dissolved in 44 ml MeOH and cooled in an ice-H_2O bath. To the solution was added H_2NOH•HCl (610 mg, 8.8 mmol, 2.0 eq) and Na_2CO_3 (930 mg, 8.8 mmol, 2.0 eq) and the resultant mixture was slowly warmed to rt. Upon stirring 5h TLC analysis indicated complete consumption of starting material. The reaction mixture was diluted with sat. NH_4Cl (20 ml), extracted with Et_2O (3 x 30 ml), and the combined organic extracts were washed with brine (1 x 30 ml), dried over Na_2SO_4, filtered, and concentrated *in vacuo*. The crude mixture was purified by flash chromatography (70:30 hexanes:EtOAc) to yield 1.2 g of product as of a colorless oil in 93% yield. IR: 3203, 2954, 1653, 1454 cm^{-1}; 1H NMR (approximate 1:1 E/Z mixture): δ 0.96-1.12 (m, 6H), 1.39 (dd, 1H, J = 14.7, 6.6),

1.44 (dd, 1H, J = 14.3, 6.3), 1.63 (dd, 1H, J = 13.2, 5.1), 1.66 (dd, 1H, J = 12.8, 5.1), 1.81-1.96 (m, 1H), 2.07 (dd, 1H, J = 12.8, 5.9), 2.21 (dd, 1H, J = 12.8, 7.0), 2.31-2.53 (m, 3H), 2.69 (dd, 1H, J = 12.8, 9.2), 3.85-3.95 (m, 2H), 4.54 (dd, 1H, J = 15.4, 7.0), 4.87-4.99 (m, 1H), 5.10-5.16 (m, 2H), 5.90-6.01 (m, 1H), 6.79-6.81 (m, 2H), 7.19-7.41 (m, 5H); ^{13}C NMR (Carbon resonances for which both E and Z isomers of the oxime are observed are paired together in parentheses): δ (24.16, 24. 25), (24.56, 24.67), 25.06, (38.95, 39.03), 41.74, 42.78, (43.60, 43.84), (53.44, 53.95), 69.80, 72.91, 118.0, (126.87, 126.95), (128.06, 128.11), (128.26, 128.30), (134.79, 134.91), 138.7, 152.6, 156.0; HRMS (ESI) calcd for $[C_{18}H_{26}N_2O_2 + H]^+$: 303.2073, found: 303.2080.

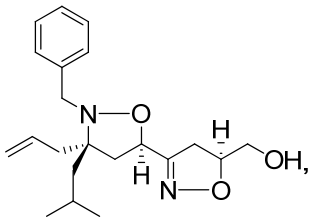

IV-12

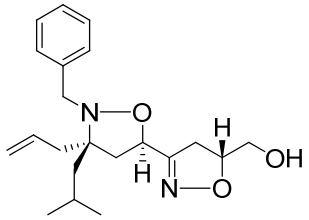

IV-13

IV-12 and IV-13: To a stirred solution of **IV-8** (1.1 g, 3.6 mmol, 1.0 eq) and allyl alcohol (250 μl, 3.6 mmol, 1.0 eq) in CH_2Cl_2 (36 ml) cooled in an ice-H_2O was added NaOCl (13 ml of a 705 mM solution, 9.0 mmol, 2.5 eq) dropwise over 30 min. The biphasic reaction mixture was allowed to slowly warm to rt and TLC analysis indicated completion consumption of the starting material after 3h. The mixture was diluted with H_2O (20 ml) and extracted with CH_2Cl_2 (3 x 30 ml). The combined organic extracts were washed with brine (1 x 30ml), dried over Na_2SO_4, filtered, and concentrated *in vacuo*. Flash chromatography (70:30 hexanes/EtOAc) of the crude product yielded 810 mg (colorless oil) of product in 63% yield as a 1:1 diastereomeric mixture at C5 of ring B. The diastereomers were separated by HPLC (70:30 hexanes:EtOAc).

((*S*)-3-((3*S*,5*R*)-3-allyl-2-benzyl-3-isobutylisoxazolidin-5-yl)-4,5-dihydroisoxazol-5-yl)methanol (IV-12): IR: 3409, 2954, 1455, 1048, 871 cm-^{1}; ^{1}H NMR: δ 0.97 (s, 3H), 0.98 (s, 3H), 1.38 (dd, 1H, J = 6.8, 14.6), 1.64 (dd, 1H, J = 4.9, 14.6), 1.69 (dd, 1H, J = 6.8, 6.8 "apparent triplet"), 1.85-1.93 (m, 1H), 4.60 (dd, 1H, J = 7.3, 13.7), 2.40-2.45 (m, 2H), 2.48 (dd, 1H, J = 8.3, 12.7), 2.62 (dd, 1H, J = 7.3, 17.6), 2.84 (dd, 1H, J = 10.7, 17.6), 3.40-3.45 (m, 1H), 3.56 (ddd, 1H, J = 3.4, 6.8, 12.2), 3.84 (s, 2H), 4.57-4.63 (m,

1H), 4.67 (dd, 1H, J = 6.8, 7.8 "apparent triplet"), 5.10-5.13 (m, 2H), 5.89-5.97 (m, 1H), 7.21-7.24 (m, 1H), 7.27-7.30 (m, 2H), 7.32-7.34 (m, 2H); ^{13}C NMR (100 MHz): δ 24.04, 24.36, 25.10, 35.94, 38.76, 40.72, 43.50, 53.69, 63.56, 68.78, 70.77, 80.66, 117.92, 126.91, 128.06, 128.28, 134.77, 138.58, 161.20; HRMS (ESI) calcd for $[C_{21}H_{30}N_2O_3 + Na]^+$: 381.2154, found: 381.2148.

((*R*)-3-((3*S*,5*R*)-3-allyl-2-benzyl-3-isobutylisoxazolidin-5-yl)-4,5-dihydroisoxazol-5-yl)methanol (IV-13): IR: 3409, 2954, 1455, 1048, 876, 735 cm^{-1}; ^{1}H NMR: δ 0.97 (d, 1H, J = 2.0), 0.98 (d, 1H, J = 2.0), 1.37 (dd, 1H, J = 6.8, 14.6), 1.63 (dd, 1H, J = 4.9, 14.6), 1.73-1.77 (m, 1H), 1.85-1.93 (m, 1H), 2.28 (dd, 1H, J = 7.3, 13.7), 2.41-2.46 (m, 2H), 2.49 (dd, 1H, J = 8.8, 17.3), 2.66 (dd, 1H, J = 7.1, 17.3), 2.81 (dd, 1H, J = 10.7, 17.6), 3.45-3.50 (m, 1H), 3.60 (ddd, 1H, J = 3.4, 6.8, 12.2), 3.82 (d, 1H, J = 14.2), 3.86 (d, 1H, J = 14.2), 4.54-4.59 (m, 1H), 5.10-5.14 (m, 2H), 5.88-5.97 (m, 1H), 7.21-7.24 (m, 1H), 7.28-7.31 (m, 2H), 7.34-7.35 (m, 2H); ^{13}C NMR (100 MHz): δ 24.00, 24.41, 25.12, 35.70, 38.62, 41.05, 43.72, 53.50, 63.65, 68.39, 70.58, 80.54, 117.94, 126.89, 128.09, 128.31, 134.75, 138.57, 161.42; HRMS (ESI) calcd for $[C_{21}H_{30}N_2O_3 + Na]^+$: 381.2154, found: 381.2147.

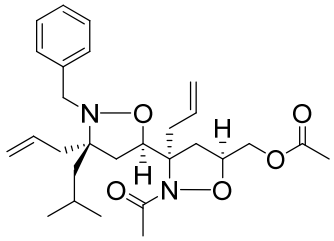

IV-18

((3*R*,3'*S*,5*S*,5'*R*)-2-acetyl-3,3'-diallyl-2'-benzyl-3'-isobutyl-3,5'-biisoxazolidin-5-yl)methyl acetate (IV-18): A solution of compound **IV-12** (210 mg, 0.59 mmol, 1.0 eq) in toluene (3.9 mL) was cooled in a dry ice-acetone bath. BF_3•OEt_2 (230 ul, 1.8 mmol, 3.0 eq) was added dropwise to the solution over 15 min and the mixture was stirred with continued cooling for 30 min. Allylmagnesium chloride (1.8 mL of a 2.0M solution in THF, 3.5 mmol, 6.0 eq) was then added dropwise over 30 min. The reaction mixture was stirred for 4 hours with continued cooling at which point TLC analysis indicated complete consumption of the starting material. Saturated NH_4Cl (5 mL) was added to the

reaction and the resultant solution was transferred to an ice-H_2O bath. After slowly warming to rt the mixture was diluted with H_2O (5 mL) and Et_2O (5 mL) and the organic and aqueous layers separated. The aqueous layer was extracted with Et_2O (3 x 5 mL). The combined organic extracts were washed with brine (5 mL), dried over Na_2SO_4, filtered, and concentrated in vacuo. The crude product was purified by flash chromatography (elution in 60:40 hexanes/EtOAc) to yield 210 mg of a ~20:1 mixture of diastereomers as a clear oil in 90% yield. The diastereomers were separated by preparative scale HPLC; a portion of the major diastereomer (**IV-14**) was peracetylated to reduce line broadening for characterization and stereochemical assignments. To a solution of **S13** (50 mg, 0.12 mmol, 1.0 eq) in DMF (600 μl) was added acetic anhydride (91 ul, 0.96 mmol, 8.0 eq) and *i*Pr_2NEt (84 μl, 0.48 mmol, 4.0 eq). The solution was irradiated in a 1000W microwave at 20% power for 20 sec. Upon cooling the irradiation was repeated and this was repeated 8 times until TLC and mass spectrometry analysis indicated formation of product. The mixture was diluted with H_2O (5 mL) and extracted with Et_2O (3 x 5 mL). The combined organic extracts were washed with H_2O (3 x 5 mL), washed with brine (5 mL), dried over Na_2SO_4, filtered, and concentrated in vacuo. The crude product was purified by flash chromatography (elution in 70:30 hexanes/EtOAc) to yield 55 mg of product as a colorless oil in 95% yield. IR: 2918, 1744, 1648, 1442, 1234, 1043 cm^{-1}; ^1H NMR: δ 0.96 (d, 3H, J = 6.3), 0.99 (d, 3H, J = 6.8), 1.31 (dd, 1H, J = 6.3, 14.6), 1.64 (dd, 1H, J = 4.9, 14.6), 1.81-1.91 (m, 2H), 1.96-2.00 (m, 2H), 1.99 (s, 3H), 2.01 (s, 3H), 2.18 (dd, 1H, J = 7.3, 14.2), 2.22 (dd, 1H, J = 7.8, 12.2), 2.47 (dd, 1H, J = 7.6, 13.9), 2.59 (dd, 1H, J = 8.1, 12.0), 3.00 (dd, 1H, J = 6.3, 13.7), 3.29 (dd, 1H, J = 8.8, 12.7), 3.58 (dd, 1H, J = 2.4, 12.2), 3.70 (d, 1H, J = 14.2), 3.77 (d, 1H, J = 14.2), 4.01-4.06 (m, 1H), 4.88 ("apparent triplet," 1H, J = 8.3), 5.07-5.14 (m, 4H), 5.63-5.71 (m, 1H), 5.80-5.89 (m, 1H), 7.15-7.19 (m, 1H), 7.25-7.28 (m, 2H), 7.31-7.33 (m, 2H); ^{13}C NMR: δ 20.73, 22.33, 23.47, 23.1, 24.73, 25.39, 29.63, 35.86, 37.06, 37.48, 39.74, 43.32, 53.85, 63.54, 71.27, 74.31, 76.29, 118.5, 119.4, 126.9, 128.1, 129.3, 132.4, 134.6, 16.9, 170.5; HRMS (ESI) calcd for[$C_{28}H_{40}N_2O_5 + Na^+$]: 507.2835; found: 507.2835.

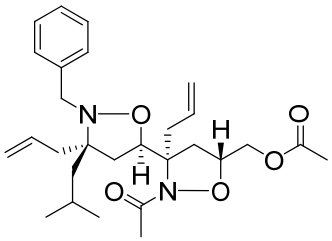

IV-19

((3*R*,3'*S*,5*R*,5'*R*)-2-acetyl-3,3'-diallyl-2'-benzyl-3'-isobutyl-3,5'-biisoxazolidin-5-yl)methyl acetate (IV-19): ^{1}H NMR: δ 0.96 (d, 3H, J = 4.9), 0.97 (d, 3H, J = 5.4), 1.30 (dd, 1H, J = 6.9, 14.6), 1.62 (dd, 1H, J = 4.9, 15.6), 1.86-1.91 (m, 1H), 1.98 (dd, 1H, J = 6.4, 13.2), 2.03 (s, 3H), 2.08 (s, 3H), 2.11 (dd, 1H, J = 7.8, 12.7), 2.19-2.24 (m, 2H), 2.37 (dd, 1H, J = 8.3, 12.7), 2.43 (dd, 1H, J = 7.1, 13.9), 2.74 (dd, 1H, J = 10.7, 13.2), 2.97 (dd, 1H, J = 6.6, 13.9); 4.76 (d, 1H, J = 14.2), 3.84 (d, 1H, J = 14.2), 3.98 (dd, 1H, J = 6.8, 11.7), 4.16-4.2 (m, 1H), 4.59-4.62 (m, 1H), 5.01-5.13 (m, 4H), 5.63-5.71 (m, 1H), 5.83-5.91 (m, 1H), 7.19-7.31 (m, 5).

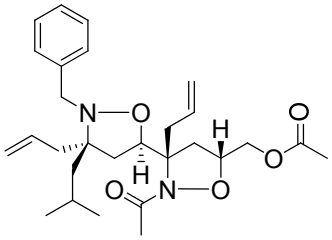

IV-20

((3*S*,3'*S*,5*R*,5'*R*)-2-acetyl-3,3'-diallyl-2'-benzyl-3'-isobutyl-3,5'-biisoxazolidin-5-yl)methyl acetate (IV-20): ^{1}H NMR: δ 0.99 (d, 3H, J = 6.8), 1.07 (d, 3H, J = 6.8), 1.34 (dd, 1H, J = 6.3, 14.7), 1.68 (dd, 1H, J = 4.9, 14.7), 1.75-1.79 (m, 1H), 1.84-1.95 (m, 2H), 1.97 (s, 3H), 2.03 (s, 3H), 2.18-2.25 (m, 3H), 2.18-2.25 (m, 3H), 2.46 (dd, 1H, J = 7.6, 13.9), 2.71 (dd, 1H, J = 5.6, 11.5), 2.92 (dd, 1H, J = 6.3, 13.7), 3.28-3.33 (m, 1H), 3.64 (d, 1H, J = 13.7), 3.70 (dd, 1H, J – 5.4, 12.7), 3.81 (d, 1H, J = 13.7), 3.88 (dd, 1H, J = 2.4, 12.2), 4.89-4.92 (m, 1H), 5.04-5.14 (m, 4H), 5.5205.60 (m, 1H), 5.81-5.90 (m, 1H), 7.18-7.29 (m, 5H).

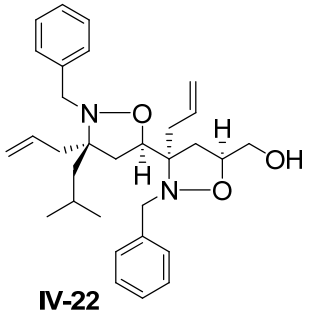

IV-22

((3*R*,3'*S*,5*S*,5'*R*)-3,3'-diallyl-2,2'-dibenzyl-3'-isobutyl-3,5'-biisoxazolidin-5-yl)methanol (IV-22): To a stirring solution of bisisoxazolidine **IV-21** (170 mg, 0.43 mmol) in THF (2.1 ml) cooled in an ice-H_2O bath was added DMAP (5 mg, 0.04 mmol) and Et_3N (64 µl, 0.46 mmol, 1.1 eq) follwed by TBSOTf (110 µl, 0.46 mmol, 1.1 eq). The reaction mixture is stirred with continued cooling for 2h at which point TLC analysis indicates completion of the reaction. The solution was diluted with sat. aq. NH_4Cl (5 ml), extracted with Et_2O (3 x 5 ml), and the combined organic extracts were washed with brine (1 x 5 ml), dried over Na_2SO_4, filtered, and concentrated *in vacuo*. The crude product was purified by flash chromatography (80:20 hexanes:EtOAc) to yield 210 mg of the TBS ether product in 98% yield. This product was dissolved in DMF (2.1 ml), BnBr (320 µl, 2.5 mmol, 6.0 eq) and *i*Pr_2NEt (210 µl, 1.2 mmol, 3.0 eq) was added, and the solution irradiated in a 1000 W microwave at 20% power (4 x 20s) with cooling and stirring between each interval. Upon cooling to ambient temperature, the mixture was diluted with H_2O (5 ml) and extracted with Et_2O (3 x 5 ml). The combined organic extracts were washed with H_2O (2 x 5 ml) and brine (1 x 5 ml), dried over Na_2SO_4, filtered, and concentrated *in vacuo*. The crude product was immediately subjected to silyl ether deprotection. To a stirring solution of the crude product in THF (2.2 ml) cooled in an ice-H_2O bath was added TBAF (820 µl of a 1M solution in THF, 0.82 mmol, 2.0 eq). The solution was stirred 1h and at this point TLC analysis showed that no starting material remained. The solution was diluted with sat. aq. NH_4Cl, extracted with Et_2O (3 x 5 ml), and the combined organic extracts were washed with brine (1 x 5 ml), dried over Na_2SO_4, filtered, and concentrated. The crude product was purified by flash chromatography (80:20 hexanes:EtOAc) to yield 160 mg of bisisoxazolidine **IV-22** as a colorless oil in 77% yield. IR: ^{1}H NMR: δ 0.82 (d, 3H, J = 6.8), 0.92 (d, 3H, J = 6.4), 1.00 (dd, 1H, J = 2.0, 6.4), 1.34 (dd, 1H, J = 5.9, 14.7), 1.55 (dd, 1H, J = 5.1, 14.4), 1.72

(dd, 1H, J = 4.9, 12.2), 1.79-1.87 (m, 1H), 2.10-2.14 (m, 2H), 2.18-2.25 (m, 2H), 2.36 (dd, 1H, J = 7.3, 15.6), 2.41 (dd, 1H, J = 7.3, 13.7), 2.61 (t, 1H, J = 10.3), 3.41-3.46 (m, 1H), 3.47-3.57 (m, 2H), 3.69 (d, 1H, J = 13.7), 3.74 (d, 1H, J = 13.7), 3.93-3.99 (m, 1H), 4.09-4.17 (m, 2H), 5.00-5.13 (m, 4H), 5.83-5.96 (m, 2H), 7.17-7.25 (m, 10H); ^{13}C NMR: δ 23.57, 24.75, 25.31, 35.04, 36.63, 37.01, 38.04, 43.48, 53.76, 54.49, 65.10, 67.68, 68.27, 69.15, 75.09, 76.12, 117.7, 118.3, 126.3, 126.7, 127.3, 127.9, 128.0, 128.9, 134.7, 135.1, 138.7, 139.5; HRMS (ESI) calcd for $[C_{31}H_{42}N_2O_3 + Na]^+$: 513.3093; found: 513.3099.

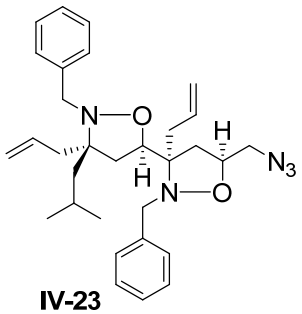

IV-23

(3*R*,3'*S*,5*S*,5'*R*)-3,3'-diallyl-5-(azidomethyl)-2,2'-dibenzyl-3'-isobutyl-3,5'-biisoxazolidine (IV-23): To a solution of isoxazolidine **IV-22** (110 mg, 0.22 mmol, 1.0 eq) in 2.2 ml anhydrous CH_2Cl_2 was added Et_3N (61 μl, 0.44 mmol, 2.0 eq) and methanesulfonyl chloride (34 μl, 0.44 mmol, 2.0 eq). The solution was stirred at ambient temperature for 30 min, at which time TLC analysis indicated completion of the reaction. The reaction mixture was diluted with H_2O (5 ml) and CH_2Cl_2 (5 ml), the layers were separated, and the aqueous layer was extracted with CH_2Cl_2 (3 x 5 ml). The combined organic extracts were washed with brine, dried over Na_2SO_4, filtered, and concentrated *in vacuo*. The crude product was dissolved in DMSO (2.2 ml) and sodium azide was added (140 mg, 2.2 mmol). The flask was fitted with a condenser and the reaction heated at 100 °C for 3 h. At that time TLC analysis indicated completion of the reaction. The cooled reaction mixture was diluted with water and extracted with Et_2O (3 x 5 ml). The combined organic extracts were washed with H_2O (2 x 5 ml) and brine (1 x 5 ml), dried over Na_2SO_4, filtered, and concentrated *in vacuo*. The crude product was purifed by flash chromatography (95:5 hexanes/EtOAc) to yield 76 mg of product as a colorless oil in 67% yield. IR: 2925, 2099, 1494, 1262, 1049, 824 cm^{-1}; ^{1}H NMR: δ 0.84 (d, 3H, J =

6.8), 0.93 (d, 1H, J = 6.8), 1.00 (d, 1H, J = 6.8), 1.33 (dd, 1H, J = 14.2, 5.9), 1.57 (dd, 1H, J = 14.7, 4.9), 1.72 (dd, 1H, J = 12.7, 5.9), 1.81-1.89 (m, 1H), 2.11 (dd, 1H, J = 11.7, 7.8), 2.18-2.24 (m, 2H), 2.29-2.37 (m, 2H), 2.42 (dd, 1H, J = 13.7, 7.3), 2.51 (dd, 1H, J = 11.2, 9.3), 2.80, dd, 1H, J = 12.7, 4.4), 3.26 (dd, 1H, J = 12.7, 7.8), 3.64 (d, 1H, J = 15.1), 3.69 (d, 1H, J = 13.7), 3.75 (d, 1H, J = 13.7), 3.75 (d, 1H, J = 15.1), 3.95-4.00 (m, 1H), 4.06-4.11 (m, 1H), 5.03-5.13 (m, 4H), 5.84-5.95 (m, 2H), 7.15-7.39 (m, 10H): ^{13}C NMR: δ 23.60, 24.73, 25.39, 35.47, 37.65, 37.90, 38.36, 43.54, 53.85, 54.30, 68.25, 69.51, 74.20, 75.75, 117.8, 118.2, 126.3, 126.9, 127.6, 127.8, 128.0, 129.1, 134.7, 135.1, 138.8, 139.1; HRMS (ESI) calcd for $[C_{31}H_{41}N_5O_2 + Na]^+$: 538.3158, found: 538.3162.

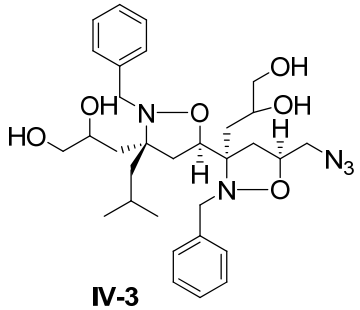

IV-3

3,3'-((3*R*,3'*S*,5*S*,5'*R*)-5-(azidomethyl)-2,2'-dibenzyl-3'-isobutyl-3,5'-biisoxazolidine-3,3'-diyl)dipropane-1,2-diol (IV-5): To a solution of bis-isoxazolidine **S16** (20 mg, 0.04 mmol, 1.0 eq) in *t*BuOH (300 μl), THF (80 μl) and H_2O (20 μl) was added NMO (25 mg, 0.10 mmol, 2.4 eq) followed by OsO4 (100 μl of a 2.5 wt% solution in *t*BuOH, 0.01 mmol, 0.2 eq). The reaction mixture was stirred for 5h at which time TLC and mass spectrometry indicated completion of the reaction. Na_2SO_3 (20 mg) was added to quench excess reagent and the mixture was stirred 1 h. The mixture was then diluted with EtOAc (5 mL) and H_2O (5 mL) and the layers separated. The aqueous layer was extracted with EtOAc (3 x 5 mL). The combined organic extracts were washed with brine (1 x 10 mL), dried over Na_2SO_4, filtered, and concentrated in vacuo. The crude product was purified by flash chromatography (elution in 90:10 EtOAc/MeOH) to yield 22 mg of product as a colorless oil in 93% yield. ^{1}H NMR (400 MHz): δ 0.95-1.00 (m, 6H), 1.37-1.95 (m, 8H), 1.99-2.53 (m, 4H), 3.03-3.39 (m, 2H), 3.42-3.52 (m, 2H), 3.84-3.91 (m, 3H), 3.97-4.56 (m, 3H), 7.13-7.38 (m, 10H); HRMS (ESI) calcd for $[C_{31}H_{45}N_5O_6 + H]^+$: 584.3448, found: 584.3461.

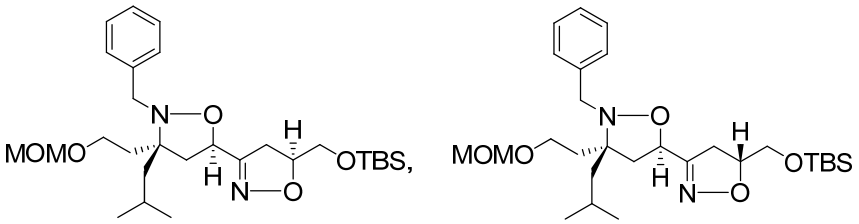

IV-25 **IV-26**

IV-25 and **IV-26**: To a solution of **IV-24** (1.8 g, 5.1 mmol, 1.0 eq) in tol (51 mL) was added allyl alcohol (3.5 mL, 51 mmol, 10 eq) followed by dropwise addition of NaOCl (18 mL of a 705 mM solution in H_2O, 13 mmol, 2.5 eq). Upon stirring 3 h TLC analysis indicated completion of the reaction. The aqueous and organic layers were separted and the aqueous extracted with EtOAc (3 x 25 mL). The combined organic extracts were washed with brine (2 x 20 mL), dried over Na_2SO_4, filtered, and concentrated in vacuo. Analysis of the crude ^{1}H NMR mixture indicated a 1.5:1 mixture of diastereomers. Purification by flash chromatography (elution in 40/60 hexanes:EtOAc) yielded 1.66 g of product as a colorless oil in 80% yield. To the product (1.66 g, 4.1 mmol, 1.0 eq), as a mixture of diastereomers, in THF (41 mL) cooled in an ice-H_2O bath was added DMAP (50 mg, 0.41 mmol, 0.1 eq) and Et_3N (1.3 mL, 9.0 mmol, 2.2 eq) followed by TBSOTf (2.1 mL, 9.0 mmol, 2.2 eq). Upon stirring with continued cooling for 1 h TLC analysis indicated complete consumption of starting material. The reaction mixture was diluted with sat. NH_4Cl (20 mL) and CH_2Cl_2 (20 mL) and the layers separated. The combined aqueous was extracted with CH_2Cl_2 (3 x 20 mL) and the combined organic extracts were washed with brine (25 mL), dried over Na_2SO_4, filtered, and concentrated in vacuo. Following TBS protection of the primary alcohols the two diastereomers were purified and separated by flash chromatography (20:80 hexanes/EtOAc) to give a 95% combined yield of **IV-25** and **IV-26**.

(*S*)-3-((3*S*,5*R*)-2-benzyl-3-isobutyl-3-(2-(methoxymethoxy)ethyl)isoxazolidin-5-yl)-5-((tert-butyldimethylsilyloxy)methyl)-4,5-dihydroisoxazole (IV-25): ^{1}H NMR: δ -0.01 (s, 3H), 0.00 (s, 3H), 0.82 (s, 9H), 0.97 (d, 3H, J = 5.1), 0.99 (d, 3H, J = 5.1), 1.37 (dd, 1H, J = 7.0, 14.5), 1.61 (dd, 1H, J – 5.1, 14.1), 1.82-1.89 (m, 2H), 1.91-1.94 (m, 2H), 2.50 (dd, 1H, J = 8.6, 12.9), 2.59 (dd, 1H, J = 6.6, 12.9), 2.67 (dd, 1H, J = 7.6, 17.4), 2.79 (dd, 1H, J = 10.4, 17.8), 3.36 (s, 3H), 3.54-3.57 (m ,1H), 3.70-3.74 (m, 1H), 3.82 (s, 2H), 4.52-4.60 (m, 1H), 4.62 (s, 2H), 4.66-4.70 (m, 1H), 7.19-7.33 (m, 5H).

(*R*)-3-((3*S*,5*R*)-2-benzyl-3-isobutyl-3-(2-(methoxymethoxy)ethyl)isoxazolidin-5-yl)-5-((tert-butyldimethylsilyloxy)methyl)-4,5-dihydroisoxazole (IV-26): ^{1}H NMR: δ 0.04 (s, 3H), 0.06 (s, 3H), 0.87 (s, 9H), 0.97-1.00 (m, 6H), 1.37 (dd, 1H, J = 6.6, 14.0), 1.76 (dd, 1H, J = 5.1, 14.5), 1.82-1.99 (m, 3H), 2.41 (dd, 1H, J = 6.4, 12.7), 2.52 (dd, 1H, J = 8.8, 12.7), 2.81 (d, 2H, J = 9.0), 3.36 (s, 3H), 3.56 (dd, 1H, J = 4.7, 10.9), 3.63 (dd, 1H, J = 4.7, 10.9), 3.71 (dd, 1H, J = 14.3, 17.1), 4.56-4.99 (m, 1H), 4.62 (s, 2H), 4.75-4.78 (m, 1H), 7.22-7.34 (m, 5H).

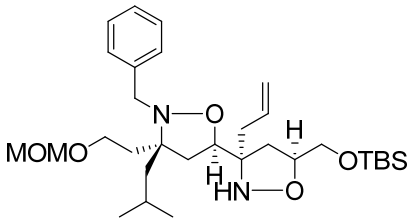

IV-27

(3*R*,3'*S*,5*S*,5'*R*)-3-allyl-2'-benzyl-5-((tert-butyldimethylsilyloxy)methyl)-3'-isobutyl-3'-(2-(methoxymethoxy)ethyl)-3,5'-biisoxazolidine (IV-27): A solution of compound **IV-25** (520 mg, 1.0 mmol, 1.0 eq) in toluene (6.7 mL) was cooled in a dry ice-acetone bath. BF_3•OEt_2 (380 ul, 3.0 mmol, 3.0 eq) was added dropwise to the solution over 15 min and the mixture was stirred with continued cooling for 30 min. Allylmagnesium chloride (3.0 mL of a 2.0M solution in THF, 6.0 mmol, 6.0 eq) was then added dropwise over 30 min. The reaction mixture was stirred for 5 hours with continued cooling at which point TLC analysis indicated complete consumption of the starting material. Saturated NH_4Cl (10 mL) was added to the reaction and the resultant solution was transferred to an ice-H_2O bath. After slowly warming to rt the mixture was diluted with H_2O (10 mL) and Et_2O (10 mL) and the organic and aqueous layers separated. The aqueous layer was extracted with Et_2O (3 x 5 mL). The combined organic extracts were washed with brine (5 mL), dried over Na_2SO_4, filtered, and concentrated in vacuo. The crude product was purified by flash chromatography to yield 480 mg of a >20:1 mixture of diastereomers as a colorless oil in 86% yield. ^{1}H NMR: δ -0.02 (s, 3H), -0.01 (s, 3H), 0.84 (s, 9H)., 0.98 (s, 3H), 1.00 (s, 3H), 1.37-1.40 (m, 1H), 1.53-1.55 (m, 1H), 1.58-1.63 (m, 1H), 1.81-1.87 (m, 3H), 1.93-2.02 (m, 3H), 2.25-2.32 (m, 1H), 2.34-2.38 (m, 1H), 3.35 (s, 3H), 3.67-3.71 (m, 2H), 3.84-3.88 (m, 1H), 3.94-2.99 (m, 1H), 4.07 (bs, 1H), 4.60 (s, 2H), 5.00-5.04 (m 2H), 5.36 (bs, 1H), 5.90 (bs, 1H), 7.21-7.31 (m, 5H).

IV-28 and **IV-29**: A solution of compound **IV-25** (350 mg, 0.67 mmol, 1.0 eq) in toluene (4.5 mL) was cooled in a dry ice-acetone bath. $BF_3 \bullet OEt_2$ (260 ul, 2.0 mmol, 3.0 eq) was added dropwise to the solution over 15 min and the mixture was stirred with continued cooling for 30 min. Allylmagnesium chloride (2.0 mL of a 2.0M solution in THF, 4.0 mmol, 6.0 eq) was then added dropwise over 30 min. The reaction mixture was stirred for 5 hours with continued cooling at which point TLC analysis indicated complete consumption of the starting material. Saturated NH_4Cl (10 mL) was added to the reaction and the resultant solution was transferred to an ice-H_2O bath. After slowly warming to rt the mixture was diluted with H_2O (10 mL) and Et_2O (10 mL) and the organic and aqueous layers separated. The aqueous layer was extracted with Et_2O (3 x 5 mL). The combined organic extracts were washed with brine (5 mL), dried over Na_2SO_4, filtered, and concentrated in vacuo. The crude product was purified by flash chromatography to yield 240 mg of a 2:1 mixture of diastereomers as a colorless oil in a combined 63% yield. The stereochemistry has not been verified for these compounds.

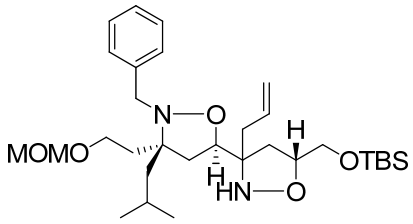

IV-28

(5R**)-3-allyl-2'-benzyl-5-((tert-butyldimethylsilyloxy)methyl)-3'-isobutyl-3'-(2-(methoxymethoxy)ethyl)-3,5'-biisoxazolidine**:

Less polar diastereomer: ^{1}H NMR: δ -0.06 (s, 3H), -0.05 (s, 3H), 0.83 (s, 9H), 0.97 (d, 3H, J = 2.4), 0.98 (d, 3H, J = 2.4), 1.20-12.5 (m, 1H), 1.37 (dd, 1H, J = 6.4, 14.2), 1.55 (dd, 1H, J = 4.4, 14.2), 1.77-1.83 (, 1H), 1.86-1.90 (m, 1H), 1.93-1.99 (m, 1H), 2.00-2.05 (m, 2H), 2.22 (dd, 1H, J = 8.8, 12.7), 2.38 (m, 2H), 3.36 (s, 3H), 3.61-3.76 (m, 3H), 3.82 (d, 1H, J = 14.2), 3.99-4.00 (m, 1H), 4.61 (s, 2H), 5.04-5.08 (m, 2H), 5.72-5.80 (m,1H), 7.22-7.33 (m, 5H).

More polar diastereomer: ^{1}H NMR: δ 0.04 (s, 6H), 0.88 (s, 9H), 0.98 (d, 3H, J = 14.9), 0.99 (d, 3H, J = 14.9), 1.30 (m, 1H), 1.38 (dd, 1H, J = 6.1, 14.4), 1.61 (dd, 1H, J = 5.1, 14.4), 1.79-1.89 (m, 3H), 1.93-2.01 (m, 3H), 2.27-2.32 (m, 1H), 2.41 (dd, 1H, J = 5.6,

13.9), 3.36 (s, 3H), 3.58 (dd, 1H, J = 3.7, 10.0), 3.64-3.71 (m, 3H), 3.85 (d, 1H, J = 14.2), 4.60 (s, 2H), 4.99-5.02 (m, 2H), 5.33 (bs, 1H), 5.89 (bs, 1H), 7.20-7.32 (m, 5H).

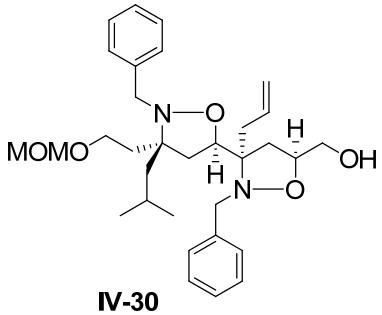

IV-30

((3*R*,3'*S*,5*S*,5'*R*)-3-allyl-2,2'-dibenzyl-3'-isobutyl-3'-(2-(methoxymethoxy)ethyl)-3,5'-biisoxazolidin-5-yl)methanol (IV-30): To a solution of **IV-27** (160 mg, 0.28 mmol, 1.0 eq) was in DMF (1.4 ml), BnBr (220 µl, 1.7 mmol, 6.0 eq) and *i*Pr_2NEt (150 µl, 0.9 mmol, 3.0 eq) was added, and the solution irradiated in a 1000 W microwave at 20% power (4 x 20s) with cooling and stirring between each interval. Upon cooling to ambient temperature, the mixture was diluted with H_2O (5 ml) and extracted with Et_2O (3 x 5 ml). The combined organic extracts were washed with H_2O (2 x 5 ml) and brine (1 x 5 ml), dried over Na_2SO_4, filtered, and concentrated *in vacuo*. The crude product was immediately subjected to silyl ether deprotection. To a stirring solution of the crude product in THF (1.4 ml) cooled in an ice-H_2O bath was added TBAF (850 µl of a 1M solution in THF, 0.82 mmol, 3.0 eq). The solution was stirred 2 h and at this point TLC analysis showed that no starting material remained. The solution was diluted with sat. aq. NH_4Cl, extracted with Et_2O (3 x 5 ml), and the combined organic extracts were washed with brine (1 x 5 ml), dried over Na_2SO_4, filtered, and concentrated. The crude product was purified by flash chromatography (80:20 hexanes:EtOAc) to yield 90 mg of bisisoxazolidine **IV-30** as a colorless oil in 60% yield. ^{1}H NMR: δ 0.83 (d, 3H, J = 6.8), 0.93 (d, 3H, J = 6.8), 1.38 (dd, 1H, J = 5.4, 14.2), 1.51 (dd, 1H, J = 5.4, 14.2), 1.61-1.63 (m, 1H), 1.75-1.94 (m, 3H), 2.18 (dd, 1H, J = 7.8, 12.2), 2.23 (dd, 1H, J = 8.5, 12.5), 2.33 (dd, 1H, J = 7.0, 13.4), 2.39 (dd, 1H, J = 7.3, 13.2), 2.59-2.63 (m, 1H), 3.36 (s, 3H), 3.44-3.54 (m, 2H), 3.61 (d, 1H, J =15.1), 3.68 (d, 1H, J = 14.2), 3.68-3.72 (m, 1H), 3.75 (d, 1H, J = 14.2), 3.96-4.00 (m, 1H), 4.08-4.19 (m, 3H), 4.62 (s, 2H), 4.68 (d, 1H, J = 5.9), 5.05 (dd, 1H, J = .15, 16.6), 5.08 (dd, 1H, J = 1.5, 10.3), 5.82-5.90 (m, 1H), 7.18-7.35 (m, 10H).

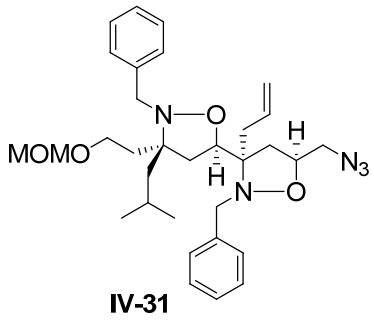

IV-31

(3*R*,3'*S*,5*S*,5'*R*)-3-allyl-5-(azidomethyl)-2,2'-dibenzyl-3'-isobutyl-3'-(2-(methoxymethoxy)ethyl)-3,5'-biisoxazolidine (IV-31): To a solution of isoxazolidine **IV-30** (80 mg, 0.15 mmol, 1.0 eq) in 1.5 ml anhydrous CH_2Cl_2 cooled in an ice-H_2O bath was added Et_3N (24 µl, 0.17 mmol, 1.1 eq) and methanesulfonyl chloride (13 µl, 0.17 mmol, 1.1 eq). The solution was stirred with continued cooling for 15 min, at which time TLC analysis indicated completion of the reaction. The reaction mixture was diluted with H_2O (5 ml) and CH_2Cl_2 (5 ml), the layers were separated, and the aqueous layer was extracted with CH_2Cl_2 (3 x 5 ml). The combined organic extracts were washed with brine, dried over Na_2SO_4, filtered, and concentrated *in vacuo*. The crude product was dissolved in DMSO (1.5 ml) and sodium azide was added (98 mg, 1.5 mmol, 1.5 eq). The flask was fitted with a condenser and the reaction heated at 100 °C for 6 h. At that time TLC analysis indicated completion of the reaction. The cooled reaction mixture was diluted with water and extracted with Et_2O (3 x 5 ml). The combined organic extracts were washed with H_2O (2 x 5 ml) and brine (1 x 5 ml), dried over Na_2SO_4, filtered, and concentrated *in vacuo*. The crude product was purifed by flash chromatography (70:30 hexanes/EtOAc) to yield 69 mg of product as a colorless oil in 72% yield. ^{1}H NMR: δ 0.84 (d, 3H, J = 6.8), 0.93 (d, 3H, J = 6.4), 1.35 (dd, 1H, J = 5.6, 14.4), 1.53 (dd, 1H, J = 5.4, 14.2), 1.71 (dd, 1H, J = 5.4, 12.2), 1.78-1.88 (m, 2H), 1.91-1.97 (m, 1H), 2.17 (dd, 1H, J = 7.6, 12.0), 2.24 (dd, 1H, J = 8.6, 12.5), 2.31 (dd, 1H, J = 7.8, 13.7), 2.38 (dd, 1H, J = 6.8, 13.7), 2.54 (m, 1H), 2.87 (dd, 1H, J = 4.4, 12.7), 3.30 (dd, 1H, J = 7.6, 12.5), 3.36 (s, 3H), 3.67 (d, 1H, J = 14.2) 3.66-3.71 (m, 2H), 3.75 (d, 1H, J = 13.7), 3.98-4.03 (m, 1H), 4.08 -4.15 (m 2H), 4.62 (s, 2H), 5.04 (dd, 1H, J = 2.0, 17.1), 5.07 (dd, 1H, J = 2.2, 10.0), 5.82 *m, 1H), 7.16-7.26 (m, 10H).

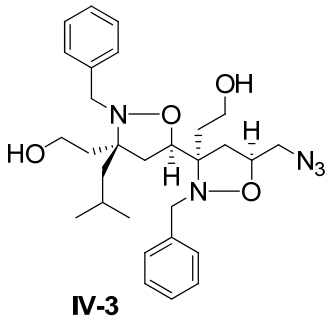

IV-3

2,2'-((3*R*,3'*S*,5*S*,5'*R*)-5-(azidomethyl)-2,2'-dibenzyl-3'-isobutyl-3,5'-biisoxazolidine-3,3'-diyl)diethanol (IV-3): To a solution of **IV-31** (42 mg, 0.07 mmol, 1.0 eq) in CH_3CN (750 μl) and H_2O (750 μl) was added $NaIO_4$ (18 mg, 0.08 mmol, 1.2 eq) and the mixture was stirred 2 h at rt at which point TLC analysis indicated complete consumption of starting material. The reaction mixture was diluted with H_2O and Et_2O and the layers separated. The aqueous was extracted with Et_2O (3 x 5 mL) and the combined organic extracts were washed with brine (10 mL), dried over Na_2SO_4, filtered and concentrated in vacuo. The crude aldehyde was dissolved in MeOH (700 μl) and $NaBH_4$ (8 mg, 0.2 mmol, 3.0 eq) was added to the solution. The reaction was stirred 30 min at which point TLC analysis indicated consumption of starting material. The reaction mixture was diluted with H_2O (5 mL) and Et_2O (5 mL) and the layers separated. The combined organic extracts were washed with brine (10 mL), dried over Na_2SO_4, filtered and concentrated in vacuo. The crude product was placed on ice and 1 mL of a 50% *i*PrOH/MeOH mixture added. After stirring 1 h ESI-MS analysis conversion to product. The product was purified by flash chromatography (elution in 70:30 hexanes/EtOAc) to yield 5 mg of **IV-3** as a colorless oil in 14% yield. 0.98 ('apparent triple', 6H, J = 7.3), 1.53-1.59, m, 1H), 1.64-1.70 (m, 3H), 1.82-1.95 (m, 2H), 2.12-2.25 (m, 2H), 2.31 (dd, 1H, J = 7.3, 12.2), 3.11 (bs, 1H), 3.30 Ibs, 1H). 3.71-3.79 (m, 3H), 3.83-3.96 (m, 5H), 4.08-4.11 (^{27}m, 1H), 4.15-4.18 (m, 1H), 7.21-7.36 (m, 10H).

G. Appendix of Select ^{1}H NMR spectra and HPLC traces

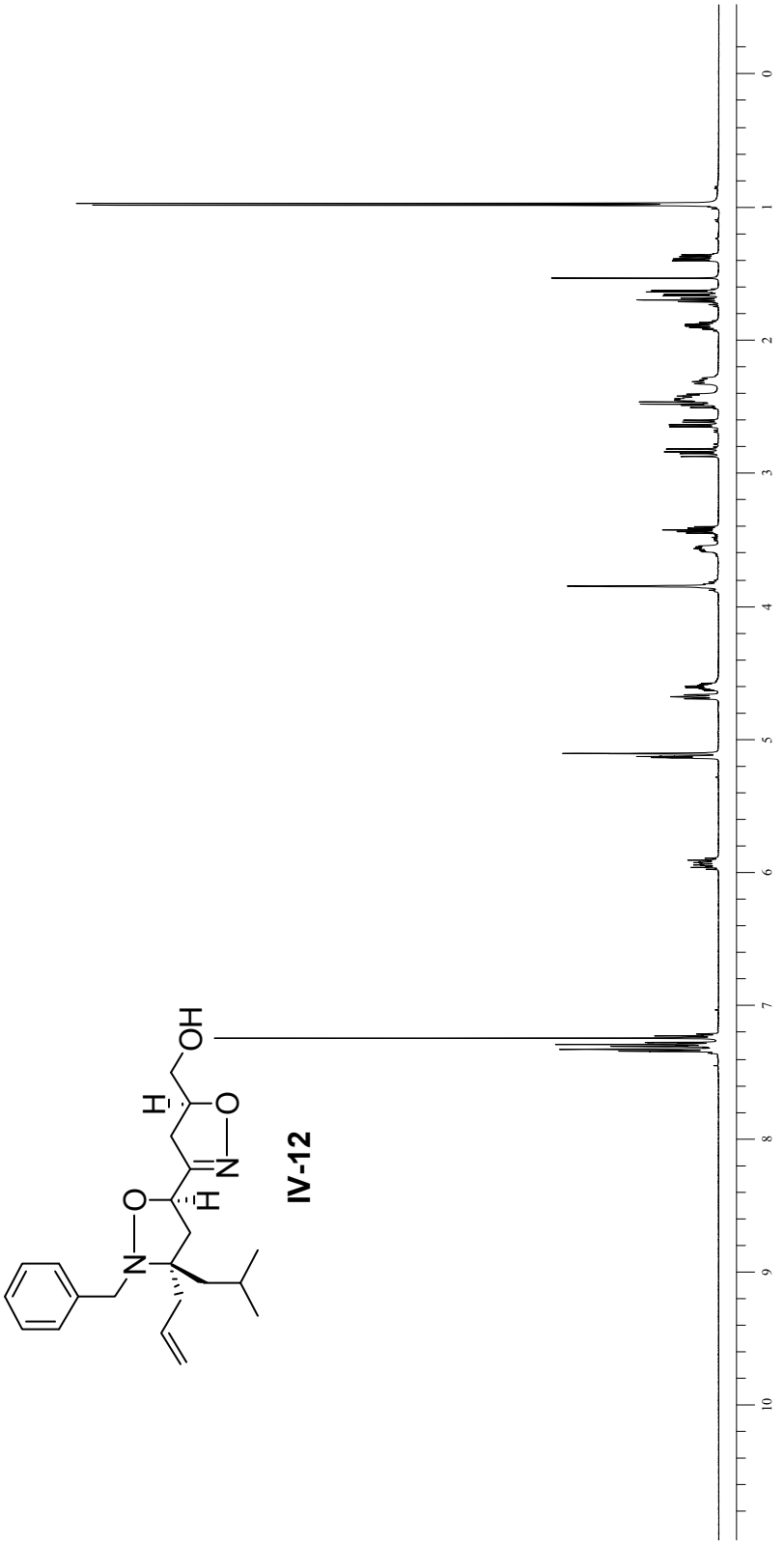

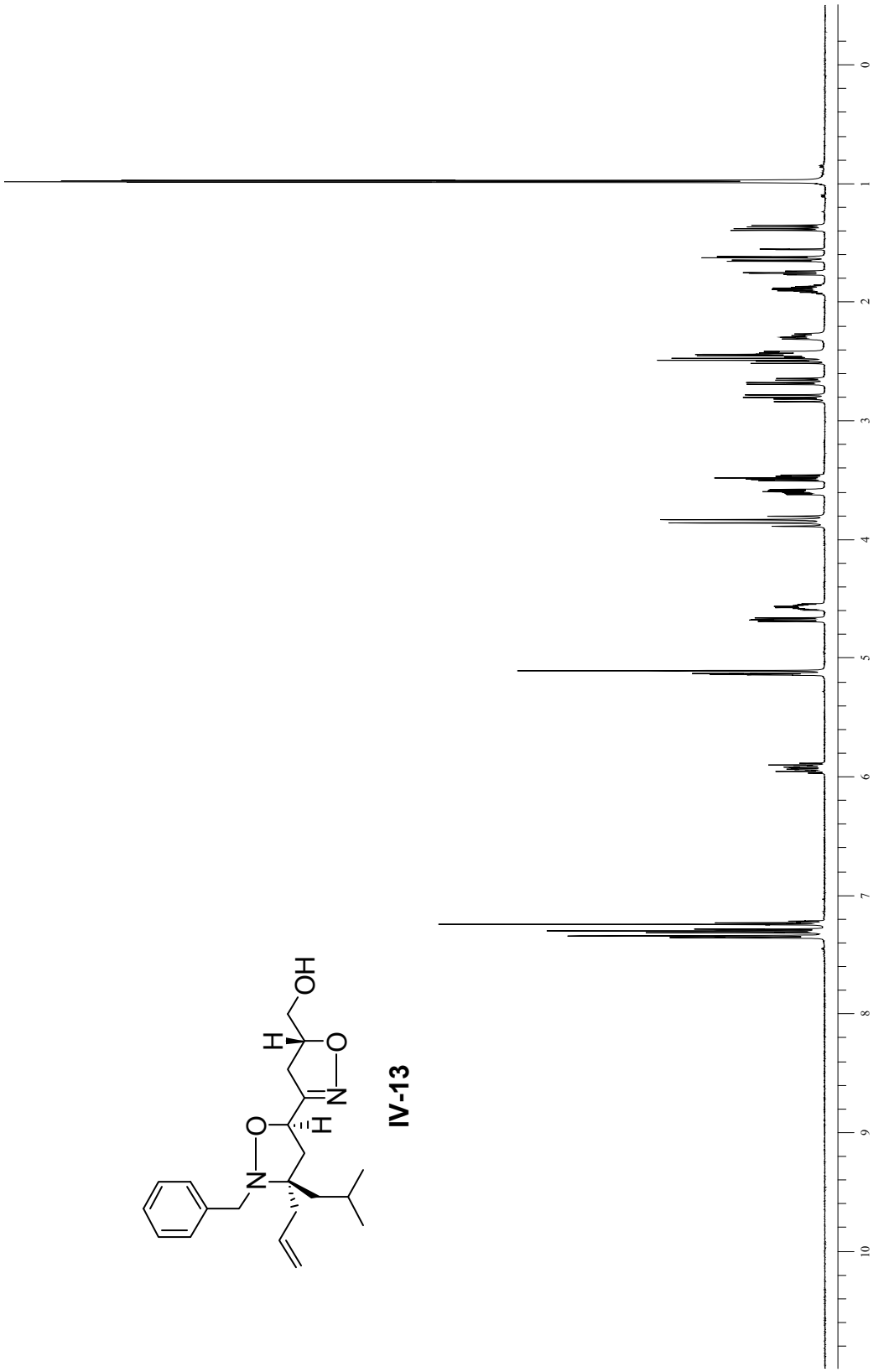

IV-13

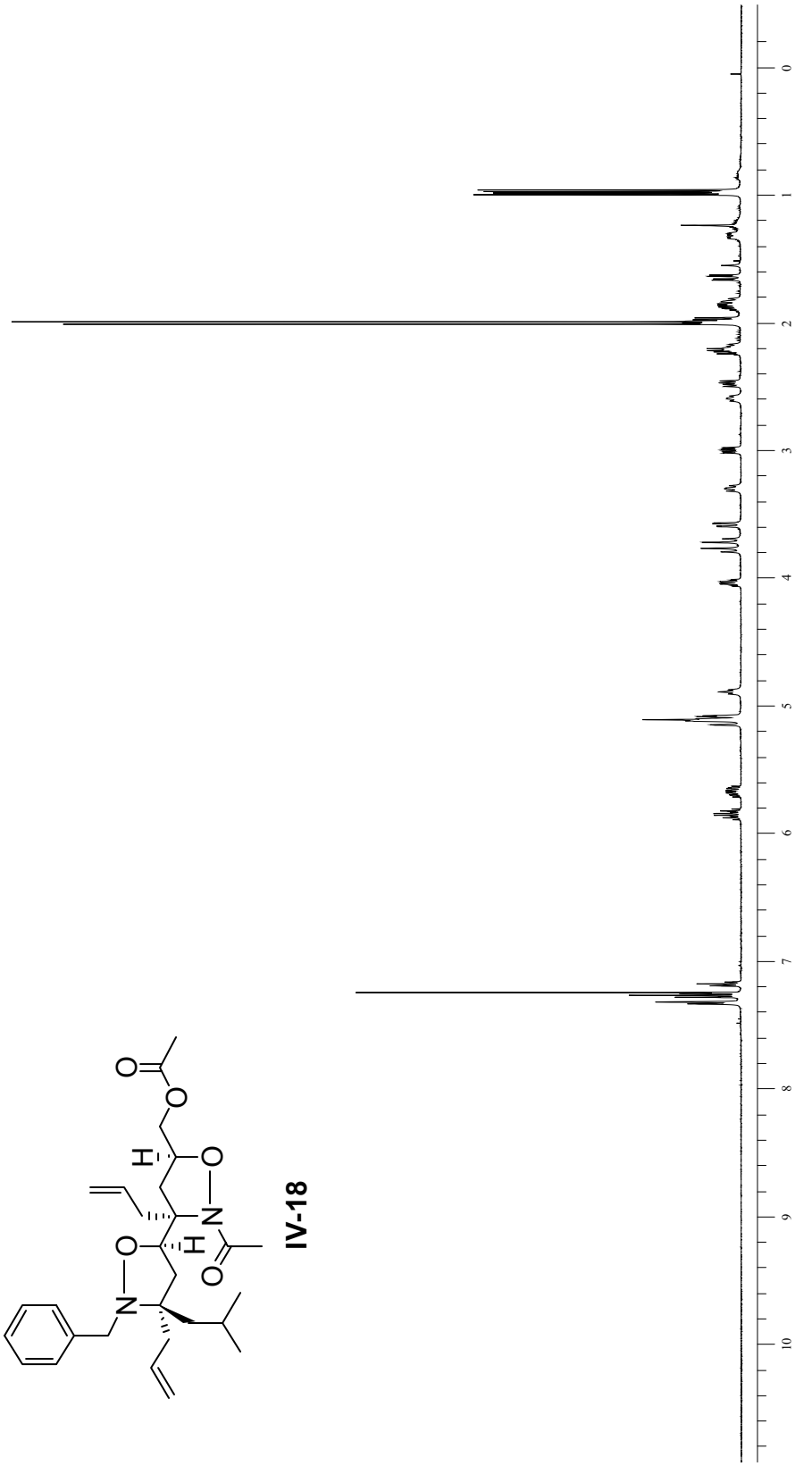

IV-18

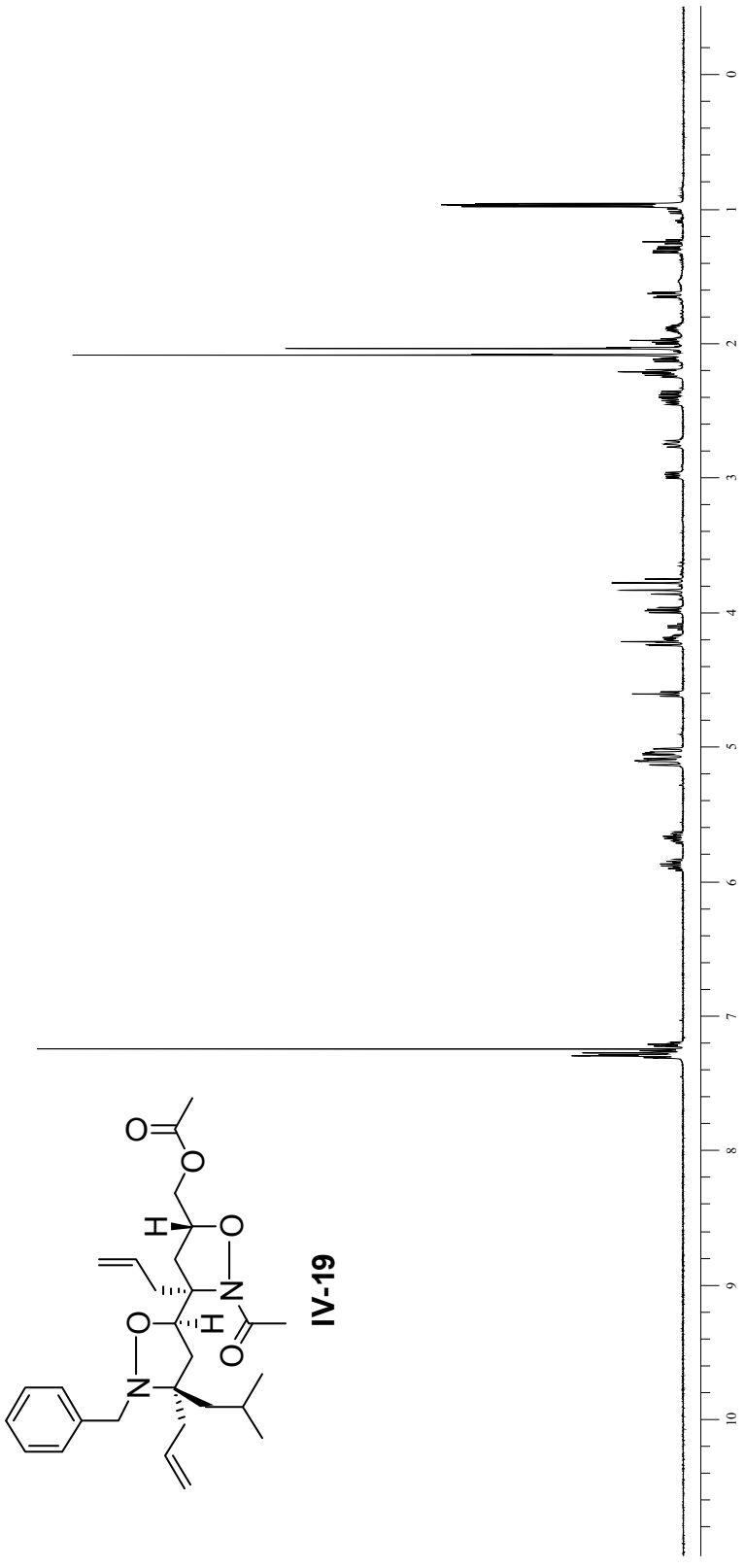
IV-19

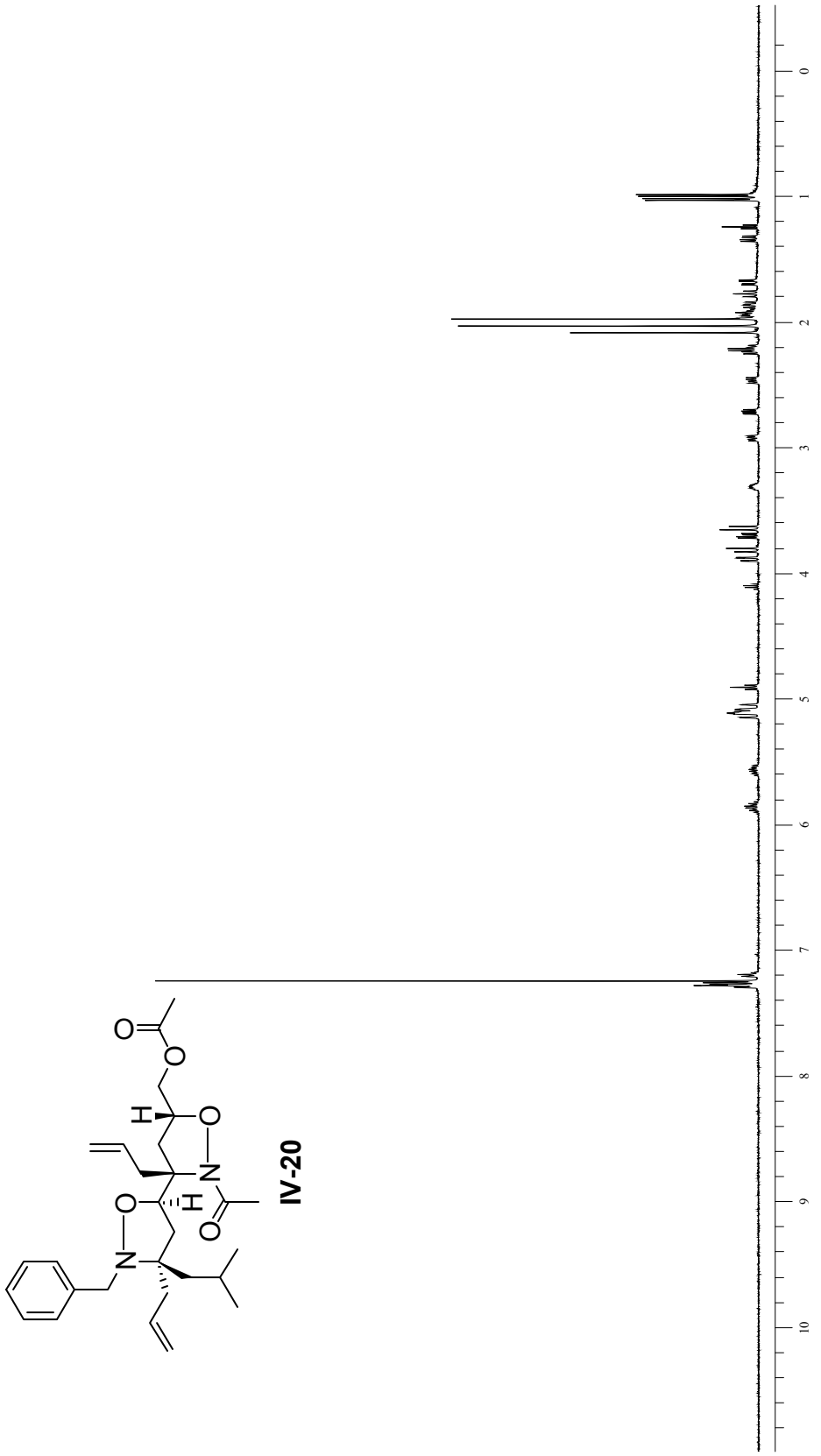
IV-20

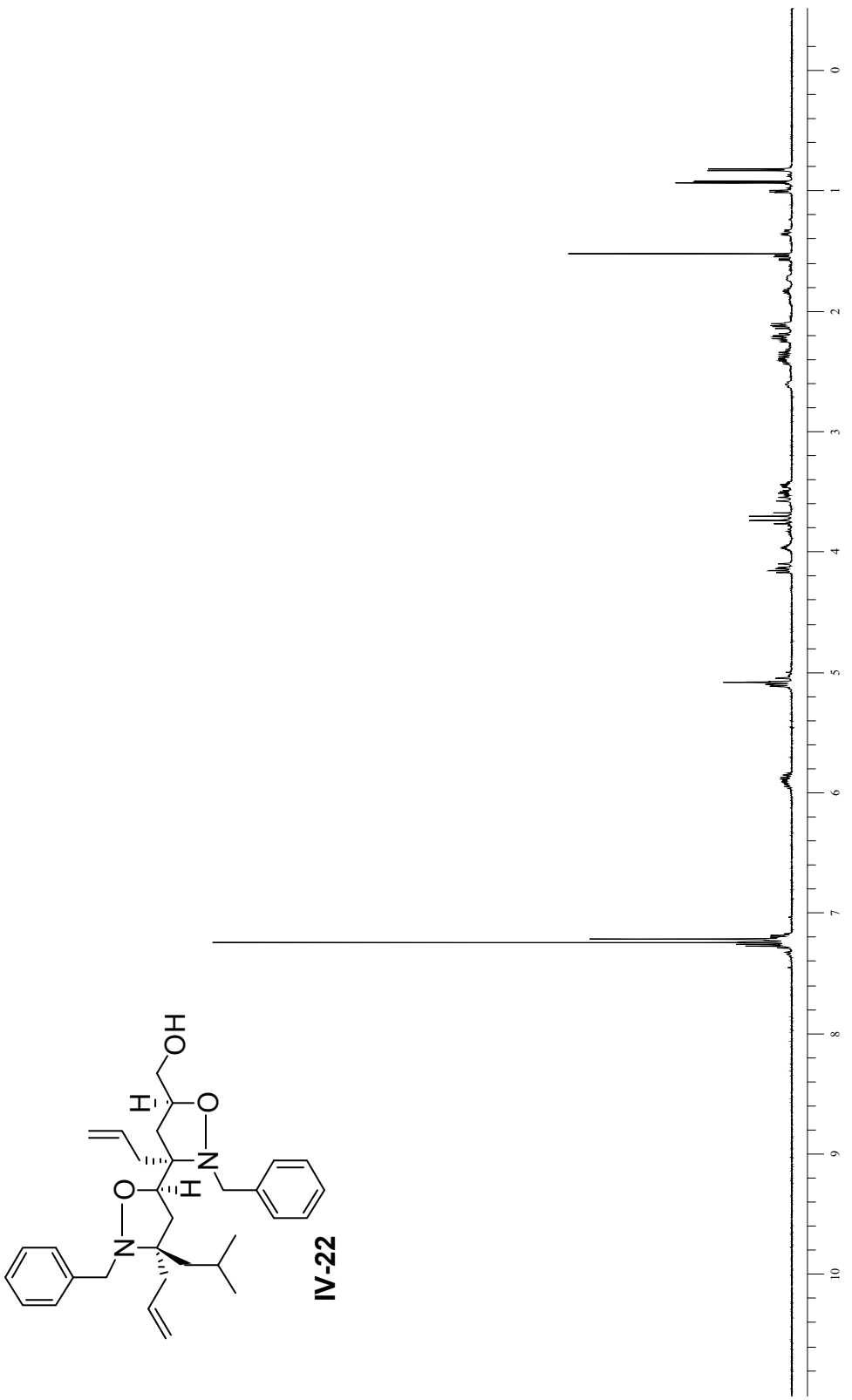

IV-22

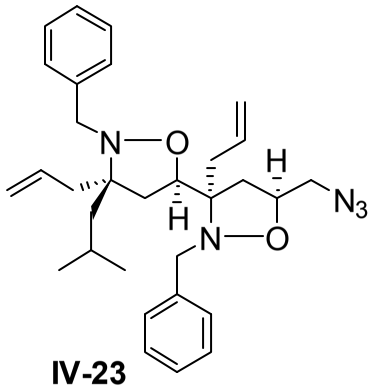

IV-23

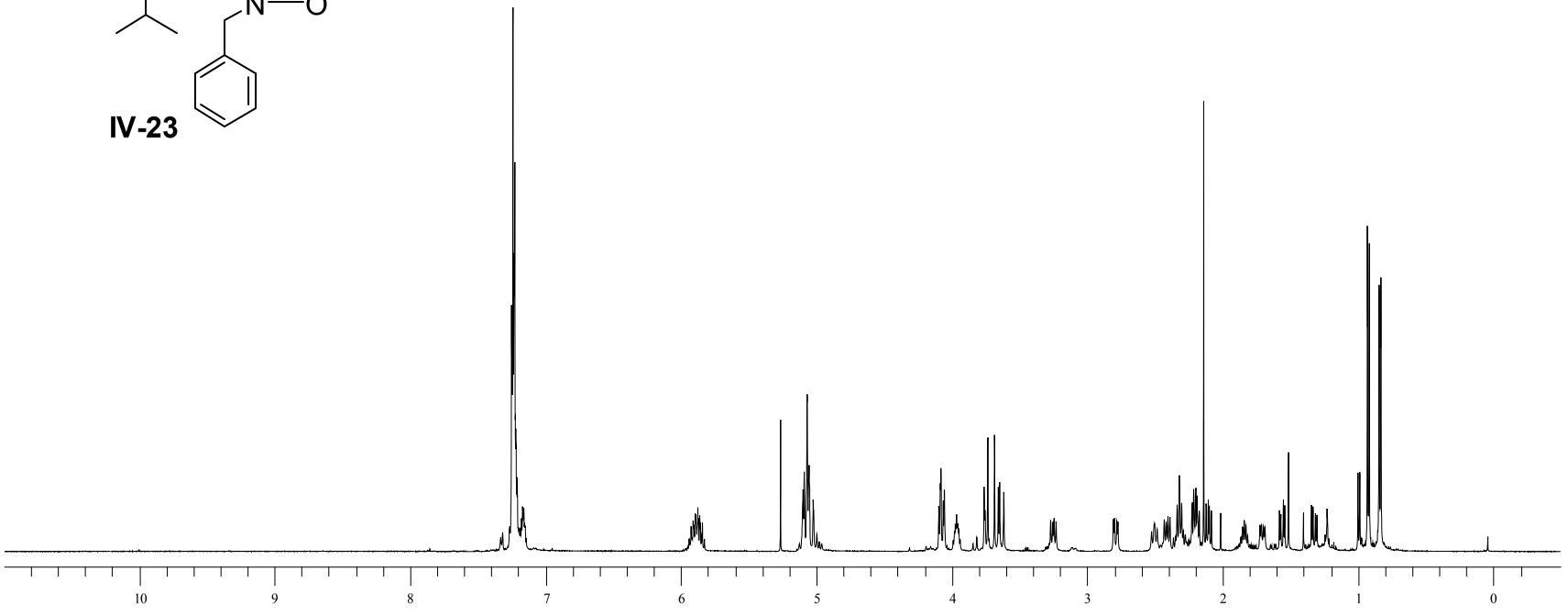

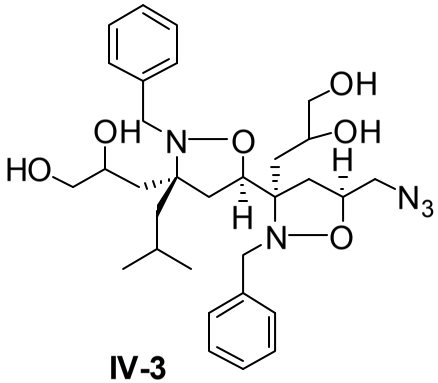

IV-3

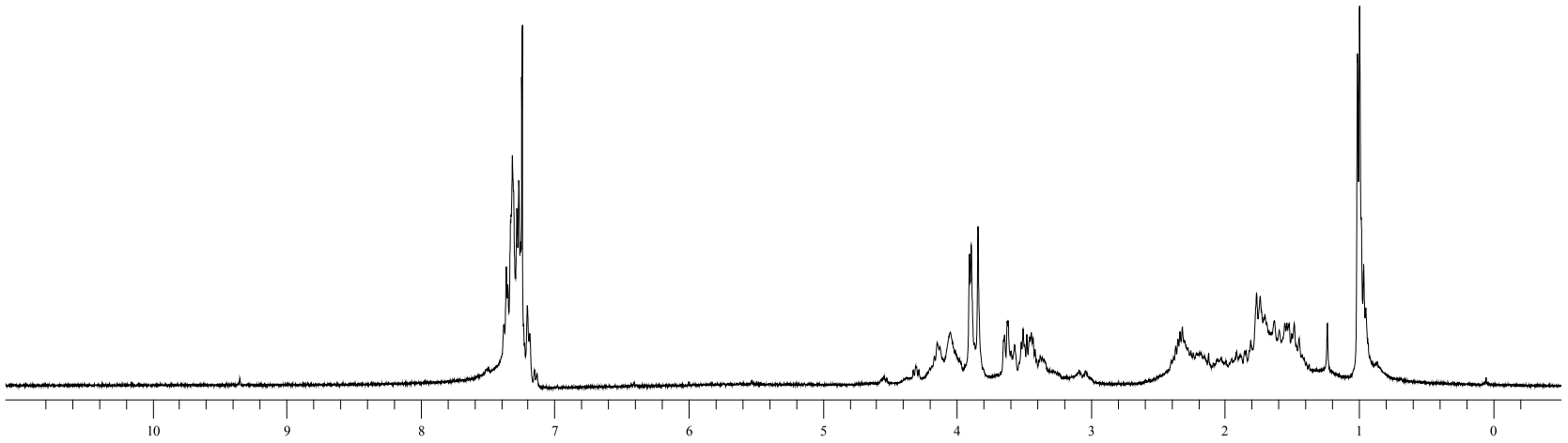

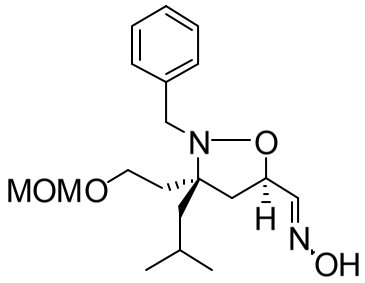

IV-24

less polar E/Z isomer

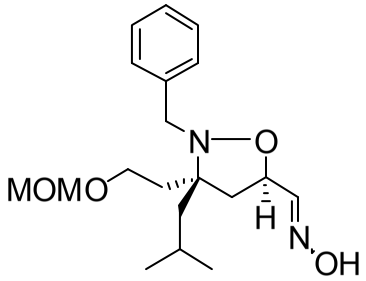

IV-24

more polar E/Z isomer

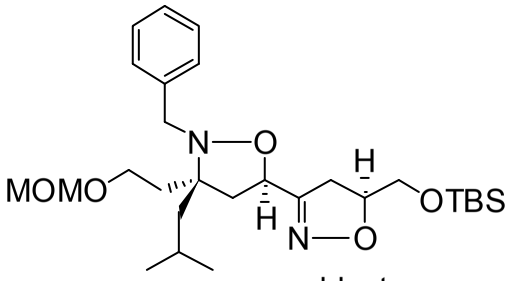

syn-adduct

IV-25

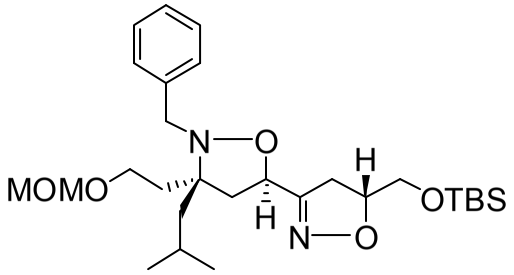

anti-adduct

IV-26

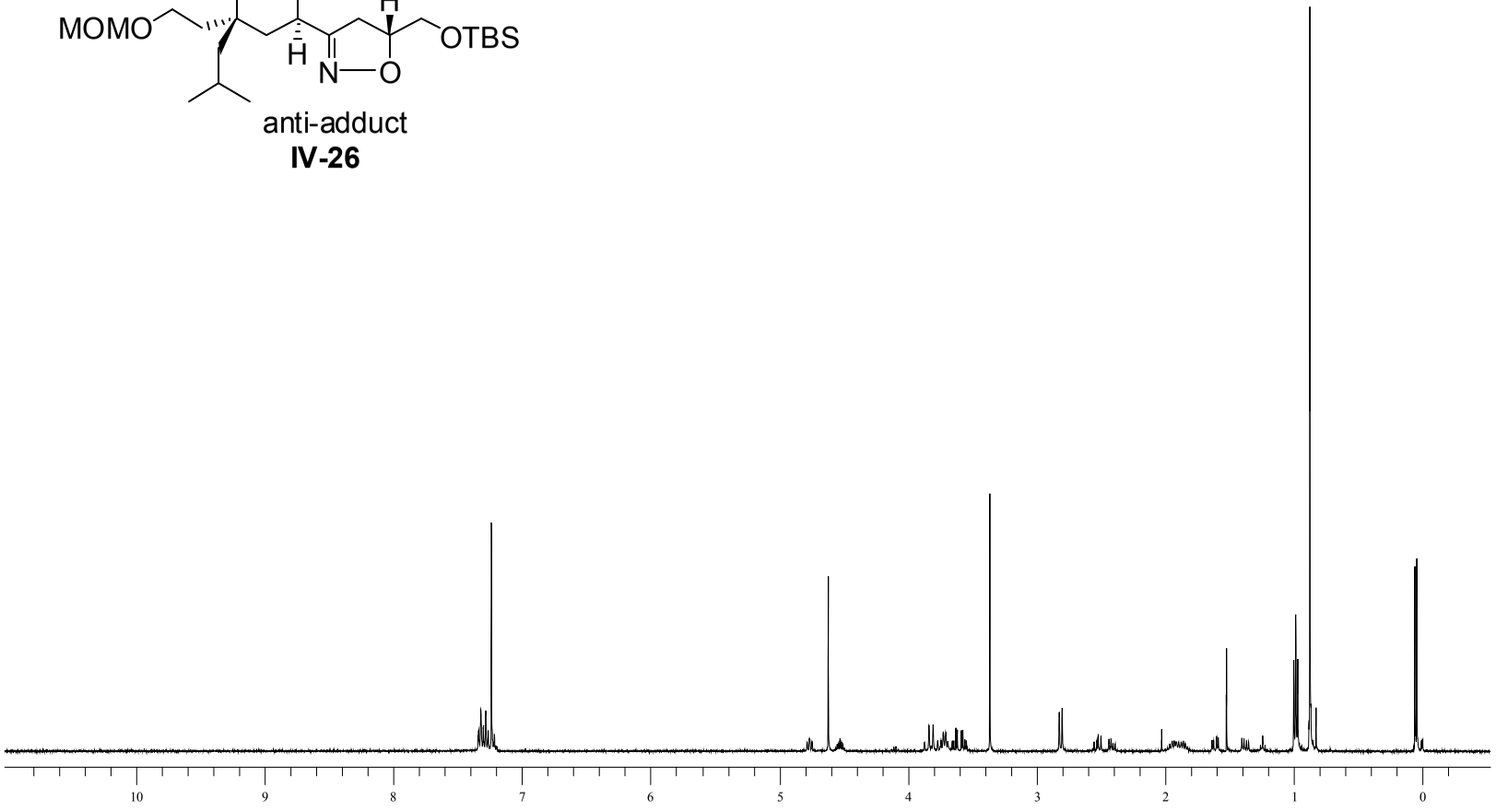

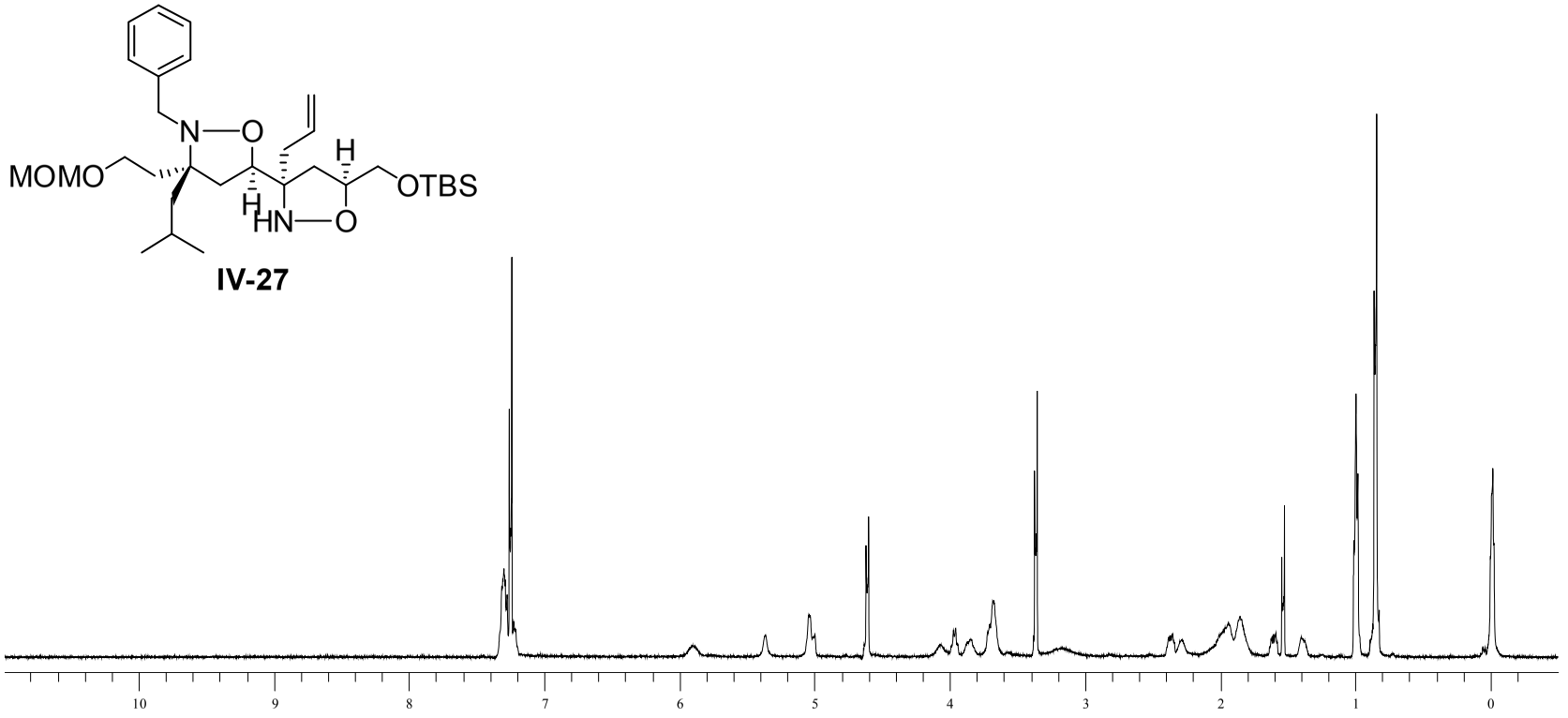
MOMO
N
O
H
H
HN
O
OTBS
IV-27
10
9
8
7
6
5
4
3
2
1
0

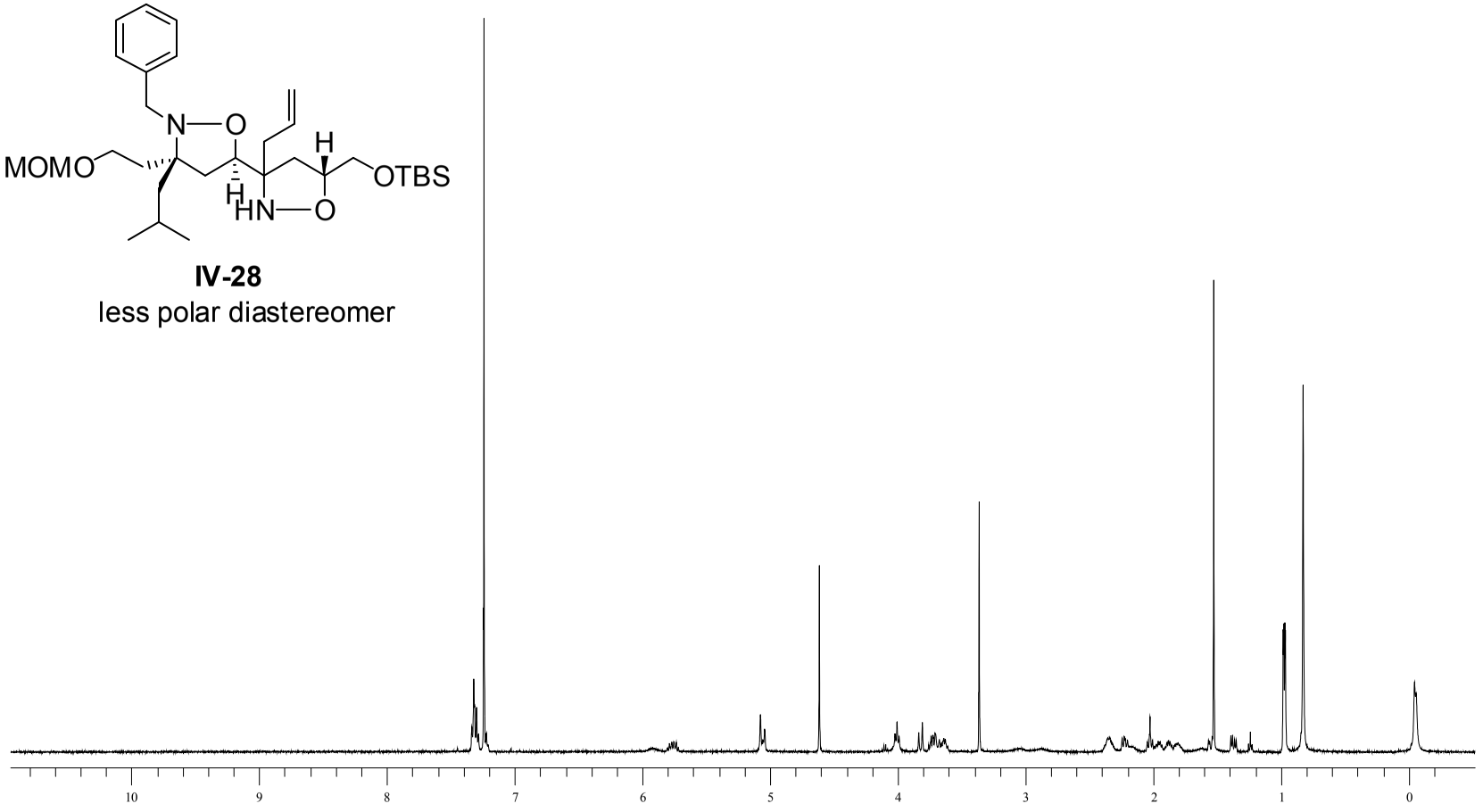

IV-28
less polar diastereomer

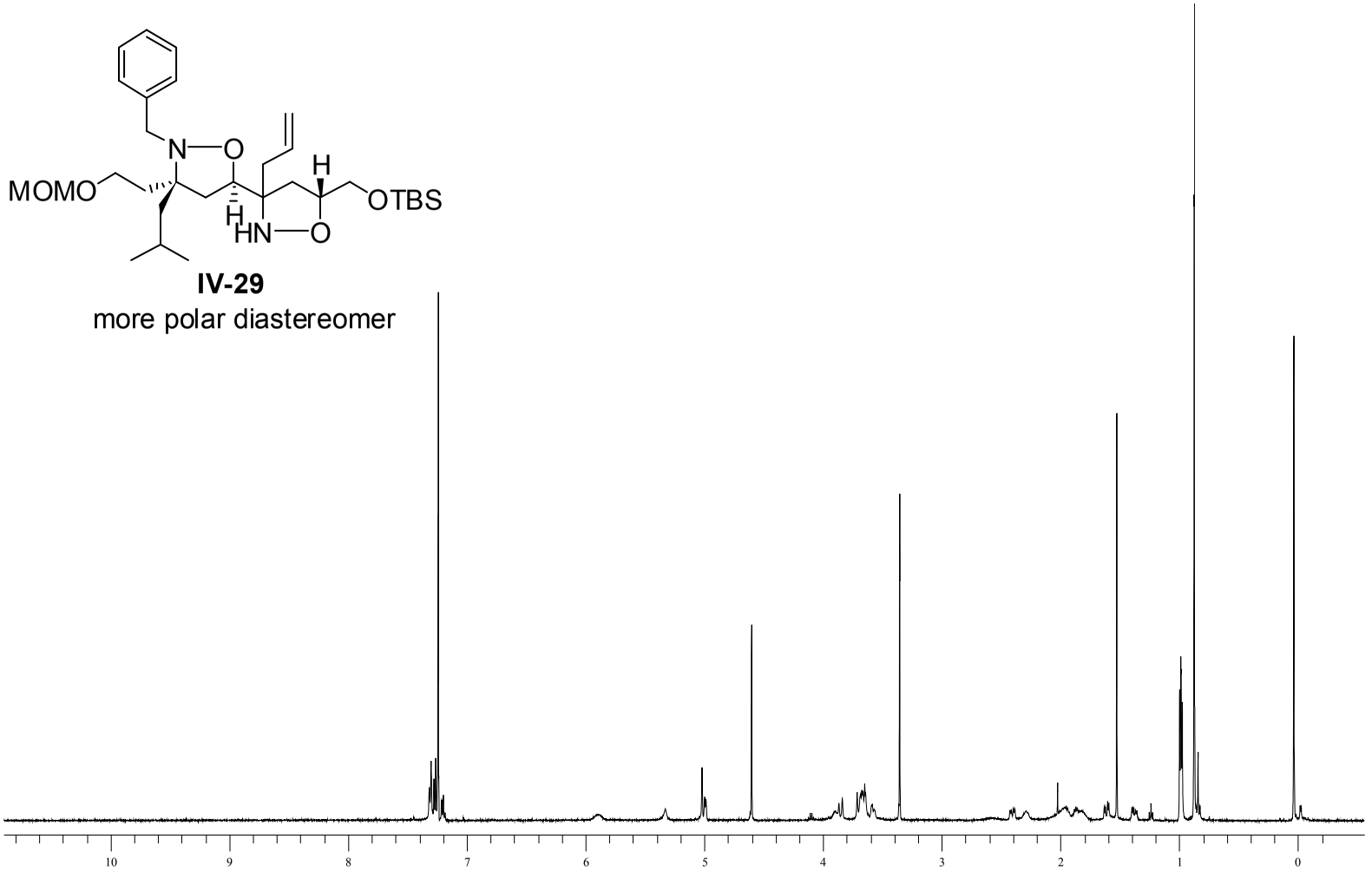
MOMO
N
O
H
H
HN
O
OTBS
IV-29
more polar diastereomer
10
9
8
7
6
5
4
3
2
1
0

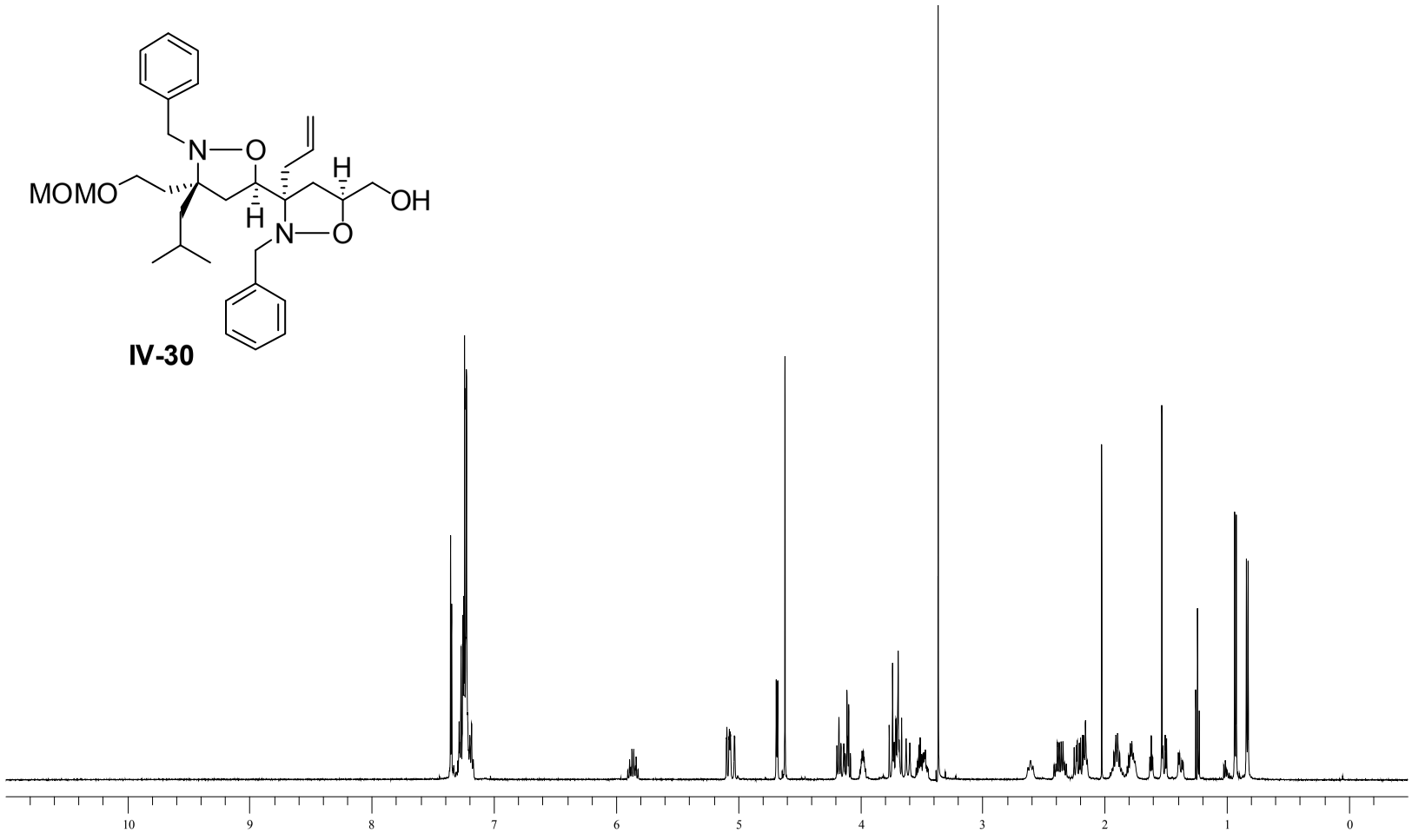
MOMO
N
O
H
H
N
O
OH
IV-30
10
9
8
7
6
5
4
3
2
1
0

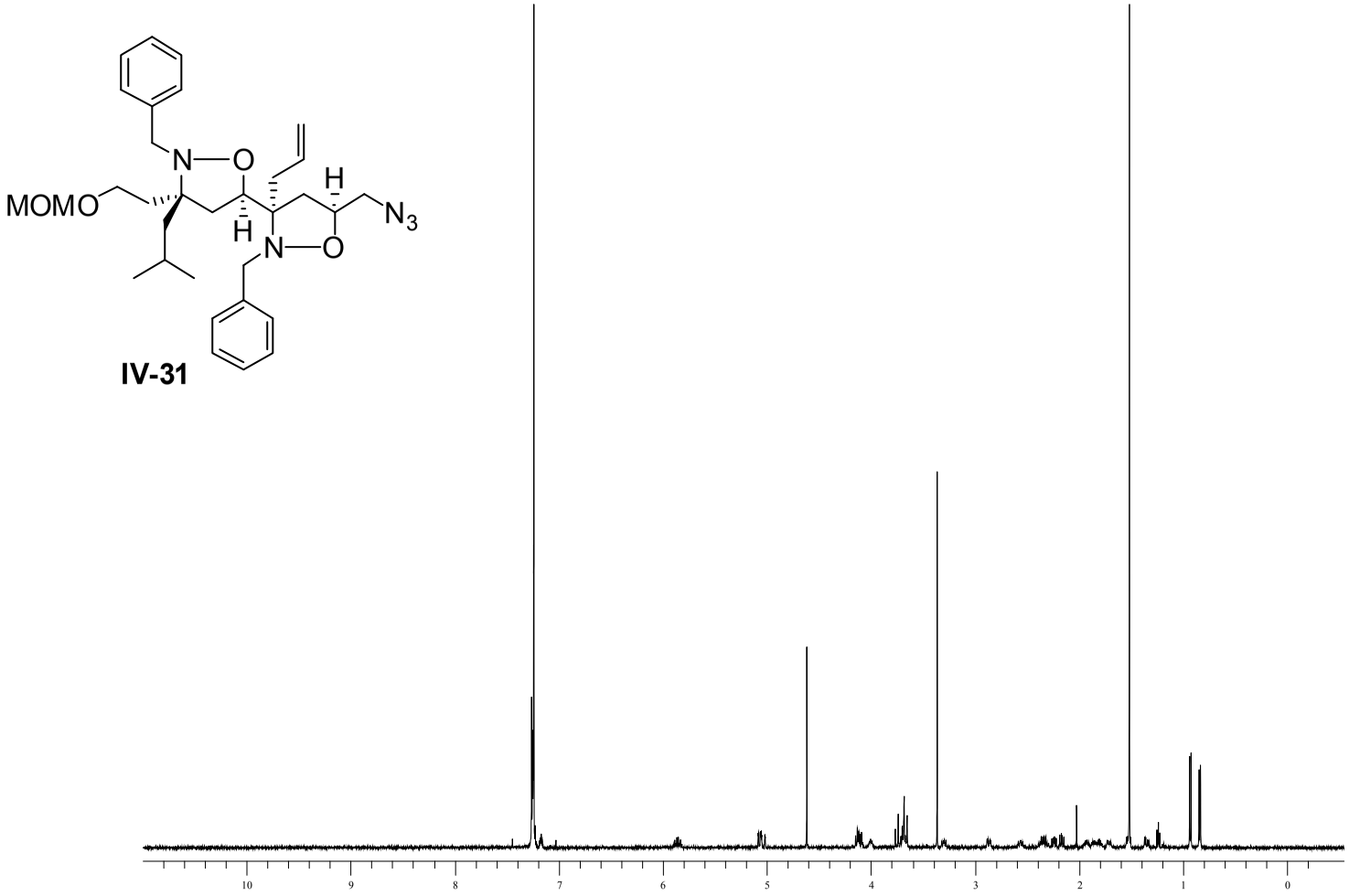

IV-31

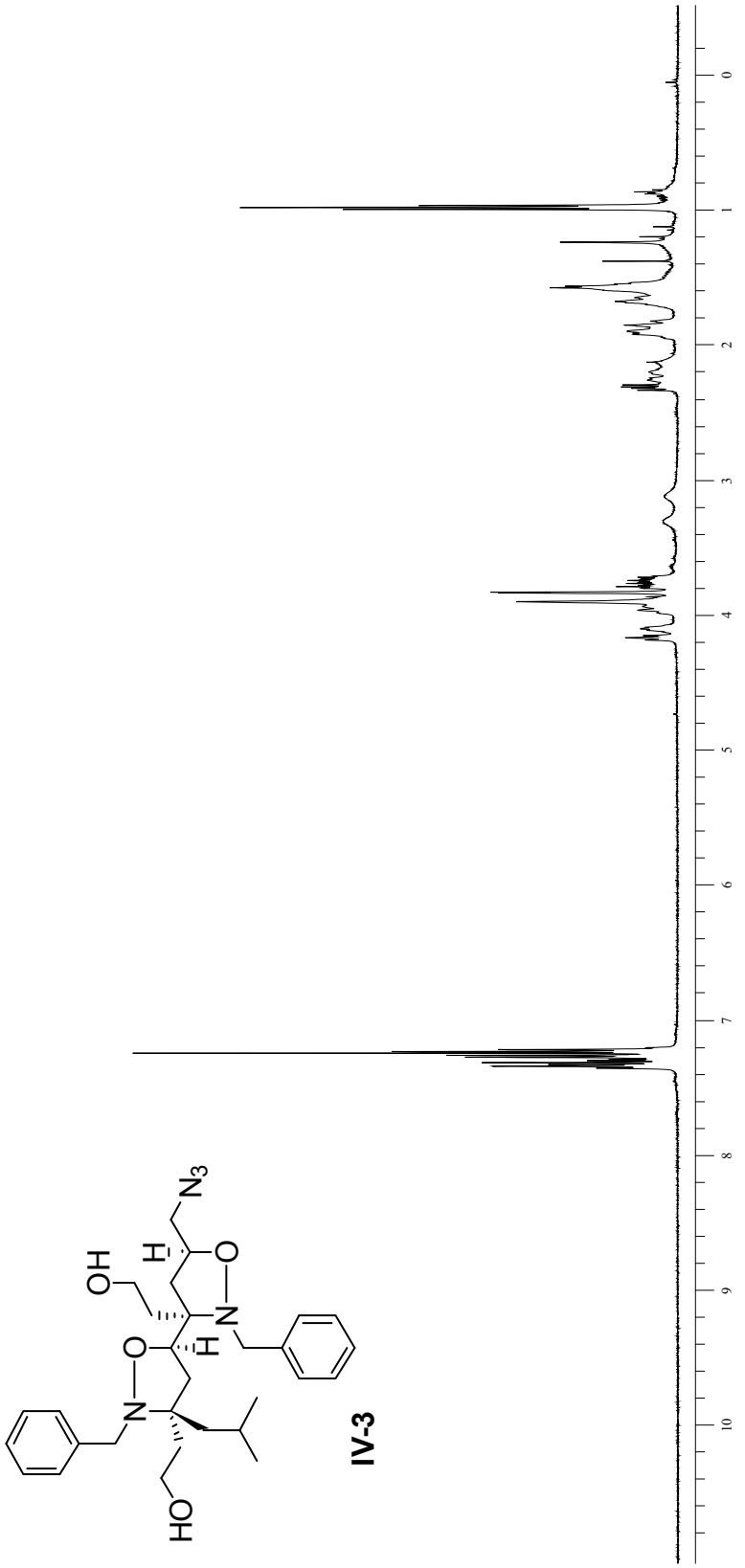
N3
H
O
OH
H
N
O
N
HO
IV-3

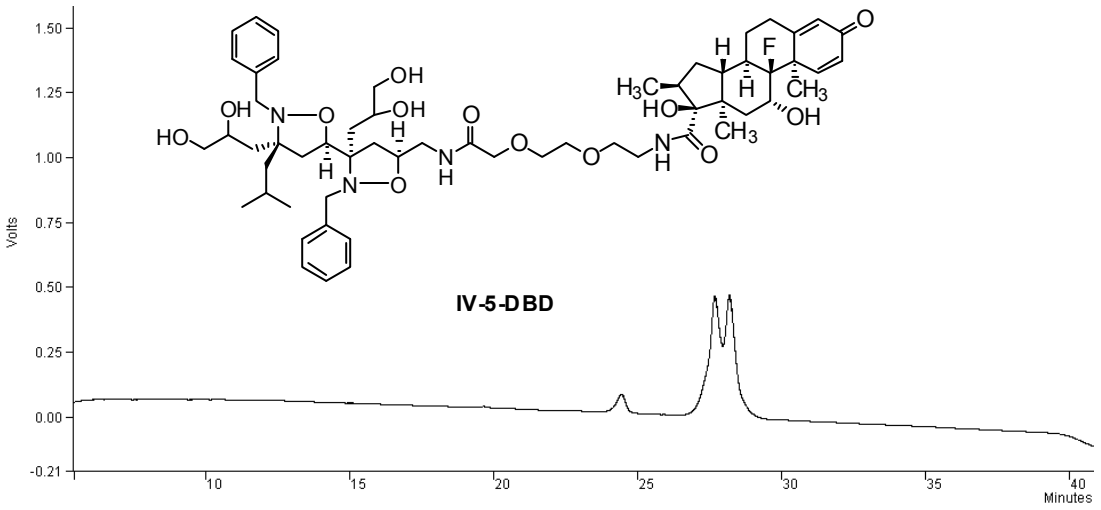

H. References

1. Minter, A. R.; Brennan, B. B.; Mapp, A. K., *J Am Chem Soc* **2004,** *126* (34), 10504-5.

2. Buhrlage, S. J.; Brennan, B. B.; Minter, A. R.; Mapp, A. K., *J Am Chem Soc* **2005,** *127* (36), 12456-7.

3. Drysdale, C. M.; Duenas, E.; Jackson, B. M.; Reusser, U.; Braus, G. H.; Hinnebusch, A. G., *Mol Cell Biol* **1995,** *15* (3), 1220-33.

4. Mapp, A. K.; Ansari, A. Z., *ACS Chem Biol* **2007,** *2* (1), 62-75.

5. Majmudar, C. Y.; Mapp, A. K., *Curr Opin Chem Biol* **2005,** *9* (5), 467-74.

6. Ernst, P.; Wang, J.; Huang, M.; Goodman, R. H.; Korsmeyer, S. J., *Molecular and Cellular Biology* **2001,** *21* (7), 2249-2258.

7. Liu, Y. P.; Chang, C. W.; Chang, K. Y., *FEBS Lett* **2003,** *554* (3), 403-9.

8. Frangioni, J. V.; LaRiccia, L. M.; Cantley, L. C.; Montminy, M. R., *Nat Biotechnol* **2000,** *18* (10), 1080-5.

9. Zor, T.; Mayr, B. M.; Dyson, H. J.; Montminy, M. R.; Wright, P. E., *J Biol Chem* **2002,** *277* (44), 42241-8.

10. Zor, T.; De Guzman, R. N.; Dyson, H. J.; Wright, P. E., *J Mol Biol* **2004,** *337* (3), 521-34.

11. Liu, B.; Alluri, P. G.; Yu, P.; Kodadek, T., *J Am Chem Soc* **2005,** *127* (23), 8254-5.

12. Casey, R. J.; Desaulniers, J. P.; Hojfeldt, J. W.; Mapp, A. K., *Bioorg Med Chem* **2008**.

13. Tanaka, M., *Proc. Nat. Acad. Sci., USA* **1996,** *15*, 1220-1233.

14. Wu, Y.; Reece, R. J.; Ptashne, M., *EMBO J* **1996,** *15* (15), 3951-63.

15. Ohashi, Y.; Brickman, J. M.; Furman, E.; Middleton, B.; Carey, M., *Mol Cell Biol* **1994,** *14* (4), 2731-9.

16. Smith, A. B., 3rd; Knight, S. D.; Sprengeler, P. A.; Hirschmann, R., *Bioorg Med Chem* **1996,** *4* (7), 1021-34.

17. Smith, A. B., 3rd; Favor, D. A.; Sprengeler, P. A.; Guzman, M. C.; Carroll, P. J.; Furst, G. T.; Hirschmann, R., *Bioorg Med Chem* **1999,** *7* (1), 9-22.

18. Smith, A. B., III; et. al., *J. Am. Chem. Soc.* **1999,** (121), 9286-9298.

19. Minter, A. R., *PhD Thesis* **2005**.

20. De Guzman, R. N.; Goto, N. K.; Dyson, H. J.; Wright, P. E., *Journal of Molecular Biology* **2006,** *355* (5), 1005-1013.

21. Goto, N. K.; Zor, T.; Martinez-Yamout, M.; Dyson, H. J.; Wright, P. E., *Journal of Biological Chemistry* **2002,** *277* (45), 43168-43174.

22. Minter, A. R.; Fuller, A. A.; Mapp, A. K., *J Am Chem Soc* **2003,** *125* (23), 6846-7.

23. Kanemasa, S. N., M; Kamimura, A.; Hori, K. J., *J. Am. Chem. Soc.* **1994,** *116*, 2324-2439.

24. Bode, J. W.; Fraefel, N.; Muri, D.; Carreira, E. M., *Angew Chem Int Ed Engl* **2001,** *40* (11), 2082-2085.

25. Pangborn, A. B.; Giardello, M. A.; Grubbs, R. H.; Rosen, R. K.; Timmers, F. J., *Organometallics* **1996,** *15* (5), 1518-1520.

26. Still, W. C. K., M.; Mitra, A., *J. Org. Chem.* **1978,** *43*, 2923.

27. Fuller, G. N.; Su, X.; Price, R. E.; Cohen, Z. R.; Lang, F. F.; Sawaya, R.; Majumder, S., *Mol Cancer Ther* **2005,** *4* (3), 343-9.

Chapter V

Conclusions and Future Directions

A. Conclusions

My thesis work focused on the successful design, synthesis, and evaluation of small molecule transcriptional activation domains. At the outset of my PhD work there was a single example of a small molecule TAD (iTAD **V-1**) shown to activate transcription in a cell-free assay. In collaboration with several colleagues we showed that iTAD **V-I** also up-regulates transcription in cells. Consistent with this, a preponderance of evidence supporting that the molecules function by a similar mode of action as their endogenous counterparts was collected using a combination of organic chemistry, NMR spectroscopy, and biological evaluations. Further an interaction with a single coactivator protein, CBP, contained in the transcriptional machinery was correlated with iTAD function (Figure **V-1b**).

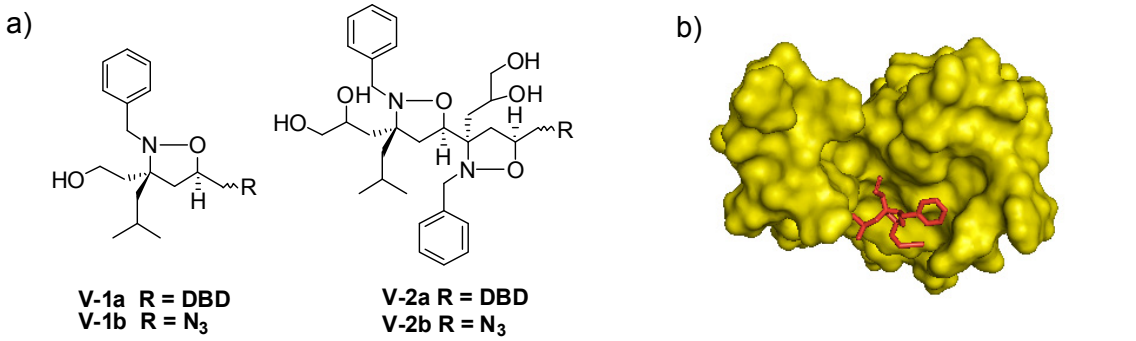

Figure V-1. iTADs are potent TADs that interact with endogenous coactivators. a) Monomeric and dimeric iTADs are potent TADS. b) iTAD **V-1b** bound to the CBP KIX domain.

B. Future Directions

1) Small Molecule TADs Based on Other Scaffolds

TAD binding sites within coactivators appear to be somewhat permissive, not requiring a single placement of particular sidechains.[1] In Chapter II it was shown that analogous to the endogenous system a variety of stereochemical and position iTAD **V-1** isomers all potently activated transcription suggesting the small molecules function via a similar mechanism.[2] An important implication of these experiments is that isoxazolidines are unlikely to be the only suitable scaffold for the construction of small molecule transcriptional activation domains, but rather a variety of conformationally constrained scaffolds should also functional well. As an initial evaluation of this prediction, amphipathic spiro-oxindoles (**V-3**-**V-5**) have been synthesized and preliminary evaluated in a cell-free assay. Spiro-oxindole **V-3b** binds masking protein MDM2 and inhibits the p53•MDM2 interaction.[3] Evidence suggests that masking proteins and coactivators may sample TAD sequences differently;[4] thus small molecule inhibitors are predicted to serve as an excellent starting point for the design of small molecule TADs. Thus, spiro-oxindoles **V-4** and **V-5** were designed to incorporate polar functionality generating small molecules that mimic the amphipathic character of endogenous TADs and iTADs. In a cell-free assay **V-3** did not activate transcription but amphipathic analogs **V-4** and **V-5** both activated transcription; **V-4** activated to a level comparable to the positive control ATF14 and the maximal activation by **V-5** was approximately half that of ATF14. This data supports that a variety of appropriately functionalized amphipathic scaffolds function as TADs.

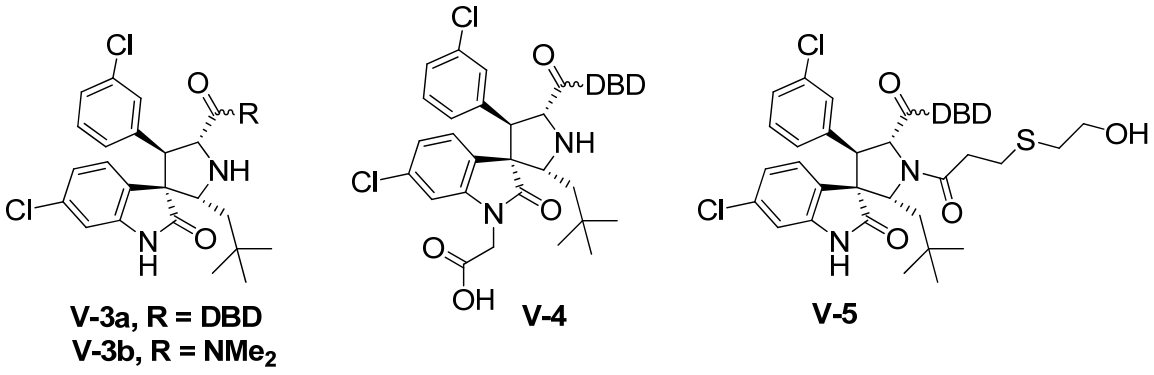

Figure V-2. Spiro-oxindoles evaluated as TADs. **V-3** does not activate transcription whereas **V-4** and **V-5** activate in a cell-free assay.

2) Cooperative Recruitment of CBP

Prevailing evidence suggests that transcriptional activators initiate transcription by assembling the large, multicomponent transcriptional machinery complex through interaction with several distinct binding partners with some evidence suggesting that each interaction contributes differentially to function. In Chapter III it was shown that iTADs exhibit a similar molecular recognition profile with the ability of isoxazolidines to activate transcription being linked to the ability to bind a particular coactivator, CBP (Creb Binding Protein). In fact, characterization of iTADs in complex with the KIX domain of CBP revealed a remarkable similarity to endogenous TADs that utilize the same site.

Based on the binding site selection of iTADs, these molecules may synergize with Creb, a TAD that binds a second site on the KIX domain of CBP, to activate transcription (Figure V-3). In vitro evidence shows that the two sites are bound cooperatively and emerging evidence suggests that some promoters require two KIX-binding activators for function.[5-10] For example, it has been found that binding of the KIX domain by either MLL or Tax, activators that bind the same KIX site as iTADs, facilitates binding of Creb to the second site. In one study Creb activation was only achieved in the presence of two KIX binding proteins. In fact NMR experiments have revealed a small but perhaps significant allosteric change in the Creb binding site upon binding of the protein domain by MLL.[5]

To investigate this possibility we are collaborating with Professor Thomas Kodadek. The Kodadek research group has reported an example of a peptoid based TAD that binds the same site within the CBP KIX domain as Creb.[11] iTADs and peptoid TADs will be attached to polyamides that target different sequences in the minor groove of DNA. A reporter plasmid containing the two appropriate binding sequences will be constructed and utilized to investigate the ability of the two KIX binding ligands to cooperatively activate transcription.

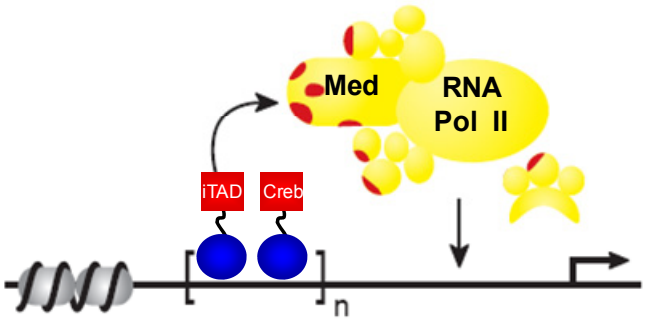

Figure V-3. Cooperative recruitment of CBP.

3) Small Molecule Inhibitors of Transcription

The fact that iTADs bind a site within CBP targeted by endogenous TADs and the observation that small structural changes alter the binding profile for this site suggests some degree of specificity for a small molecule inhibitor of TADs that bind this site may be possible. This will likely require, however, molecules that bind more tightly than **V-1**. Based upon the binding model of iTAD **V-1** presented in Chapter III structure based design of isoxazolidines with enhanced affinity for the KIX domain is predicted to be possible. A general schematic depicting the inhibition of transcription is shown in Figure V-4.

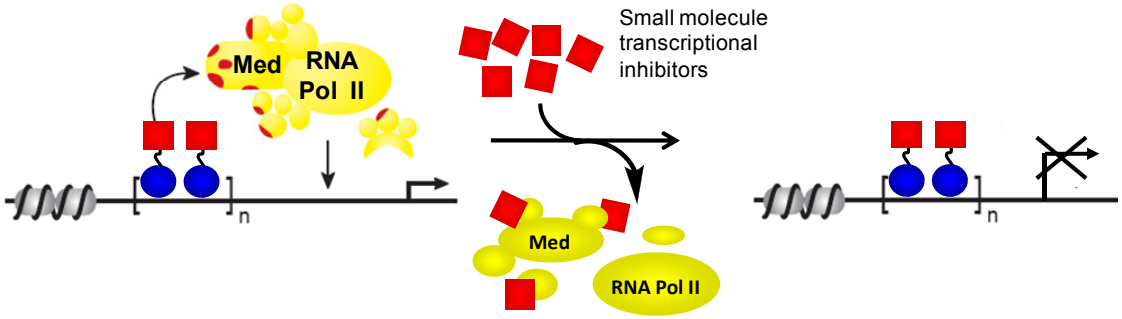

Figure V-4. Schematic of small molecule inhibition of transcription.

The binding model for iTADs with the KIX domain is based upon the reported MLL•KIX solution structure. Five MLL residues, one polar (T2857) and four hydrophobic (I2849, F2852, V2853 and L2854), make extensive contacts with KIX upon binding (Figure V-5a and V-5b).[5] The benzyl, isobutyl and alcohol sidechains of iTAD **V-1** are predicted to project into the same subsites as F2852, L2854, and T2857,

respectively. Figure V-5c shows **V-1** placed in the KIX domain binding pocket. The particular picture simply removed MLL and inserted **V-1** thus the structural reorganization of the protein upon binding the small molecule is not accounted for; nonetheless the picture is sufficient to suggest that a C4 substituent on the ring of the isoxazolidine may project into the same local binding pocket as V2853. Thus, isoxazolidines such as **V-6** containing a C4 alkyl substituent are predicted to have enhanced affinity for the KIX domain as a result of this additional interaction. C4 substituents on molecules such as **V-5** can be installed by either utilization of a substituted allylic alcohol in the cycloaddition forming the isoxazoline ring or by alkylation of the isoxazoline ring following the cycloaddition reaction. **V-6** and related analogs are currently being prepared for evaluation as inhibitors of KIX targeting TADs.

The larger bis-isoxazolidines (such as **V-2**) presented in Chapter IV interact with a large surface area of KIX than monomeric iTAD **V-1** resulting in an overall greater affinity for the protein and thus also offer an excellent starting point for the design of inhibitors. The binding model for bis-isoxazolidines, such as **V-2**, is that ring A projects functionality into the same subsites as **V-1** with a ring B substituent positioned analogous to MLL residue I2849. Further enhancement of binding affinity and complex lifetime for bis-isoxazolidine is predicted to be achieved by identifying a perhaps more optimal placement of sidechains on ring B, perhaps with analogs such as **V-7** and **V-8** (Figure V-5d) which closely mimic the functionality of MLL. Combination of this strategy with addition of a C4 substituent on ring A, as illustrated with compound **V-9** (Figure V-5d), as discussed above has potential to yield perhaps the most potent inhibitors. Beyond CBP these molecules should be an excellent starting points for designing inhibitors of other TAD•coactivator complexes as a wide variety of functional groups can be appended and displayed similarly to a helix.

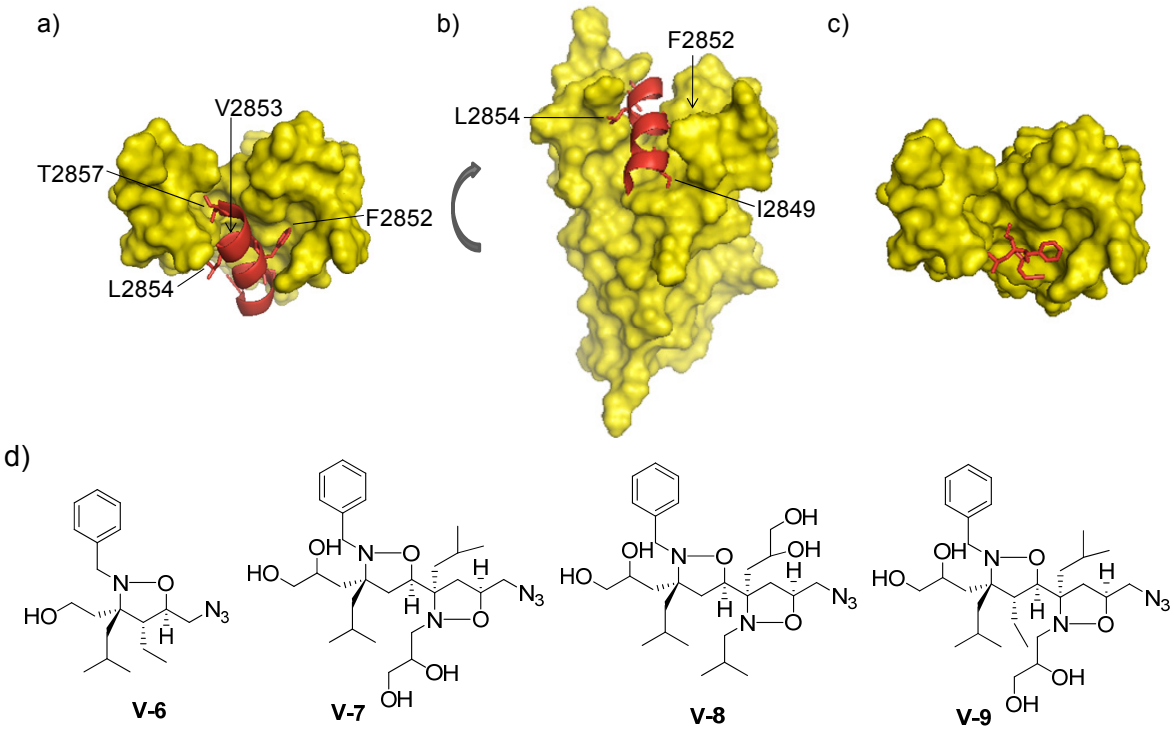

Figure V-5. Design of small molecule CBP inhibitors.

4) Realization of Small Molecule Transcriptional Activators as Therapeutics

The advances we have made in the field of small molecule transcriptional activators bring us closer to being able to construct an ideal small molecule based artificial transcriptional activator, but there remains much work to be done. An ideal small molecule based artificial transcriptional activator was defined in Chapter I as a molecule that can be delivered to a specific tissue, localize to the nucleus, and upregulate transcription of a specific gene to the appropriate level in a signal responsive fashion. Such tools are highly sought after due to the implication of misregulated or miscued transcriptional activators in disease. For example, the onset of nearly 40 different cancers is implicated with malfunctioning transcriptional activators.[1] The work here demonstrated that small molecules can upregulate transcription in cells by a mode of action that mimics their endogenous counterparts. A minimal transcriptional activator, consisting of only DBD and TAD function, can now be constructed and paves the way for addressing issues such as delivery and signal responsiveness.

C. References

1. Mapp, A. K.; Ansari, A. Z., *ACS Chem Biol* **2007,** *2* (1), 62-75.

2. Buhrlage, S. J.; Brennan, B. B.; Minter, A. R.; Mapp, A. K., *J Am Chem Soc* **2005,** *127* (36), 12456-7.

3. Ding, K.; Lu, Y.; Nikolovska-Coleska, Z.; Qiu, S.; Ding, Y.; Gao, W.; Stuckey, J.; Krajewski, K.; Roller, P. P.; Tomita, Y.; Parrish, D. A.; Deschamps, J. R.; Wang, S., *J Am Chem Soc* **2005,** *127* (29), 10130-1.

4. Ansari, A. Z.; Reece, R. J.; Ptashne, M., *Proc Natl Acad Sci U S A* **1998,** *95* (23), 13543-8.

5. De Guzman, R. N.; Goto, N. K.; Dyson, H. J.; Wright, P. E., *Journal of Molecular Biology* **2006,** *355* (5), 1005-1013.

6. Campbell, K. M.; Lumb, K. J., *Biochemistry* **2002,** *41* (47), 13956-64.

7. Ernst, P.; Wang, J.; Huang, M.; Goodman, R. H.; Korsmeyer, S. J., *Molecular and Cellular Biology* **2001,** *21* (7), 2249-2258.

8. Geiger, T. R.; Sharma, N.; Kim, Y. M.; Nyborg, J. K., *Mol Cell Biol* **2008,** *28* (4), 1383-92.

9. Ramirez, J. A.; Nyborg, J. K., *J Mol Biol* **2007,** *372* (4), 958-69.

10. Ghee, M.; Baker, H.; Miller, J. C.; Ziff, E. B., *Brain Res Mol Brain Res* **1998,** *55* (1), 101-14.

11. Liu, B.; Alluri, P. G.; Yu, P.; Kodadek, T., *J Am Chem Soc* **2005,** *127* (23), 8254-5.

Appendix

A Flexible and Selective Route to β-proline Analogs

A. Introduction

Nonnatural molecules that mimic key protein structural motifs such as helices and β-turns have found application as catalysts, sensors, materials and as inhibitors of protein-protein interactions. A key advantage of these so-called 'foldamers' compared to proteins is their often enhanced structural and proteolytic stability relative to their natural counterparts. Foldamers composed of β-amino acids, for example (Figure 1), can adopt stable and predictable secondary structures, are resistant to proteolytic degradation and can be more densely functionalized than their natural α-amino acid counterparts.[1, 2] Further, it was recently demonstrated that β-amino acid foldamers can assemble into higher order structures, a critical step towards proteomimetics that mimic the structure *and* function of natural proteins.[3]

One class of β-peptides that has been less studied includes oligomers composed of β-prolines, in particular the analogs containing the nitrogen moiety within the ring, although the monomeric units have been utilized in a number of applications.[4, 5] Early solution studies of unfunctionalized β-proline oligomers (4 or more subunits) suggested the existence of multiple rotameric states, precluding thorough structural characterization.[6] However, the introduction of two substituents at C2 of the beta proline (**3**) leads to a strong preference for the *Z*-amide bond isomer.[7] Indeed, CD analysis of the homooligomers of disubstituted β-prolines indicated the adoption of regular structure for the pentameric and hexameric species. Although an exciting advance, a major roadblock for further implementing these more substituted β-proline oligomers is the synthetic difficulties associated with selectively installing a range of functional groups adjacent to the nitrogen and along the backbone.

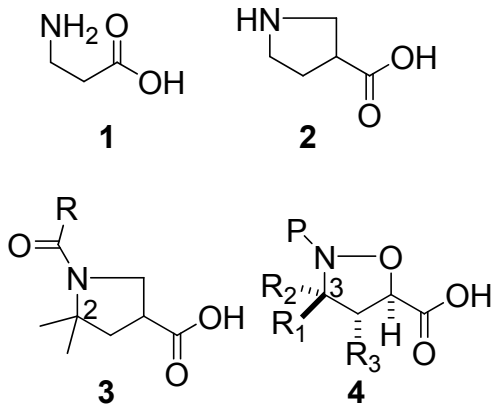

Figure 1. Structural classes of β-amino acids. **1**: basic β-amino acid; **2**: β-proline monomer; oligomers of **2** populate multiple rotomer states; **3**: disubstituted β-proline; oligomers of **3** adopt regular structure; **4**: trisubstituted isoxazolidine β-proline.

Several former colleagues have previously reported a general synthetic strategy for densely functionalized $\beta^{3,3}$-amino acids, $\beta^{2,3,3}$-amino acids, and cyclic β-amino acids using a chiral isoxazoline as the key intermediate.[8, 9] We hypothesized that a similar strategy could be developed for β-proline analogs in which one carbon has been replaced by an oxygen, a substitution that should confer advantageous aqueous solubility properties while minimally perturbing the amide bond in the context of oligomers. In this approach, a 1,3-dipolar cycloaddition using the conditions of Kanemasa and Carreira establishes the stereochemistry at C5 (**7**) and introduces the first substituent adjacent to the nitrogen (Figure 2).[10, 11] Additional substitution at C4 of the isoxazoline ring of **7** can be incorporated by using a disubstituted double bond in the cycloaddition and/or through a separate alkylation step post-cycloaddition.[8, 9] Selective nucleophilic attack at the C=N bond then provides the additional C3 substituent in **8**. Finally, oxidative cleavage of the C5 diol moiety would provide the requisite carboxylic acid at this position (**9**). Here we describe the development and implementation of this synthetic strategy for a range of β-proline analogs, including those with substitution patterns not accessible by previous methodologies.

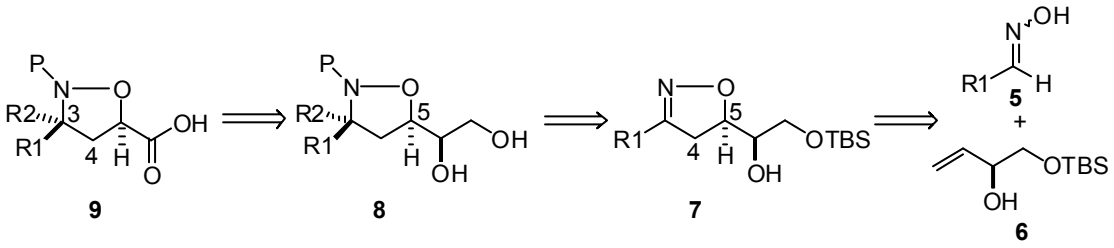

Figure 2. Isoxazoline strategy for the synthesis of di- and tri-substituted β-prolines.

B. Disubstituted Isoxazolidine β- prolines

The first step in the synthesis of disubstituted isoxazolidine β-prolines is a 1,3-dipolar cycloaddition between a nitrile oxide and a chiral allylic alcohol to yield a single detectable diastereomer of isoxazoline **7** (Scheme 1). The allylic alcohol **6** is readily generated as either stereoisomer from (*R*)- or (*S*)-glycidol,[12, 13] enabling access to either enantiomer of the isoxazoline cycloaddition product; for this study only the (*S*)-isomer of the allylic alcohol was used as it provided β-proline analogs with stereochemistry analogous to L-proline. Consistent with previous reports, the cycloaddition proceeds in excellent yield with either an isobutyl (**5a**) or ethyl (**5b**) R1 substituent.[8, 9] Subsequent protection of the secondary alcohol as a silyl ether produced isoxazoline **10** in excellent yield. Protection of the secondary alcohol was necessary for the introduction of carbamate protecting groups utilized in solid phase synthesis (Boc, Fmoc, Cbz). Although alkyl groups can be added to N2 without protection of the secondary alcohol, carbonate formation was a significant side reaction during carbamate formation.

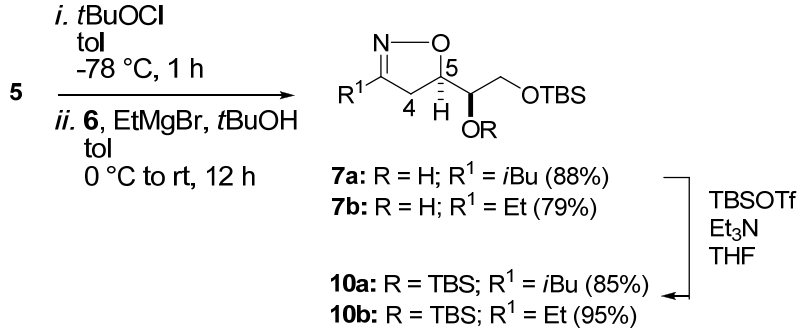

Scheme 1. Synthesis of the key isoxazoline intermediates.

Installation of the second functional group at C3 was accomplished by the combination of isoxazoline **10** with either a stabilized Grignard reagent (**11**, **13** and **16**) or

an organolithium reagent (**12**, **14**, **15**) in the presence of BF_3•Et_2O (Table 1). In all examples, the major diastereomer isolated results from addition to the *re* face of the C=N bond, with good (7:1) to excellent (>20:1) diastereomeric ratios observed. In this way, alkyl, aryl and heteroaryl functional groups can be positioned at C3. Protection of the secondary alcohol prior to this reaction is not a requirement, but the isolation and purification of the product is facilitated with the protection.

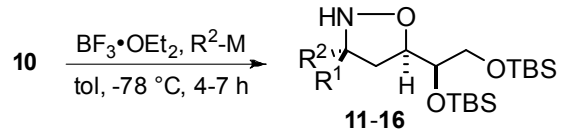

product	R^1	R^2-M	yield	d.r.[a]
11[b]	*i*Bu	BnMgBr	80%	10:1
12[b]	*i*Bu	PhLi	60%	7:1
13[b]	*i*Bu	allylMgCl	76%	8:1
14[b]	*i*Bu	MeLi	64%	7:1
15	*i*Bu	thienylLi	73%	20:1
16	Et	2-methylallylMgCl	79%	8:1

[a]Diastereomeric ratios determined due to ^{1}H NMR spectral integration. [b]Prepared by Bin Chen.

Table 1. Nucleophile addition to isoxazoline **10**.

Conversion of isoxazolidines **11-16** to the β-proline analogs required only protection at N2 followed by unmasking of the C5 diol moiety and oxidative cleavage to the carboxylic acid (Figure 3). Protection of the ring nitrogen with a solid phase synthesis compatibility group was anticipated to be a challenging step. Due to significant steric hindrance and concomitant nucleophilicity of the nitrogen, we have previously found that alkyl groups can only be added to that position using microwave-accelerated conditions. Despite significant large steric profile of the protecting groups, it was possible to protect the nitrogen with a BOC, FMOC or Cbz group, all commonly used in solid-phase peptide synthesis. Although installation of the Cbz group consistently provided the highest yields, likely due to its smaller steric profile. The TBS groups were then removed in situ by addition of TBAF. The resulting diols were oxidatively cleaved in a 2-step procedure in which a $NaIO_4$ cleavage produced an intermediate aldehyde; due to instability of the

aldehyde, this intermediate was immediately oxidized to the more stable carboxylic acid without purification. This was accomplished by treatment with sodium perchlorate to cleanly produce the desired isoxazolidine β-proline analogs shown (**17-22)** in good overall yields (over the four steps shown) and with no detectable epimerization. Despite the polarity of **17-22** the molecules were readily purified using standard flash chromatography.

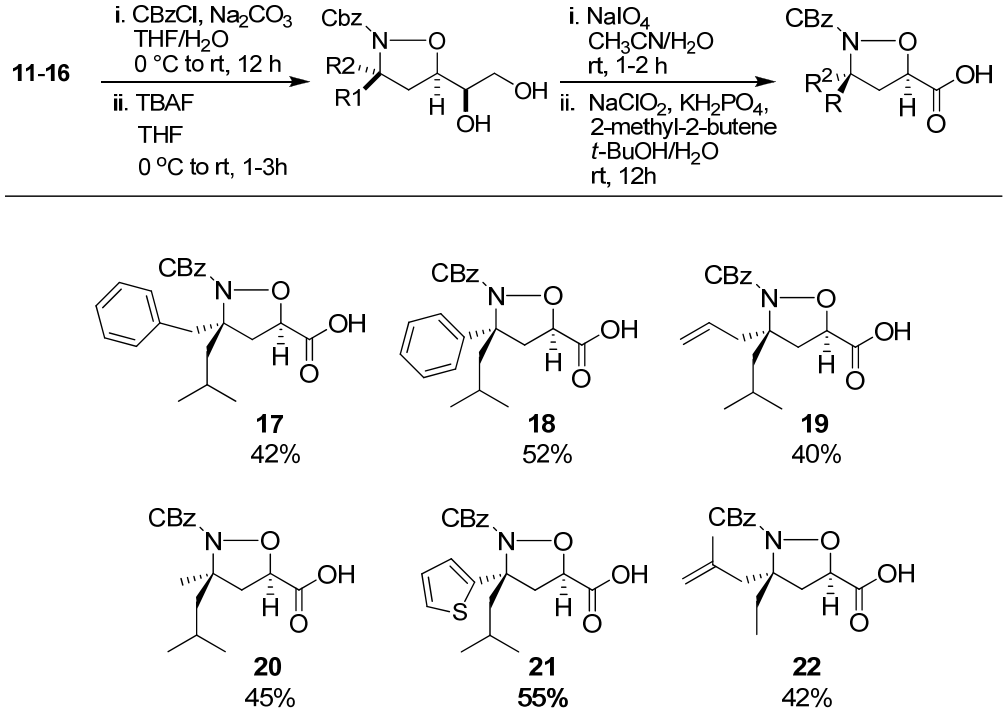

Figure 3. Conversion of isoxazolidines **11-16** to β-prolines. Isoxazolidine β-prolines **17-20** were prepared by Bin Chen.

A key feature of this synthetic approach to β-prolines is that diverse functionality can be introduced at multiple stages from choice of oxime in the first step to late-stage modification of sidechains of densely functionalized analogs. For example, we prepared an amphipathic isoxazoldine β-proline, **26**, bearing a hydrophobic (isobutyl) and polar (hydroxyl) functional group at the carbon adjacent to the nitrogen. From **13**, the nitrogen was protected with an Fmoc group in 92% yield. The double bond of isoxazolidine **23** was oxidatively cleaved and protected as the MOM ether. Subsequently the silyl ethers

were selectively removed by treatment wth 20% HCl in MeOH. In the final step the pendant diol of **25** was oxidatively cleaved to yield isoxazolidine β-proline **26**.

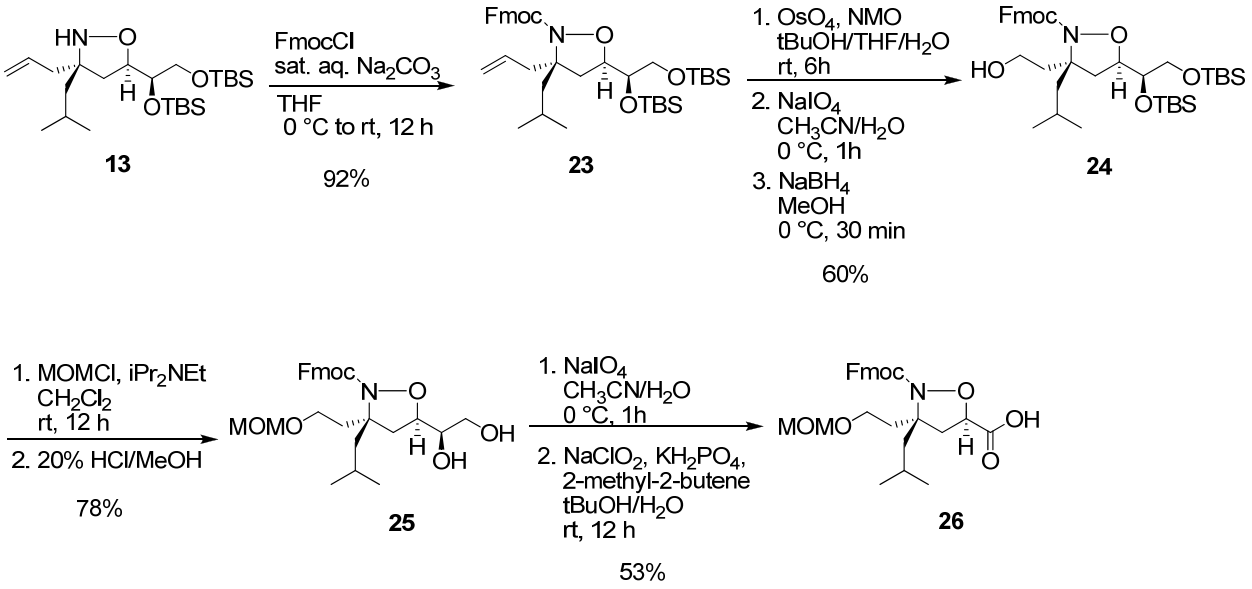

Scheme 2. Synthesis of amphipathic isoxazolidine β-proline **26**.

C. Synthesis of Trisubstituted Isoxazolidine β-prolines

As described earlier, we envisioned that one advantage of our synthetic strategy would be that it could be used to access *trisubstituted* β-proline analogs. Although not expected to strongly impact the conformational preferences of oligomers, functional groups at C4 of the isoxazolidine ring could be useful for *inter*-oligomer interactions, facilitating the formation of higher order assemblies. A C4 substituent can be introduced at the cycloaddition stage through the use of allylic alcohols containing disubstituted double bonds or via an alkylation reaction with the isoxazolidine. We have elected for the alkylation strategy has it offers a more convergent synthesis. Deprotonation of isoxazolidine **10b** (Figure 4) with LDA and the addition of benzyl bromide proceeded in good yield (62%) to provide **27** as a single stereoisomer. Nucleophilic attack at the C=N bond proceeded with either an organolithium reagent (**28**) or a stabilized Grignard (**29**, **30**) reagent. The C4 and C5 substituents exert opposing steric effects in this reaction. In the case of **28**, the additional steric hindrance lead to an attenuated yield (55%) relative to

the earlier example (Table 1: **15**), although only a single stereoisomer was observed. In the second example, a better overall yield was obtained of a 1.2:1 mixture of diastereomers. In all cases, the relative stereochemistry was verified by NOESY with the indicated enhancements.

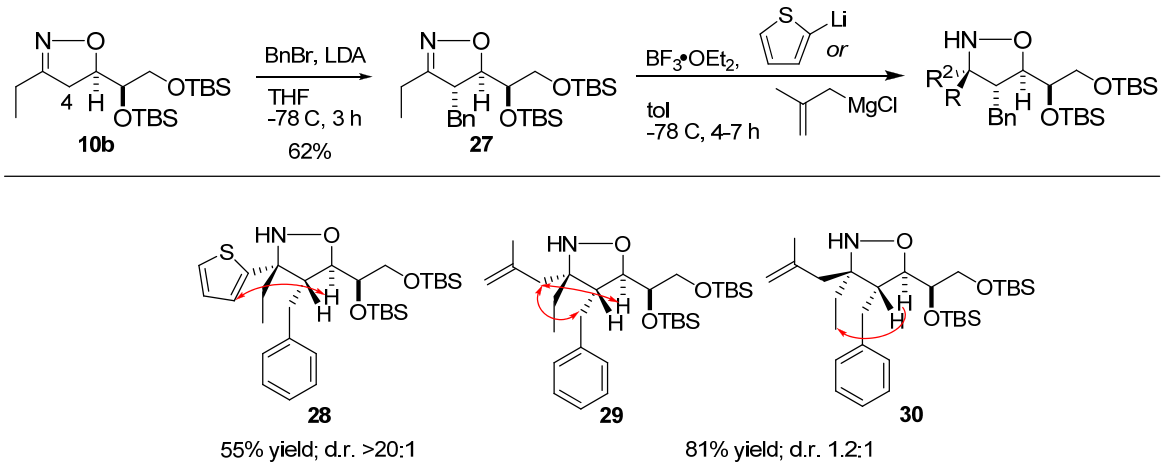

Figure 4. Nucleophile addition to C4 substituted isoxazolidines. NOE assignments were conducted on derivates containing a N2 CBz functionality.

Conversion of isoxazolidines **28-30** to β-proline analogs occurred using the same conditions as outlined in Figure 3. Despite the additional steric hindrance in these isoxazolidines, Cbz protection proceeded without incident as did the deprotection/oxidative cleavage sequence to produce the protected amino acids in good overall yield. Although only three examples are presented here, these results suggest that the strategy should be utilizable for a wider range of substrates by variation of both the initiation oxime substituent in the initial cycloaddition, alternative alkylating agents and the organometallic reagents used in Table 1.

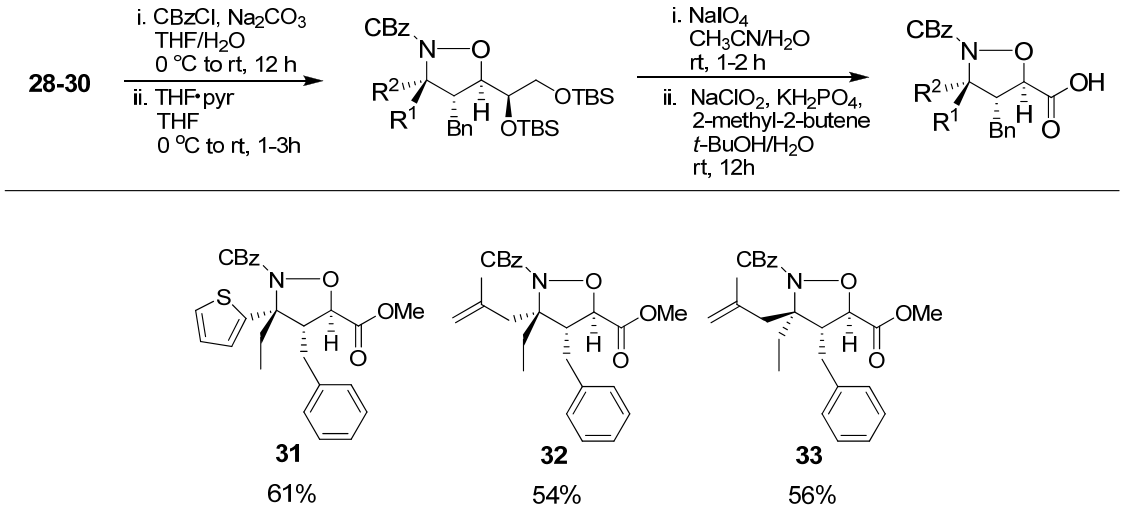

Figure 5. Generation of tri-substituted β-amino acids.

D. Conclusions

In conclusion we have reported flexible synthetic methods to yield $\beta^{(3,3)}$- and $\beta^{(3,3,4)}$-proline peptidomimetic building blocks. In the case of $\beta^{(3,3)}$-prolines the substitution pattern should confer conformational preferences analogous to the disubstituted analogs previously reported by Gellman and co-workers.[6, 7] Either way we predict these densely functionalized molecules will possess interesting properties for a variety of applications. The synthetic advantages of the approach we present here compared to the methods utilized by Gellman and co-workers include control of stereochemistry at every step, access to either enantiomers of product, and access to greater side chain diversity. For example, in Figure 4 we show incorporation of a hydroxyl side chain, although one can envision straight forward manipulation for incorporation of a wider range of functional groups including amines, secondary alcohol, ketones, aldehydes, amides, and others. $\beta^{(3,3,4)}$-prolines may adopt similar folds due to avoidance of the same steric interaction between the 3-position substitutents and the amide or exhibit new secondary structure. Given our success with generating bis-isoxazolidines that bind protein surfaces we anticipate similar functionalization of β-prolines will yield molecules that can also bind with transcriptional coactivator proteins and a library of more diversely substituted β-proline dimers and oligomers will be found to interact with a wide range of protein partners.

E. Experimentals

Unless otherwise noted, starting materials were obtained from commercial suppliers and used without further purification. THF, benzene, and toluene were dried by passage through activated alumina columns and degassed by stirring under a dry N_2 atmosphere. All reactions involving air- or moisture-sensitive compounds were performed under a dry N_2 atmosphere. BF_3•OEt_2, Et_3N, *i*Pr_2NH, MeOH and furan were distilled from CaH_2. Ac_2O was distilled from K_2CO_3. Purification by flash column chromatography was carried out with E. Merck Silica Gel 60 (230-400 mesh) according to the procedure of Still, Kahn, and Mitra. ^1H and ^{13}C NMR spectra were recorded in $CDCl_3$ at 500 MHz and 125 MHz, respectively, unless otherwise specified. IR spectra were measured as thin films on NaCl plates. Compounds **7a** and **10a** have been reported previously. NOE experiments determining the relative stereochemistry of compounds **28-30** were performed on CBz protected compounds.

General.

Unless otherwise noted, starting materials were obtained from commercial suppliers and used without further purification. THF, benzene, and toluene were dried by passage through activated alumina columns and degassed by stirring under a dry N_2 atmosphere. All reactions involving air- or moisture-sensitive compounds were performed under a dry N_2 atmosphere. BF_3•OEt_2, Et_3N, *i*Pr_2NH, MeOH and furan were distilled from CaH_2. Ac_2O was distilled from K_2CO_3. Purification by flash column chromatography was carried out with E. Merck Silica Gel 60 (230-400 mesh) according to the procedure of Still, Kahn, and Mitra. ^1H and ^{13}C NMR spectra were recorded in $CDCl_3$ at 500 MHz and 125 MHz, respectively, unless otherwise specified. IR spectra were measured as thin films on NaCl plates. Compounds **7a** and **10a** have been reported previously.

General procedure for nucleophile addition to isoxazolines.

To a solution of isoxazoline **7b** or **10b** (0.8 mmol, 1 eq) in toluene (5 mL) cooled in a dry ice-acetone bath was added BF_3•OEt_2 (0.31 mL, 2.5 mmol, 3.1 eq), and the resulting mixture was stirred with continued cooling for 30 min. A solution of organolithium reagent or Grignard reagent (5.8 mmol, 7.2 eq) was then added dropwise

over 15 min. The reaction mixture was allowed to stir with continued cooling until the starting material had been consumed as ascertained by TLC analysis, typically within 4 h. Saturated $NaHCO_3$ (15 mL) was added slowly to consume any remaining organolithium reagent or Grignard reagent and the mixture was diluted with EtOAC (12 mL). The mixture was then extracted with EtOAc (3 x 20 mL). The organic extracts were combined, washed with H_2O (3 x 15 mL) and brine (1 x 30 mL), dried over Na_2SO_4, and concentrated. The major and minor diastereomers were separated and the major diasteromer was carried on to subsequent steps. In one case, nucleophilic addition provided a 1.2:1 mixture of diastereomers and both were individually carried on to subsequent steps.

General procedure for Cbz protection and TBS deprotection of isoxazolidines.

A solution of isoxazolidine (0.3 mmol, 1 eq) in THF (1.0 mL) was cooled in an ice-H_2O bath. To the stirring solution was added CbzCl (125 μl, 0.9 mmol, 3 eq). Sat. aq. Na_2CO_3 was added to adjust the pH to 10 and the biphasic reaction mixture was stirred at rt for 12 h. The reaction mixture was then partitioned between 5 mL each H_2O and EtOAc, and the aqueous layer was extracted with EtOAc (3 x 5 mL). The combined organic extracts were dried over Na_2SO_4 and concentrated *in vacuo*. The crude mixture was passed through a short plug of SiO_2 (15:1 hexanes/EtOAc) and concentrated. The residue was dissolved in THF, cooled in an ice-H_2O bath, and 4 eq TBAF (1 M in THF) or HF•Pyr (3.0 eq) was added dropwise. HF•pyr was used for the deprotection of isoxazolidines containing a C4 substituent as the deprotection with TBAF proceeded very slowly. After 1 h, the ice-H_2O bath was removed and the progress of the reaction was monitored by TLC analysis. The reaction was then diluted with H_2O (10 mL) and extracted with Et_2O or EtOAc (3 x 5 mL). The organic extracts were combined, washed with H_2O (3 x 5 mL) and brine (1 x 10 mL), dried over Na_2SO_4, filtered, and concentrated *in vacuo*. The diol was then used in the subsequent oxidative cleavage reactions after passing through a plug of silica to eliminate the nonpolar impurities (1:9 MeOH/CH_2Cl_2).

General procedure for the oxidative cleavage of diols.

To a stirring solution of crude amine diol (0.1 mmol, 1.0 eq) dissolved in 2 ml *t*-BuOH /THF/H_2O (10:3:1) or CH_3CN (500 μl) and H_2O (500 μl) was added $NaIO_4$ (21

mg, 0.1 mmol, 1.2 eq). The reaction mixture was stirred at rt until the starting material was fully consumed as ascertained by TLC analysis. The mixture was worked-up one of two ways. In the first method, the reaction mixture was diluted with 5 ml $CHCl_3$ and filtered through a layer of Celite using $CHCl_3$ for extra washing. Alternatively, the mixture was diluted with H_2O (5 ml) and extracted with Et_2O (3 x 5 ml), the combined organic extracts were washed with brine (1 x 5 ml), dried over $MgSO_4$, and filtered. Concentration *in vacuo* of the combined filtrate from either procedure then provided a crude oil that was immediately dissolved in *t*-BuOH (1 mL) and 2-methyl-2-butene (4.7 mmol, 47 eq). A solution of $NaClO_2$ (0.9 mmol, 9.2 eq) and KH_2PO_4 (7 eq) in H_2O was added dropwise to give a pale yellow reaction mixture. The reaction was stirred at rt until TLC analysis indicated completion of the oxidation, typically within 3 h. The mixture was diluted with 10 mL sat. aq. $NaHCO_3$ and EtOAc. The aqueous layer was then extracted 3 x 5 mL with EtOAc and the combined organic extracts were dried over Na_2SO_4, filtered, and concentrated to provide the crude product mixture. Compounds containing a substituent at the C4 position were isolated as the methyl ester. The methyl ester was generated by treatment of the crude acid (30 mg, 0.07 mmol, 1.0 eq) in benzene (1.4 ml) and MeOH (470 µl) with $TMSCHN_2$ (350 µl of a 2M solution in Et_2O, 0.70 mmol, 10 eq.). The resulting mixture was stirred for 10 min, at which time TLC analysis indicated complete conversion to the methyl ester. The solvent was removed by rotary evaporation and the product purified by flash chromatography.

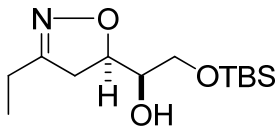

7b

2-(*tert*-Butyl-dimethyl-silanyloxy)-(1*R*)-1-[(5*R*)-3-ethyl-4,5-dihydro-isoxazol-5-yl]-ethanol (7b): To a solution of oxime derived from 3-methylbutyraldehyde (480 mg, 6.6 mmol, 1.0 eq) in toluene (33 mL) cooled in a dry ice-acetone bath shielded from light was added *t*-BuOCl (790 µl, 6.6 mmol, 1.0 eq) over 20 min. The resulting mixture was stirred 2 h with continued cooling at which time TLC analysis indicated complete conversion to the hydroximinoyl chloride. In a separate flask, chiral allylic alcohol[refs] (1.7 g, 1.7 mmol, 1.3 eq) was dissolved in toluene (66 mL) and cooled in an ice-H_2O

bath. To this solution was added *t*-BuOH (2.1 mL, 22 mmol, 3.3 eq) followed by dropwise addition of EtMgBr (6.6 mL of a 2.0 M solution in Et_2O, 20 mmol, 3.0 eq) and the solution stirred 1 h with continued cooling. The solution of hydroximinoyl chloride was then transferred via canula to the allylic alcohol solution and the mixture allowed to slowly warm to ambient temperature and stirred 15 h. Sat aq. NH_4Cl (10 mL) was added to the reaction mixture followed by further dilution with H_2O (40 mL). The organic and aqueous layers were separated and the aqueous extracted with CH_2Cl_2 (3 x 40 mL). The combined organic extracts were washed with brine (1 x 30 mL), dried over $MgSO_4$, filtered, and concentrated. Purification by flash chromatography yielded 1.4 g of isoxazoline **7b** as a clear oil in 79% yield as a single stereoisomer. IR: 3365, 2929, 2857, 1115, 1059, 837 cm^{-1}; ^1H NMR: δ 0.06 (s, 6H), 0.88 (s, 9H), 1.15 (t, 3H, J = 7.33), 2.32-2.57 (m, 2H), 2.95-2.98 (m, 2H), 3.56-3.73 (m, 3H), 4.62 (ddd, 1H, J = 11.4, 7.7, 2.6); ^{13}C NMR: δ -5.48, -5.47, 10.82, 18.22, 21.17, 25.82, 38.91, 63.93, 72.98, 79.15, 160.59; HRMS (ESI) calcd for $[C_{13}H_{27}NO_3Si + Na]^+$: 296.1658, found: 296.1655.

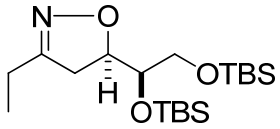

10b

(5*R*)-5-[(1*R*)-1,2-Bis-(*tert*-butyl-dimethyl-silanyloxy)-ethyl]-3-ethyl-4,5-dihydro-isoxazole (10b): To a solution of isoxazoline **7b** (1.4 g, 5.1 mmol, 1.0 eq) in THF (26 mL) cooled in an ice-H_2O bath was added DMAP (63 mg, 0.51 mmol, 0.10 eq) and Et_3N (1.6 mL, 11 mmol, 2.2 eq). TBSOTf (2.6 mL, 11 mmol, 2.2 eq) was added dropwise and the solution slowly warmed to ambient temperature. The reaction was complete in 2 h as indicated by TLC analysis. The mixture was again cooled in an ice-H_2O bath, diluted with sat. aq. NH_4Cl (15 mL) and extracted with Et_2O (3 x 15 mL). The combined organic extracts were washed with brine (1 x 20 mL), dried over $MgSO_4$, filtered, and concentrated *in vacuo*. Purification of the crude product by flash chromatography (95:5 hexanes/EtOAc) yielded 1.9 g of isoxazoline **10b** in 95% yield as a clear oil. IR: 2929, 2856, 1462, 1254, 1090, 835 cm^{-1}; ^1H NMR: δ 0.04 (s, 3H), 0.04 (s, 3H), 0.06 (s, 3H), 0.07 (s, 3H), 0.85 (s, 9H), 0.87 (s, 9H), 1.14 (t, 3H, J = 7.3), 2.25-2.37 (m, 2H), 2.88 (d, 2H, J = 9.3), 3.56 (dd, 1H, J = 9.0, 1.7), 3.62-3.69 (m, 2H), 4.59-4.63 (m, 1H); ^{13}C NMR:

δ -5.52, -4.86, -4.36, 10.73, 18.01, 18.24, 21.25, 25.69, 25.83, 38.24, 64.19, 74.24, 80.05, 159.43; HRMS (ESI) calcd for $[C_{19}H_{41}NO_3Si_2 + Na]^+$: 410.2523, found: 410.2517.

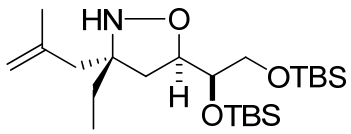

16

(5*R*)-5-[(1*R*)-1,2-Bis-(*tert*-butyl-dimethyl-silanyloxy)-ethyl]-(3*S*)-3-ethyl-3-(2-methyl-allyl)-isoxazolidine (16): Compound **16** was prepared following the general procedure using isoxazoline **10b** (800 mg, 2.1 mmol, 1.0 eq) and the nucleophile 2-methylallylmagnesium chloride (30 mL of a 0.5 M solution in THF, 15 mmol, 7.2 eq). Purification of the crude product by flash chromatography (95:5 hexanes/EtOAc) yielded 730 mg of the major diastereomer (d.r. 8:1) as a clear oil in 79% yield. ^{13}C NMR: δ -5.44, -5.42, -4.58, -4.43, 9.47, 18.00, 18.31, 24.44, 25.56, 25.88, 41.64, 41.3, 42.19, 64.61, 67.18, 68.06, 75.43, 113.90, 114.72; HRMS (ESI) calcd for $[C_{23}H_{49}NO_3Si_2 + Na]^+$: 466.3149, found: 466.3145.

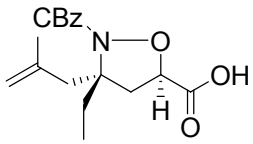

22

(3*S*, 5*R*)-3-Ethyl-3-(2-methyl-allyl)-isoxazolidine-2,5-dicarboxylic acid 2-benzyl ester (22): Compound **22** was prepared according to the general procedure from isoxazolidine **10a** (44 mg, 0.10 mmol, 1.0 eq). Purification by flash chromatography (95:5 CH_2Cl_2:MeOH + 2% acetic acid) of the crude product yielded 14 mg of **18** as a clear oil in 42% yield. IR: 2927, 2363, 1696, 1559, 1456 cm^{-1}; ^{1}H NMR: δ 0.39 (t, 3H, J = 7.3), 1.78-1.85 (m, 1H), 1.97-2.04 (m, 1H), 2.37 (d, 1H, J = 13.7), 2.50 (dd, 1H, J = 12.7, 7.3), 2.69 (d, 1H, J = 13.7), 2.82 (dd, 1H, J = 12.9, 8.1), 4.53-4.56 (m, 1H), 4.82 (s, 1H), 4.95 (s, 1H), 5.22 (s, 2H), 7.33-7.41 (m, 3H), 7.43-7.45 (m 2H); ^{13}C NMR: δ 8.63, 24.24, 31.97, 42.30, 45.67, 68.46, 69.50, 85.70, 117.16, 129.51, 129.63, 129.69, 143.17, 166.67; HRMS (ESI) calcd for $[C_{18}H_{23}NO_5 + Na]^+$: 356.1474, found: 356.1472.

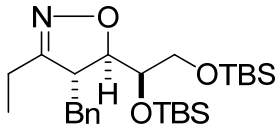

27

(4*R*, 5*R*)-4-Benzyl-5-[(1*R*)-1,2-bis-(*tert*-butyl-dimethyl-silanyloxy)-ethyl]-3-ethyl-4,5-dihydro-isoxazole (23): Distilled diisopropylamine (760 µl, 5.4 mmol, 1.5 eq) was added to 25 mL THF and the solution was cooled in an ice-H_2O bath. To the solution was added *n*-BuLi (3.4 mL of a 1.7 M solution in hexanes, 5.6 mmol, 1.6 eq). The mixture was stirred for 10 min and transferred to a dry ice/acetone bath. A solution of isoxazoline **10b** (1.4 g, 3.6 mmol, 1.0 eq) in 5 mL THF was added over 15 min and the mixture was stirred 1 h with continued cooling. BnBr (1.4 mL, 11 mmol, 3.0 eq) in 5 mL THF was subsequently added and the mixture continued to stir while being cooled until complete by TLC analysis (3 h). The mixture was diluted with sat. aq. NH_4Cl (10 mL), extracted with Et_2O (3 x 20 mL), washed with brine (20 mL), dried over $MgSO_4$, filtered, and concentrated *in vacuo*. The crude product was purified by flash chromatography (98:2 hexanes:EtOAc) to yield 1.1 g of isoxazoline **23** as a clear oil in 62% yield. IR: 2929, 2856, 1462, 1254, 1090, 835 cm^{-1}; ^1H NMR: δ -0.04 (s, 6H), -0.02 (s, 3H), -0.02 (s, 3H), 0.82 (s, 9H), 0.83 (s, 9H), 1.14 (t, 3H, J = 7.3), 2.10-2.20 (, 1H), 2.34-2.43 (m, 1H), 2.65 (dd, 1H, J = 9.9, 13.6), 3.01 (dd, 1H, J = 5.5, 13.6), 3.17-3.21 (m, 1H), 3.35-3.45 (m, 2H), 3.52 (dd, 1H, J = 6.9, 9.9), 4.33 (dd, 1H, J = 2.9, 5.9), 7.13-7.15 (m, 2H), 7.19-7.30 (m, 3H); ^{13}C NMR: δ -5.51, -5.46, -4.80, -4.27, 10.67, 18.04, 18.25, 20.14, 25.78, 25.92, 37.60, 52.05, 63.73, 74.20, 76.69, 77.01, 77.33, 84.59, 126.71, 128.74, 128.90, 138.14, 161.51; HRMS (ESI) calcd for $[C_{26}H_{47}NO_3Si_2 + Na]^+$: 500.2992, found: 500.2999.

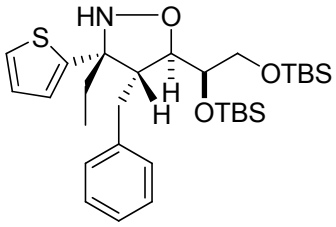

28

(4*R*, 5*R*)-4-Benzyl-5-[(1*R*)-1,2-bis-(*tert*-butyl-dimethyl-silanyloxy)-ethyl]-(3*R*)-3-ethyl-3-thiophen-2-yl-isoxazolidine (28): Prepared following the general procedure by additional of 2-thienyllithium (3.9 mL of a 1 M solution, 3.9 mmol, 7.2 eq) to isoxazoline **27** (260 mg, 0.54 mmol, 1.0 eq). Purification of the crude product by flash chromatography (98:2 hexanes:EtOAc) gave 170 mg of **28** as a clear oil in 55 % yield as a single diastereomer. ^{1}H NMR: δ -0.08 (s, 3H), -0.02 (s, 3H), 0.00 (s, 3H), 0.04 (s, 3H), 0.89 (s, 9H), 0.89 (s, 9H), 0.96 (t, 3H, J = 6.8), 1.82 (bs, 1H), 1.96 (t, 1H, J = 12.0), 2.54 (bs, 1H), 2.62-2.66 (m, 1H), 2.78-2.80 (m, 2H), 3.44 (dd, 1H, J = 9.8, 5.4), 3.59 (t, 1H, J = 9.0), 4.16 (d, 1H, J = 7.3), 7.01-7.03 (m, 1H), 7.05-7.06 (m, 3H), 7.16-7.19 (m, 1H), 7.22-7.25 (m, 2H), 7.36 (d, 1H, J = 4.9); ^{13}C NMR: δ -5.49, -5.43, -4.55, -4.52, 9.52, 17.94, 18.28, 25.91, 25.93, 30.82, 37.14, 56.73, 64.04, 72.04, 75.20, 84.15, 124.52, 124.65, 125.69, 126.26, 128.51, 128.89, 139.68, 144.52; HRMS (ESI) calcd for $[C_{30}H_{51}NO_3SSi_2 + Na]^+$: 584.3026, found: 584.3032.

29 and **30**: Prepared according to the general procedure by addition of 2-methylallylmagnesium chloride (12 mL of a 0.5 M solution in THF, 6.0 mmol, 7.2 eq) to isoxazoline **27** (400 mg, 0.83 mmol, 1.0 eq). A 1.2:1 diastereomeric ratio of products was determined by crude ^{1}H NMR. Purification by flash chromatography (98:2 hexanes:EtOAc) yielded 190 mg of diastereomer **29** and 160 mg of diastereomer **30**, both as colorless oils, for a combined yield of 81 %.

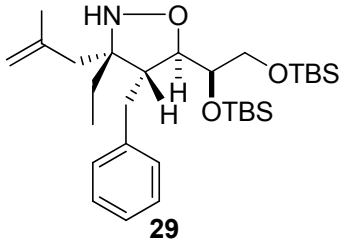

29

(4*R*, 5*R*)-4-Benzyl-5-[(1*R*)-1,2-bis-(*tert*-butyl-dimethyl-silanyloxy)-ethyl]-(3*S*)-3-ethyl-3-(2-methyl-allyl)-isoxazolidine (29): IR: 2928, 2857, 1471, 1254, 1093, 836 cm^{-1}; ^{1}H NMR: δ -0.17 (s, 3H), -0.13 (s, 3H), -0.06 (s, 3H), -0.04 (s, 3H), 0.81 (s, 9H), 0.84 (s, 9H), 1.08 (t, 3H, J = 7.7), 1.28-1.36 (m, 1H), 1.70-1.79 (m, 1H), 1.91 (s, 3H), 2.18 (d, 1H, J = 13.2), 2.36 (d, 1H, J = 13.2), 2.47-2.53 (m, 1H), 2.56-2.64 (m, 2H), 2.97 (dd, 1H, J = 12.5, 2.9), 3.34 (dd, 1H, J = 9.5, 5.1), 3.58 (dd, 1H, J = 9.5, 8.1), 4.06 (d, 1H, J = 6.6),

4.75 (s, 1H), 4.87-4.88 (m, 1H), 5.34 (bs, 1H), 7.12-7.27 (m, 5H); ^{13}C NMR: δ -5.51, -5.39, -4.82, -4.43, 9.14, 17.91, 18.31, 24.94, 25.86, 25.95, 26.05, 36.67, 37.55, 53.71, 64.06, 68.48, 75.70, 76.70, 77.01, 77.33, 85.03, 11.93, 126.32, 128.63, 128.86, 140.25, 143.92; HRMS (ESI) calcd for $[C_{30}H_{55}NO_3Si_2 + Na]^+$: 556.3618, found: 556.3615.

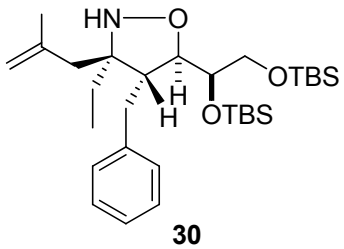

30

(4*R*, 5*R*)-4-Benzyl-5-[(1*R*)-1,2-bis-(*tert*-butyl-dimethyl-silanyloxy)-ethyl]-(3*R*)-3-ethyl-3-(2-methyl-allyl)-isoxazolidine (30): IR: 2953, 2928, 2857, 1471, 1254, 1093, 836 cm^{-1}; ^{1}H NMR: δ -0.15 (s, 3H), -0.07 (s, 3H), -0.01 (s, 3H), 0.84 (s, 9H), 0.89 (s, 9H), 1.03 (t, 3H, J = 7.7), 1.51-1.59 (m, 1H), 1.64-1.73 (m, 1H), 1.89 (s, 3H), 2.28 (d, 1H, J = 13.2), 2.33 (d, 1H, J = 13.3), 2.51-2.68 (m, 3H), 3.02 (dd, 1H, J = 12.5, 2.2), 3.37 (dd, 1H, J = 9.5, 5.1), 3.49-3.53 (m, 1H), 4.12 (d, 1H, J = 6.59), 4.91 (s, 1H), 5.02 (s, 1H), 7.16-7.22 (m, 3H), 7.25-7.28 (m, 2H); ^{13}C NMR: δ -5.54, -5.43, -4.73, -4.37, 8.13, 17.90, 18.27, 24.31, 24.90, 25.91, 25.93, 35.34, 40.54, 53.56, 64.00, 67.81, 75.11, 84.15, 115.89, 126.24, 128.56, 128.94, 140.26, 141.49; HRMS (ESI) calcd for $[C_{30}H_{55}NO_3Si_2 + Na]^+$: 556.3618, found: 556.3615.

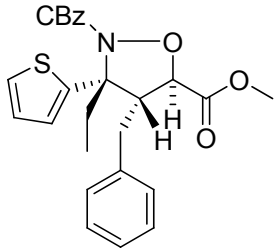

31

(3*R*, 4*R*, 5*R*)-4-Benzyl-3-ethyl-3-thiophen-2-yl-isoxazolidine-2,5-dicarboxylic acid 2-benzyl ester 5-methyl ester (31): Isoxazolidine **28** (67 mg, 0.12 mmol, 1.0 eq) was treated according to the general procedure to yield 34 mg of **27** as a clear oil in 61% yield. IR: 2950, 1710, 1454, 1327, 697 cm^{-1}; ^{1}H NMR: δ 0.93 (t, 3H, J = 7.2), 2.09 (d, 1H, J = 14.3, 9.6), 2.14 (dd, 1H, J = 14.1, 7.0), 2.40-2.49 (m, 1H), 2.54 (dd, 1H, J = 14.5,

5.5), 3.26-3.33 (m, 4H), 4.41 (d, 1H, J = 9.4), 6.91 (dd, 1H, J = 3.9, 1.2), 6.93-6.96 (m, 3H), 7.00-7.02 (m, 2H), 7.07-7.09 (m, 1H), 7.11-7.14 (m, 2H), 7.15-7.18 (m, 3H), 7.31 (dd, 1H, J = 5.1, 1.2); ^{13}C NMR: δ 7.66, 29.18, 34.14, 52.34, 53.73, 67.51, 71.17, 78.94, 124.84, 125.04, 126.69, 126.77, 127.96, 128.03, 128.34, 128.39, 128.82, 137.38, 145.18, 169.53; HRMS (ESI) calcd for $[C_{26}H_{27}NO_5S + Na]^+$: 488.1508, found: 488.1507.

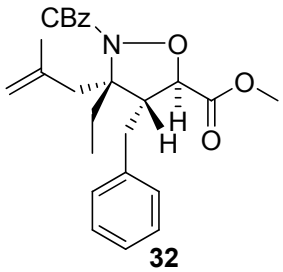

32

(3*S*, 4*R*, 5*R*)-4-Benzyl-3-ethyl-3-(2-methyl-allyl)-isoxazolidine-2,5-dicarboxylic acid 2-benzyl ester 5-methyl ester (32): Isoxazolidine **29** (43 mg, 0.08 mmol, 1.0 eq) was treated according to the general procedure to yield 19 mg of **32** as a clear oil in 54% yield. IR: 3468, 2923, 2852, 1695, 1455, 1348, 1115cm^{-1}; ^{1}H NMR: δ 0.93 (t, 3H, J = 7.3), 1.65-1.72 (m, 1H), 1.76 (s, 3H), 2.31-2.38 (m, 1H), 2.41 (d, 1H, J = 14.2), 2.66 (d, 1H, J = 13.7), 2.93 (dd, 1H, J = 13.9, 10.0), 3.02 (dd, 1H, J = 13.7, 5.4), 3.19-3.23 (m, H), 3.40 (s, 3H), 4.44 (d, 1H, J = 9.3), 5.11 (d, 1H, J = 12.2), 5.19 (d, 1H, J = 12.2), 7.22-7.25 (m, 3H), 7.30-7.43 (m, 7H); HRMS (ESI) calcd for $[C_{26}H_{31}NO_5 + Na]^+$: 460.2100, found: 460.2093.

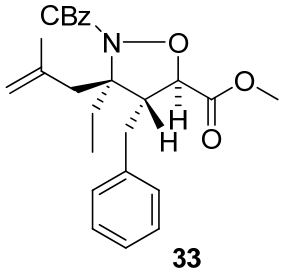

33

(3*R*, 4*R*, 5*R*)-4-Benzyl-3-ethyl-3-(2-methyl-allyl)-isoxazolidine-2,5-dicarboxylic acid 2-benzyl ester 5-methyl ester (33): Isoxazolidine **30** (37 mg, 0.07 mmol, 1.0 eq) was treated according to the general procedure to yield 17 mg of **33** as a clear oil in 56% yield. IR: 3469, 2924, 2852, 1695, 1455, 1348, 1115 cm^{-1}; ^{1}H NMR: δ 0.95 (t, 3H, J = 7.6), 1.67-1.74 (m, 4H), 2.02-2.09 (m, 1H), 2.24 (d, 1H, J = 14.6), 2.67 (dd, 1H, J = 13.7,

10.7), 2.93 (dd, 1H, J = 13.7, 4.9), 3.03 (d, 1H, J = 14.6), 3.26 (s, 3H), 3.31-3.36 (m, 1H), 4.28 (d, 1H, J = 9.8), 4.72 (s, 1H), 4.95 (s, 1H), 5.21 (s, 2H), 7.11-7.38 (m, 10H); ^{13}C NMR: δ 10.05, 22.53, 23.20, 29.00, 33.67, 36.97, 44.89, 54.50, 6.52, 70.74, 81.20, 117.13, 17.91, 129.67, 129.72, 130.32, 141.94, 163.91; HRMS (ESI) calcd for $[C_{26}H_{31}NO_5 + Na]^+$: 460.2100, found: 460.2098.

F. Selected ^{1}H NMR spectra

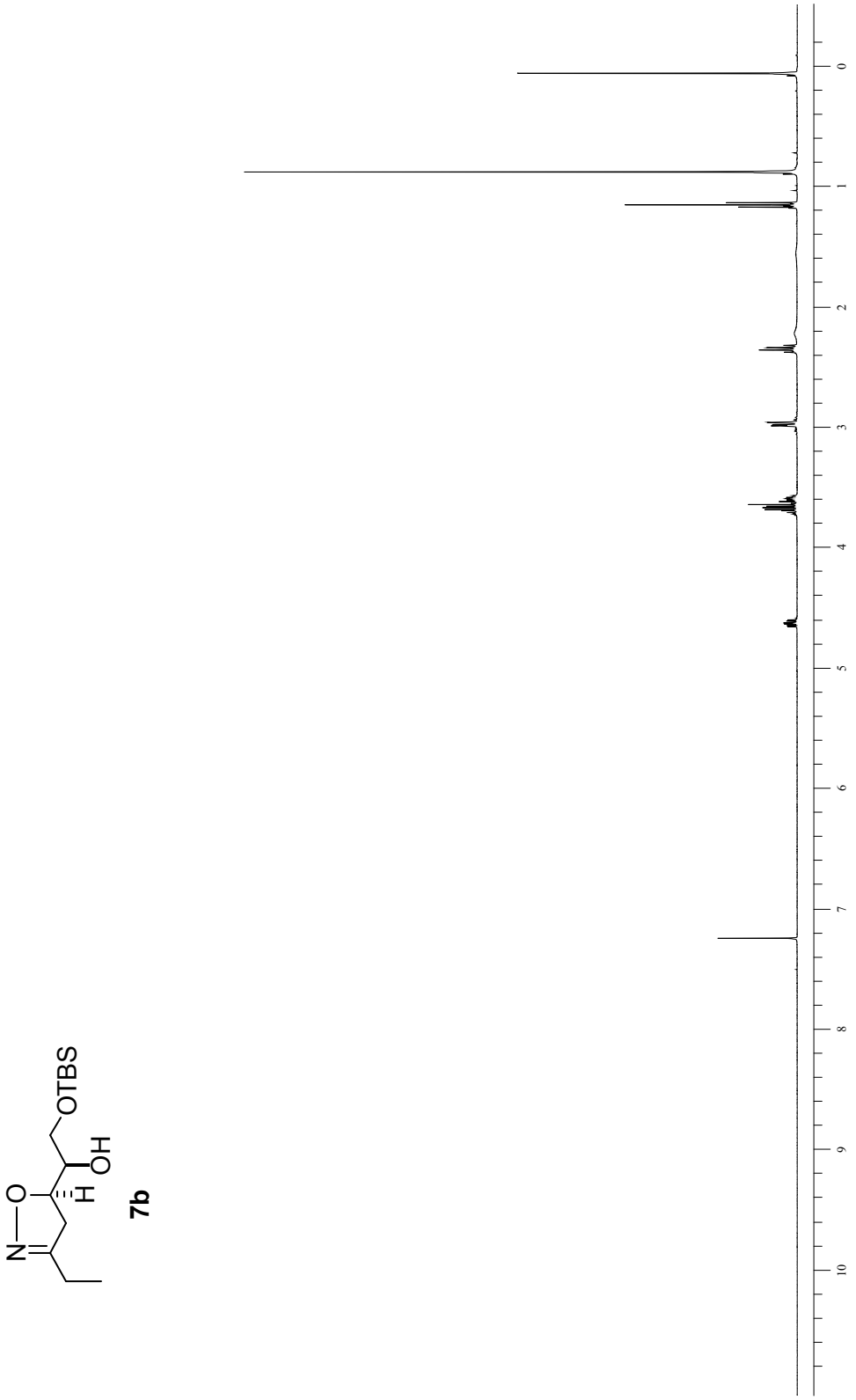

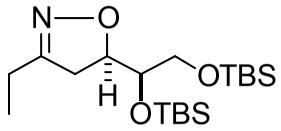

10b

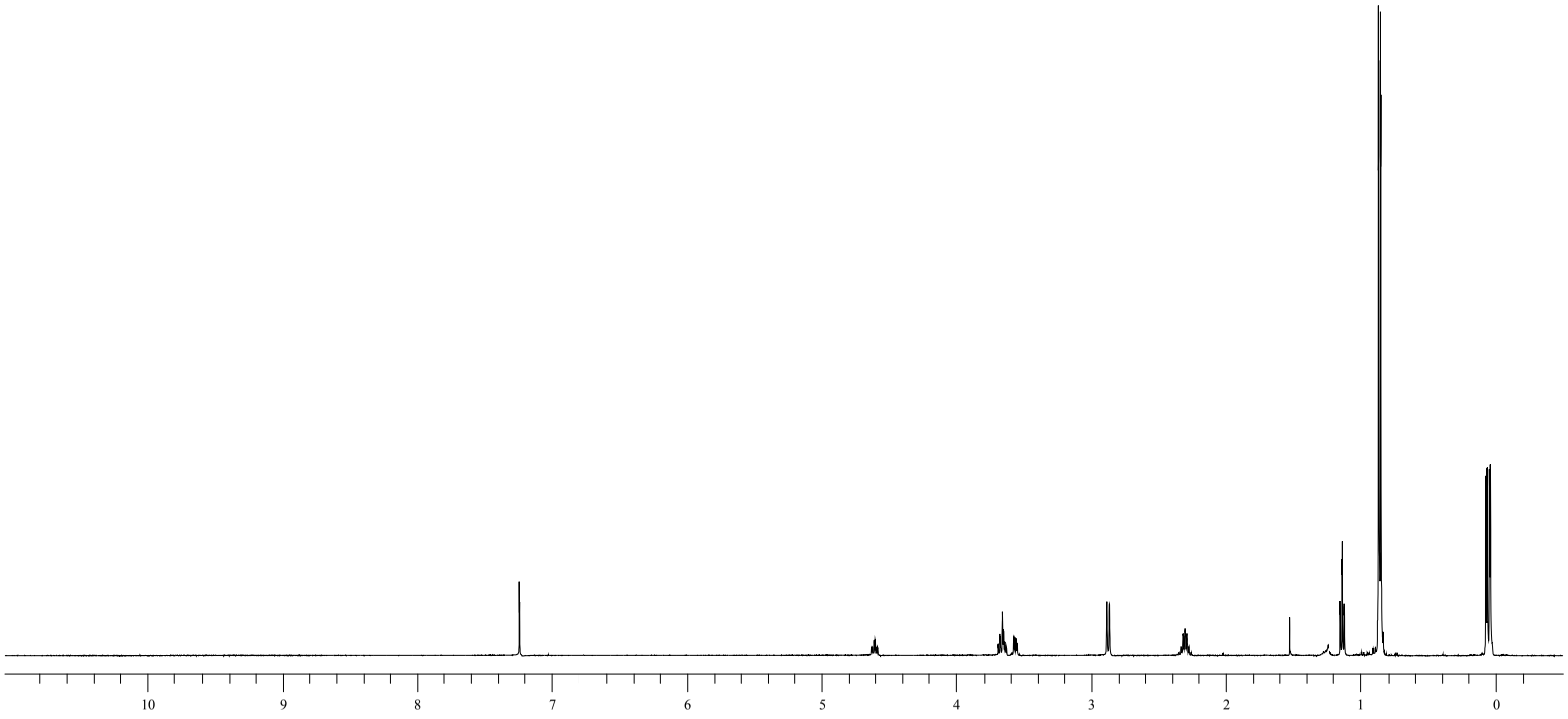

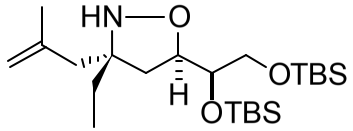

16

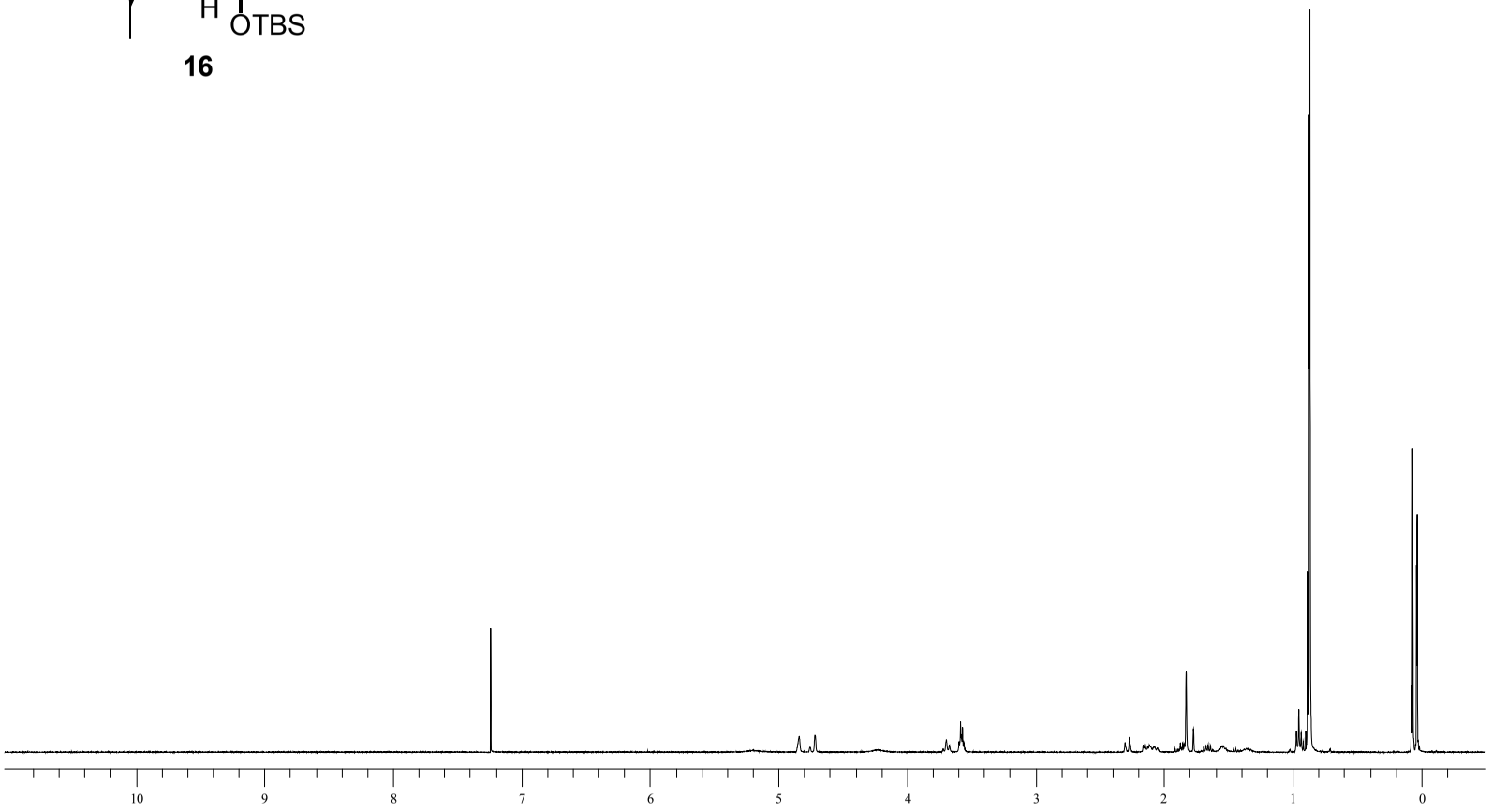

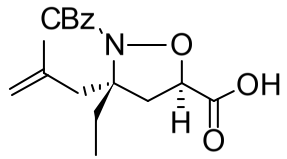

22

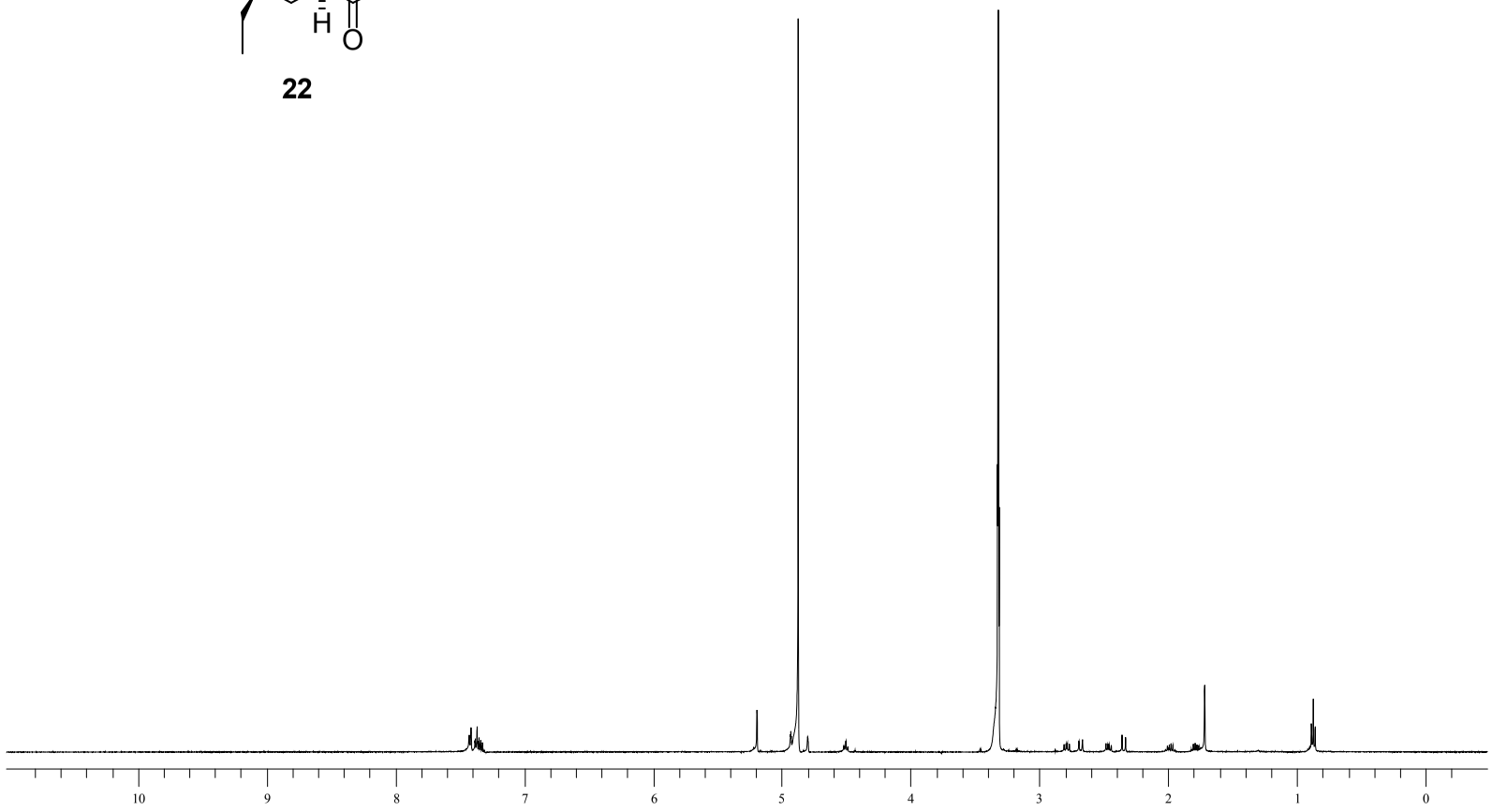

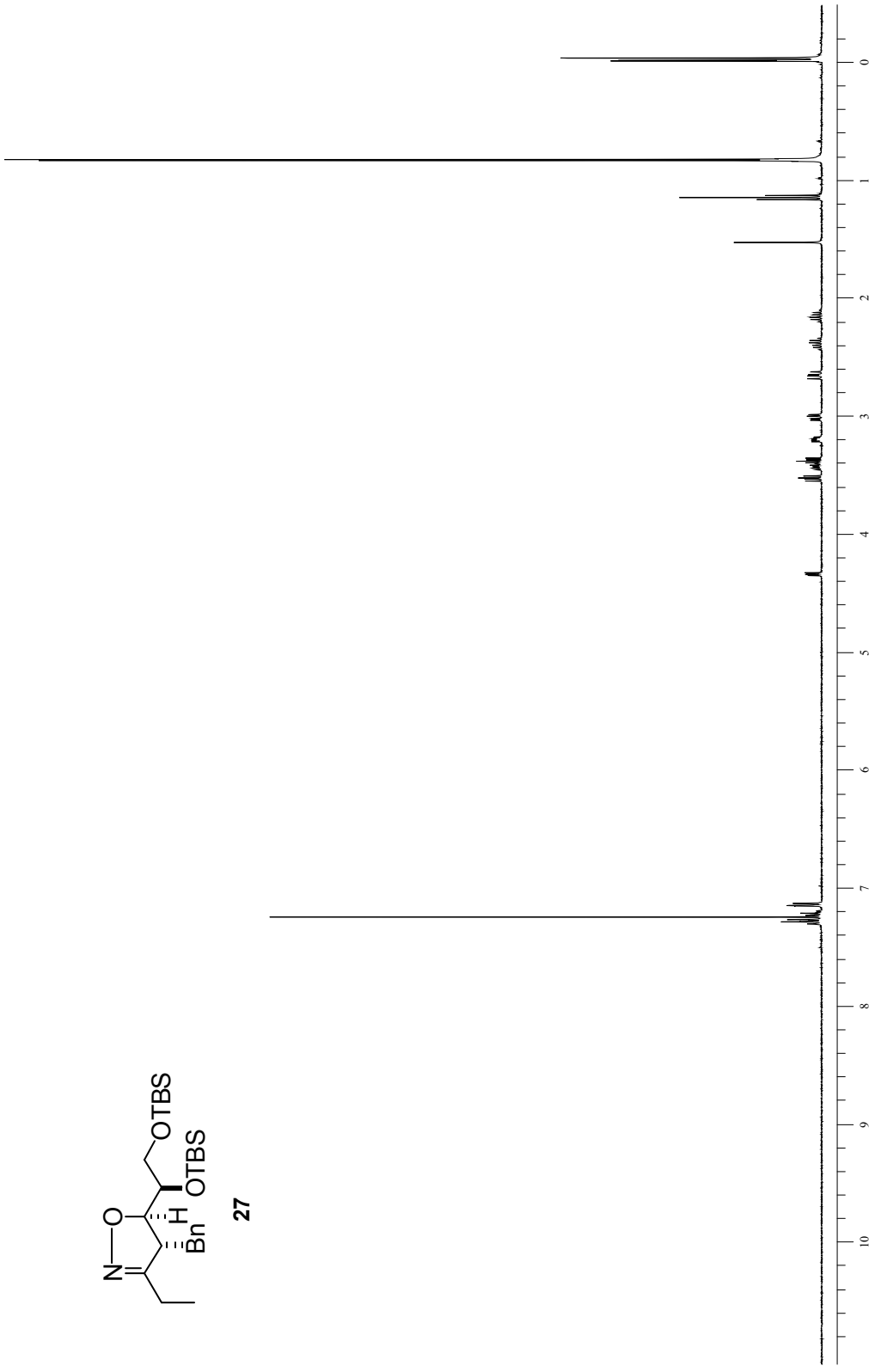

27

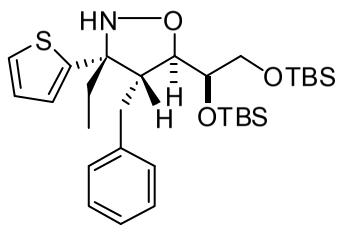

28

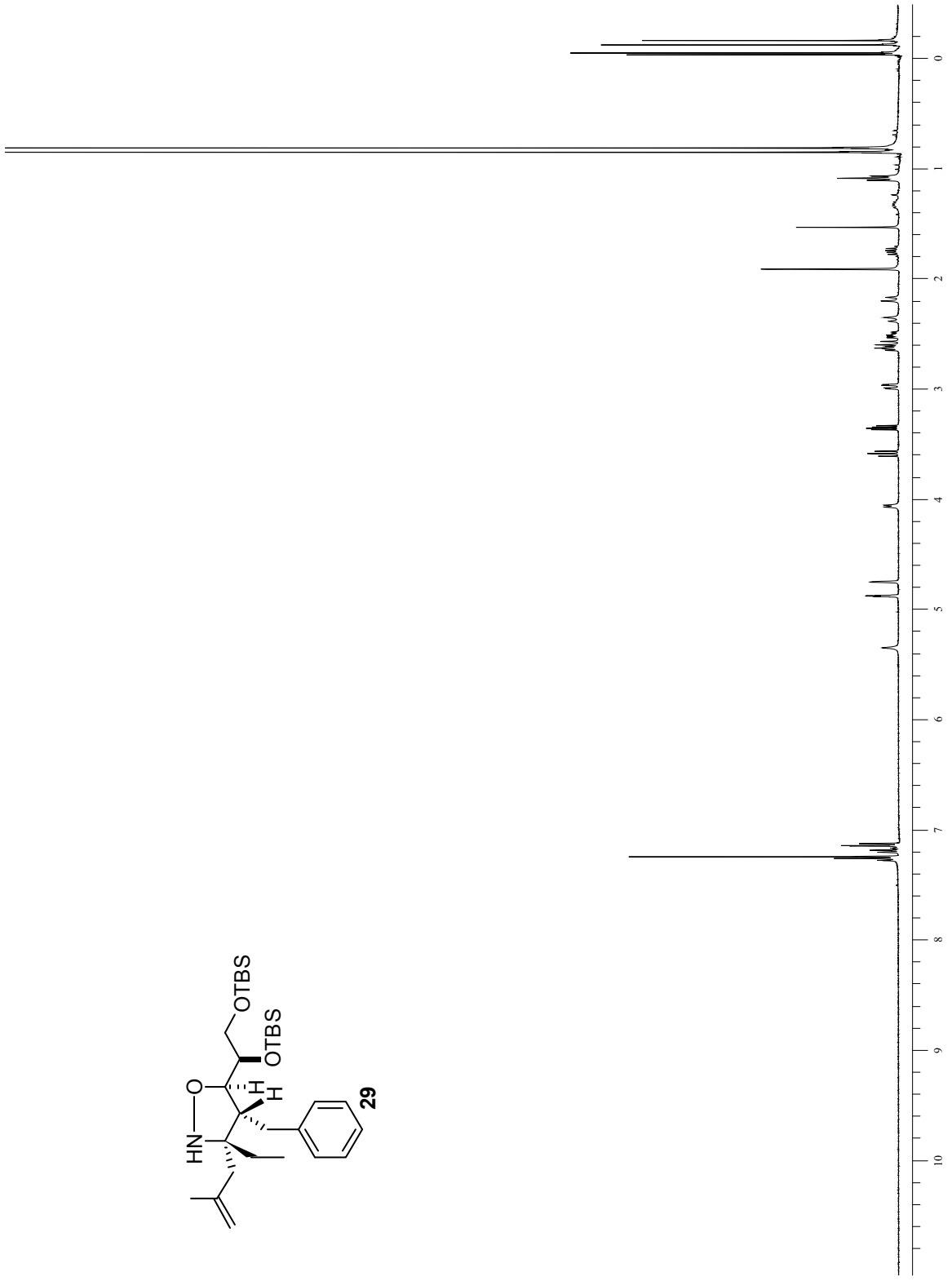
OTBS
OTBS
H
O
HN
29

S

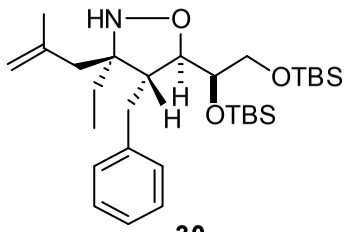

30

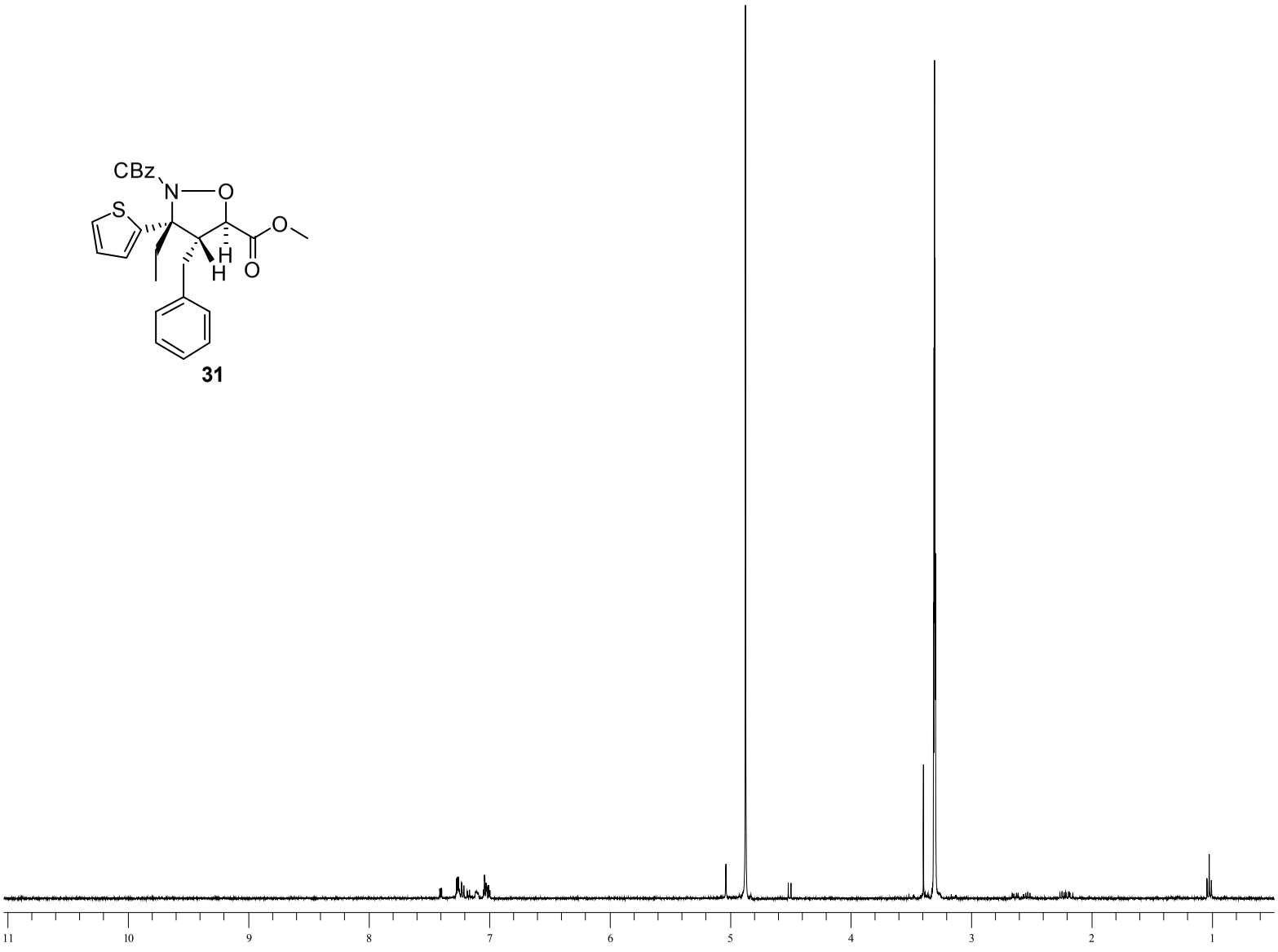
CBz
N
O
S
O
O
H
H
31
11
10
9
8
7
6
5
4
3
2
1

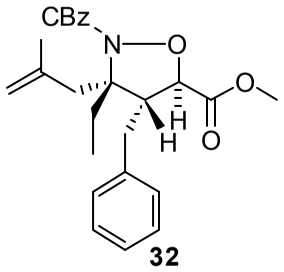

32

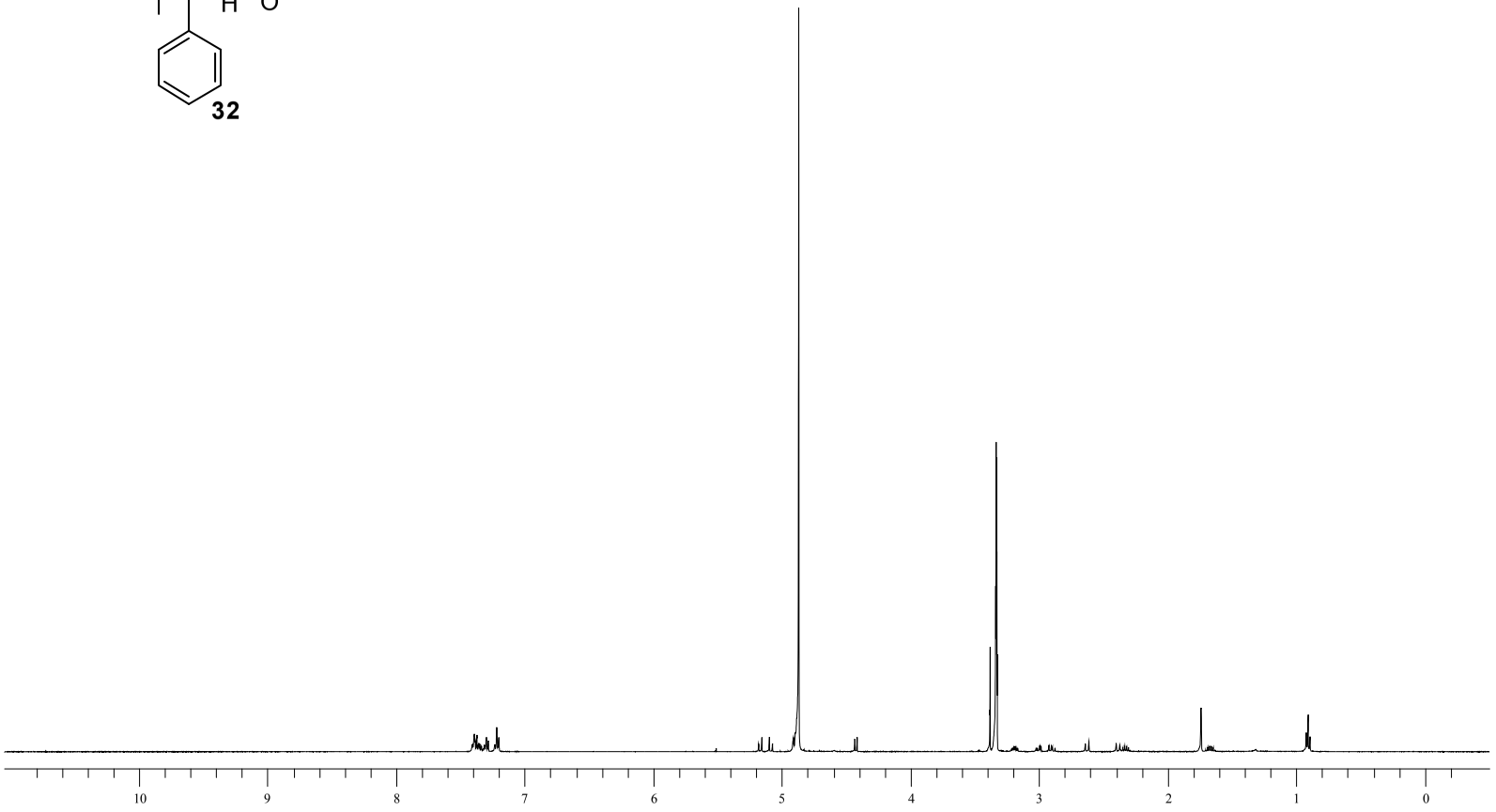

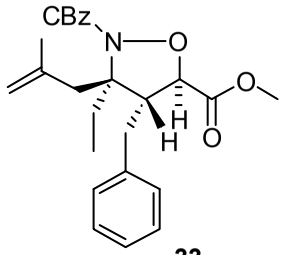

33

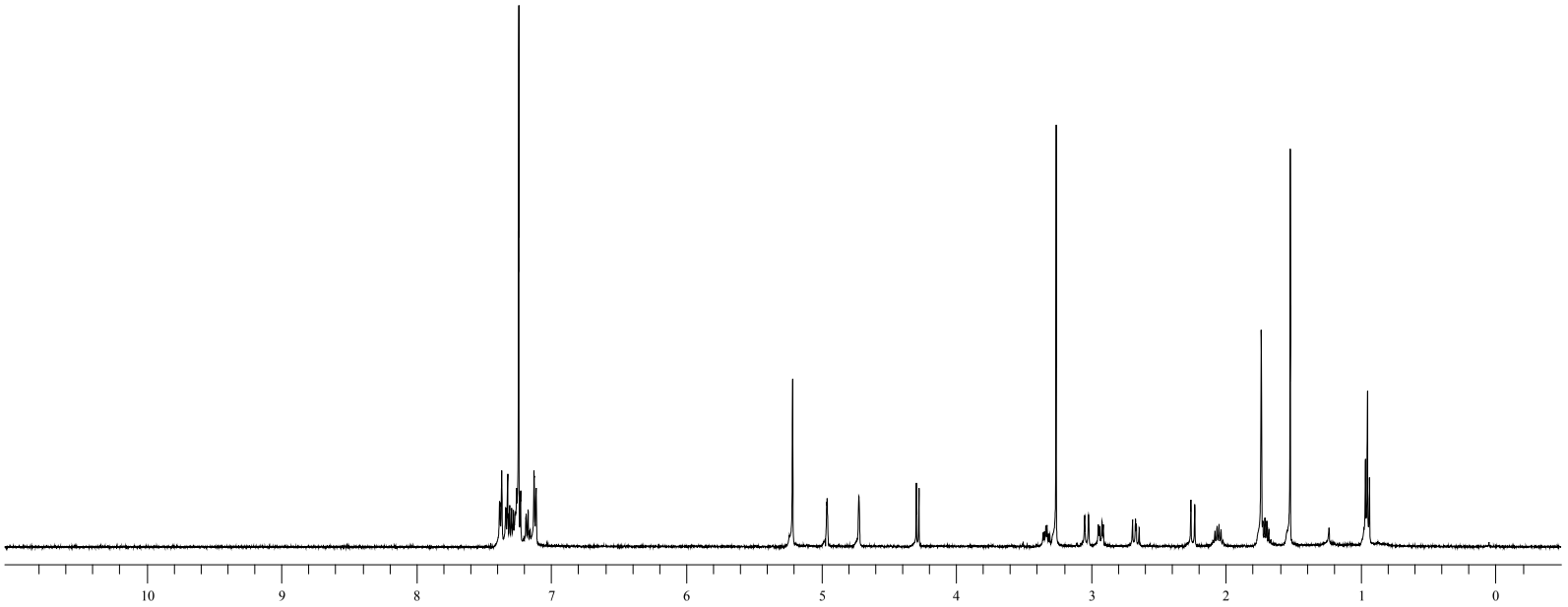

G. References

1. Hill, D. J.; Mio, M. J.; Prince, R. B.; Hughes, T. S.; Moore, J. S., *Chem Rev* **2001,** *101* (12), 3893-4012.

2. Cheng, R. P.; Gellman, S. H.; DeGrado, W. F., *Chem Rev* **2001,** *101* (10), 3219-32.

3. Cheng, R. P.; DeGrado, W. F., *J Am Chem Soc* **2002,** *124* (39), 11564-5.

4. Larsson, O. M.; Thorbek, P.; Krogsgaard-Larsen, P.; Schousboe, A., *J Neurochem* **1981,** *37* (6), 1509-16.

5. Johnson, G.; Drummond, J. T.; Boxer, P. A.; Bruns, R. F., *J Med Chem* **1992,** *35* (2), 233-41.

6. Huck, B. R.; Langenhan, J. M.; Gellman, S. H., *Org Lett* **1999,** *1* (11), 1717-20.

7. Huck, B. R.; Fisk, J. D.; Guzei, I. A.; Carlson, H. A.; Gellman, S. H., *J Am Chem Soc* **2003,** *125* (30), 9035-7.

8. Minter, A. R.; Fuller, A. A.; Mapp, A. K., *J Am Chem Soc* **2003,** *125* (23), 6846-7.

9. Fuller, A. A.; Chen, B.; Minter, A. R.; Mapp, A. K., *J Am Chem Soc* **2005,** *127* (15), 5376-83.

10. Kanemasa, S. N., M; Kamimura, A.; Hori, K. J., *J. Am. Chem. Soc.* **1994,** *116*, 2324-2439.

11. Bode, J. W.; Fraefel, N.; Muri, D.; Carreira, E. M., *Angew Chem Int Ed Engl* **2001,** *40* (11), 2082-2085.

12. Davoille, R. J. R., D. T.; Christie, S. D. R., *Tet. Lett.* **2000,** *41*, 1255-1259.

13. Wang, J. C. J., G. J., *J. Org. Chem.* **1999,** *64*, 8090-8097.